NASA Contractor Report 181787

PLAN, FORMULATE, DISCUSS AND CORRELATE A NASTRAN FINITE ELEMENT VIBRATIONS MODEL OF THE BOEING MODEL 360 HELICOPTER AIRFRAME

R. Gabel, P.F. Lang, L.A. Smith and D.A. Reed
BOEING HELICOPTERS
Philadelphia, Pa. 19142

Contract NAS1-17497

April 1989

National Aeronautics and
Space Administration

Langley Research Center
Hampton, Virginia 23665-5225

FOREWORD

Boeing Helicopters, together with other U.S. helicopter manufacturers, is engaged in a finite element applications program designed to emplace in the United States a superior capability to utilize finite element analysis models in support of helicopter airframe structural design. The Boeing effort is being performed under U.S. Government Contract NAS1-17497. The contract is monitored by NASA Langley Research Center, Structures Directorate.

This report reviews the modeling plan and presents results for the formulation and correlation of a NASTRAN finite element vibrations model of the Boeing Model 360 helicopter.

Key NASA and Boeing personnel in the program are listed below:

NASA Langley

P. H. Clark, Contracting Officer

J. W. Owens, Contract Specialist

J. H. Cline, Technical Representative

R. G. Kvaternik, Leader, Rotorcraft Structural Dynamics Group

Boeing Helicopters

J. M. Kelleher, Contract Administrator

R. Gabel, Dynamics Unit Manager

D. A. Reed, Engineering Specialist, Dynamics

P. F. Lang, Senior Engineer, Dynamics

L. A. Smith, Senior Engineer, Structures Technology

P. S. Skopowski, Engineering Specialist Environmental Test

P. T. Tran, Associate Engineer, Environmental Test

N. Dorofee, Dynamics Technician

BLANK
PAGE

TABLE OF CONTENTS

1.0 Introduction

INTRODUCTION

The NASA Langley Research Center is sponsoring a rotorcraft structural dynamics program with the overall objective to establish in the United States a superior capability to utilize finite element analysis models for calculations to support industrial design of helicopter airframe structures. Viewed as a whole, the program is planned to include efforts by NASA, universities, and the U.S. helicopter industry. In the initial phase of the program, teams from the major U.S. manufacturers of helicopter airframes will apply extant finite element analysis methods to calculate static internal loads and vibrations of helicopter airframes of both metal and composite construction, conduct laboratory measurements of the structural behavior of these airframes, and perform correlations between analysis and measurements to build up a basis upon which to evaluate the results of the applications. To maintain the necessary scientific observation and control, emphasis throughout these activities will be on advance planning, documentation of methods and procedures, and thorough discussion of results and experiences, all with industry-wide critique to allow maximum technology transfer between companies. The finite element models formed in this phase will then serve as the basis for the development, application, and evaluation of both improved modeling techniques and advanced analytical and computational techniques, all aimed at strengthening and enhancing the technology base which supports industrial design of helicopter airframe structures. Here again, procedures for mutual critique have been established, and these procedures call for a thorough discussion among the program participants of each method prior to the applications and of the results and experiences after the applications. The aforementioned rotorcraft structural dynamics program has been given the acronym DAMVIBS (Design Analysis Methods for VIBrationS).

This report presents the results of an effort under the DAMVIBS Program by Boeing Helicopters to plan, formulate, discuss and correlate a NASTRAN finite element vibrations model of the Boeing Model 360 helicopter airframe.

2.0 Modeling and Correlation Plan Objectives

MODELING AND CORRELATION PLAN OBJECTIVES

The principal objectives of the modeling plan are to (1) define guides for formulating and coding the NASTRAN model and (2) define test cases for demonstrating adequacy of the model. The objective of the correlation plan is to provide guides for correlation of predicted and measured vibration characteristics.

MODELING AND CORRELATION PLAN OBJECTIVES

MODELING PLAN

- DEFINE GUIDES FOR MODELING AND CODING THE NASTRAN MODEL OF THE BOEING MODEL 360 COMPOSITE AIRFRAME
    1) STATIC (STRESS) MODELING
    2) MASS MODELING
    3) VIBRATION MODELING BY MODIFICATION OF THE STATIC MODEL

- DEFINE TEST CASES FOR DEMONSTRATING ERROR FREE CALCULATIONS FOR
    1) STATIC LOADS
    2) NORMAL MODES
    3) FORCED RESPONSE

CORRELATION PLAN

- DEFINE GUIDES FOR CORRELATION OF PREDICTED AND MEASURED VIBRATION CHARACTERISTICS
    1) BASIS OF CORRELATION
    2) TYPE AND NUMBER OF PLOTS

3.0 Description of Boeing Model 360 Helicopter

PRECEDING PAGE BLANK NOT FILMED

DESCRIPTION OF BOEING MODEL 360 HELICOPTER

The Model 360 prototype is a tandem rotor helicopter with a rear loading ramp designed for aerial transport of passengers and/or cargo. The airframe is basically an all-composite airframe using modularized construction techniques. Design gross weight is 30,500 pounds. The rotor system is a four-bladed counter-rotating design with a normal speed of 269 RPM. Primary power is provided by two T55-L-11 turbo-shaft engines mounted inside of the aft pylon. The landing gear configuration is a retractable design with a single forward gear and dual aft gear. Normal crew is a pilot, copilot and crew chief.

ORIGINAL PAGE
BLACK AND WHITE PHOTOGRAPH

DESCRIPTION OF BOEING MODEL 360 HELICOPTER

MODEL 360 OVERALL DIMENSIONS AND GENERAL ARRANGEMENT

The accompanying three-view drawing shows the general arrangement and typical overall dimensions for the Model 360 prototype. Overall length exclusive of the rotors is 51 feet. The center to center rotor dimension is 34.39 feet and the rotor diameter is 49.7 feet. Including the rotors and landing gear, the overall length and width are 83.3 and 13 feet, respectively.

Two Lycoming T55-L-11 engines drive 90° angle gearboxes and cross shafts into a combining transmission. The combining transmission, in turn, drives interconnect shafts to the forward and aft rotor transmissions. The overall gear ratio is 64.045 which reduces the power turbine speed to the normal rotor speed of 269 RPM.

The airframe is of all composite construction with a low frontal area. The cockpit contains dual pilot/copilot stations and all accompanying controls and instruments. The main cabin is a constant section with a forward left-hand escape hatch, a forward right-hand cabin door and an aft ramp. An aft pylon structure bridges the ramp and supports the aft transmission and rotor, the engines and an auxiliary power unit. Fuel is contained in three crashworthy cells below the cabin floor.

MODEL 360 OVERALL DIMENSIONS AND GENERAL ARRANGEMENT

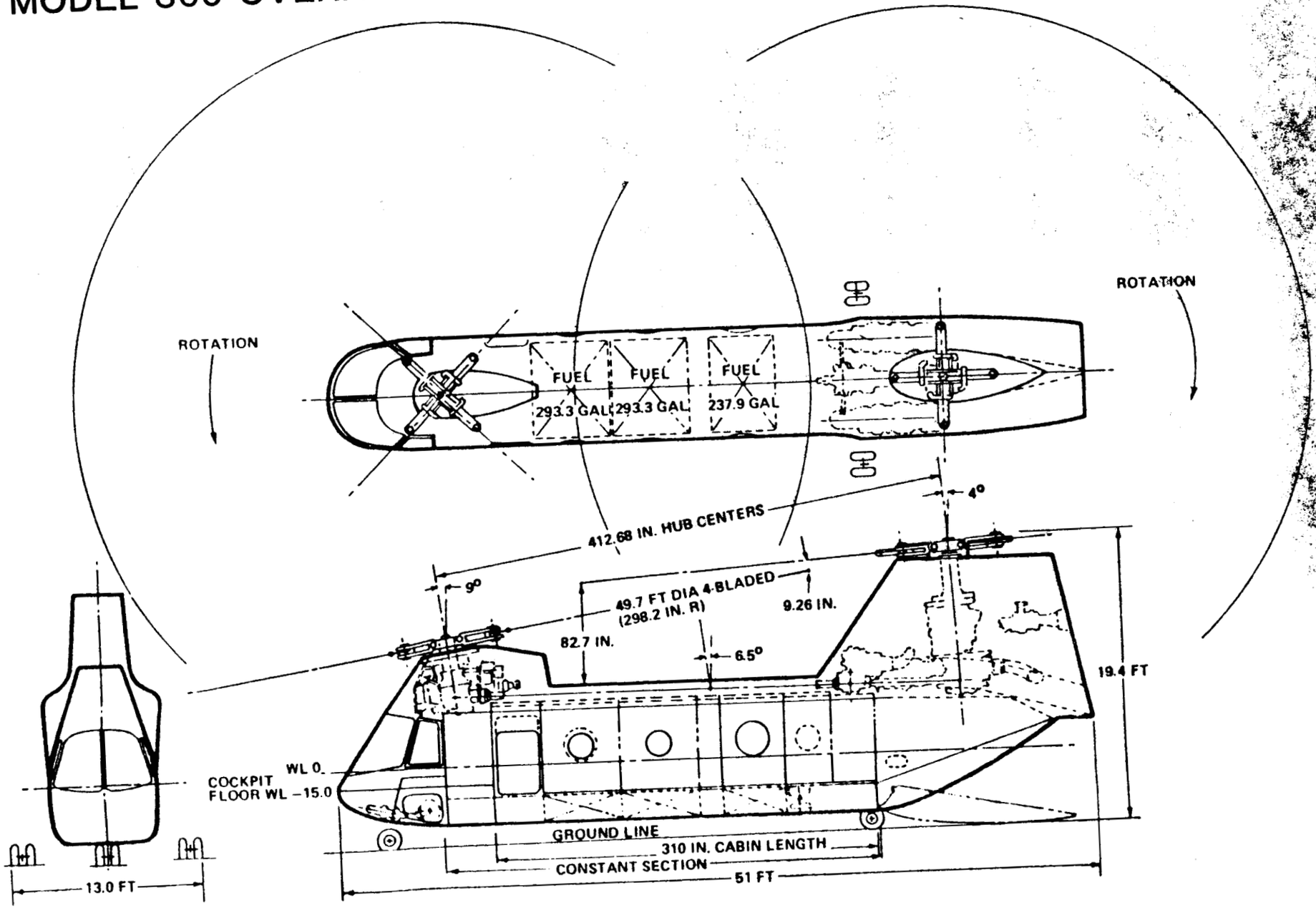

MODEL 360 AIRFRAME AND SUBSYSTEM MODULES

The Model 360 airframe consists of seven subsystem modules as illustrated in this figure. These subsystems include the tunnel, cockpit module, nose enclosure, fuselage, ramp, main landing gear module and cabin floor/fuel assembly. The tunnel, ramp and nose enclosure are considered to be nonstructural since they are designed to neither contribute to the overall stiffness nor support any major components. The cockpit module and cabin floor/fuel assembly, on the other hand, support significant masses. The dynamic behavior of both of these subsystem modules is controlled by supporting the modules on mass-tuned, anti-resonant isolators.

MODEL 360 AIRFRAME AND SUBSYSTEM MODULES

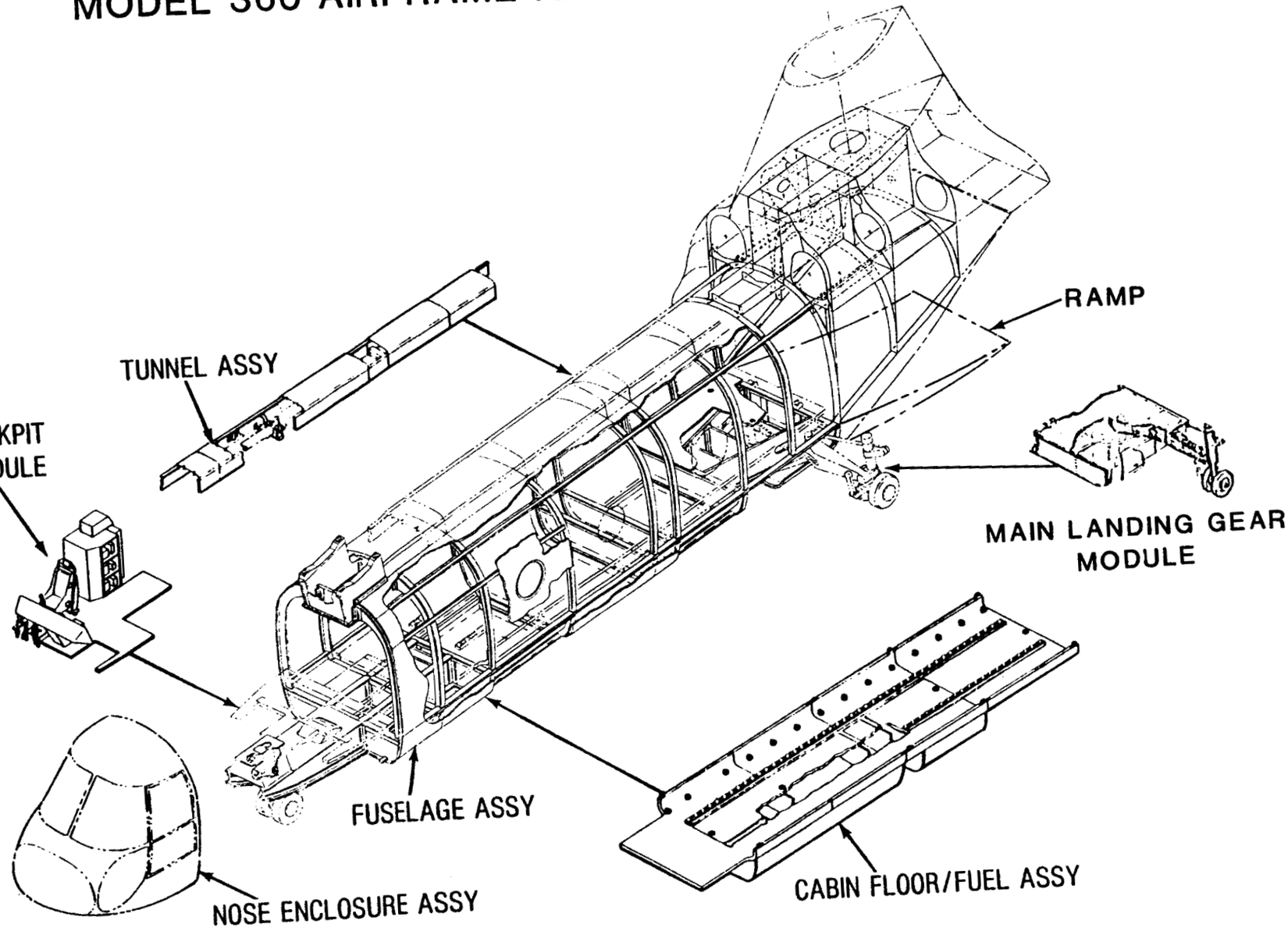

MODEL 360 PRIMARY STRUCTURE

The Model 360 has an all composite semi-monocoque fuselage with a primary structure of frames, longerons and stressed, honeycomb-sandwich, skin panels and bulkheads. Frames are located only where major concentrated loads enter the aircraft, leading to skin panel sizes which vary from approximately 2 foot by 6 foot to 6 foot by 6 foot. At major frames in the cabin section, deep webs in the frame below the floor line aid in redistribution of loads. Four main longerons are sized to carry overall fuselage vertical and lateral bending loads. All major components are mixed modulus construction to meet strength and stiffness requirements.

Butt-line beams bridge the two major frames at Stations 82 and 120 to support the forward transmission. The two beams which support the cockpit are cantilevered forward of Station 82 and bridge the two frames (Stations 120 and 160) aft of Station 82. A large double-box structure bridging the frames at Stations 430, 476 and 528 supports the aft transmission (transmission mounted between Station 476 and 528) and transfers the rotor loads to the lower fuselage structure. Assembly of the major modules is achieved by a bonded/bolted joining of the subassemblies. Bolts are used to provide pressure during the adhesive cure and are sized to carry the design limit loads as a redundant load path.

MODEL 360 PRIMARY STRUCTURE

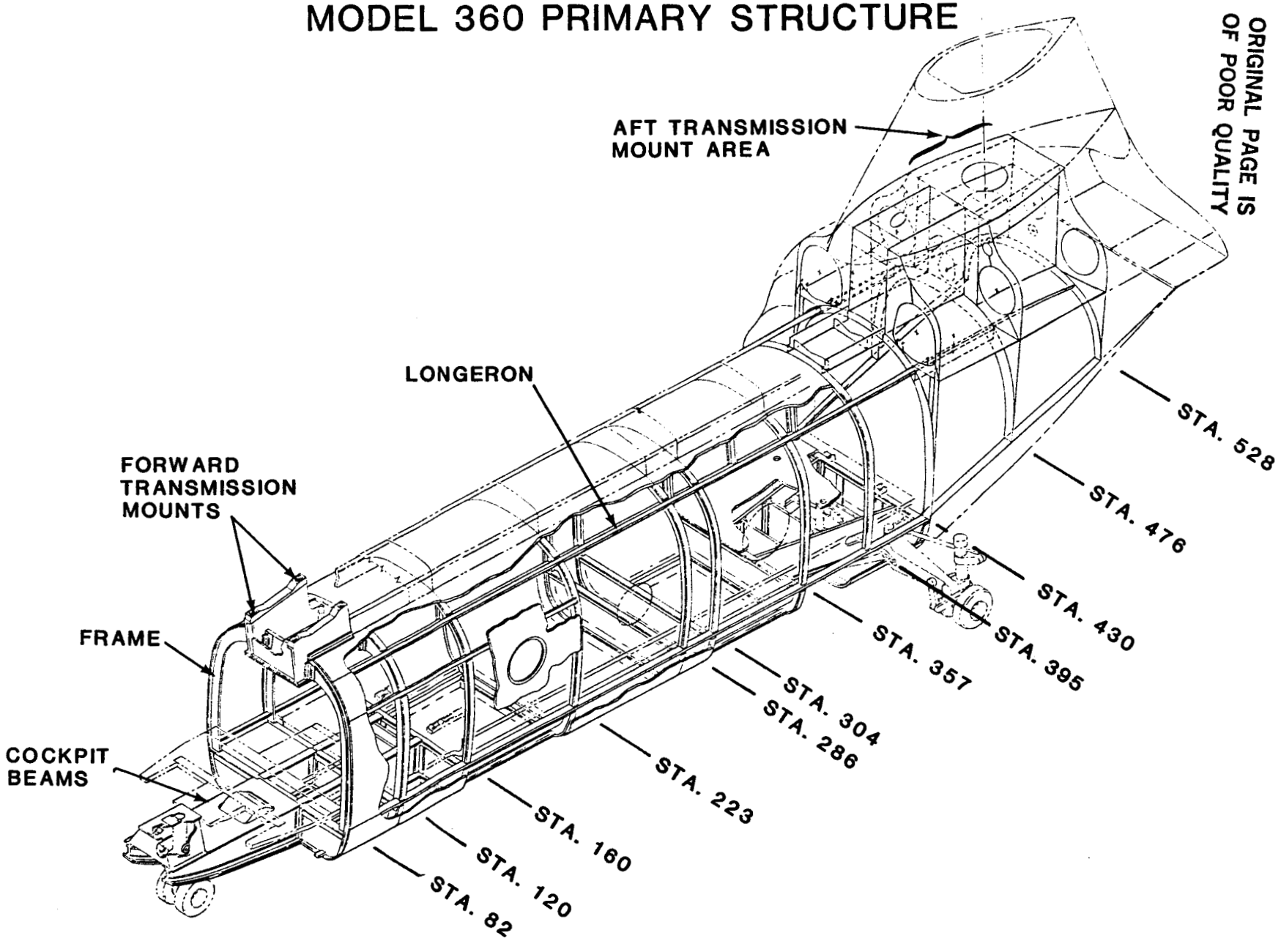

ORIGINAL PAGE IS OF POOR QUALITY

MODEL 360 FUSELAGE ASSEMBLY

A photograph of the partially completed fuselage assembly is shown on the following page. Visible in the photograph are the access for the forward left-hand escape hatch, a portion of the cockpit beams and the partially completed forward transmission support structure.

ORIGINAL PAGE
BLACK AND WHITE PHOTOGRAPH

MODEL 360 FUSELAGE ASSEMBLY

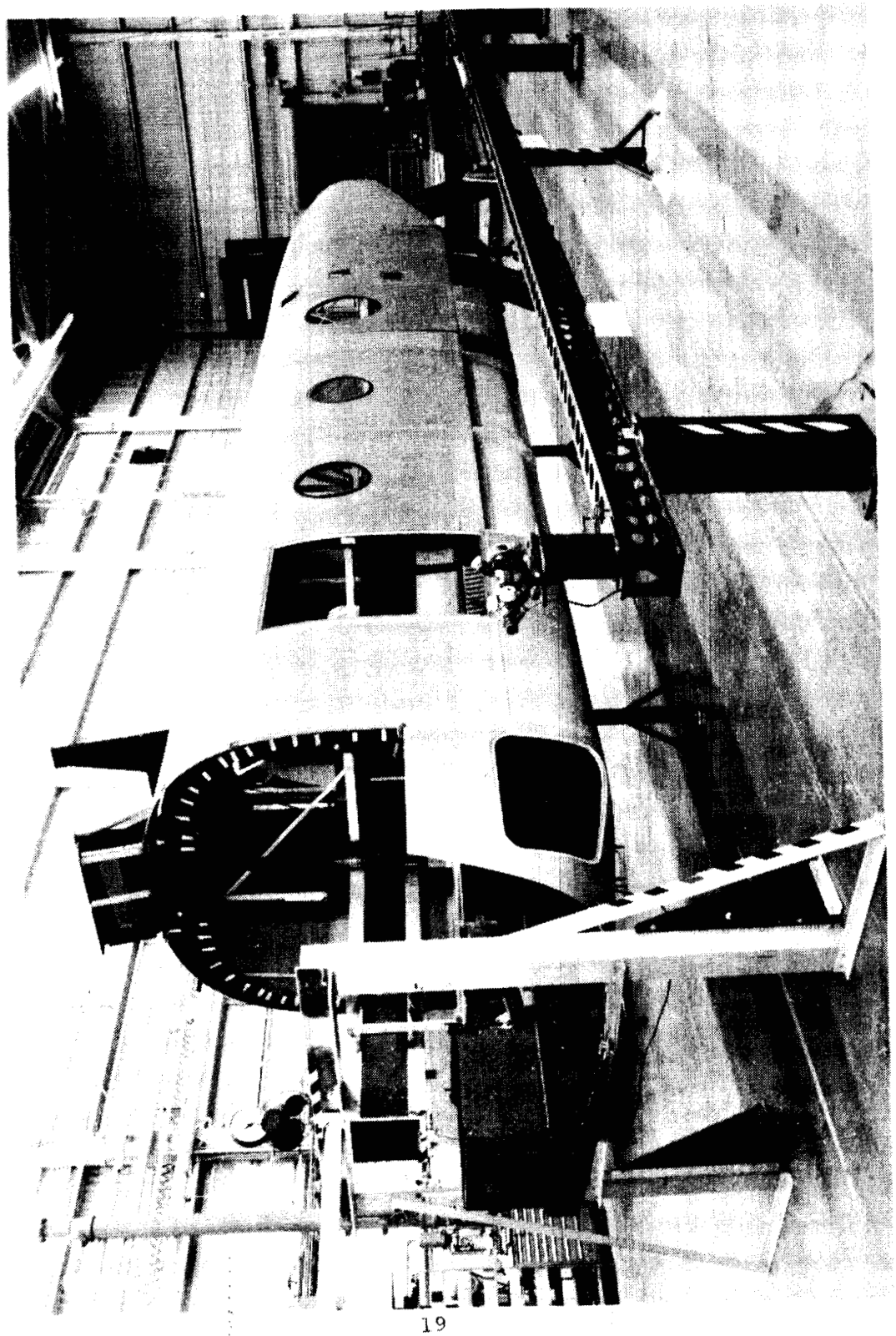

MODEL 360 SECONDARY STRUCTURE

A number of secondary structural elements are provided solely for aerodynamic fairing or utility functions and are not considered to be load carrying structure. These include:

1.) drive shaft tunnel covers
2.) nose enclosure
3.) forward transmission fairing
4.) cabin door, escape hatch and windows
5.) aft pylon fairings
6.) tail cone
7.) aft cargo ramp
8.) landing gear compartment doors
9.) cargo hatches
10.) engine access panels

MODEL 360 SECONDARY STRUCTURE

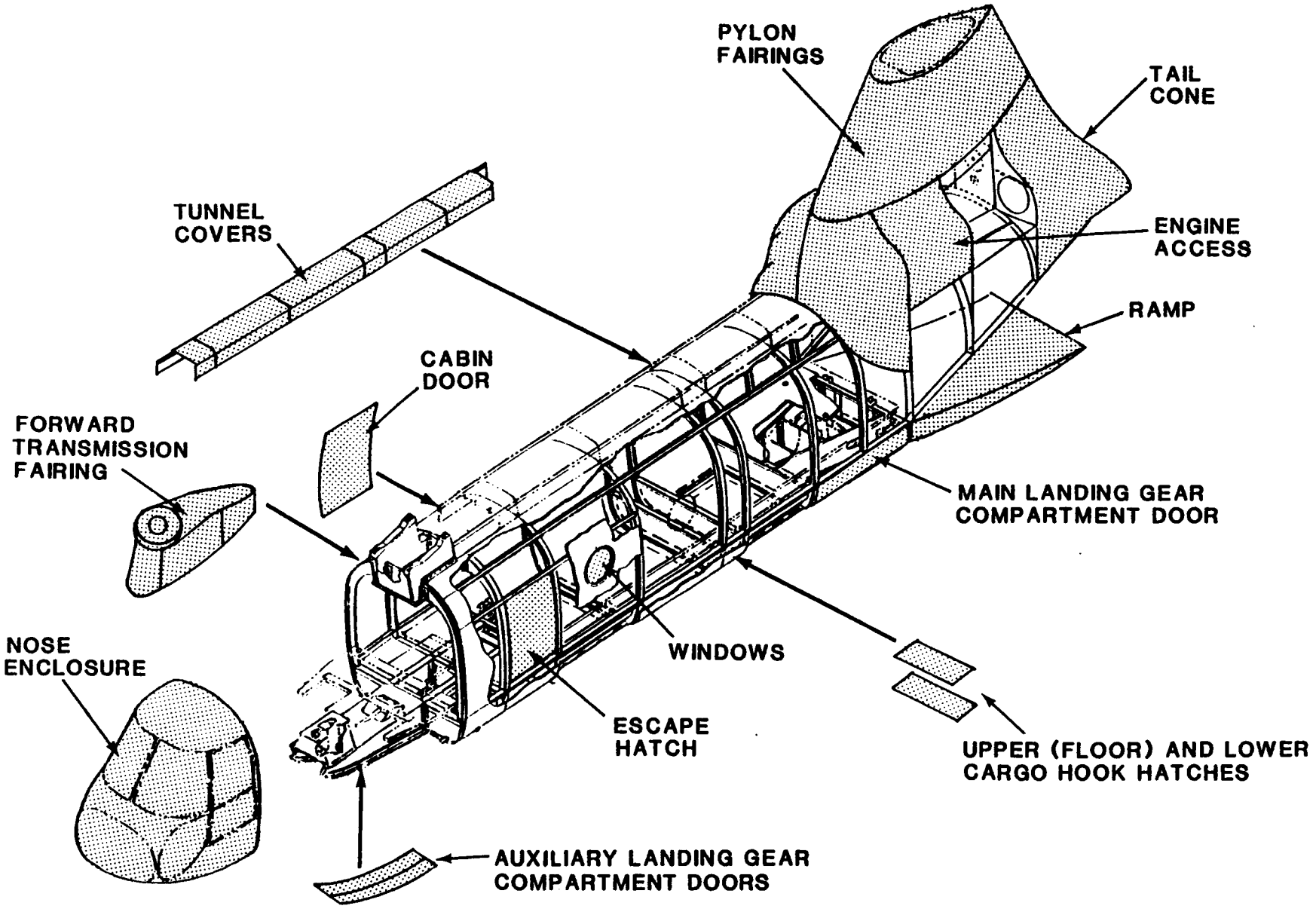

MODEL 360 TYPICAL FRAME CONSTRUCTION

This drawing illustrates construction of a typical frame. Graphite inner and outer caps are joined by a web consisting of graphite face sheets and a nomex core. A skin panel splice plate is bonded to the web around the outer perimeter of the frame to provide an attachment surface for the skin panels. The skin panel splice plate is cut away at the longeron locations to accept the longeron outer cap.

MODEL 360 TYPICAL FRAME CONSTRUCTION

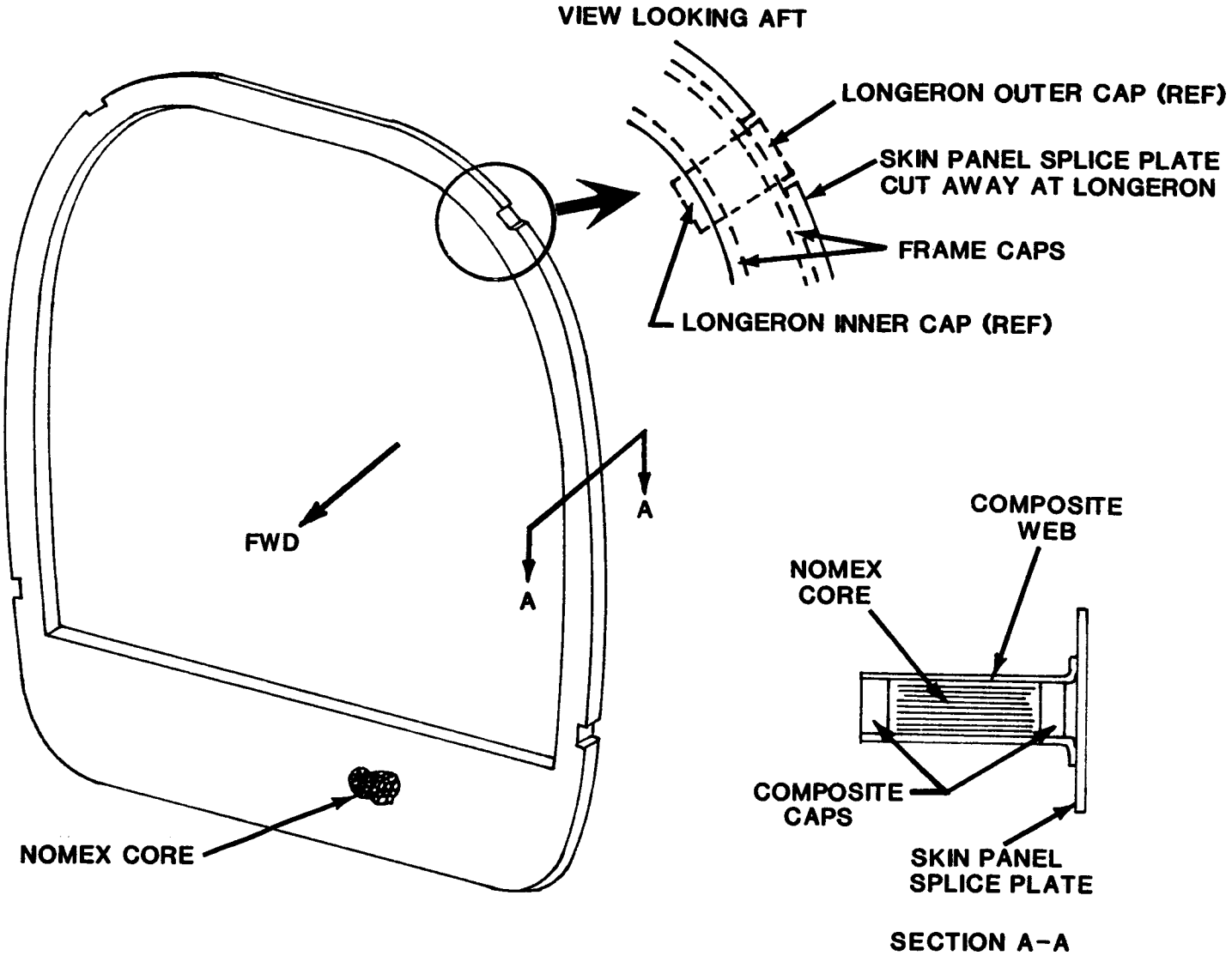

MODEL 360 TYPICAL SKIN PANEL AND LONGERON

Typical skin panel and longeron assemblies are shown in this figure. Skin panels are of sandwich construction with kevlar skins and a nomex core. The skins are formed into a flange at the edges of the panel for assembly to the skin splice plate of the frames shown in the previous illustration. The panels are secured by a fully bonded joint in addition to mechanical fasteners. The fasteners provide pressure during the adhesive cure and are sized to carry design loads as a redundant load path.

The longerons consist of graphite caps and face sheets with a nomex core. Notches in the core of the inner cap sub-assembly are provided at the frame locations to permit installation of the longerons. The outer cap is bonded in place after the inner cap has been assembled with the frames.

MODEL 360 TYPICAL SKIN PANEL AND LONGERON

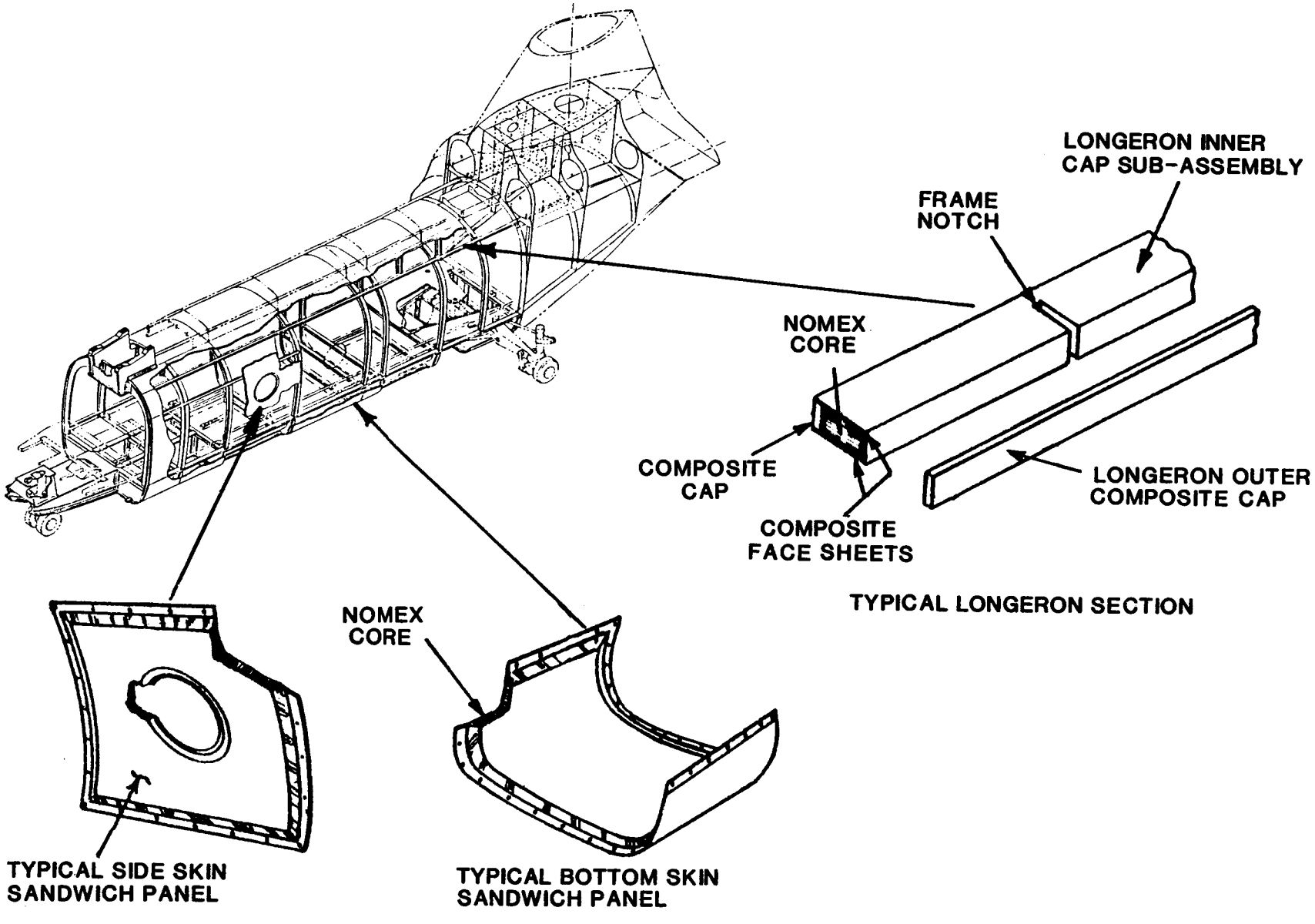

MODEL 360 FUSELAGE INTERIOR VIEW

The accompanying photograph of the fuselage interior shows the frames, longerons and the deep frame web below the floor.

ORIGINAL PAGE
BLACK AND WHITE PHOTOGRAPH

MODEL 360 FUSELAGE INTERIOR VIEW

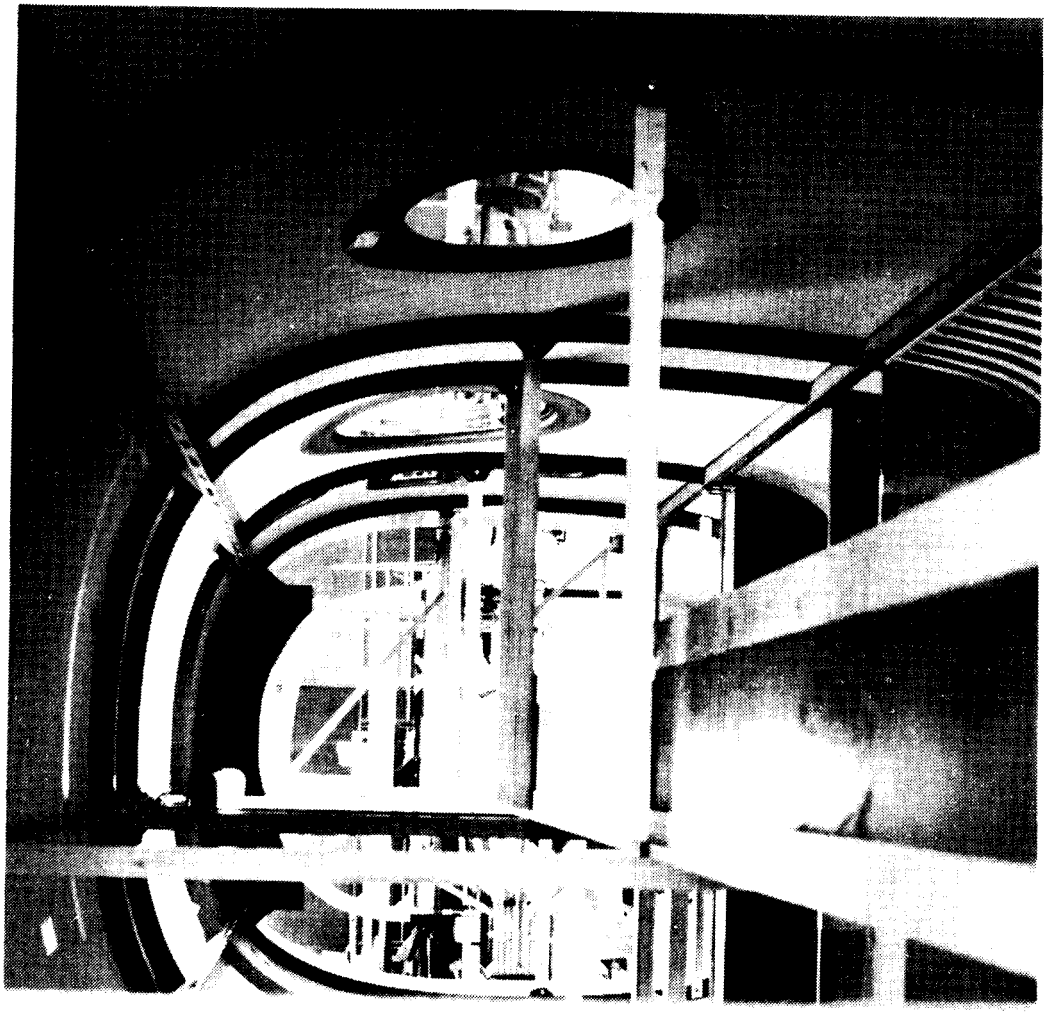

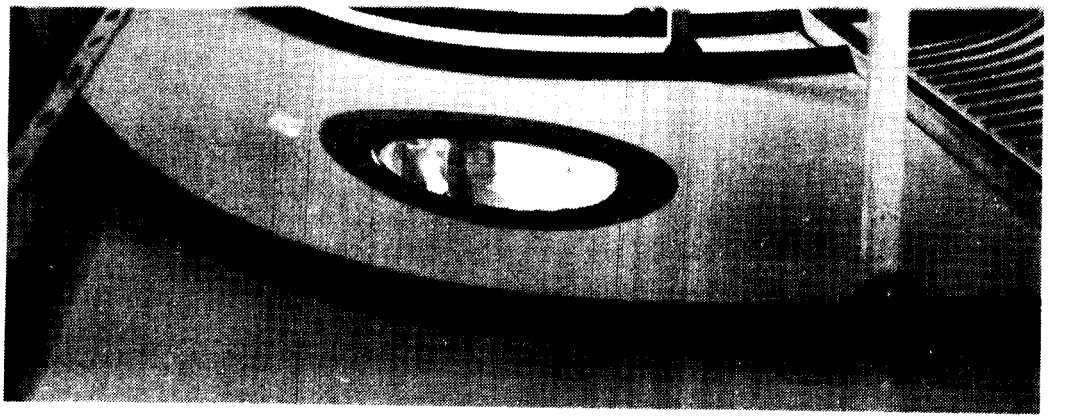

ISOLATED COCKPIT AND FLOOR/FUEL MODULES

The cockpit module and the cabin floor/fuel module are both isolated from the airframe by mass-tuned anti-resonant isolators. The anti-resonant isolation is stiff at low frequencies and dynamically soft at the tuned isolation frequency.

The cockpit isolators are tuned to minimize cockpit vibration at both 4/rev (blade passage frequency) and 8/rev. At 4/rev, the isolators act in the vertical, lateral, pitch and roll axes. Isolation at 8/rev is in the vertical direction only. The floor/fuel isolators are single frequency units designed to provide only 4/rev vertical isolation.

ORIGINAL PAGE
BLACK AND WHITE PHOTOGRAPH

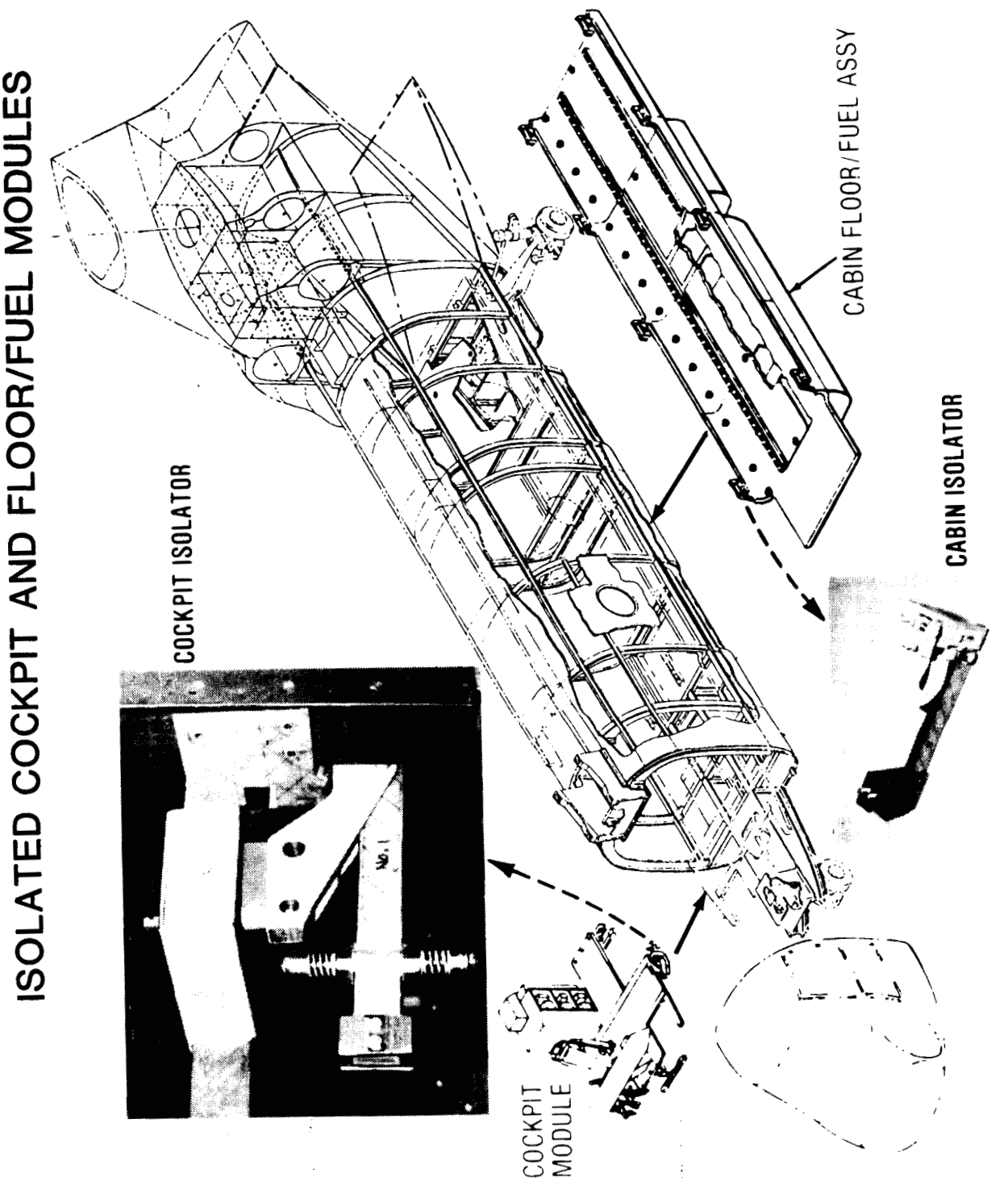

MODEL 360 FORWARD TRANSMISSION AND ROTOR SHAFT

As shown in this illustration, the Model 360 utilizes a composite rotor shaft and transmission cover. The rotor shaft is cantilevered from the transmission with the load path to the airframe being through the transmission upper cover. Mechanically, the transmission is a modified CH-47C transmission.

ORIGINAL PAGE
BLACK AND WHITE PHOTOGRAPH

MODEL 360 FWD TRANSMISSION AND ROTOR SHAFT

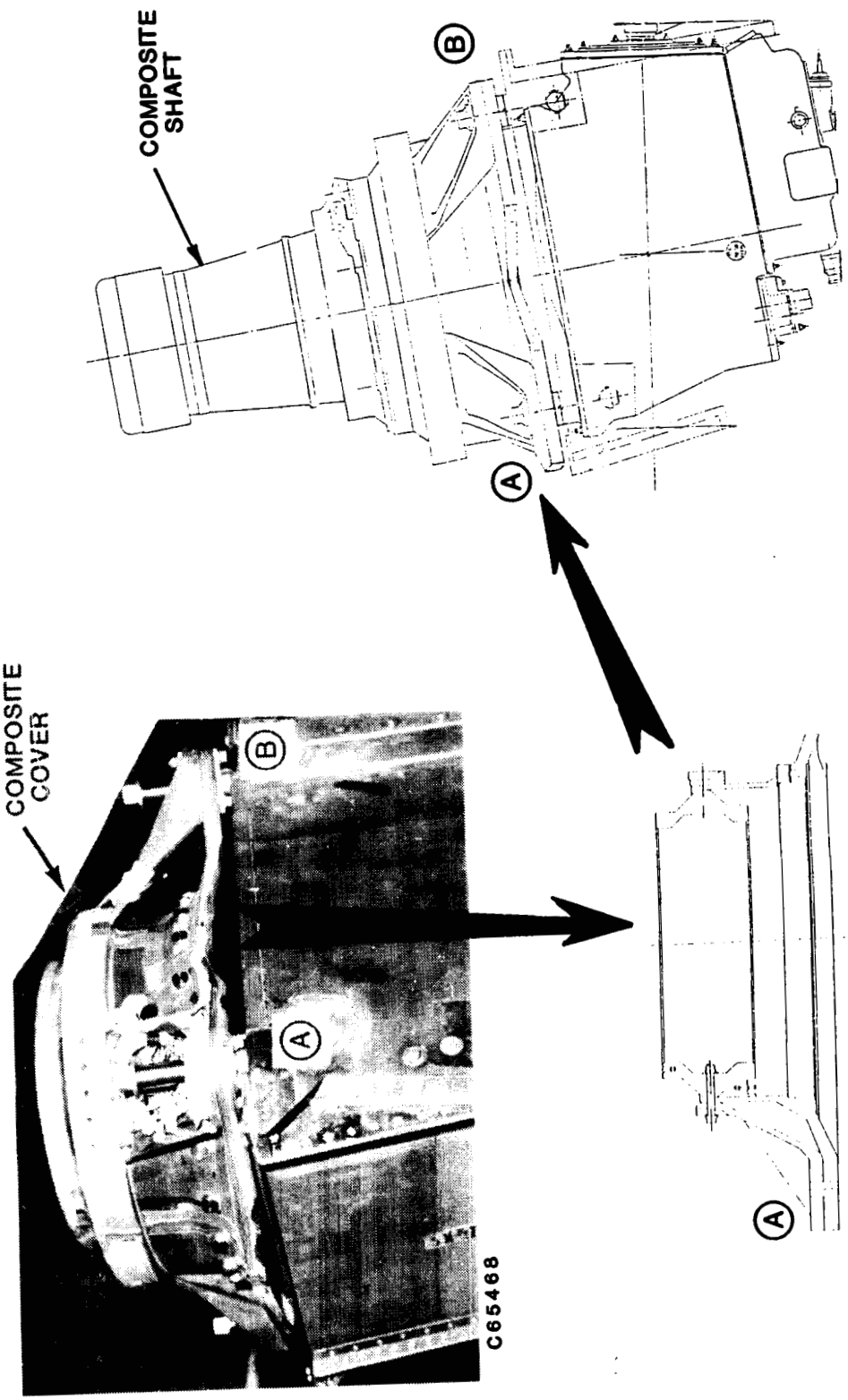

MODEL 360 AFT TRANSMISSION AND ROTOR SHAFT

Functionally, the aft rotor installation is the same as the forward installation. In both cases, the rotor shaft is cantilevered from the transmission cover. However, as shown in this illustration, the configuration of the aft transmission cover is totally different. In addition, the structural attachment points are located above, rather than below, the transmission. The aft rotor shaft is also approximately three times longer than the forward rotor shaft.

MODEL 360 AFT TRANSMISSION AND ROTOR SHAFT

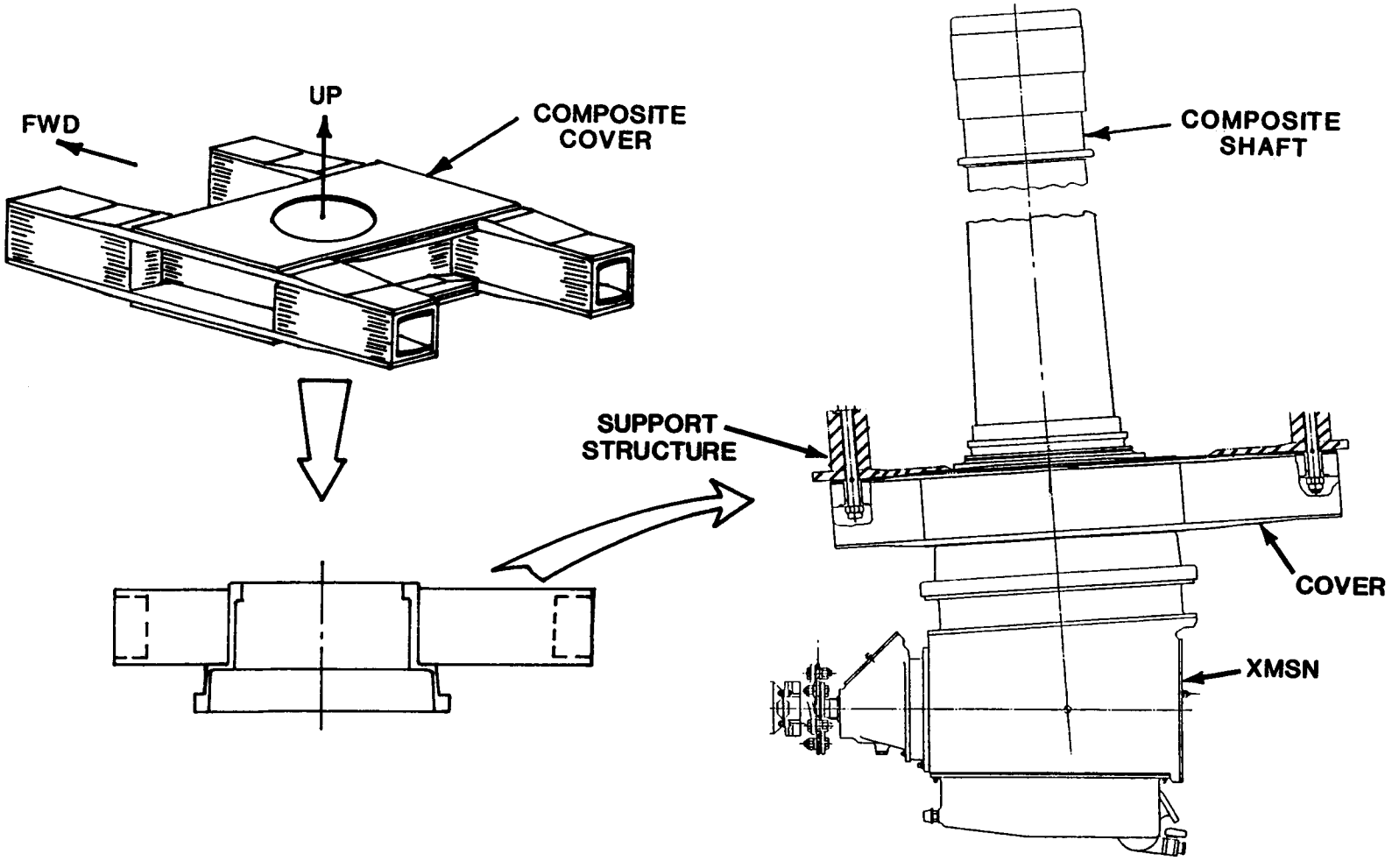

MODEL 360 ENGINE SUPPORT STRUCTURE

The engines are mounted on the aft fuselage on either side of the aft pylon structure and are fully enclosed within the pylon aerodynamic fairing. The forward engine support fittings are attached to a lateral beam (extending the full width of the airframe) at Frame 430. The aft support fittings are attached to the engine deck at Station 451. At the forward engine support, two attachment points provide longitudinal, lateral and vertical load paths to the primary structure. At the aft support, a vertical link pivoted at both engine and airframe attachments provides only a vertical load path.

MODEL 360 ENGINE SUPPORT STRUCTURE

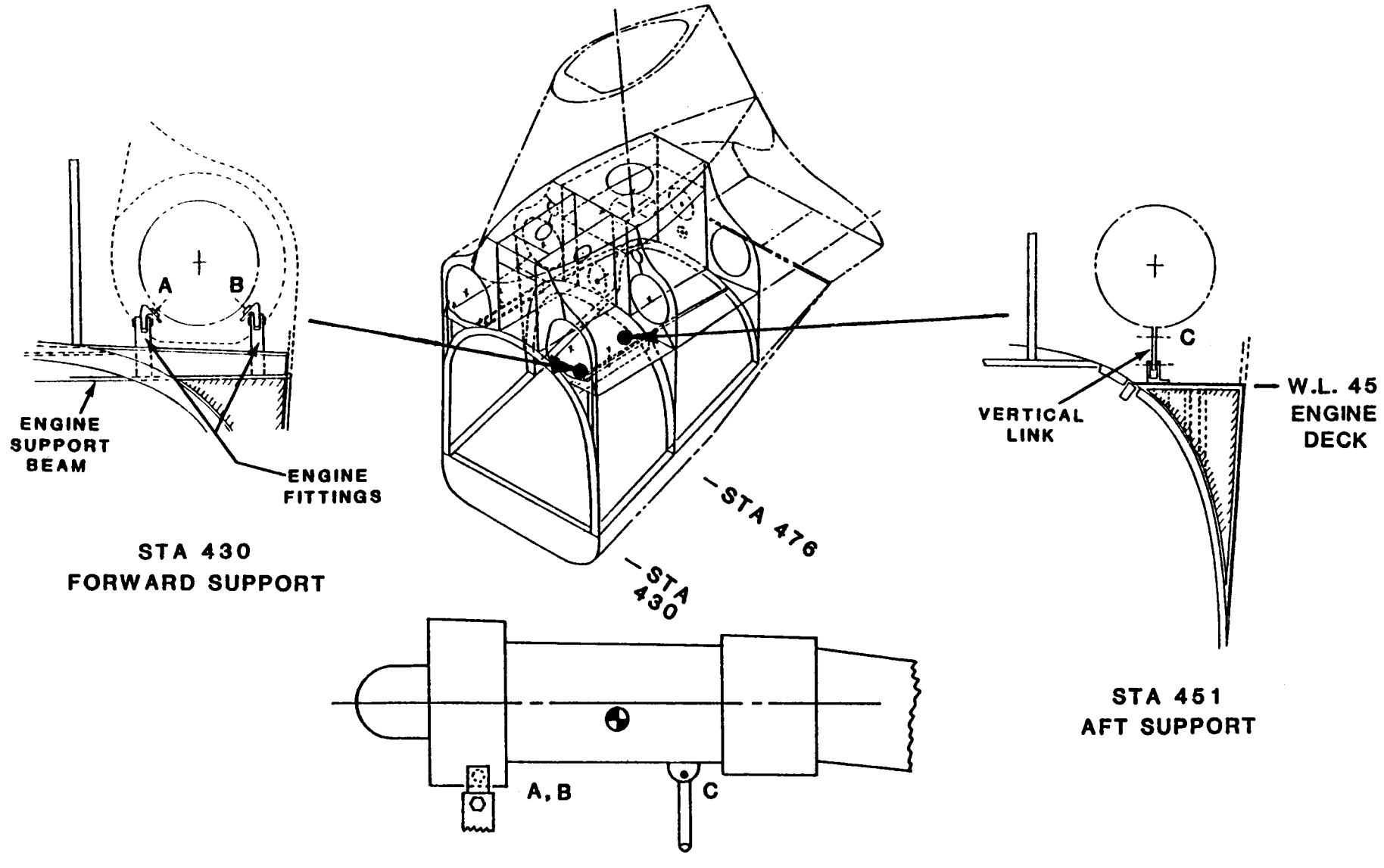

MODEL 360 MAIN LANDING GEAR

The retractable main landing gear, located just forward of station 430, is attached to a drag beam which is pivoted in the structure about a near vertical axis. The strut, in turn, is pivoted at the end of the drag beam about the longitudinal axis. Rotation of the drag beam about its pivot axis is restrained by a drag link which transfers loads through a bellcrank system and actuator to the structure. Similarly, roll motion of the strut is restrained by a stabilizer link connected directly to the structure. In the extended position,the gear is locked in place by an internal latch in the actuator. A latch pin inserted between the structure and the bellcrank mechanism is used to lock the gear in the retracted position.

The structure and the fittings which house the drag beam pivot are designed to provide only shear restraint. As its name implies, the pivot or shear pin is also designed solely as a shear restraint. Vertical loads along the axis of the shear pin are carried by a bearing block which shears the load back to the frame at station 430.

MODEL 360 MAIN LANDING GEAR

- EXTENDED: INTERNAL LATCH IN ACTUATOR
- RETRACTED: BELLCRANK PINNED TO STRUCTURE

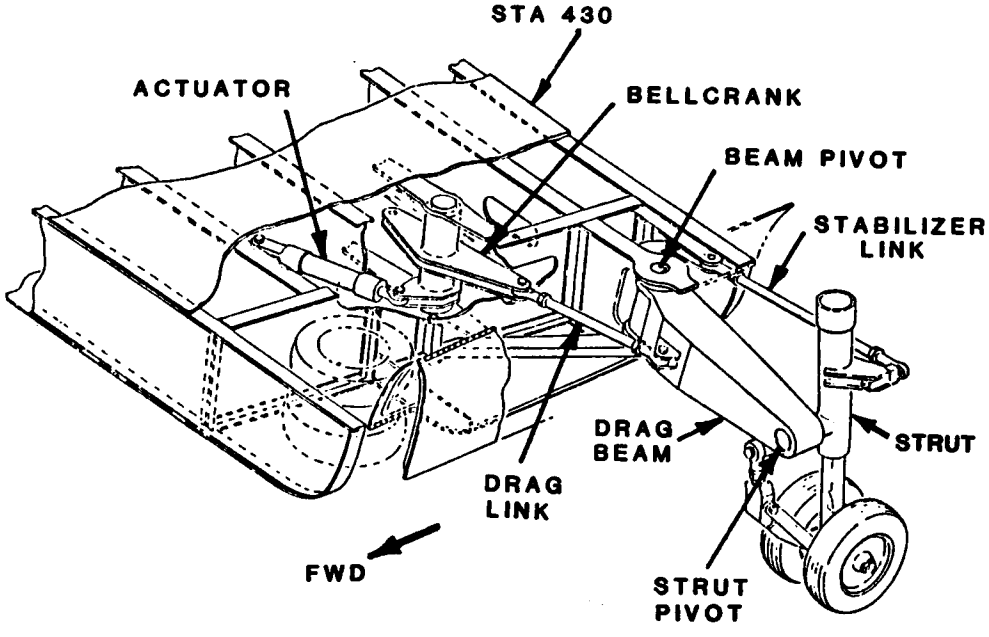

EXTENDED

RETRACTED

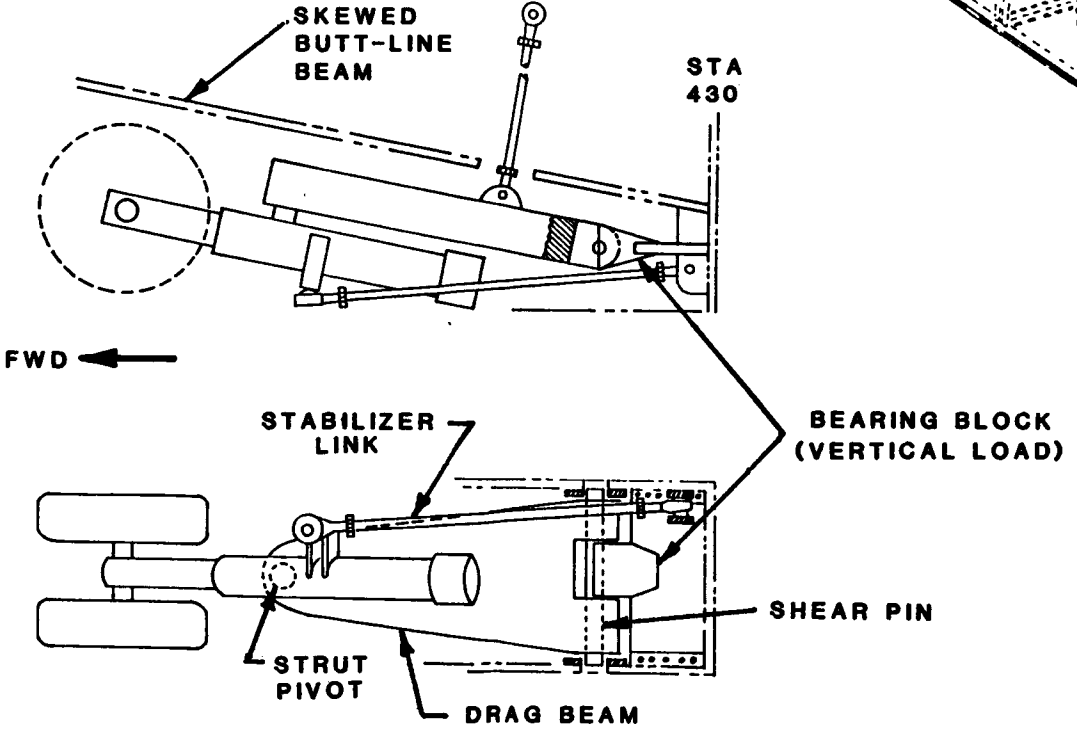

MODEL 360 FORWARD LANDING GEAR

The forward landing gear located at the forward extremity of the cockpit beams is also retractable. Two fittings located on either side of the strut provide support points for the pivot pin on which the strut rotates in the fore and aft direction. In the extended position, a latch pin fixes the top of strut to the structure. When retracted, an internal latch in the folding actuator locks the gear in the stowed position.

MODEL 360 FORWARD LANDING GEAR

EXTENDED

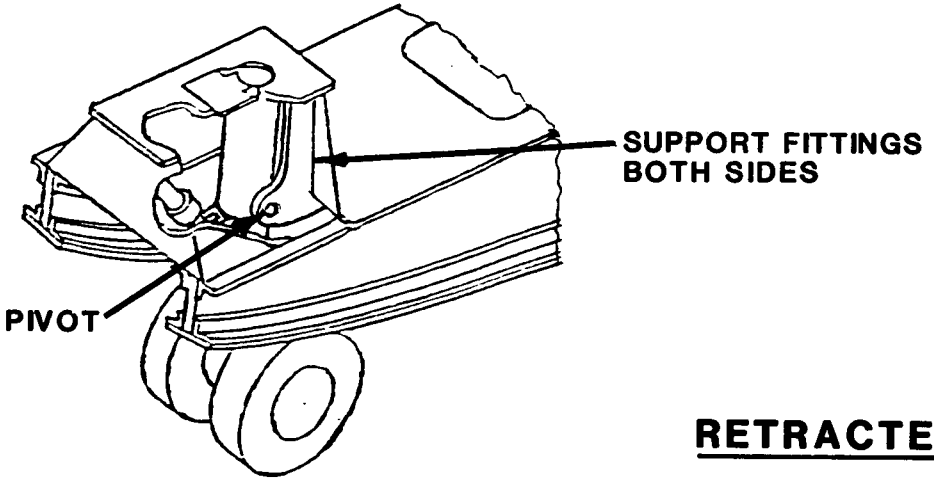

- EXTENDED: LATCH PIN THROUGH STRUCTURE INTO TOP OF STRUT
- RETRACTED: INTERNAL LATCH IN FOLDING ACTUATOR

RETRACTED

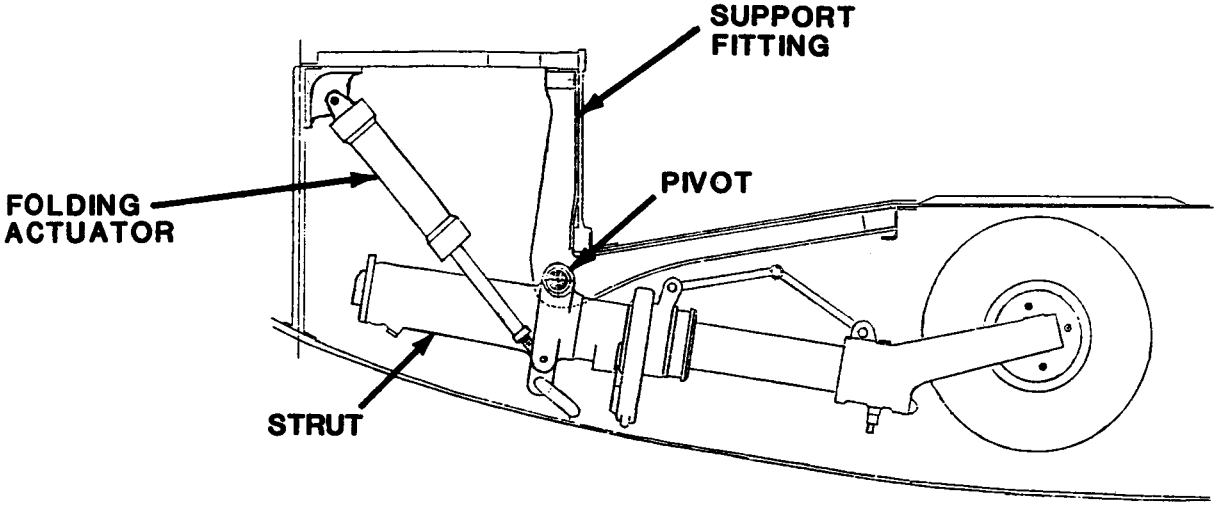

MODEL 360 WEIGHTS SUMMARY

The accompanying tabulation summarizes the weight break down for the aircraft when empty and at the design gross weight.

MODEL 360 WEIGHTS SUMMARY

ITEM	WEIGHT	
	KG	LB
ROTOR GROUP	1448	3192
BODY GROUP	1808	3987
ALIGHTING GEAR	399	881
FLIGHT CONTROLS GROUP	803	1771
ENGINE SECTION	126	277
PROPULSION GROUP (INCL DRIVE SYSTEMS)	2793	6159
AUXILIARY POWER PLANT GROUP	79	174
INSTRUMENTS & NAV GROUP	102	225
HYDRAULICS GROUP	69	152
ELECTRICAL GROUP	268	591
AVIONICS GROUP	237	523
FURNISH. & EQUIP. GROUP	297	654
AIR CONDITIONING	58	128
ANTI-ICING	7	16
AUXILIARY GEAR GROUP	349	769
WEIGHT EMPTY	8843	19499
FIXED USEFUL LOAD	230	508
FUEL	2429	5356
PAYLOAD	2330	5137
DESIGN GROSS WEIGHT	13832	30500

4.0 Modeling Guides

4.1 Static Modeling Guides

PRECEDING PAGE BLANK NOT FILMED

PAGE 44 INTENTIONALLY BLANK

STATIC MODELING GUIDES - SUPPLEMENT BREAKDOWN

The aircraft is divided into five sub-structures or superelements for static modeling. A superelement numbering scheme was employed to facilitate both formulation of the model and possible future superelement-type analyses.

The Model 360 prototype aircraft contains no manufacturing splice joints; therefore, boundaries between superelements can be chosen to minimize the number of common nodes. The five superelements are indicated in the figure and described below:

1.) Forward Fuselage/Cockpit; Station .254 m (10.0 in.) to station 3.55 m (140 in.); this area covers the cockpit, forward rotor transmission and rotor shaft, forward landing gear, cockpit floor pallet, longerons and skin panels. Boundary grids at station 140.

2.) Center Fuselage; Station 3.55 m (140 in.) to station 8.74 m (344 in.); this area includes center section fuselage frames, longerons, skin panels and drive shaft tunnel beams. Boundary grids at station 140 and 344.

3.) Center Fuselage Cabin Floor; Station 3.05 m (120 in.) to station 10.02 m (430 in.); cabin floor including attached auxiliary and main fuel tanks. Boundary grids at the eighth floor isolation points 2 @ frame 160, 2 @ frame 286, 2 @ frame 357 and 2 @ frame 430.

4.) Main Landing Gear; Below water line - .381 m (-15.0 in.) station 8.74 m (344 in.) to station 10.92 m (430 in.); this area includes main landing gear and support structure. Boundary grids at station 344; along water line -15 from station 344 to Sta 430 and at station 430.

5.) AFT Pylon and Fuselage; above water line -.381 m (-15 in.) station 8.74 m (344 in.) to station 10.92 m (430 in.) and station 10.92 m (430 in.) to 13.41 m (528 in.); this area includes aft fuselage frames, skin panels, combiner transmission support beams, engine support structure, engines and aft transmission and rotorshaft. Boundary grids at station 344, along water line -15 from station 344 to station 430 and at station 430.

STATIC MODELING GUIDES
SUPERELEMENT BREAKDOWN

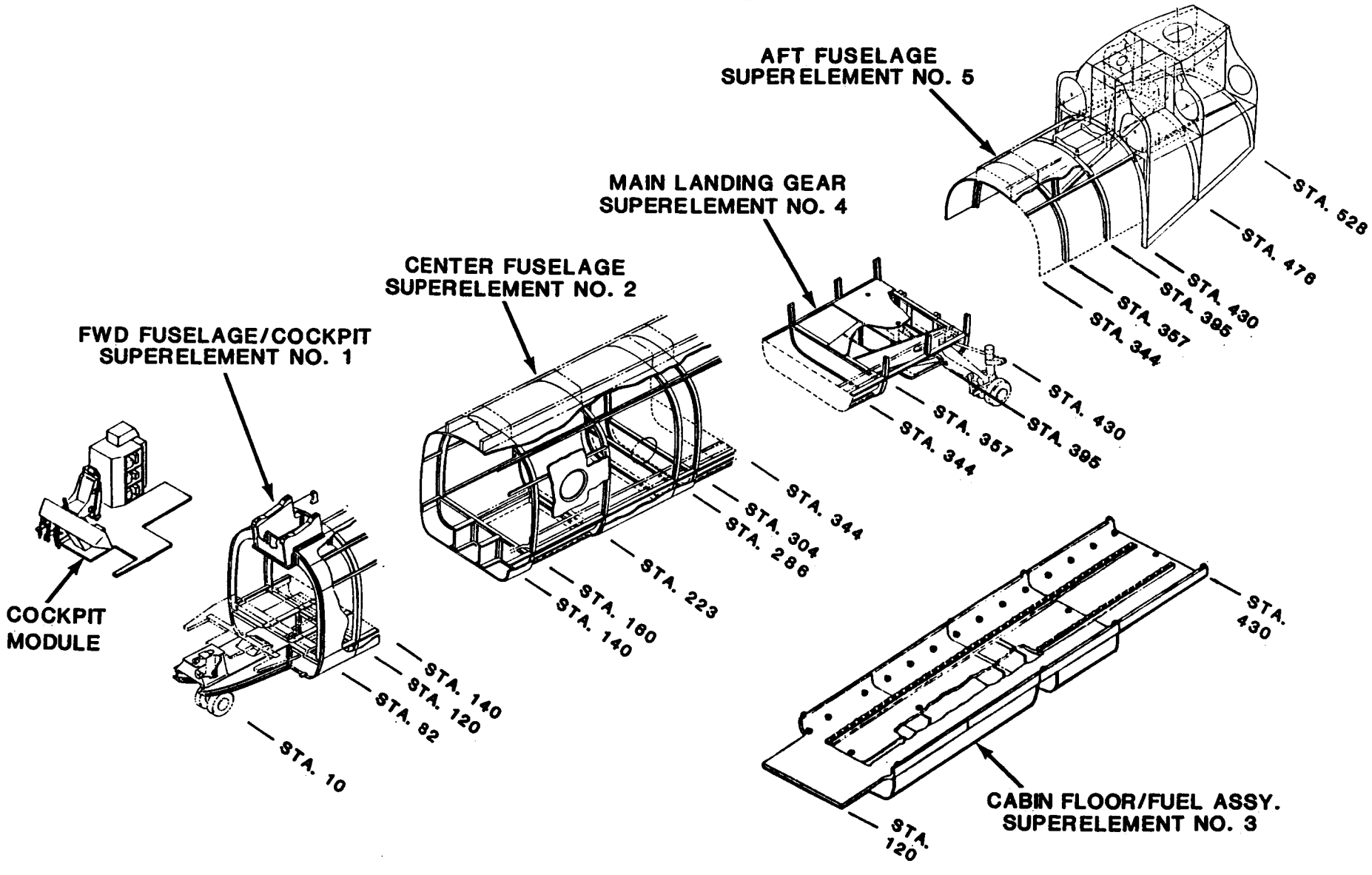

STATIC MODELING GUIDES

NODE AND ELEMENT NUMBERING

A numbering system has been developed to facilitate use of the NASTRAN output and permit automatic node and element generation. The system provides a means of locating the node or element within the model and identifies elements by type. The system is both straightforward and easily applied.

The format for node point identification is $YYYMZ_1Z_2$. Fields (YYY) are the station location and fields (MZ_1Z_2) are the set identification numbers. Field (M) is odd on the right side and even on the left side. Node numbers for canted frames use a station number at approximately the center of the plane defined by the frame.

Element identification is given in an $XYMZ_1Z_2$ format. In this format, field (X) is the superelement number, field (Y) is the element type (CBAR, CONROD, etc) and fields (MZ_1Z_2) are the set identification numbers.

Intentional gaps are provided in the numbering sequence to allow for additional nodes and elements. The numbering sequence always begins and ends at the centerline of the aircraft to aid in automatic model generation. For symmetric portions of the structure, the nodes and elements are established for one side of the aircraft and then mirrored to create a complete model simply by incrementing the code number (M).

STATIC MODELING GUIDES
NODE AND ELEMENT NUMBERING

NODES

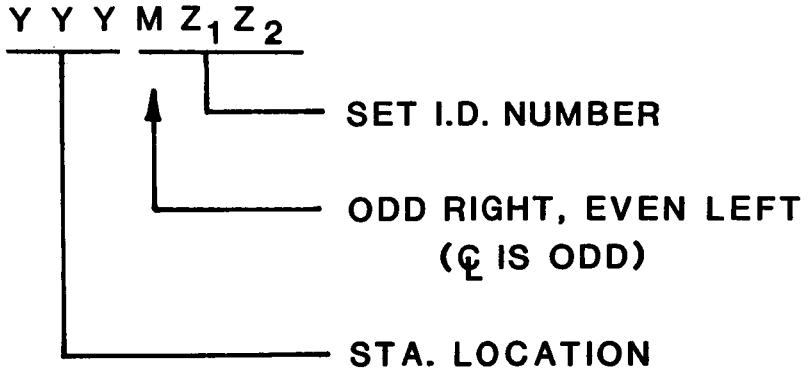

ELEMENTS

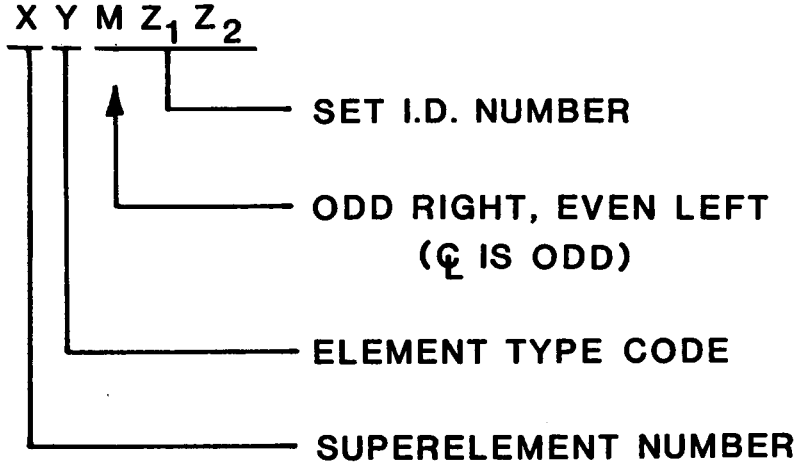

ELEMENT TYPE CODE

3 --- CBAR
4 --- CONROD
5 --- CQUAD4
6 --- CSHEAR
7 --- CTRIA3

STATIC MODELING GUIDES

NODE AND ELEMENT NUMBERING - FRAMES

Specific detail is provided in the accompanying figure to illustrate application of the node and element numbering system to a typical frame.

Six digit node identification numbers of the form $YYYMZ_1Z_2$ are used as described previously. In the illustration, the node numbers all begin with 082 indicating station 82. Looking forward in the aircraft, the right hand side of the frame begins with field (M) as an odd number. Fields (Z_1Z_2), on the outer cap start with 01 at butt line zero on the top of the frame and proceed clockwise to butt line zero on the bottom. Numbers on the inner cap follow the same sequence except the starting value of field (Z_1) is incremented by 5. On the left side of the frame, field (M) is on even numbered and the numbers in fields (Z_1Z_2) proceed in a counter-clockwise direction. Intentional gaps are provided in the sequence to permit insertion of additional nodes.

Element identification in the $XYMZ_1Z_2$ format follows a similar pattern. All the element numbers begin with 1 indicating superelement number one. This is followed by the element type in field (Y). The numbering sequence in fields (MZ_1Z_2) is the same as that used for the node numbers.

STATIC MODELING GUIDES
NODE AND ELEMENT NUMBERING – FRAMES

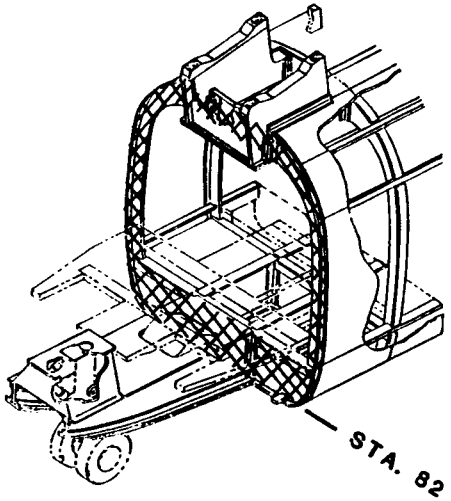

TYPICAL NUMBERING

NODE 082101

- MZ_1Z_2 , SET I.D. NUMBER
- M, ODD RIGHT, EVEN LEFT (℄ IS ODD)
- YYY, STA. LOCATION

ELEMENT 16102

- MZ_1Z_2 , SET I.D. NUMBER
- M, ODD RIGHT, EVEN LEFT (℄ IS ODD)
- Y, ELEMENT TYPE
- X, SUPERELEMENT I.D.

ELEMENT TYPE CODE (Y)

(3) CBAR	(6) CSHEAR
(4) CONROD	(7) CTRIA3
(5) CQUAD4	

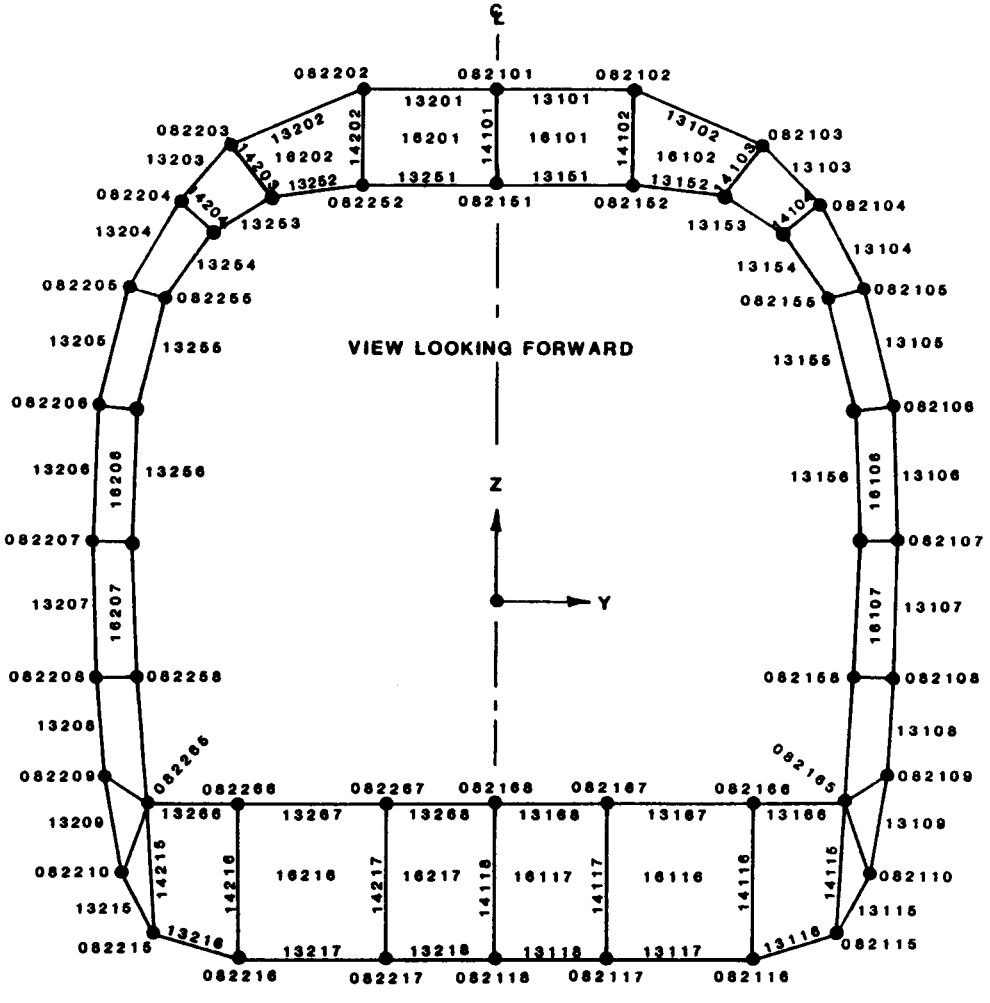

STATION 82 FRAME *

*** SOME NODE AND ELEMENT NUMBERS OMITTED FOR CLARITY**

STATIC MODELING GUIDES

NODE AND ELEMENT NUMBERING - OUTER SHELL

This figure illustrates the application of the node and element numbering system to a portion of the outer shell in superelement two.

The node numbering procedure here is identical to that used for the frames. The right side (odd) and left side (even) series start at the top centerline and proceed in opposite directions around the outer surface. At the frame stations, the nodes correspond to those on the frame outer cap.

Element numbering follows the same general procedure with one exception. Proceeding from forward to aft, each panel bay is incremented by 2 in field (Z_1). Where the length of the superelement is such that there are more than five bays, field (M) is incremented by 2 and the sequence in fields (Z_1Z_2) is repeated.

STATIC MODELING GUIDES
NODE AND ELEMENT NUMBERING - OUTER SHELL

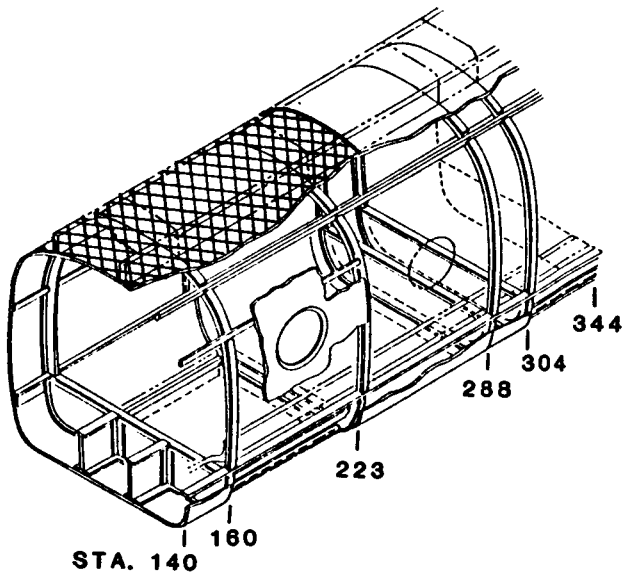

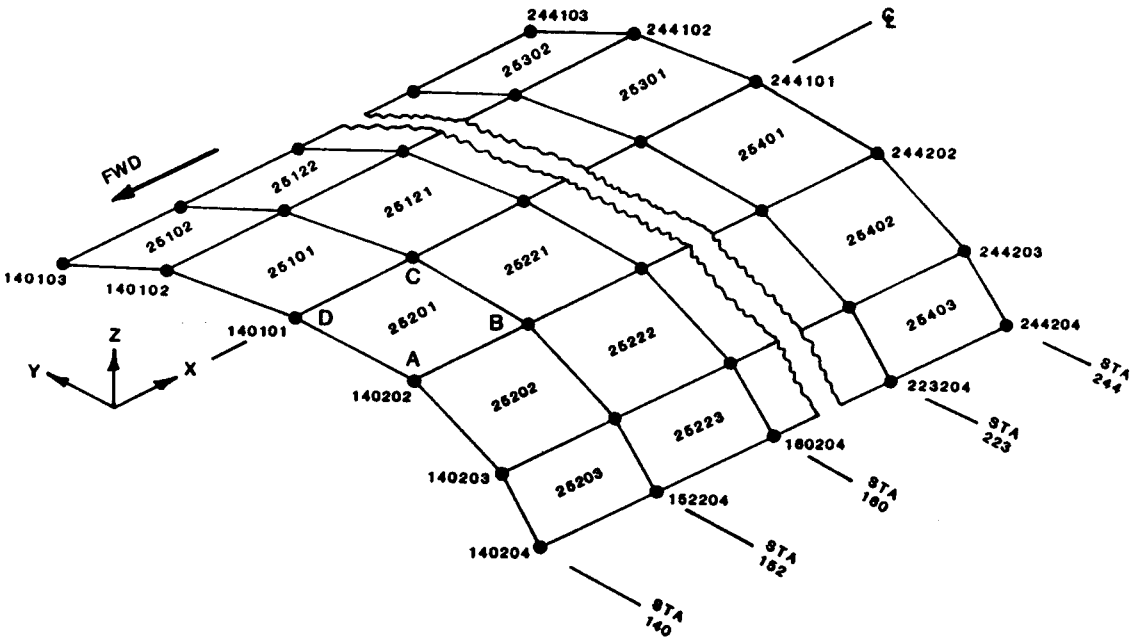

CROWN SKIN STA. 140 TO 244*

TYPICAL NUMBERING

NODE 082101

- MZ_1Z_2 . SET I.D. NUMBER
- M, ODD RIGHT, EVEN LEFT (℄ IS ODD)
- YYY, STA. LOCATION

ELEMENT 16102

- MZ_1Z_2 . SET I.D. NUMBER
- M, ODD RIGHT, EVEN LEFT (℄ IS ODD)
- Y, ELEMENT TYPE
- X, SUPERELEMENT I.D.

ELEMENT TYPE CODE (Y)

(3) CBAR	(6) CSHEAR
(4) CONROD	(7) CTRIA3
(5) CQUAD4	

* SOME NODE AND ELEMENT NUMBERS OMITTED FOR CLARITY

STATIC MODELING GUIDES

NODE AND ELEMENT NUMBERING - FLOORS AND DECKS

In the figure, the use of the node and element numbering system for typical floor and deck structure is shown. The deck shown in the illustration is part of the main landing gear support structure in superelement four.

The node numbering procedure here follows logically from those previously shown. The right side (odd) and left side (even) series start at butt line zero and proceed outboard in opposite directions. If the floor or deck has more than one element thickness, the series continues around to the lower surface in exactly the same manner as a frame.

In each panel bay, numbering of the deck planar elements proceeds from inboard to outboard. Forward to aft, the procedures is the same as that described for the outer shell. The numbering sequence for longitudinal axial elements (longitudinal caps in the illustration) proceeds from forward to aft. Where there is more than one axial element, an inboard to outboard sequence is also established by incrementing either field (M), (Z_1) or both (note that both possibilities are illustrated).

STATIC MODELING GUIDES
NODE AND ELEMENT NUMBERING - FLOORS AND DECKS

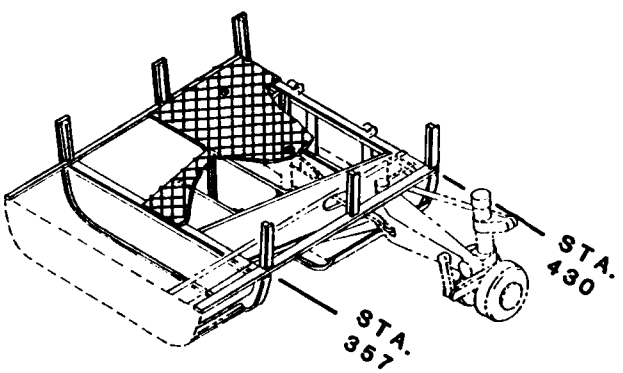

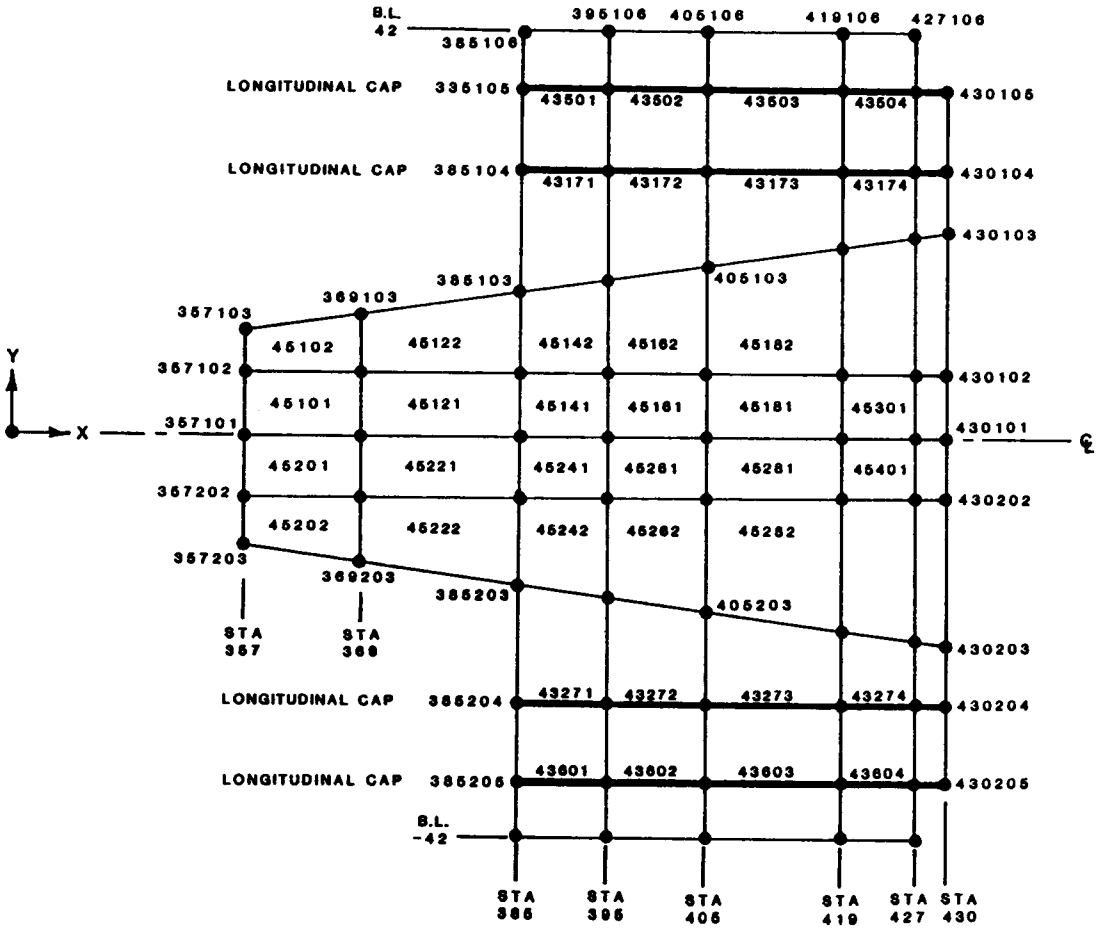

TYPICAL NUMBERING

NODE 082101
- MZ_1Z_2 , SET I.D. NUMBER
- M, ODD RIGHT, EVEN LEFT (℄ IS ODD)
- YYY, STA. LOCATION

ELEMENT 16102
- MZ_1Z_2 , SET I.D. NUMBER
- M, ODD RIGHT, EVEN LEFT (℄ IS ODD)
- Y, ELEMENT TYPE
- X, SUPERELEMENT I.D.

ELEMENT TYPE CODE (Y)

(3) CBAR	(6) CSHEAR
(4) CONROD	(7) CTRIA3
(5) CQUAD4	

MAIN LANDING GEAR DECK *

*** SOME NODE AND ELEMENT NUMBERS OMITTED FOR CLARITY**

STATIC MODELING GUIDES

NODE AND ELEMENT NUMBERING - BULKHEADS

The accompanying figure illustrates the use of the node and element numbering system for a typical bulkhead. The station 120 bulkhead shown is part of the forward fuselage/cockpit superelement (superelement one).

Node numbering on the outer mold line follows the same convention used for frames. Interior node numbers begin at the top centerline and proceed inboard to outboard and top to bottom with the odd series on the right and the even series on the left. Element numbering follows the same procedure.

STATIC MODELING GUIDES

NODE AND ELEMENT NUMBERING – BULKHEADS

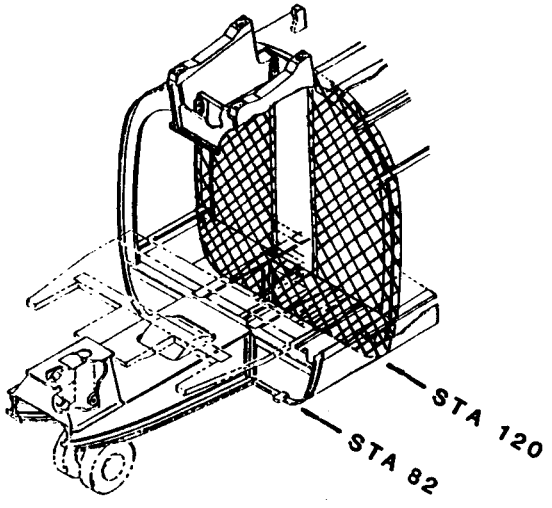

TYPICAL NUMBERING

NODE 0 8 2 1 0 1

- MZ_1Z_2 , SET I.D. NUMBER
- M, ODD RIGHT, EVEN LEFT (℄ IS ODD)
- YYY, STA. LOCATION

ELEMENT 1 6 1 0 2

- MZ_1Z_2 , SET I.D. NUMBER
- M, ODD RIGHT, EVEN LEFT (℄ IS ODD)
- Y, ELEMENT TYPE
- X, SUPERELEMENT I.D.

ELEMENT TYPE CODE (Y)

(3) CBAR	(6) CSHEAR
(4) CONROD	(7) CTRIA3
(5) CQUAD4	

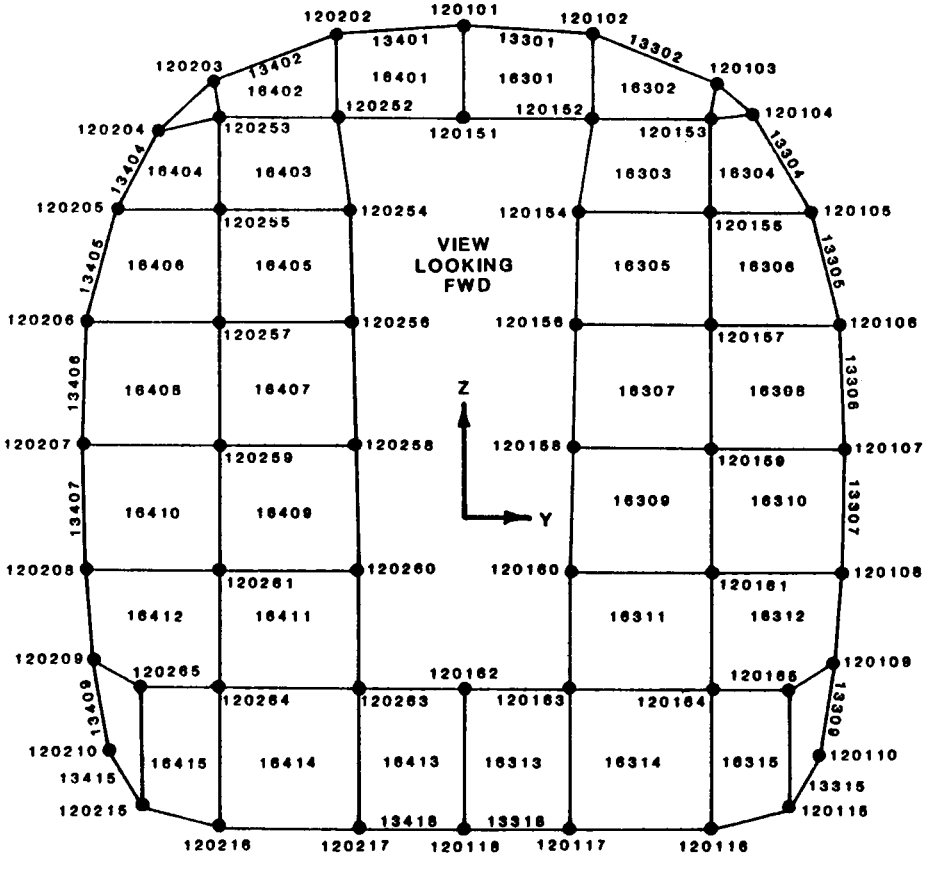

STATION 120 BULKHEAD*

*SOME NODE AND ELEMENT NUMBERS OMITTED FOR CLARITY

STATIC MODELING GUIDES

PLANNING PHASE MODEL 360 NASTRAN STRUCTURAL MODEL

For purposes of illustration, the accompanying figure shows an earlier NASTRAN model of the Boeing Model 360 helicopter airframe. All nodes are shown and members connecting nodes are indicated. This figure does not, however, indicate the types of structural elements connected to nodes.

This picture of the NASTRAN model, and similar pictures of portions of the model, help in checking the model to insure that elements are properly connected and that grid point coordinates are reasonably correct.

STATIC MODELING GUIDES

PLANNING PHASE MODEL 360 NASTRAN STRUCTURAL MODEL

1347 STRUCTURAL NODES
2989 STRUCTURAL ELEMENTS

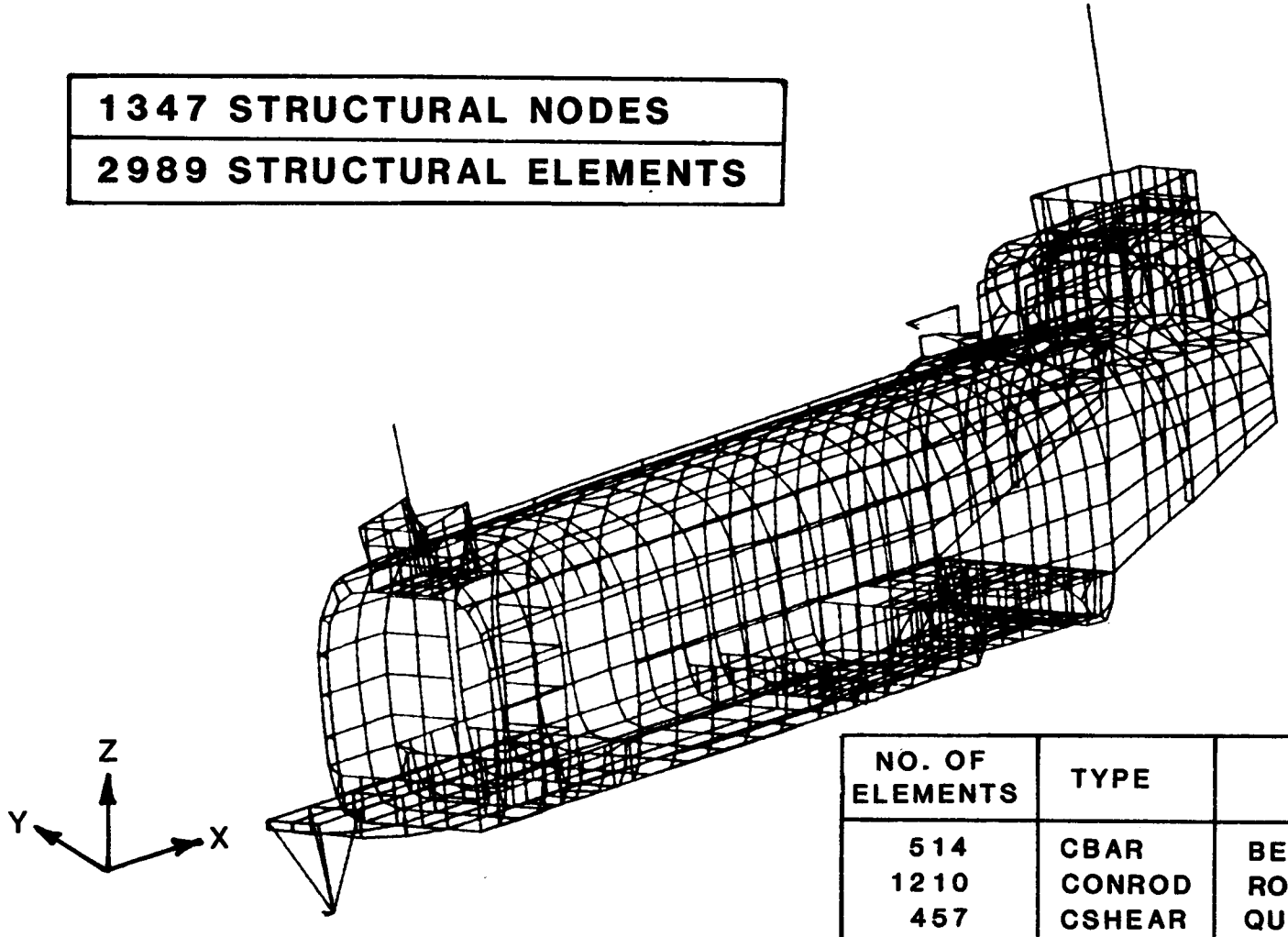

NO. OF ELEMENTS	TYPE	DESCRIPTION
514	CBAR	BEAM
1210	CONROD	ROD
457	CSHEAR	QUADRILATERAL SHEAR
758	CQUAD4	QUADRILATERAL PLATE
50	CTRIA3	TRIANGULAR PLATE

STATIC MODELING GUIDES

STRUCTURE NOT MODELED

Items not to be modeled as structure include:

1.) drive shaft tunnel covers
2.) nose enclosure
3.) forward transmission fairing
4.) cabin door, escape hatch and windows
5.) aft pylon fairings
6.) tail cone
7.) aft cargo ramp
8.) landing gear compartment doors
9.) cargo hatches
10.) engine access panels
11.) drive shafting (except forward and aft rotor shafts)
12.) fittings (except for those in the rotor to airframe and primary airframe load paths)
13.) rotor systems

STATIC MODELING GUIDES
STRUCTURE NOT MODELED

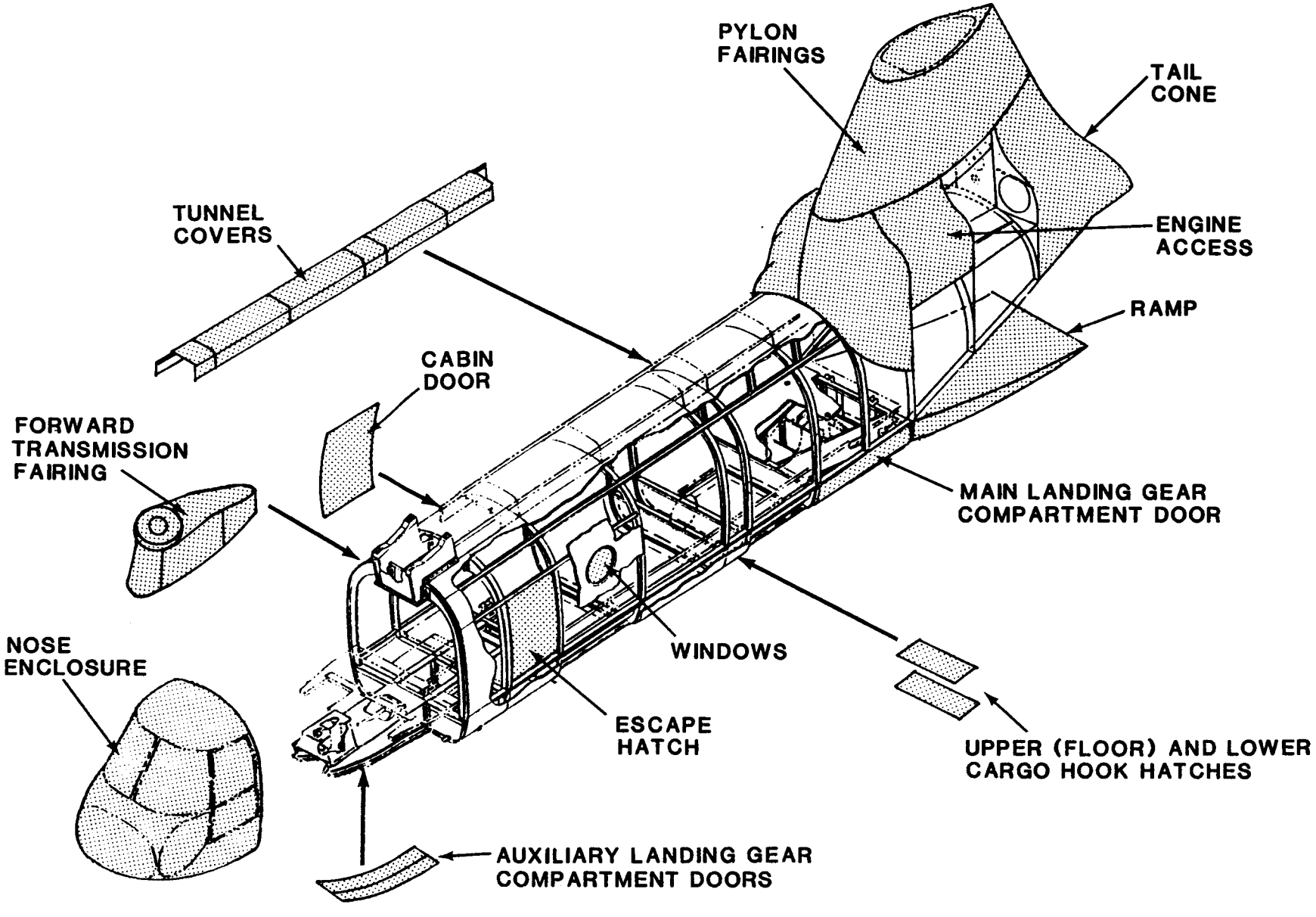

STATIC MODELING GUIDES

COMPOSITE MATERIAL APPLICATIONS

All primary and secondary structure in the Model 360 helicopter is fabricated from laminated composite materials except the landing gear oleos and the main landing gear drag beams, drag links, and stabilizer bars. Kevlar is used over a nomex core in skin panels while glass is used over a nomex core in floor panels. Mixed modulus materials which consist of a combination of glass and graphite are used in frame caps, webs, most fittings and much of the structure in the pylons. The figure shows the approximate distributions of the various materials throughout the aircraft.

STATIC MODELING GUIDES
COMPOSITE MATERIAL APPLICATIONS

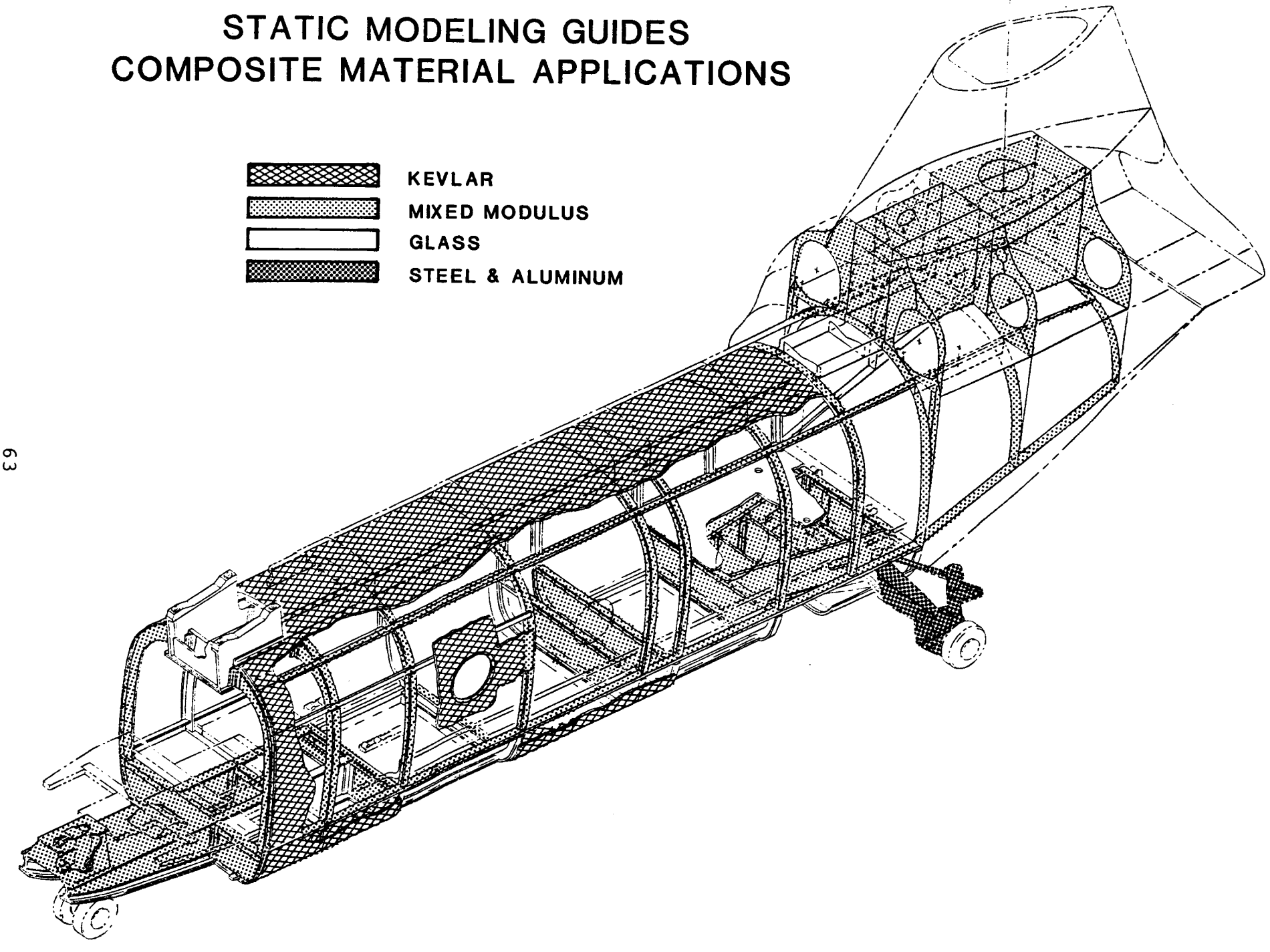

STATIC MODELING GUIDES

SUMMARY OF SIGNIFICANT GROUND RULES

Significant ground rules for static modeling are summarized in the accompanying figure and discussed below.

1) CBARS with low bending stiffness are used extensively in lieu of CONRODS to eliminate the need to specify SPC's which can cause inadvertent ties to ground. Boeing studies show that CBARS substituted for CONRODS lead to low inplane bending and torsion loads and nearly identical axial loads.

2) Static analysis of composite materials in NASTRAN produces loads for individual lamina, which results in excessive output. As an alternative, overall laminate properties are input to NASTRAN. A detailed lamina stress analysis, based on NASTRAN results, is performed outside of NASTRAN and only for critical areas.

3) Honeycomb sandwich floor and outer skin panels are modeled with flat plate elements carrying shear, bending and inplane loads.

4) Modeling of frames considers only inplane stiffness.

5) Longerons carry axial load only; however, CBARS with low bending stiffness are used for modeling. This will permit evaluation of shear effects if desired.

6) Isolator static stiffness values are used between the isolated floors and the airframe. This model is correct only for static loads analysis. Because the isolators are mass tuned, the tuning weights and associated linkages are required for dynamic analysis.

7. The concept of "effective skins" is not employed in the modeling. This is implicit in the use of QUAD4 skin elements.

STATIC MODELING GUIDES
SUMMARY OF SIGNIFICANT GROUND RULES

- CBARS WITH LOW BENDING STIFFNESS USED IN PLACE OF CONRODS TO ELIMINATE SPEC'S.
- OVERALL LAMINATE PROPERTIES CALCULATED AND INPUT TO NASTRAN. LAMINA ANALYSIS IN NASTRAN PRODUCES EXCESSIVE OUTPUT.
- HONEYCOMB SANDWICH FLOOR AND SKIN PANELS CARRY SHEAR, BENDING AND END LOAD.
- FRAME MODELING CONSIDERS ONLY INPLANE STIFFNESS.
- LONGERONS CARRY ONLY AXIAL LOAD. CBARS WITH LOW BENDING STIFFNESS USED TO PERMIT LATER EVALUATION OF SHEAR EFFECTS.
- CABIN AND COCKPIT FLOOR TIED TO AIRFRAME USING ISOLATOR STATIC STIFFNESS. TUNING WEIGHT AND ASSOCIATED LINKAGE OMITTED.
- THE CONCEPT OF "EFFECTIVE SKIN" IS NOT EMPLOYED IN THE MODELING.

STATIC MODELING GUIDES

COMPOSITE LAMINATE PROPERTIES - ANALYSIS METHOD

In general, composite laminates consist of a combination of nonisotropic materials of different types or many plies of the same material at different layup angles. As stated previously, static analysis with composite materials can be performed within NASTRAN. However, individual lamina loads are calculated for every element resulting in excessive output. As an alternative, overall laminate properties can be input to NASTRAN. Then, a detailed stress analysis, based on NASTRAN element loads, can be performed outside of NASTRAN. This external analysis can be limited to examination of only critical areas.

At Boeing, a laminate analysis program called "COMPLY", for Composite Ply analysis, is used to obtain the overall laminate properties. Program inputs, consisting of the material properties and geometry of the individual lamina, are used to form the stiffness matrix in terms of the component [A], [B] and [D] matrices where [A] is the extensional stiffness, [B] the coupling stiffness and [D] the bending stiffness. Overall laminate properties in the COMPLY program are obtained from the inverse of the [A] matrix. For a symmetric laminate, the [B] matrix is zero and the properties may be obtained from the inverse of the [A] matrix alone. In the case of an asymmetric laminate, the inverse of the full matrix is required and the properties are obtained from the [A] portion of the inverted matrix. The inverted [A] matrix is used since the diagonal terms are of the form 1/Et which provides the desired modulus values directly. Diagonal terms of the [A] matrix, on the other hand, involve Nu which is also unknown.

The COMPLY program also has the capability of performing lamina stress and/or strain analysis and can be used for post-processing of NASTRAN calculated element loads. In this application, COMPLY reduces the NASTRAN loads to element stresses or strains which may be searched so that only the most critical need be examined.

STATIC MODELING GUIDES
COMPOSITE LAMINATE PROPERTIES - ANALYSIS METHOD

INPUT TO COMPLY PROGRAM

STIFFNESS:

- MATERIAL PROPERTIES
  - E, G, Nu
- GEOMETRY
  - PLY THICKNESS (t) AND FIBER ORIENTATION

LOAD ANALYSIS:

- MATERIAL STRESS/STRAIN ALLOWABLES
  - TENSION, COMPRESSION AND SHEAR
- LOADS, USER SUPPLIED OR NASTRAN

CALCULATE

STIFFNESS MATRIX $[K] = \left[\begin{array}{c|c} A & B \\ \hline B & D \end{array}\right]$

WHERE:

[A] IS EXTENSIONAL STIFFNESS

[B] IS COUPLING STIFFNESS

[D] IS BENDING STIFFNESS

OUTPUT

STIFFNESS:

- $[K]$, $[K]^{-1}$ -- STIFFNESS MATRIX AND INVERSE
- E_X -- MODULUS OF ELASTICITY, X-DIRECTION
- E_Y -- MODULUS OF ELASTICITY, Y-DIRECTION
- G_{XY} -- SHEAR MODULUS
- Nu_{XY} -- POISSON'S RATIO
- $[A]\{1/t\}$ -- [A] MATRIX DIVIDED BY THICKNESS

LOADS:

- LAMINA STRESSES/STRAINS AND MARGINS IN THE LOAD AND FIBER DIRECTIONS

ACKNOWLEDGEMENT:

THE AUTHORS WISH TO ACKNOWLEDGE THAT THE FORMULATION AND CODING OF THE COMPLY PROGRAM IS ATTRIBUTABLE TO THE PERSONAL EFFORTS OF MR. HARLEY COLLINS.

STATIC MODELING GUIDES

COMPOSITE LAMINATE PROPERTIES - SAMPLE ANALYSIS INPUT

Figure A below shows a hypothetical laminate containing Kevlar (Ply #1 and #5), unidirectional graphite (ply #2 and #4) and woven graphite (ply #3). Using COMPLY, the user inputs the values of the material properties and the corresponding allowables for tension, compression and shear (Figure B). Next the ply number, material number, its orientation angle, and thickness are input (Figure C). The orientation angle is referenced to the X and Y direction of the laminate. Typically, groups of plies of the same material and same angle are lumped together as one ply, here shown as ply three. (Note that the angle is zero for ply three. Since it is a woven fabric with fibers at ±45° in each of the 3 plies, the properties are known and input directly.)

STATIC MODELING GUIDES

COMPOSITE LAMINATE PROPERTIES - SAMPLE ANALYSIS INPUT

PLY NO.	MATERIAL NO.	MATERIAL	THICKNESS
1	1	1-PLY KEVLAR	t = .0055
2	2	1-PLY UNIGRAPHITE	t = .0055
3	3	3-PLIES $\pm 45^{o}$ WOVEN GRAPHITE	t = .0155
4	2	1-PLY UNIGRAPHITE	t = .0055
5	1	1-PLY KEVLAR	t = .0055

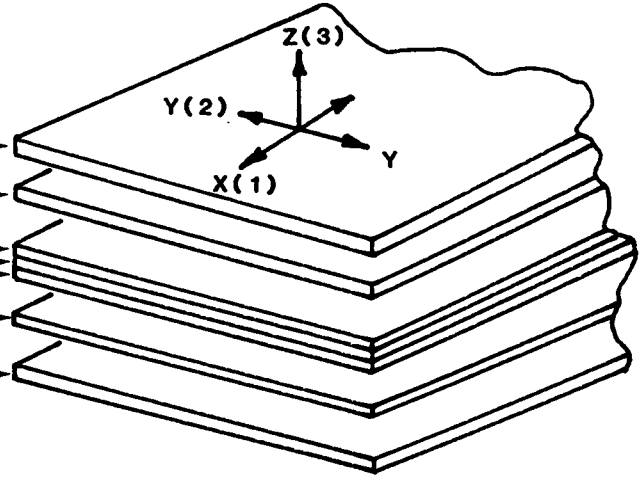

FIGURE (A) HYPOTHETICAL MIXED MODULUS LAMINATE

Material Properties	Mat 1	Mat 2	Mat 3
E1	8,000,000	12,000,000	9,000,000
E2	4,000,000	8,000,000	1,400,000
G12	1,000,000	2,000,000	980,000
NU12 (POISSON'S RATIO)	0.3000	0.2500	0.3100
Stress Allowables			
F1 tension	50,000	90,000	42,000
F1 compression	25,000	45,000	50,000
F2 tension	6,000	45,000	23,000
F2 compression	4,000	36,000	12,000
F12 shear	6,400	5,000	4,600

FIGURE (B) LAMINA PROPERTIES

Ply	Mat.No.	Angle	t	
1	1	0.0	0.0055	
2	2	0.0	0.0055	
3	3	0.0	0.0155	
4	2	0.0	0.0055	
5	1	0.0	0.0055	Total t = 0.0375

FIGURE (C) LAMINA STACKING SEQUENCE

STATIC MODELING GUIDES

COMPOSITE ANALYSIS PROPERTIES - SAMPLE ANALYSIS OUTPUT

MAT1 CARD

Continuing with the example from the previous page, COMPLY uses classical laminate theory to calculate the stiffness matrix, the inverse of the stiffness matrix and subsequently the overall laminate properties E_x (elasticity in the material x-direction), E_y (elasticity in the material y-direction), G_{xy} (the shear modulus) and Poisson's ratio Nu_{xy}. The modulus values are obtained from the diagonal terms of the inverse [A] matrix which are of the form 1/Et, where t is the total laminate thickness.

The overall laminate properties are those used for elements such as CBARS input to NASTRAN on a MAT1 card. Note that the modulus of elasticity in only one direction can be input (E_x in the example). If bending in two planes is required, the moment of inertia in the second plane must be adjusted to account for the lower value of E_y.

STATIC MODELING GUIDES

COMPOSITE LAMINATE PROPERTIES - SAMPLE ANALYSIS OUTPUT

MAT1 CARD

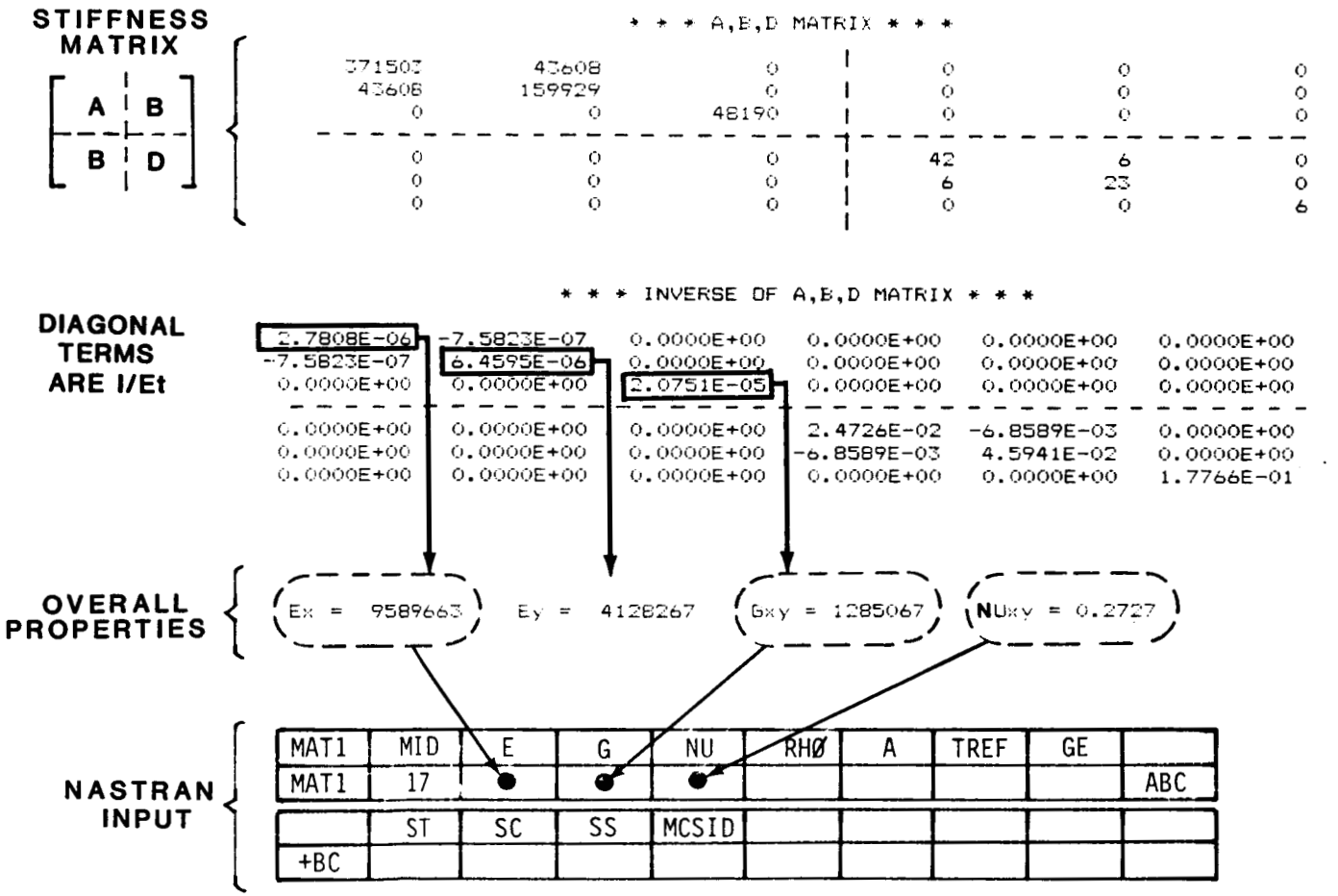

STATIC MODELING GUIDES

COMPOSITE LAMINATE PROPERTIES - SAMPLE ANALYSIS OUTPUT

MAT2 CARD

Material properties for plate elements are input on a MAT2 card which permits specification of nonisotropic properties in the form of the [G] matrix whose terms are of the form E_{ij}. Since the [A] matrix has terms of the form tE_{ij}, the [A/t] matrix in the COMPLY output is term for term the same as the [G] matrix input on the MAT2 card.

STATIC MODELING GUIDES

COMPOSITE LAMINATE PROPERTIES - SAMPLE ANALYSIS OUTPUT

MAT2 CARD

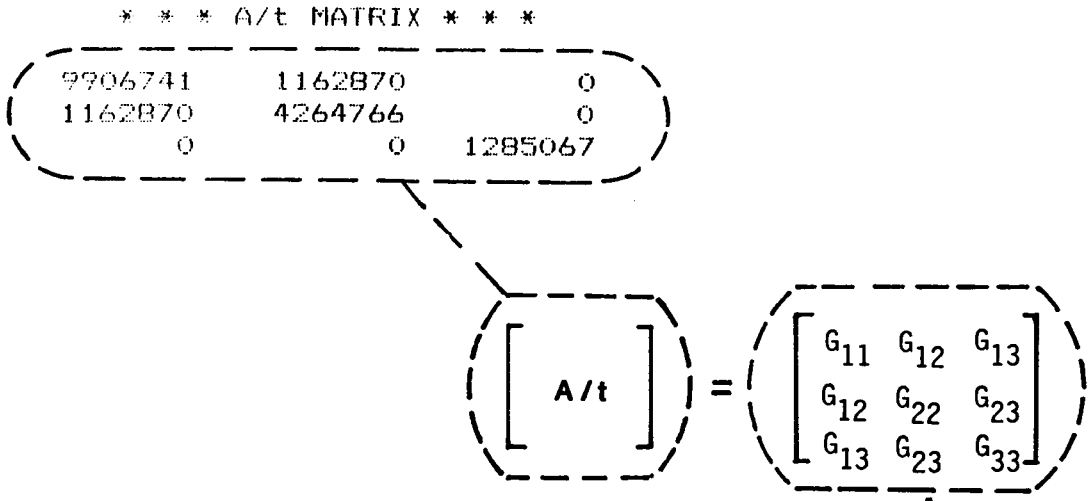

NASTRAN INPUT

MAT2	MID	G11	G12	G13	G22	G23	G33	RHØ	
MAT2	13								ABC
	A1	A2	A12	TO	GE	ST	SC	SS	
+BC									DEF
	MCSID								
+DE	1003								

COMPOSITE LAMINATE PROPERTIES - INPUT TO NASTRAN

In the case of two-dimensional elements employing a MAT1 card, NASTRAN requires values for only two of the three parameters E, G and Nu. When only two are specified, the third is calculated based on isotropic theory. If all three are specified, and the values are not consistent with isotropic theory, all three will be used in ways which may not be consistent with the user's intentions. As will be shown in the following discussion, all three values are not required for two-dimensional elements. Since composite laminates are in general nonisotropic, the usual practice is to supply only the values needed for the particular element being used.

For CBAR elements only E and G are necessary. The stiffness matrix describing bending of a bar element involves only E and the constant R. Notice that the calculation for R does not contain Nu. It does, however, contain E and G and only these are input, leaving NASTRAN to calculate its own bogus isotropic Nu which is not used. Identical reasoning applies for rod elements.

For CSHEAR elements only G and Nu from COMPLY are input. NASTRAN uses the strain energy of Equation 1 to relate motions of the corners and Equation 2 to derive the stiffness matrix $[K_{ee}]$. The constant ½ in Equation 3 is used in Equation 1 which contains only G and Nu but not E.

For CQUAD4 elements, a MAT2 card can be used to specify true nonisotropic properties such as those found in composite laminates.

STATIC MODELING GUIDES

COMPOSITE LAMINATE PROPERTIES - INPUT TO NASTRAN

- FOR 2-DIMENSIONAL ELEMENTS USING A MAT1 CARD, ONLY REQUIRED VALUES OF E, G AND Nu ARE INPUT. IF THREE VALUES NOT CONSISTENT WITH ISOTROPIC THEORY ARE SPECIFIED, NASTRAN MAY USE THE VALUES INCORRECTLY.

- CBAR REQUIRES ONLY E AND G.

$$\begin{Bmatrix} F_{za} \\ M_{ya} \\ F_{zb} \\ M_{yb} \end{Bmatrix} = \begin{bmatrix} R & -\frac{\ell}{2}R & -R & -\frac{\ell}{2}R \\ & \frac{\ell^2}{4}R + \frac{EI_y}{\ell} & \frac{\ell}{2}R & \frac{\ell^2}{4}R - \frac{EI_y}{\ell} \\ & & R & \frac{\ell}{2}R \\ \text{SYMMETRICAL} & & & \frac{\ell^2}{4}R + \frac{EI_y}{\ell} \end{bmatrix} \begin{Bmatrix} U_{za} \\ \theta_{ya} \\ U_{zb} \\ \theta_{yb} \end{Bmatrix}$$

STIFFNESS MATRIX

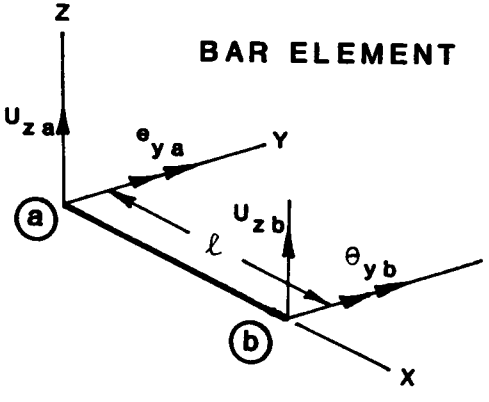

WHERE: $R = \left(\frac{\ell}{K_z AG} + \frac{\ell^3}{12 EI_y} \right)^{-1}$

- CSHEAR REQUIRES ONLY G AND Nu.

$$E = \frac{1}{2} z q_1^2 \qquad \text{STRAIN ENERGY (EQ. 1)}$$

$$E = \frac{1}{2} \{u_e\}^T [K_{ee}] \{u_e\} \qquad \text{STIFFNESS MATRIX (EQ. 2)}$$

WHERE: $z = \frac{A}{Gt} \left(1 + \frac{2 \tan^2 \theta}{1 + Nu} \right)$ (EQ. 3)

- CQUAD4 NONISOTROPIC PROPERTIES INPUT ON MAT2 CARD.

STATIC MODELING GUIDES - FRAMES

The figure shows a cabin frame and the corresponding finite element model. Frames are modeled to represent the inplane bending stiffness only. General assumptions and methods to be followed are listed below.

ASSUMPTIONS

- The caps are assumed to carry only axial loads and are represented by CBAR elements with low bending stiffness.
- The webs are assumed to carry only shear loads and are represented by CSHEAR elements.

METHODS

- Outer nodes are located at the skin line (outer mold line) and inner nodes are located at the inner mold line.
- The element representing the honeycomb sandwich web of the frame is based on the thickness of the two faceplates. The core is not modeled.
- No skin area is lumped with the cap area.
- If a cap is tapered between nodes, the average cap area is used.
- Cap areas are not reduced for local notches.
- Web holes and stiffeners are ignored.
- CONROD elements are placed between CSHEAR elements as panel breakers to maintain the aspect ratio near one. Typically, a rod area (A) of .001 is used and the modulus (E) is assumed to be the same as the shear element.

STATIC MODELING GUIDES - FRAMES

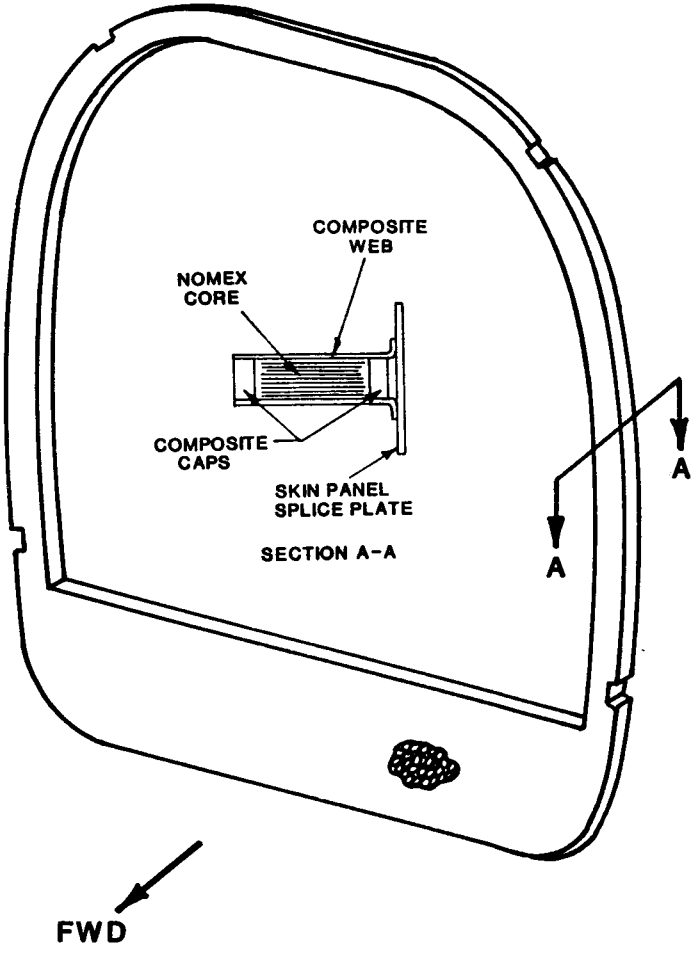

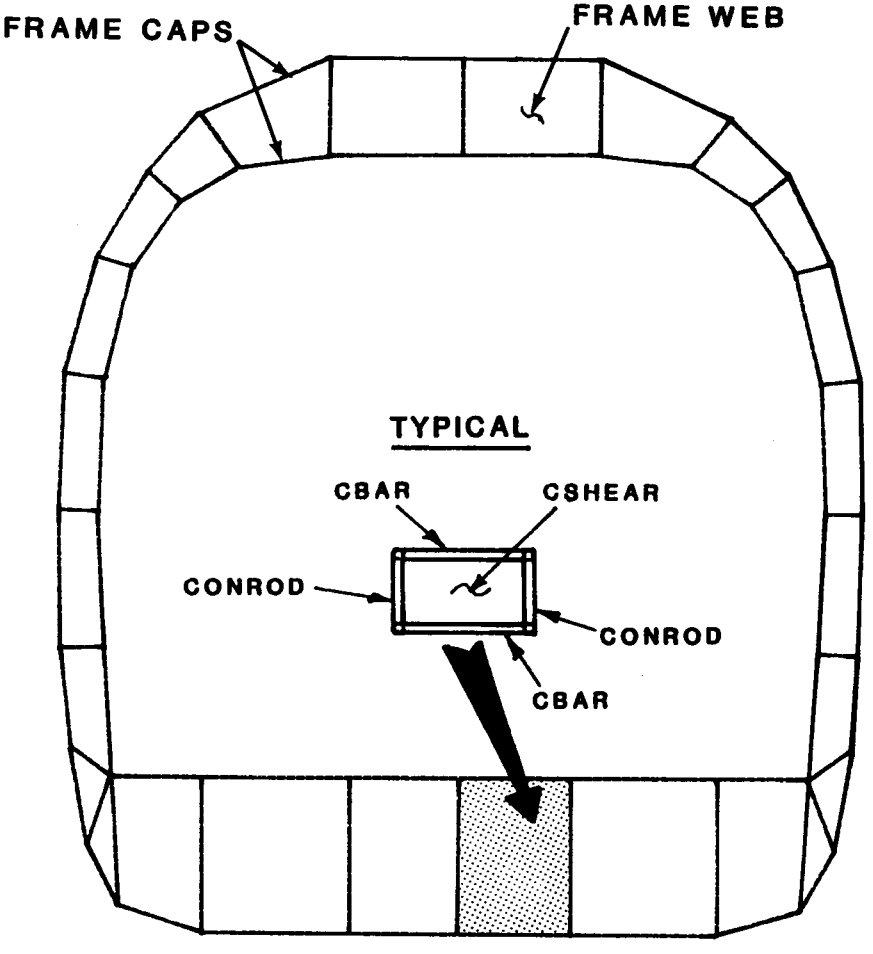

STRUCTURAL COMPONENT	TYPE OF LOADING	ELEMENT TYPE
CAPS	AXIAL	CBAR
WEBS	SHEAR	CSHEAR

STATIC MODELING GUIDES

AREAS FOR EQUIVALENT FRAME STIFFNESS

One of the more time consuming tasks involved in the modeling of frames is the calculation of equivalent frame stiffness properties. Outer node points on the frame must be located at the skin line, while inner node points are most conveniently located at the edge of the inner cap. Typically, the centroids of the cap areas do not correspond to the desired grid point locations. Therefore, equivalent cap areas at the node points which provide the correct frame bending stiffness must be determined. As indicated in the figure, the calculation is quite simple; however, a typical frame requires the calculation of equivalent inner and outer cap areas at approximately 25 locations (50 equivalent areas/frame).

STATIC MODELING GUIDES
AREAS FOR EQUIVALENT FRAME STIFFNESS

REAL FRAME CROSS SECTION

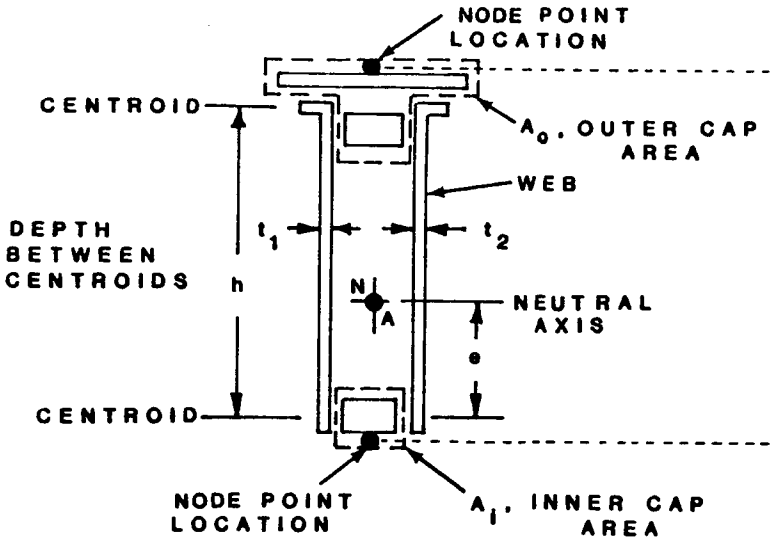

NASTRAN FRAME CROSS SECTION MODEL

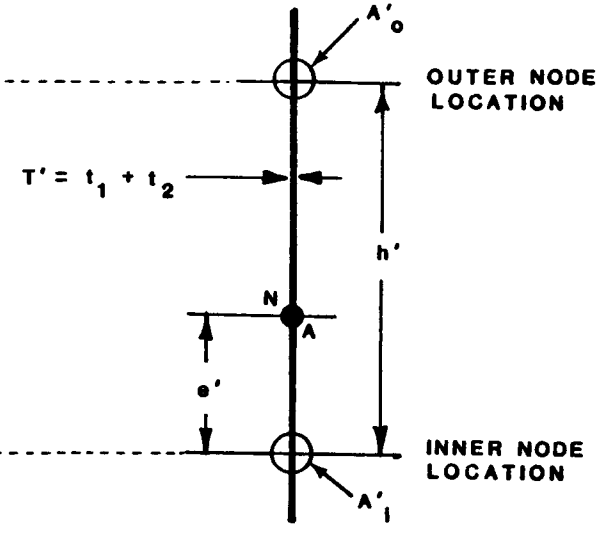

$$e = \frac{A_o h}{A_o + A_i}$$

$$I_{N/A} = A_o (h-e)^2 + A_i e^2$$

INERTIA ABOUT NEUTRAL AXIS

$$e' = \frac{A'_o h'}{A'_o + A'_i} \quad \text{AND} \quad I_{N/A} = A'_o (h'-e')^2 + A'_i e'^2$$

$$A'_o = \left(\frac{h}{h'}\right)^2 A_o \quad \text{AND} \quad A'_i = \left(\frac{h}{h'}\right)^2 A_i$$

AREAS FOR EQUIVELANT STIFFNESS

$$e' = \frac{A_o h'}{A'_o + A'_i} = \frac{h'e}{h} \quad \text{AND}$$

$$I_{N/A} = \left(\frac{h}{h'}\right)^2 A_o \left(h' - \frac{h'e}{h}\right)^2 + \left(\frac{h}{h'}\right)^2 A_i \left(\frac{h'}{h}\right)^2 e^2 = A_o (h-e)^2 + A_i e^2$$

SAME AS REAL FRAME

STATIC MODELING GUIDES

HONEYCOMB SANDWICH STRUCTURE

Honeycomb sandwich panels are the most widely used type of structure in the Model 360. Honeycomb structures include bulkheads, butt-line beams, decks, floors and outer skin panels. These members are made of laminated composite skins or webs over a nomex honeycomb core. Generally, caps are located at edges and often buried in the panel. For purposes of analysis, honeycomb structures are divided into two categories: (1) those treated as shear panels, which includes all applications except the floors and skin panels and (2) those treated as plate elements with membrane and out-of-plane bending stiffness.

Material properties of the cap areas, E and G, are calculated from the individual plies using the COMPLY program as previously described.

In the case of most shear panels, the web is generally made up of a single material with known material properties (G and Nu) and use of the COMPLY program is not necessary. Total thickness is the sum of the two faceplates.

Material properties of plate elements are calculated using the total core thickness plus the two faceplates. Near zero stiffness values are used for the core so that it only affects the total laminate thickness.

STATIC MODELING GUIDES
HONEYCOMB SANDWICH STRUCTURE

SANDWICH PANEL EXPLODED VIEW

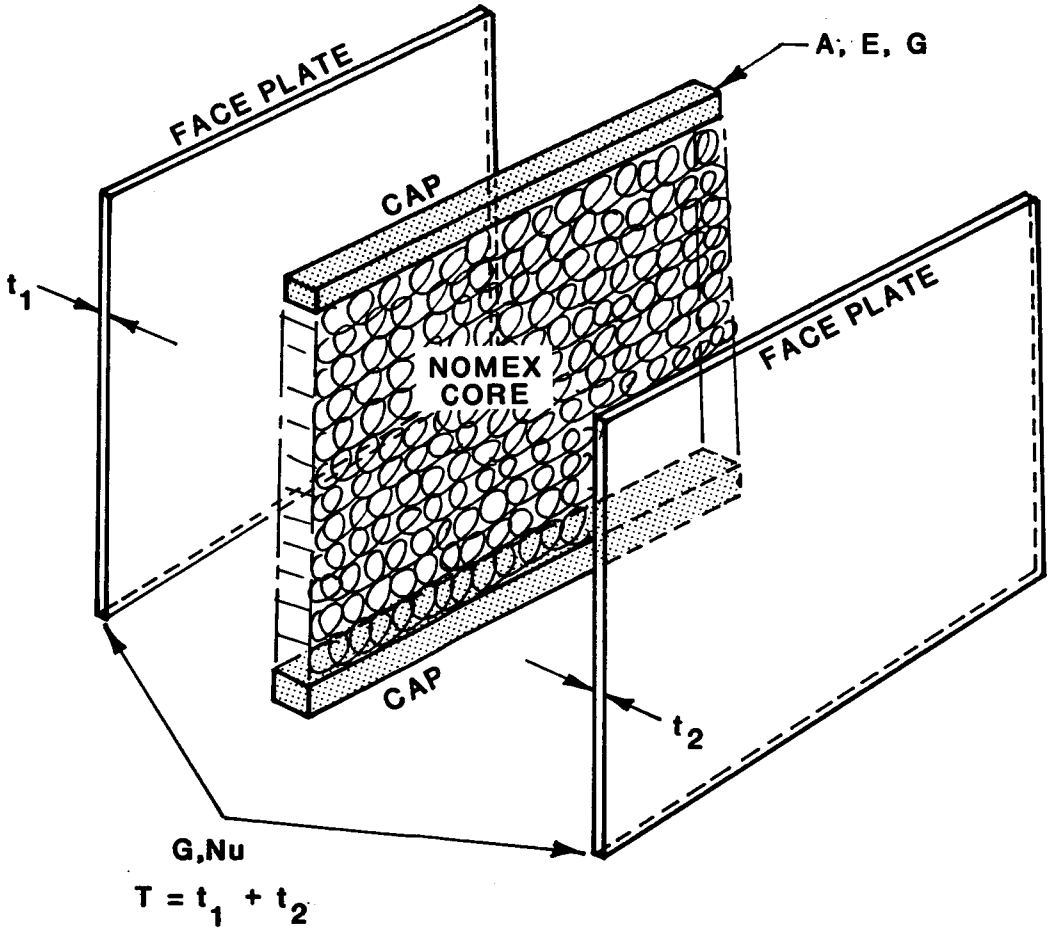

INPUTS TO NASTRAN

BAR ELEMENTS

CAPS = CBAR

A, E, G, AND I = near zero

SHEAR PANELS

WEBS = CSHEAR

T, G, AND Nu

PLATE ELEMENTS

WEBS = CQUAD4

T, [G] AND $12I/T^3$

WHERE I IS PER UNIT WIDTH

STATIC MODELING GUIDES - HONEYCOMB SANDWICH STRUCTURE

BULKHEADS, DECKS AND BUTT-LINE BEAMS

The figure below illustrates a typical honeycomb sandwich panel bulkhead and the corresponding NASTRAN model. With the exception of outer skin panels and floors, the following assumptions and methods apply to honeycomb sandwich panels in general.

ASSUMPTIONS

- Webs act as shear elements only and are modeled as CSHEAR elements.
- Caps (including buried caps) are assumed to carry only axial loads and are modeled as CBAR elements with low bending stiffness.

METHODS

- CSHEAR element aspect ratios are kept as close to one as possible.
- CSHEAR elements are generally modeled with interior angles as close to 90° as possible.
- The thickness of the honeycomb sandwich web is based upon the thickness of the two faceplates.
- Web holes and stiffeners are ignored.
- Cap areas are not reduced for local notches.
- CONROD elements are placed between CSHEAR elements as panel breakers to maintain the aspect ratio near one. Typically a rod area (A) of .001 is used and the modulus (E) is assumed to be the same as the shear element.
- No web area is lumped with the cap area.

STATIC MODELING GUIDES - HONEYCOMB SANDWICH STRUCTURE
BULKHEADS, DECKS AND BUTT-LINE BEAMS

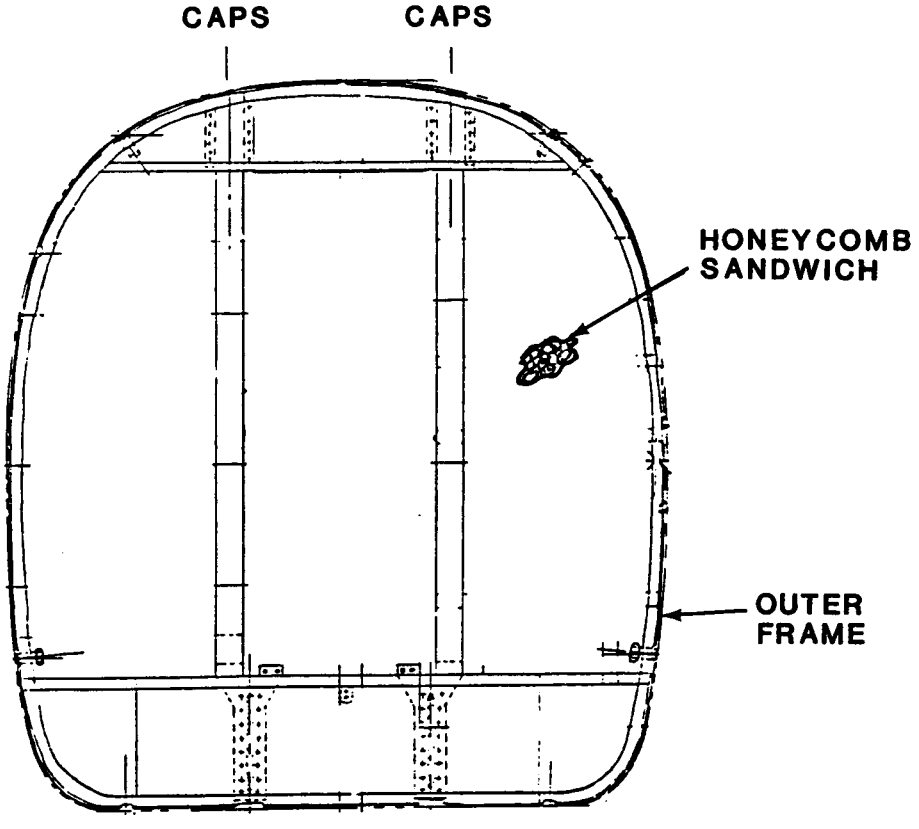

STATION 120
BULKHEAD FRAME

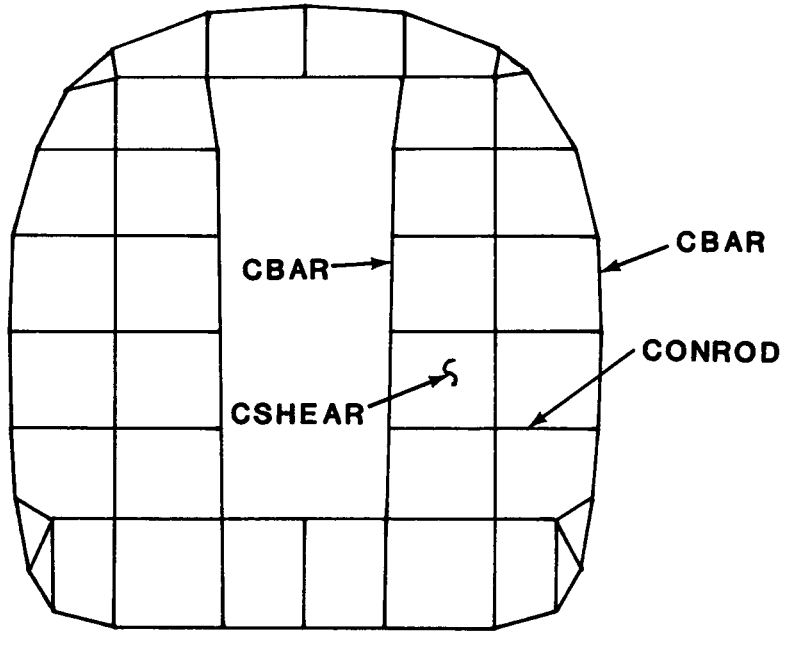

STATIC MODELING GUIDES

HONEYCOMB SANDWICH STRUCTURE - SKIN PANELS

The Model 360 outer skin panels are a special class of honeycomb sandwich panels. Their construction differs from sandwich panels described previously because they are "panned down" at the edges; i.e., the core thickness is tapered to zero. As shown in the figure, additional plies are added in the panned down area to increase buckling stability and provide additional fastener bearing area.

The primary purpose of outer skin panels is to distribute fuselage shears. However, due to the method of construction, the panels also take some end load and, to some degree, resist out of plane bending. For these reasons, it is believed that the skin panels are best idealized with CQUAD4 elements.

Panel material properties will be determined using the COMPLY program as described earlier. Calculations of the panel material properties is based on the following assumptions.

- Membrane and bending properties are computed using the total core thickness plus inner and outer skin thickness. Near zero stiffness values are used for the core so that it only affects the total laminate thickness.
- Additional edge plies are ignored.
- Edge taper is ignored.
- Window cut-outs and stiffeners are ignored.

STATIC MODELING GUIDES

HONEYCOMB SANDWICH STRUCTURE - SKIN PANELS

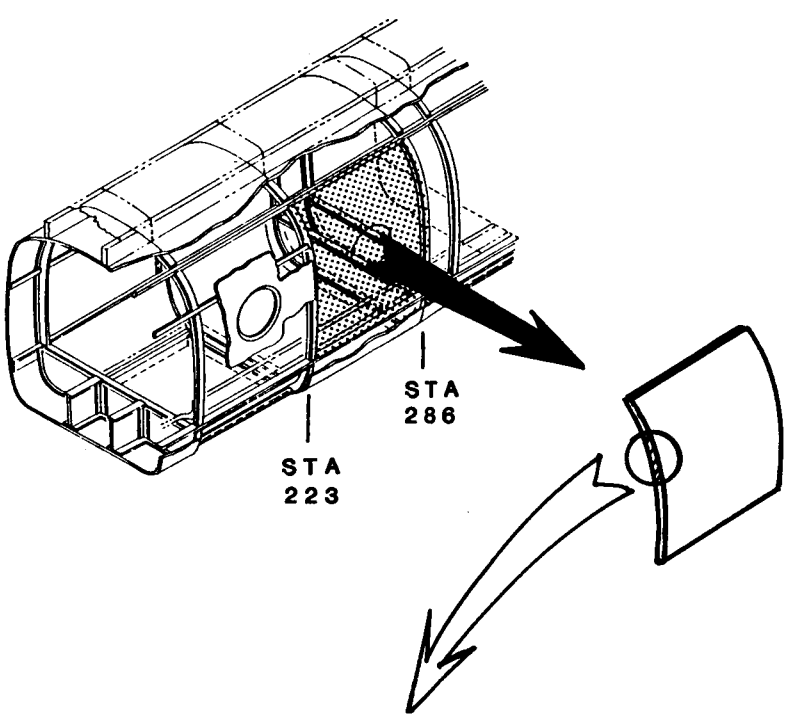

PANEL EDGE DETAIL - TYPICAL

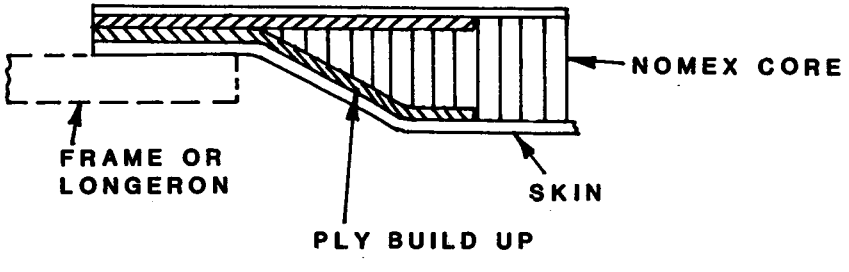

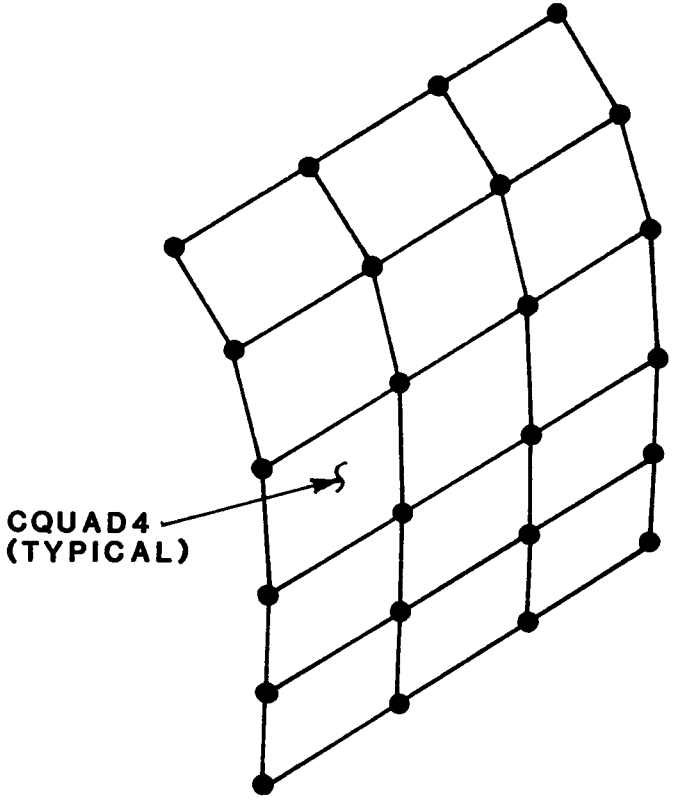

TYPICAL SKIN PANEL
NASTRAN MODEL

STATIC MODELING GUIDES

HONEYCOMB SANDWICH STRUCTURE - CABIN FLOOR

UPPER FLOOR STRUCTURE

The Model 360 cabin floor assembly is a major honeycomb sandwich substructure which supports all internal cargo and fuel. The floor assembly is supported on mass-tuned isolators which provide isolation in the vertical direction. For stress modeling, the isolator static stiffness is used.

This figure illustrates an overview of the floor assembly and the modeling of the upper floor surface (sub-floor and isolator modeling are discussed on the following pages). Because the floor panels act as bending members, they will be modeled using CQUAD4 elements for panels and CBAR elements for the caps. Major modeling assumptions include the following:

- Membrane and bending properties of panels are calculated using the total core thickness plus inner and outer skin thickness. Near zero stiffness values are used for the core.
- Node points are located at the neutral axis of the composite panel.
- Actual areas and inertias are used for caps.
- The hatch is not structural.
- CONRODS are used for lateral and longitudinal restraining links to permit vertical motion only.

STATIC MODELING GUIDES
HONEYCOMB SANDWICH STRUCTURE - CABIN FLOOR
UPPER FLOOR STRUCTURE

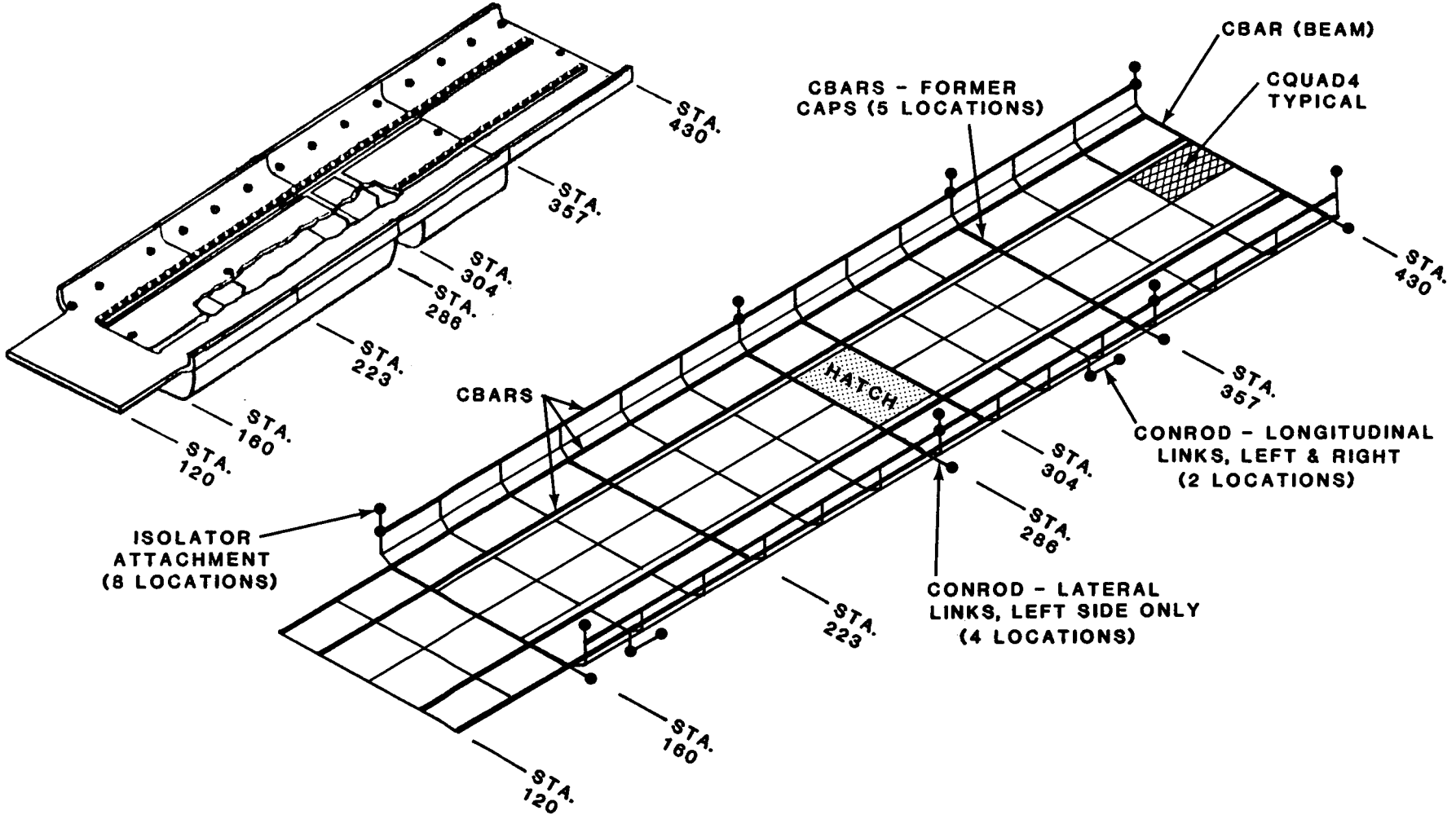

STATIC MODELING GUIDES

HONEYCOMB SANDWICH STRUCTURE - CABIN FLOOR

SUB-FLOOR STRUCTURE

The sub-floor structure is an integral portion of the overall floor assembly which is bonded and fastened with mechanical fasteners to the upper floor structure. It is divided into three bays which house three crashworthy fuel cells. Access to the fuel bays is through removable panels in the upper floor structure.

Modeling procedure will be similar to the upper floor structure. The outer surface and formers will be modeled with CQUAD4 elements and buried caps with CBAR elements.

STATIC MODELING GUIDES

HONEYCOMB SANDWICH STRUCTURE - CABIN FLOOR SUB-FLOOR STRUCTURE

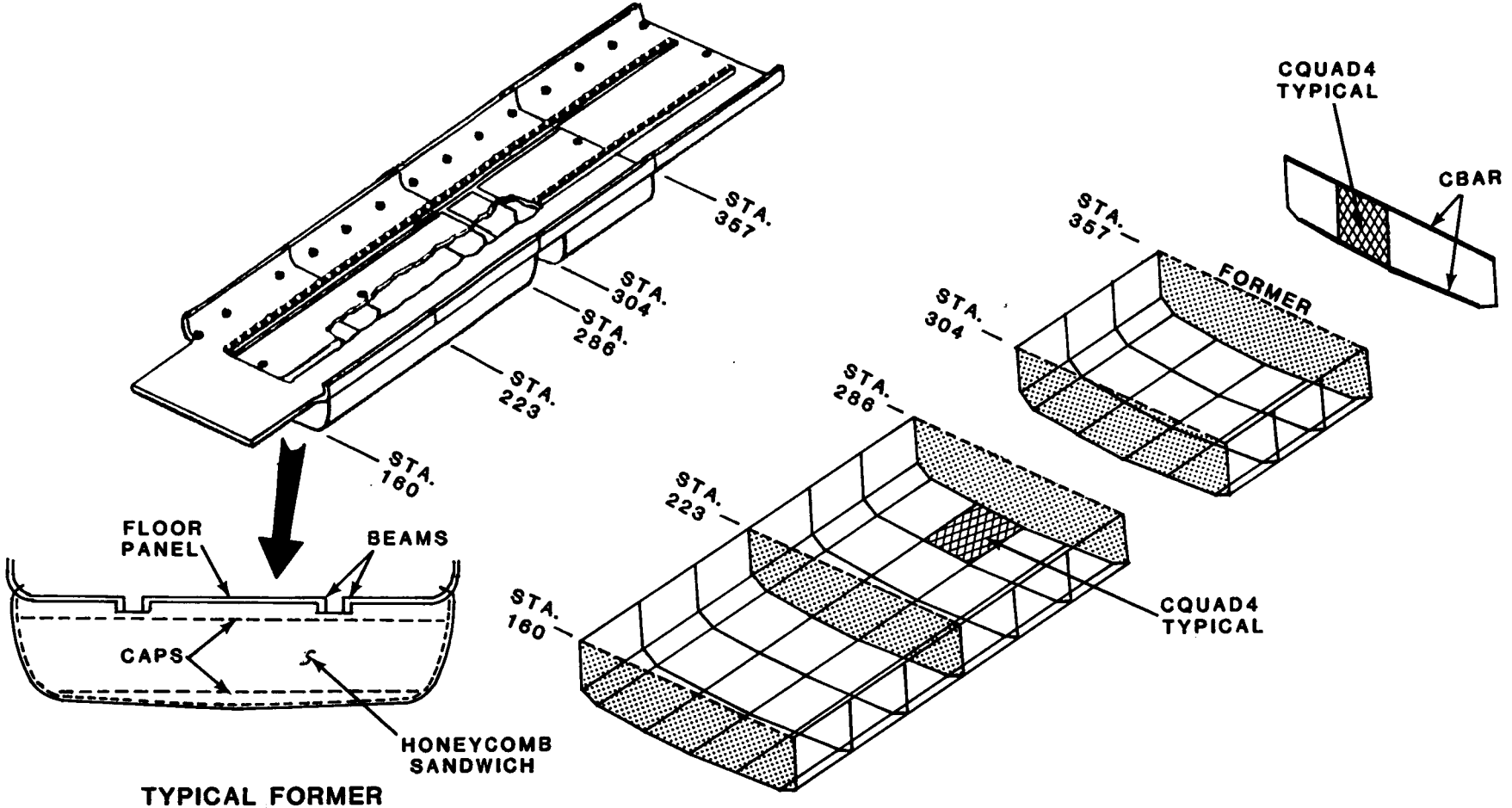

STATIC MODELING GUIDES

ISOLATOR MODELING - CABIN FLOOR

This figure illustrates the treatment of the cabin floor isolators and is generally typical of the procedure used to model the mass-tuned isolators in both the cockpit and cabin.

Fittings between the frame and the floor are modeled with CBAR elements with the isolator spring represented by a CELAS element. The drive rod and pivoted arm with the tuning weight are not modeled. This configuration duplicates the isolator static stiffness which is satisfactory for loads analysis. (Note: for dynamic analysis the locked configuration will be modeled by replacing the CELAS element with a rigid pin-ended element between points C and D.)

STATIC MODELING GUIDES

ISOLATOR MODELING - CABIN FLOOR

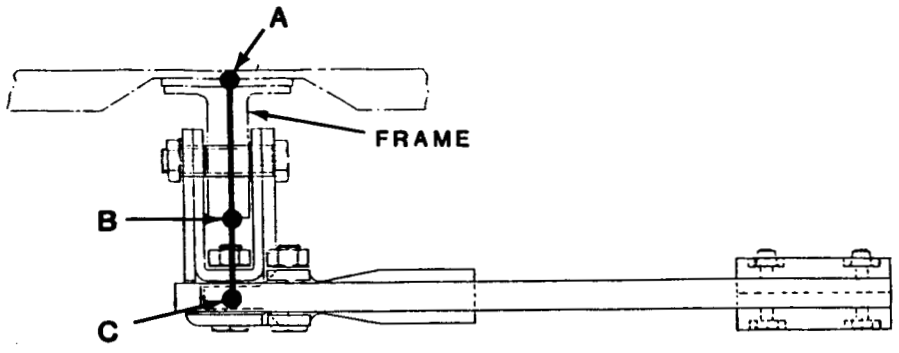

TOP VIEW

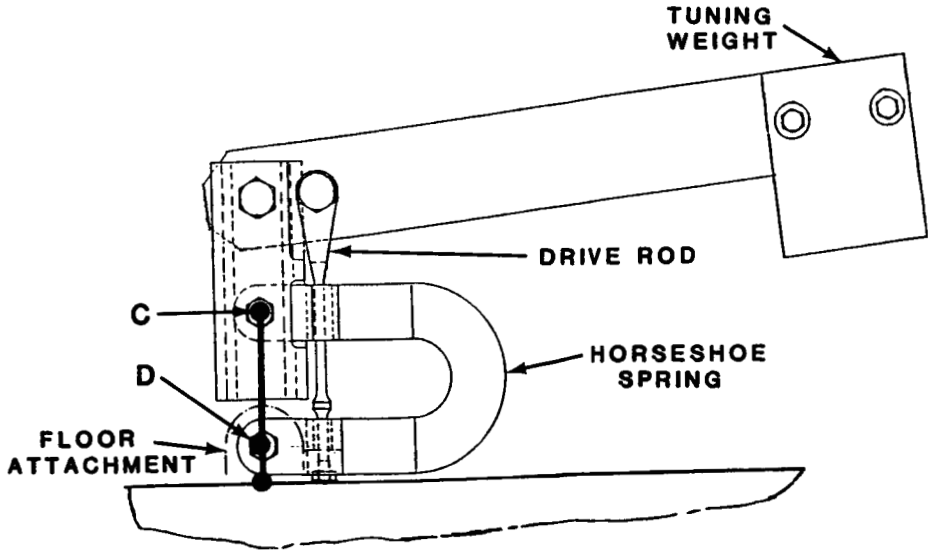

SIDE VIEW

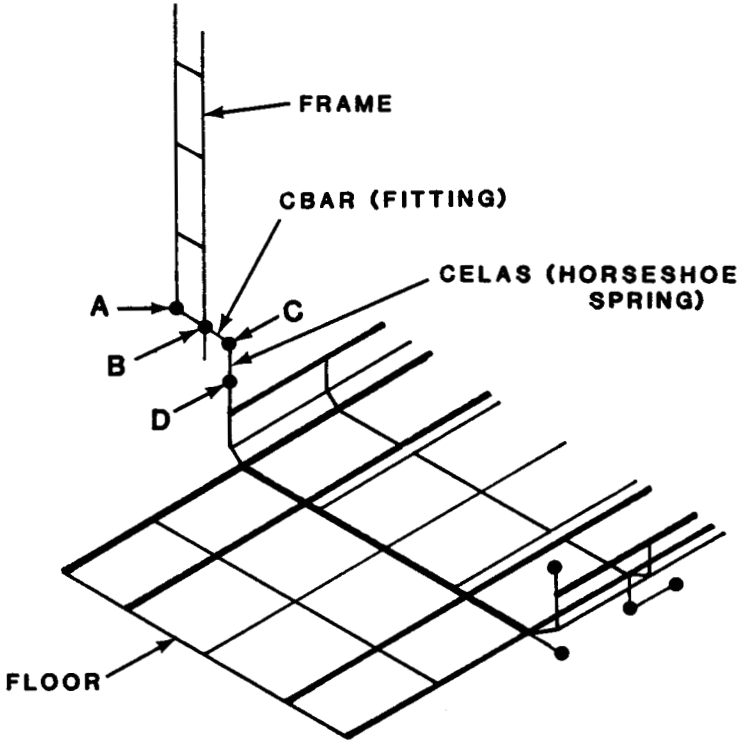

STATIC MODELING GUIDES

ROTOR SHAFTS

This figure shows a rotor shaft modeled to give an effective bending stiffness and an effective axial area. Since inner and outer diameters of the rotor shafts vary along the shaft, equivalent properties that match the deflections at the rotor hub can be obtained by integration of the shaft stiffness properties along the length of the shaft. A single bar element with the calculated equivalent constant section properties is used to represent the rotor shaft.

STATIC MODELING GUIDES
ROTOR SHAFTS

ROTOR SHAFT

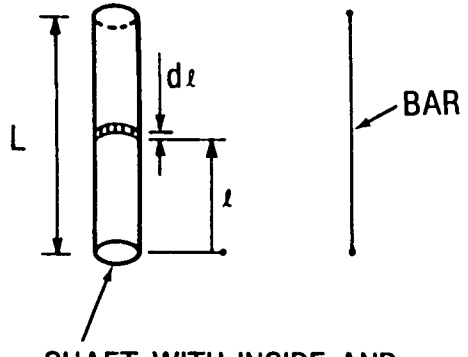

SHAFT WITH INSIDE AND OUTSIDE DIAMETERS WHICH VARY ALONG THE SHAFT LENGTH

$$I = \frac{L}{\int \frac{d\ell}{I(\ell)}}$$ (FOR EQUIVALENT BENDING STIFFNESS)

$$A = \frac{L}{\int \frac{d\ell}{A(\ell)}}$$ (FOR EQUIVALENT AXIAL STIFFNESS)

WHERE

$$A(\ell) = \frac{\pi}{4} (D_o^2 - D_i^2)$$

$$I(\ell) = \frac{\pi}{64} (D_o^4 - D_i^4)$$

D_o = OUTSIDE DIAMETER

D_i = INSIDE DIAMETER

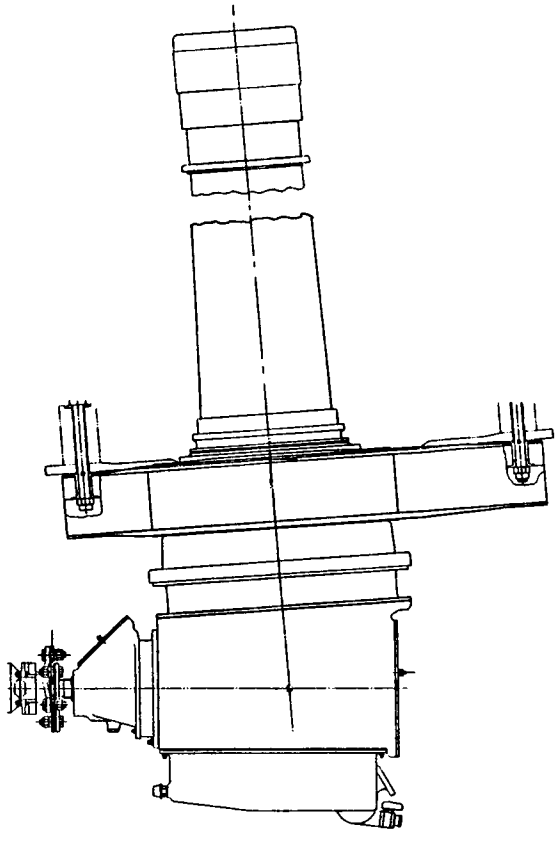

STATIC MODELING GUIDES

FORWARD TRANSMISSION COVER AND ROTOR SHAFT

The forward transmission cover is a composite part of complex shape. Its load path is from the rotor shaft bearings to the four feet of the cover. From here bolts transfer load into the pylon structure. As noted previously, the rotor shaft is modeled with an equivalent bar element. An array of CBAR elements is used to represent the bearings and transfer load from the rotor shaft to the outer cover surface. The four feet of the cover are modeled with CBAR elements. Attachment points A, B, C, D are pinned to the airframe and take no moment. Similarly, the bearings transmit no moment and the rotor shaft is pinned at the bearing locations.

STATIC MODELING GUIDES
FORWARD TRANSMISSION COVER AND ROTOR SHAFT

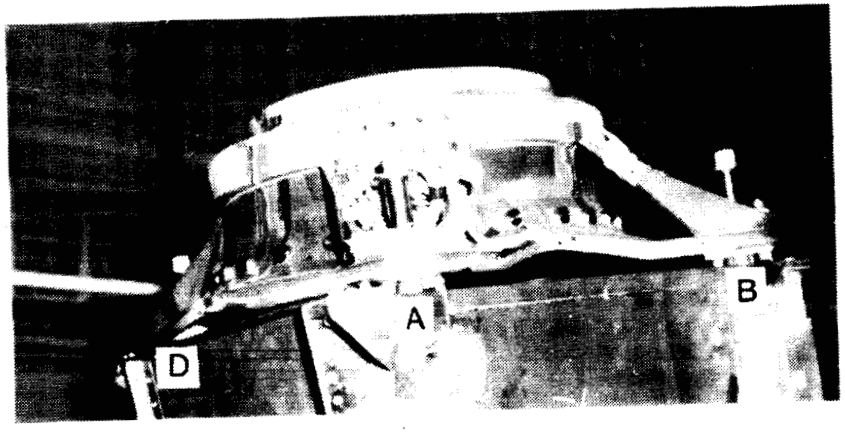

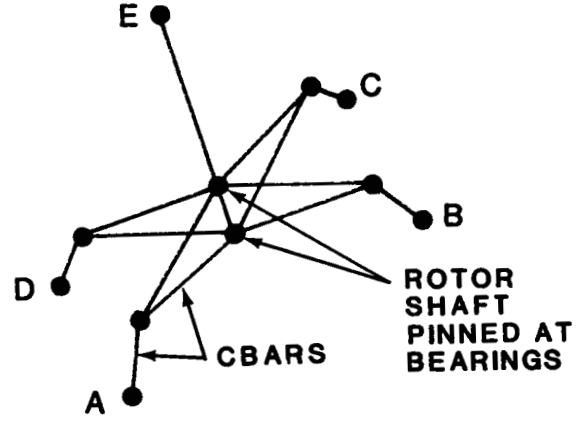

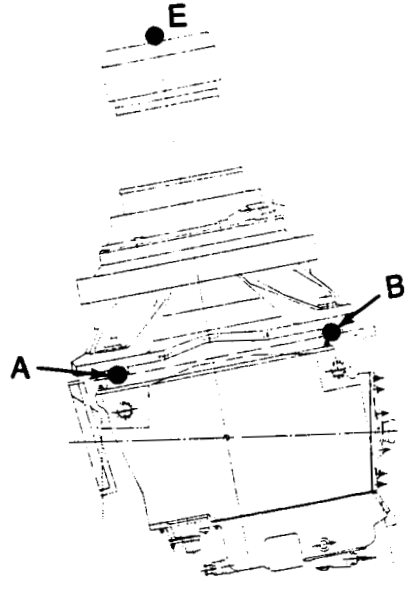

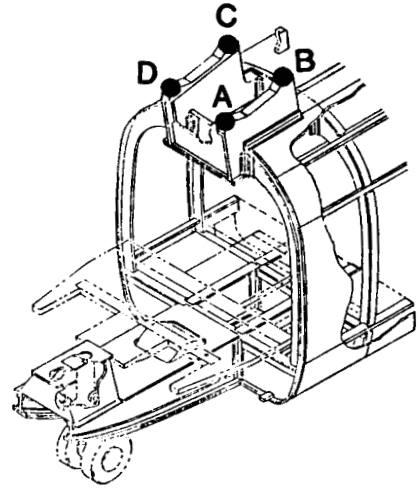

STATIC MODELING GUIDES

AFT TRANSMISSION COVER AND ROTOR SHAFT

The aft transmission cover is also of composite construction. While the load path is similar, the configuration differs form the forward rotor and the structural attachments are above rather than below the transmission.

Modeling is similar to the forward transmission. Loads are transferred from the rotor shaft through an array of CBAR elements to the four longitudinal beams which are also modeled with CBARS. The airframe attachment points and rotor shaft bearing locations are pinned so they carry no moment.

STATIC MODELING GUIDES
AFT TRANSMISSION COVER AND ROTOR SHAFT

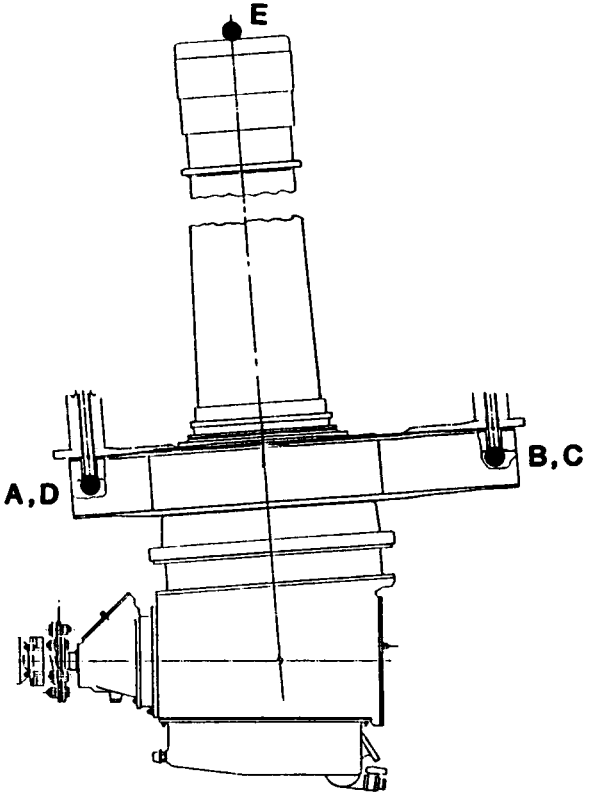

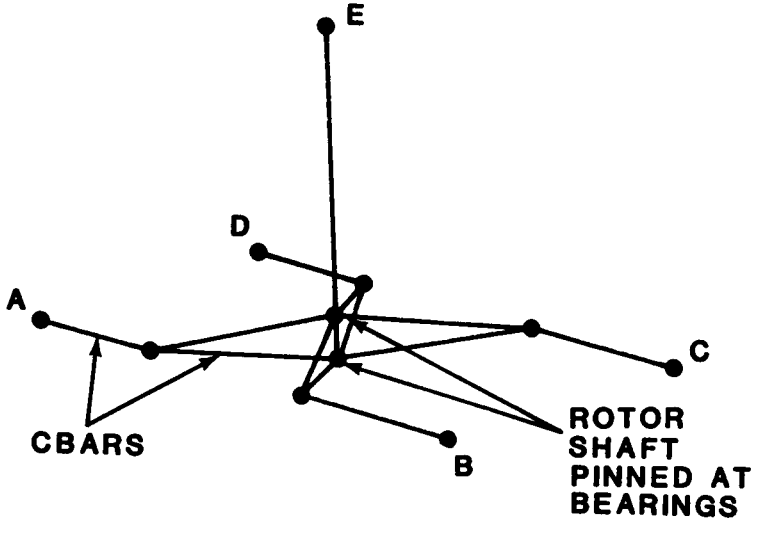

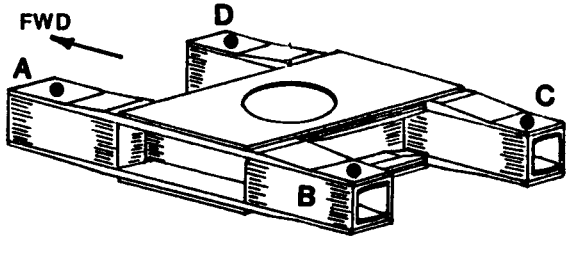

STATIC MODELING GUIDES

FORWARD LANDING GEAR

The forward landing gear is modeled in the retracted position using CONRODS and CBARS as shown. Axial and bending stiffnesses are representative of the member stiffnesses. The trunnion pin (A-B) is restrained in the axial direction at only one end to prevent it from stiffening the structure. Sufficient node points are employed to obtain a reasonable distribution of the landing gear mass.

STATIC MODELING GUIDES
FORWARD LANDING GEAR

EXTENDED

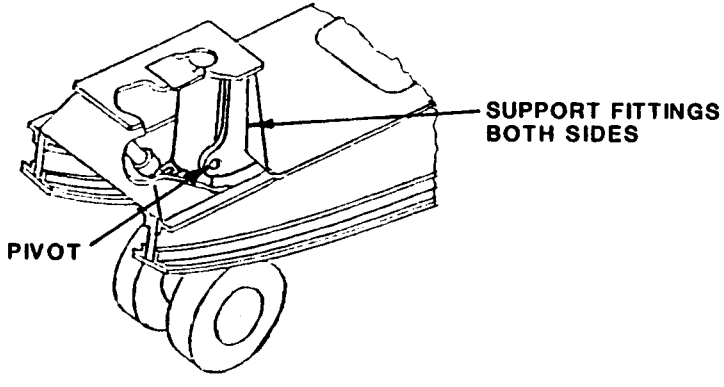

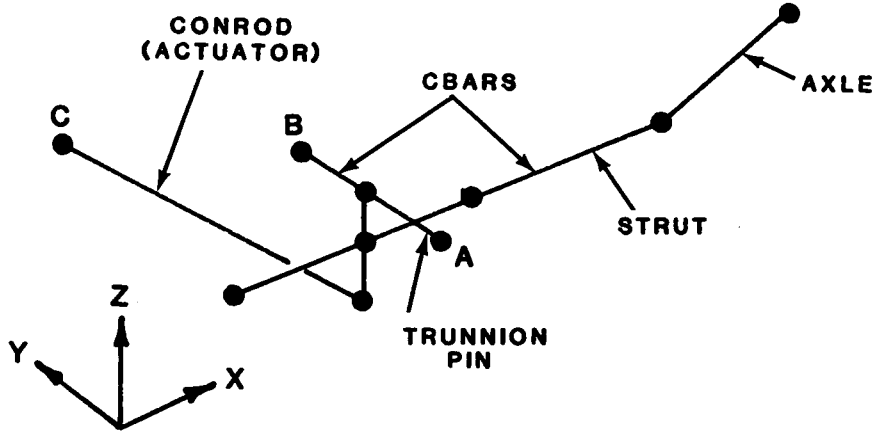

RETRACTED

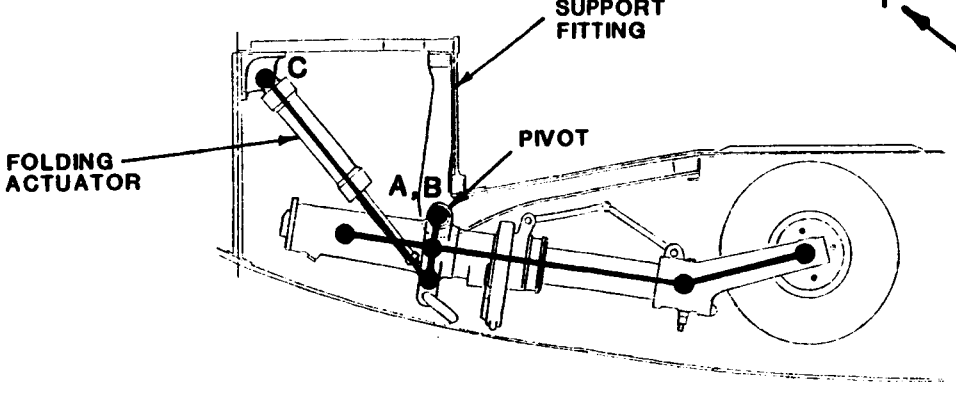

NASTRAN MODEL
RETRACTED POSITION

STATIC MODELING GUIDES

MAIN LANDING GEAR

The NASTRAN model of the main landing gear in the retracted position is shown in the accompanying figure. Proper modeling for analysis of landing gear loads requires detailed modeling of the linkage. In the stowed (retracted) flight position modeling of the linkage is necessary to obtain the correct support stiffnesses for the landing gear mass. The drag link and stabilizer link which do not carry bending loads are modeled with CONRODS. The remaining members are modeled with CBARS. End restraints on the shear pin (C-D) are specified so that it carries no axial load. A sufficient number of node points are used to permit a reasonable distribution of landing gear mass.

STATIC MODELING GUIDES
MAIN LANDING GEAR

EXTENDED

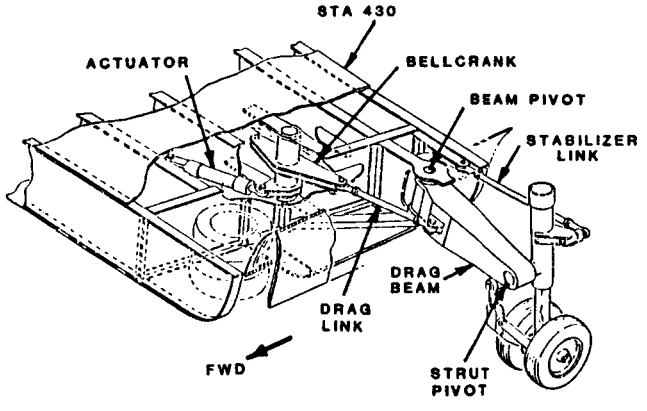

RETRACTED

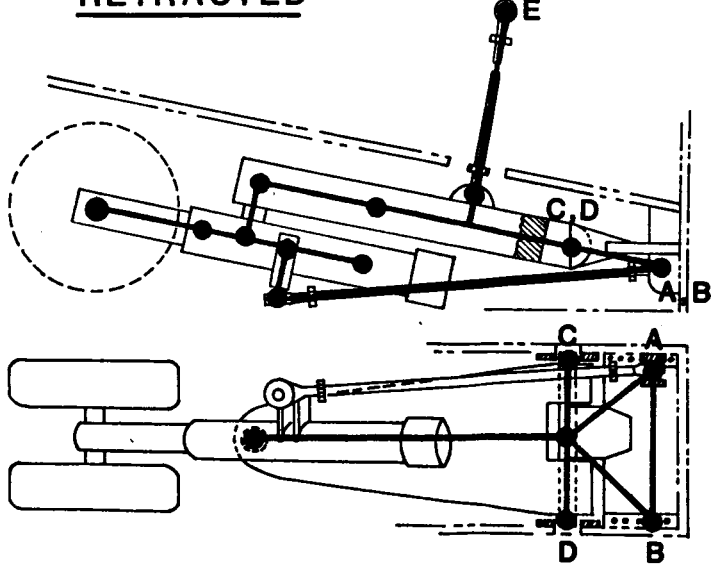

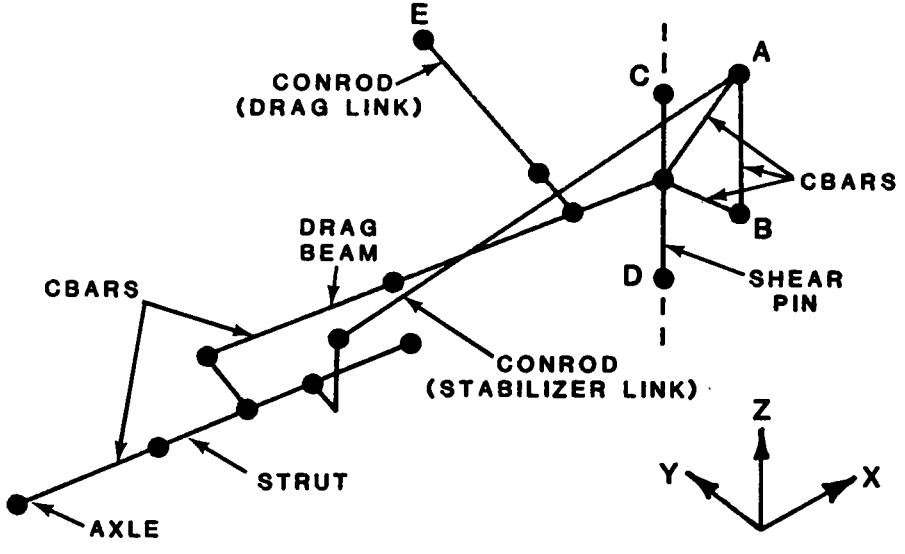

NASTRAN MODEL
RETRACTED POSITION

STATIC MODELING GUIDES

ENGINE AND ENGINE FITTINGS

This figure shows the modeling of the engine and engine support fittings. The forward engine fittings which provide vertical, lateral and longitudinal restraint are modeled with CBAR elements. At the aft support, the vertical link, which carries only vertical loads, is modeled with a CONROD. Typically, the engine is considered to be rigid and modeled with rigid elements. Engine mass is located at the center of gravity with inertia loads transferred to the attachments through the rigid engine framework.

STATIC MODELING GUIDES
ENGINE AND ENGINE FITTINGS

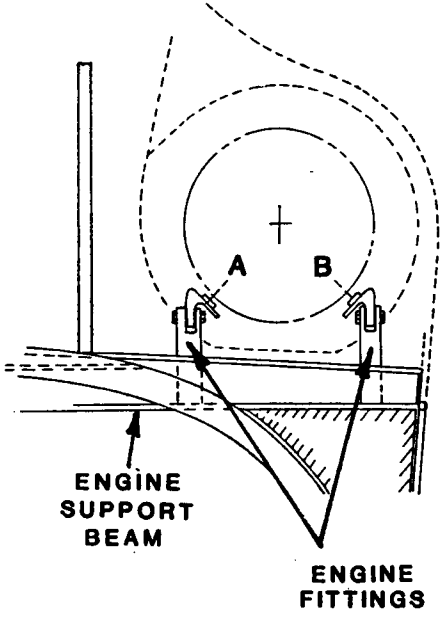

STA 480
FORWARD SUPPORT

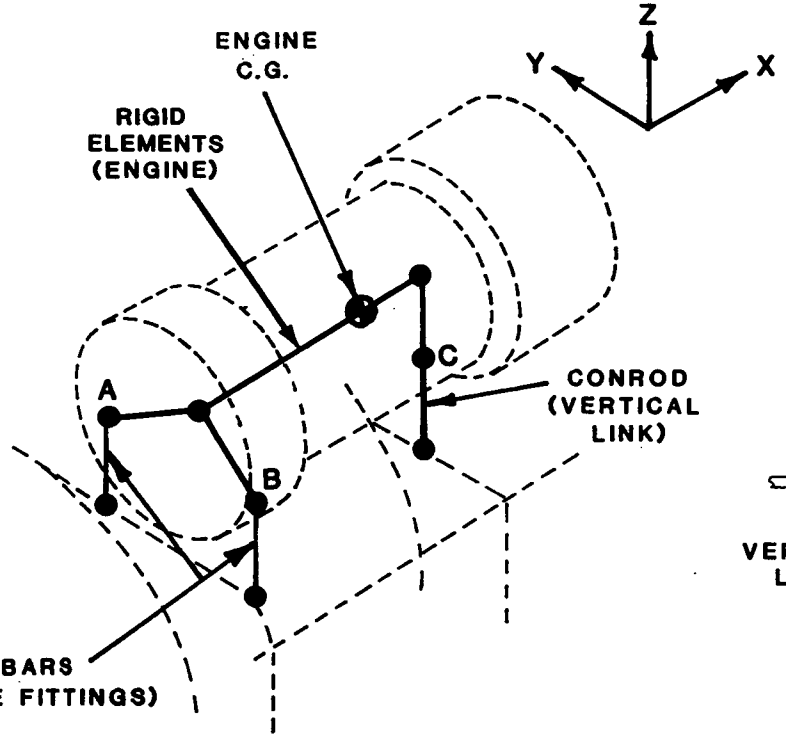

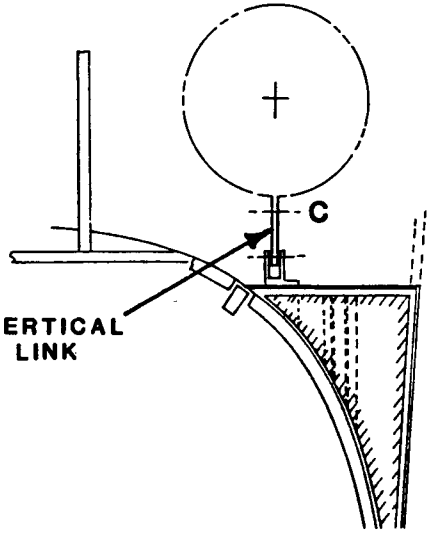

STA 451
AFT SUPPORT

BLANK
PAGE

4.2 Mass Modeling Guides

PRECEDING PAGE BLANK NOT FILMED

MASS MODELING GUIDES

GENERAL APPROACH

This chart illustrates the general approach to mass modeling.

1.) Mass data obtained from the summary weight statement is divided into two categories; namely, useful load items and those items comprising the weight empty data base. The useful load items are treated as detailed or concentrated items to facilitate analysis of different loading conditions.

2.) The weight empty data base is broken down into two categories identified as special items (basically concentrated weights) and distributed weight items.

3.) Concentrated weight items are distributed directly to assigned NASTRAN nodes .

4.) Distributed weight items are separated into unisolated items and those comprising the isolated cockpit and floor/fuel modules.

5.) The unisolated distributed items are allocated to specified frame stations using program W-17. The isolated items are allocated to specified stations on the isolated module. Both are then manually distributed to appropriate NASTRAN nodes at that station.

MASS MODELING GUIDES - GENERAL APPROACH

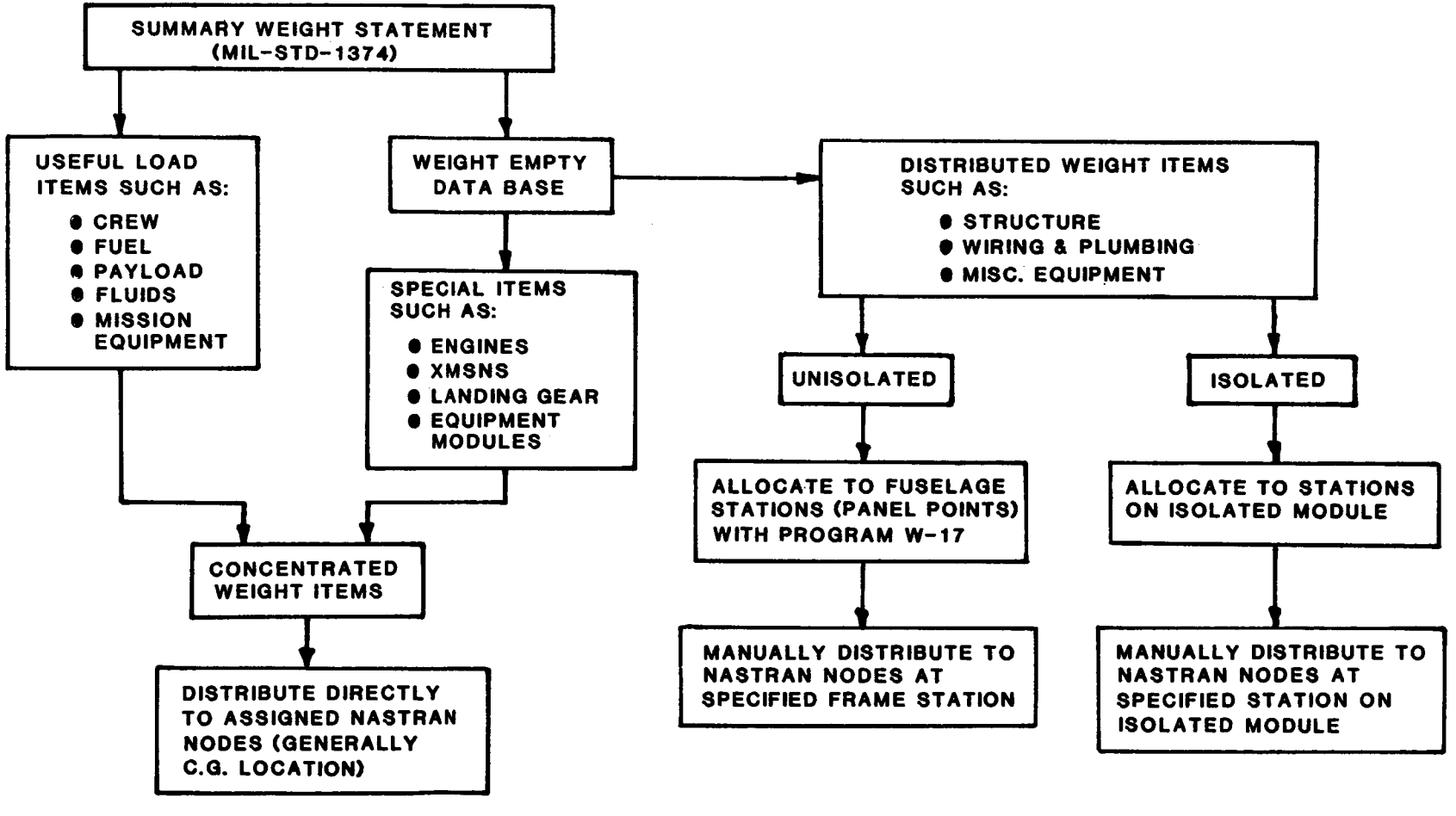

MASS MODELING GUIDES

TREATMENT OF DISTRIBUTED MASS ITEMS

The procedure for allocating aircraft distributed mass to NASTRAN nodes is as follows:

1.) Fuselage stations corresponding to frames and bulkheads where distributed mass is to be located are identified. Computer program W-17 divides the airframe into a series of non-overlapping bays with the designated stations (referred to as panel points) at their centers. Mass properties of the distributed items within each bay are then summed to form a single mass which is allocated to the designated station (panel point). A typical panel point loading is illustrated in Figure A.

2.) The panel point mass at a particular station (Figures B and C) is reviewed and the mass is distributed to NASTRAN nodes on the structure at that station. The distribution of mass at a particular station is done in a manner to preserve, within the limits of the NASTRAN model, the mass vertical and lateral c.g. location and the roll inertia at that particular station. The distribution is made by the Weights Engineer based on his knowledge of mass items near the panel point.

3.) Local roll inertias are maintained to provide good estimates of aircraft torsional frequencies. Preserving local pitch and yaw inertias at a frame station does not appear to be a requirement if the distance between frame stations for masses is reasonably small.

MASS MODELING GUIDES
TREATMENT OF DISTRIBUTED MASS ITEMS

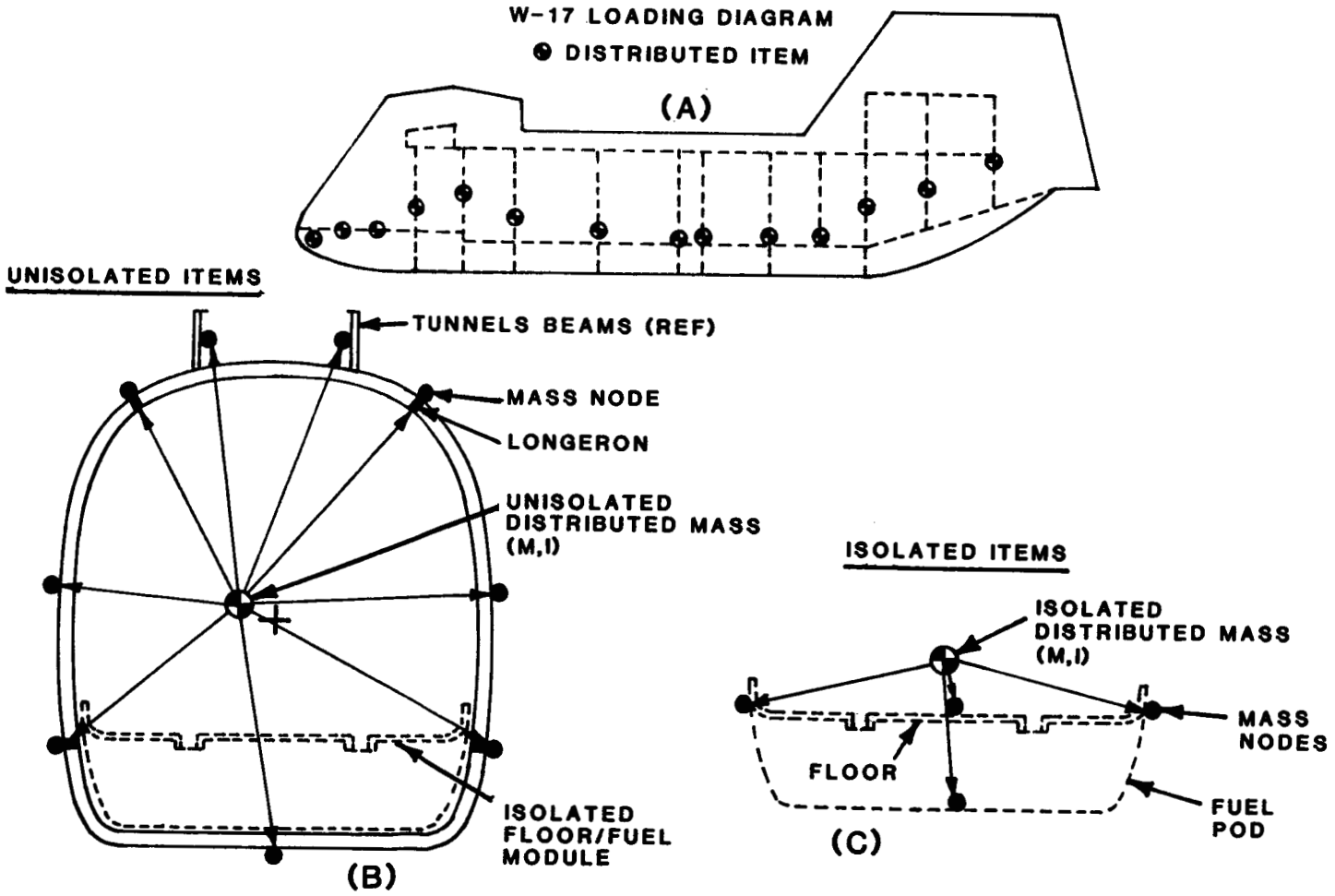

- DISTRIBUTED MASS ITEMS LUMPED AT NODES AS SHOWN
- MAINTAIN VERTICAL AND HORIZONTAL CG, AND THE ROLL INERTIA WITHIN THE LIMITS OF THE NASTRAN MODEL

MASS MODELING GUIDES

TREATMENT OF CONCENTRATED MASS ITEMS

Both empty weight special items and useful load items (mission masses) are treated more-or-less as concentrated items. Items falling into each of the above categories are as follows:

Special Items (Empty Weight)	Useful Load Items (Mission Weights)
Engine Assemblies	Pilot and Copilot
Transmissions	Fuel
Landing Gear	Cargo
Equipment Modules	Fluids
APU	Mission Equipment
Rotors & Rotating Controls	

In general, concentrated masses are represented by their actual mass and moments of inertia placed at a location corresponding to the center of gravity. This will be accomplished using a structural node where possible. Otherwise, a c.g. node will be created using RBE3 elements connected to nodes which correspond to the attachment points. Notable exceptions are:

- Rotor disc inertia is assumed to be zero; 100% rotor mass assumed for static analysis and 70% for vibration analysis

- Fuel and cargo mass are distributed to a number of assigned NASTRAN nodes to obtain a more realistic inertia loading. Center of gravity and moment of inertia are maintained within limits of the NASTRAN model.

- While broken out as a concentrated weight (as opposed to a distributed weight) the landing gear are in fact flexible appendages. For vibration analysis, the landing gear must be modeled as small substructures with an appropriate mass distribution.

MASS MODELING GUIDES
TREATMENT OF CONCENTRATED MASS ITEMS

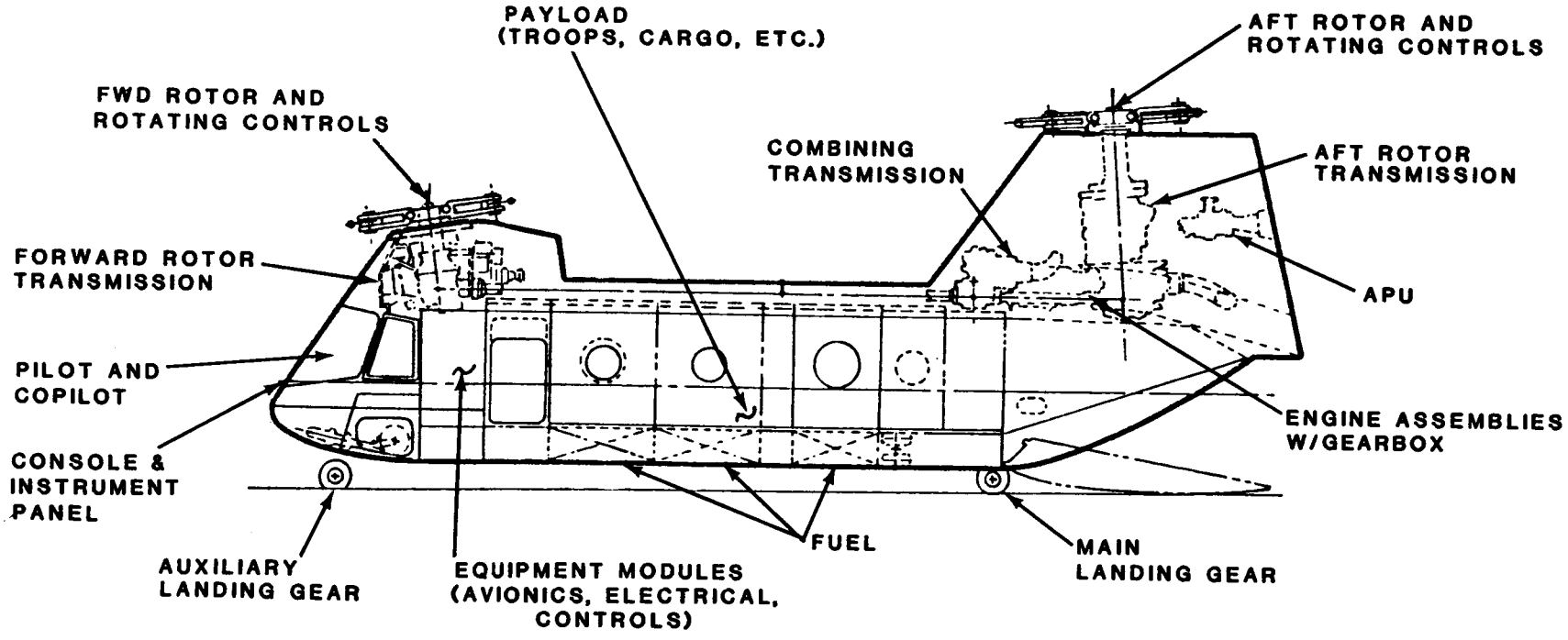

- **MASS AND MOMENT OF INERTIA LOCATED AT C.G.**
- **100% ROTOR MASS, NO DISC INERTIA**
- **FUEL AND CARGO DISTRIBUTED TO MULTIPLE NODE POINTS MAINTAINING C.G. AND INERTIA WITHIN LIMITS OF THE NASTRAN MODEL**
- **LANDING GEAR MODELED AS FLEXIBLE APPENDAGE WITH DISTRIBUTED MASS**

BLANK
PAGE

4.3 Vibration Modeling Guides

PRECEDING PAGE BLANK NOT FILMED

VIBRATION MODELING GUIDES

MODELING ASSUMPTIONS

The figure summarizes the major assumptions for the Vibration Finite Element Model.

Aircraft Configuration

- To simulate an inflight situation, the aircraft is analyzed in a free-free condition without the use of SUPPORT cards. The near zero frequencies which should be obtained for the six rigid-body modes in this fashion will serve as an additional check on the validity of the model.
- The design gross weight is selected to evaluate modeling of the floor/fuel module substructure under load.

Modeling

- The cockpit and floor isolation systems are locked to place the emphasis on correct modeling of the basic structure and avoid the complexity of modeling the isolation systems.
- In the interest of simplification, the question of effective fuel mass will be avoided and the fuel will be treated as a rigid mass.
- The issue of effective rotor mass and rotor-fuselage coupling is the subject of a separate investigation. At this time, the rotor is treated as a concentrated mass with inertias corresponding to an unbladed condition and a weight which includes 70% of the flapping mass. The 70% value is based on preliminary rotor-fuselage coupling studies.

VIBRATION MODELING GUIDES
MODELING ASSUMPTIONS

- **AIRCRAFT CONFIGURATION**
  - **FREE-FREE CONDITION**
  - **DESIGN GROSS WEIGHT**
- **MODELING**
  - **ISOLATORS LOCKED**
  - **RIGID FUEL (100% EFFECTIVE MASS)**
  - **70% ROTOR FLAPPING MASS**

VIBRATION MODELING GUIDES

CHANGES FROM STATIC TO VIBRATION FEM

There are only two minor changes from the static to the vibration model.

- Rotor flapping mass is reduced from 100% to 70% based on preliminary rotor-fuselage coupling studies.
- The static model uses the static stiffness value of the floor isolators which is correct for loads analysis. The isolation systems are locked for the dynamic analysis to place the emphasis on the basic structural modeling.

VIBRATION MODELING GUIDES
CHANGES FROM STATIC TO VIBRATION FEM

- **REDUCE ROTOR FLAPPING MASS FROM 100% TO 70%**
- **CONVERT FLOOR ISOLATION SYSTEMS TO LOCKED CONFIGURATION**

VIBRATION MODELING GUIDES

GENERALIZED DYNAMIC REDUCTION

The so-called generalized dynamic reduction is a procedure routinized in NASTRAN for drastically reducing the number of degrees of freedom when computing vibrations and other dynamic responses. This is an assumed mode method wherein the assumed modes are approximate vibration modes. The number of approximate modes chosen is 1.5 times the number of accurate modes desired.

VIBRATION MODELING GUIDES
GENERALIZED DYNAMIC REDUCTION

$$\{u_f\} = [G]\ \{u_q\}$$

- $\{u_f\}$: STATIC FEM DOF
- $[G]$: REDUCTION TRANSFORMATION
- $\{u_q\}$: GENERALIZED COORDINATES FOR MODAL ANALYSIS

THE COLUMNS OF [G]:

- APPROXIMATE THE LOWER MODES OF THE STRUCTURE
- ARE EQUAL IN NUMBER TO 1.5 x (NUMBER OF ACCURATE MODES DESIRED)

4.4 Computational Demonstration

PRECEDING PAGE BLANK NOT FILMED

COMPUTATIONAL DEMONSTRATION

A computational demonstration will be performed using the NASTRAN FEM of the Model 360 helicopter to show that the model generates reasonable (error-free) results for computations of (1) static internal member loads, (2) steady-state forced response to oscillatory excitation forces at the blade passage frequency applied at the rotor hubs, and (3) natural frequencies and mode shapes.

COMPUTATIONAL DEMONSTRATION

A COMPUTATIONAL DEMONSTRATION WILL BE PERFORMED TO SHOW THAT THE FEM GENERATES REASONABLE (ERROR FREE) RESULTS FOR:

- **STATIC INTERNAL LOADS**
- **STEADY-STATE FORCED RESPONSE**
- **NATURAL FREQUENCIES AND MODE SHAPES**

COMPUTATIONAL DEMONSTRATION

DEMONSTRATION CASES

To satisfy the objectives of the computational demonstration, NASTRAN runs will be performed at the design gross weight of 30,500 lb. for the following:

1.) Rigid-body check

2.) Static analysis for internal loads under a 3.0 g symmetric pull-up

3.) Normal modes analysis for natural frequencies and mode shapes

4.) Forced vibration analysis for representative b/rev loads

All demonstration cases will be performed using the latest version of MSC/NASTRAN available through Boeing Computer Services (BCS).

COMPUTATIONAL DEMONSTRATION
DEMONSTRATION CASES

FOR 30,500 LB DESIGN GROSS WEIGHT PERFORM FOLLOWING:

- **RIGID-BODY CHECK**
- **STATIC ANALYSIS FOR INTERNAL MEMBER LOADS**
  - **3.0g PULL-UP FROM SYMMETRIC DIVE**
- **NORMAL MODES ANALYSIS**
  - **NATURAL FREQUENCIES AND MODES**
- **FORCED VIBRATION ANALYSIS**
  - **REPRESENTATIVE b/REV LOADS**

COMPUTATIONAL DEMONSTRATION

RIGID-BODY CHECK

The principal purpose of the rigid-body check is ensure that there are no inconsistent constraints, primarily single point constraints (SPC's), applied to the model. If the model is placed in a free-body condition with no inconsistent constraints present, then it must be capable of undergoing rigid-body motions without inducing internal forces.

As indicated in the accompanying figure, the following steps are required to perform the rigid body check:

1.) All SPC's are removed except those which are required to remove grid point singularities.

2.) All SUPPORT cards are removed and the model is constrained at one rotor hub in all directions except one.

3.) A unit SPC displacement is imposed at the hub in the free direction.

To evaluate the results, the NASTRAN output is examined to determine that the following conditions are satisfied:

1.) All grid point displacements on the model are equal to the applied displacement.

2.) All internal forces, including SPC forces, are zero.

Any deviation from these conditions indicates that unwanted constraints are present.

COMPUTATIONAL DEMONSTRATION
RIGID BODY CHECK

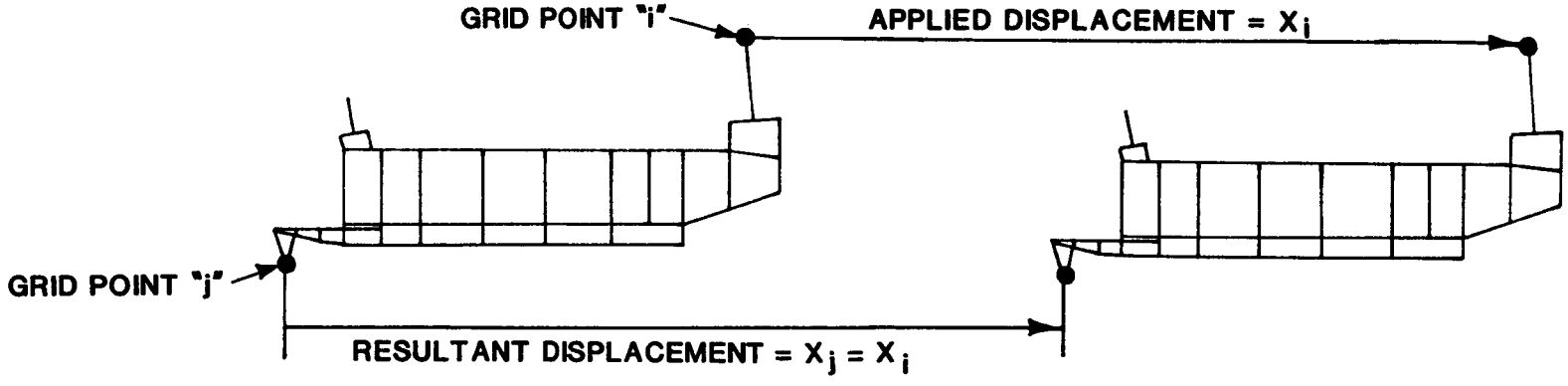

- **TO PERFORM RIGID BODY CHECK:**
  - **REMOVE ALL SPC'S EXCEPT THOSE REQUIRED TO REMOVE SINGULARITIES**
  - **REMOVE ALL SUPPORT CARDS AND CONSTRAIN ONE HUB IN ALL DIRECTIONS EXCEPT ONE**
  - **IMPOSE UNIT SPC HUB DISPLACEMENT IN FREE DIRECTION**
- **TO EVALUATE, EXAMINE OUTPUT TO DETERMINE THAT:**
  - **ALL GRID POINT DISPLACEMENTS EQUAL APPLIED DISPLACEMENT**
  - **ALL INTERNAL LOADS ARE ZERO**

COMPUTATIONAL DEMONSTRATION

STATIC INTERNAL LOADS

The demonstration case for static internal loads will be a 3.0 g pull-up from a symmetric dive at an aircraft gross weight of 30,500 lb. with a C.G. location at station 304. The analysis is performed using the static analysis solution (RIGID FORMAT 24) of MSC/NASTRAN. Applied loads for the analysis are developed from the mass model using a Boeing code which provides the inertia loads.

The items of primary interest in the NASTRAN output are the grid point displacements and the SPC forces, both of which will be examined for any errors or anomalies. In the case of the displacements it is sometimes convenient to examine the data in the form of a static deflected shape. Other information of interest which will also be reviewed includes grid point force balance and element forces.

COMPUTATIONAL DEMONSTRATION
STATIC INTERNAL LOADS

SYMMETRIC PULL-UP

GW = 30,500 LB

CG = STA. 304

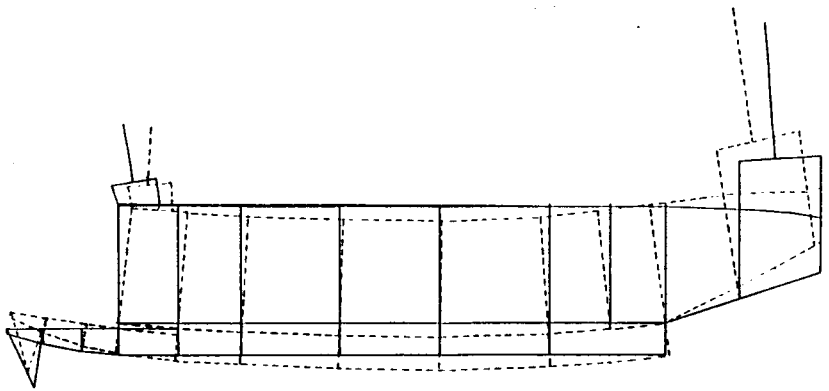

STATIC DEFLECTED SHAPE

NASTRAN OUTPUT OF PRIMARY INTEREST

- **DISPLACEMENTS**
- **SPC FORCES**
- **GRID POINT FORCE BALANCE**
- **ELEMENT FORCES**

COMPUTATIONAL DEMONSTRATION

NORMAL MODES ANALYSIS

Natural frequencies and modes will be calculated for the design gross weight of 30,500 pounds. To place emphasis on the structural modeling, the analysis will be carried out with the cockpit and floor/fuel module isolation systems locked. A NASTRAN frequency tabulation and modal vector printout will be obtained. Mode shape plots will be obtained using the NASTRAN automated plotting capability.

It should be noted here that the aircraft configuration for the demonstration cases is not the same as the test configuration for the validation test performed under another task under this contract. While the results may be similar, they will not be identical.

COMPUTATIONAL DEMONSTRATION
NORMAL MODES ANALYSIS

MODE NO.	DESCRIPTION OF MODE	FREQ. Hz
7	AFT PYLON ROLL	5.18
8	AFT PYLON PITCH	5.35
9	COCKPIT VERT (HUB OUT OF PHASE)	7.26
10	FWD XMSN PITCH (HUBS IN PHASE)	7.44
11	ENGINE YAW, FUSELAGE TORSION	7.60
13	FWD XMSN PITCH (HUBS OUT OF PHASE)	8.70
14	FWD XMSN ROLL (HUBS IN PHASE)	8.83
17	CABIN FRAME RACKING	10.53
18	COCKPIT LATERAL / TWIST	11.03
19	CABIN FRAME DIAGONAL DISTORTION	12.27
21	COCKPIT VERT (HUB IN PHASE)	14.12
25	COCKPIT LATERAL / TWIST (NO HUB)	16.93
27	CABIN FLOOR VERT	17.71
30	CABIN FRAME DISTORTION	18.91
31	COCKPIT VERT (NO HUB)	20.48

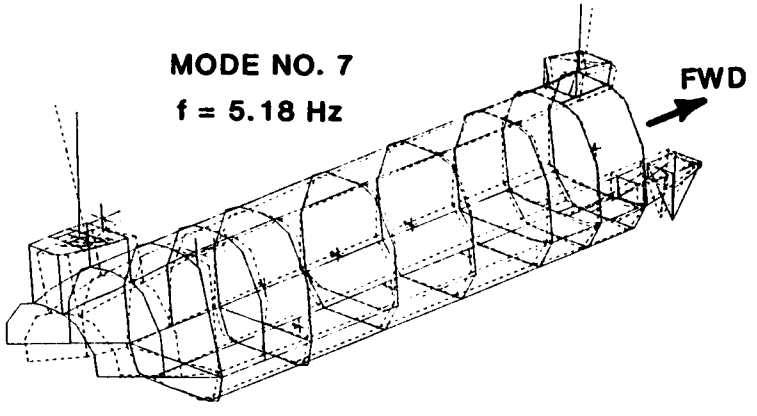

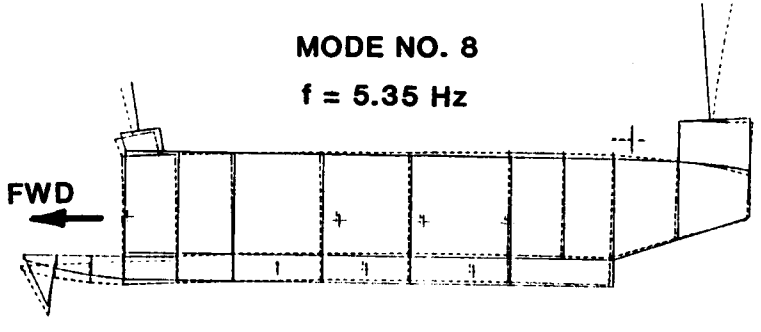

COMPUTATIONAL DEMONSTRATION

FORCED VIBRATION ANALYSIS

Airframe forced responses will be calculated using a set of typical 4/rev (17.9 Hz) rotor hub loads. Output will be a NASTRAN listing of grid point accelerations and plots of airframe acceleration.

COMPUTATIONAL DEMONSTRATION
FORCED VIBRATION ANALYSIS

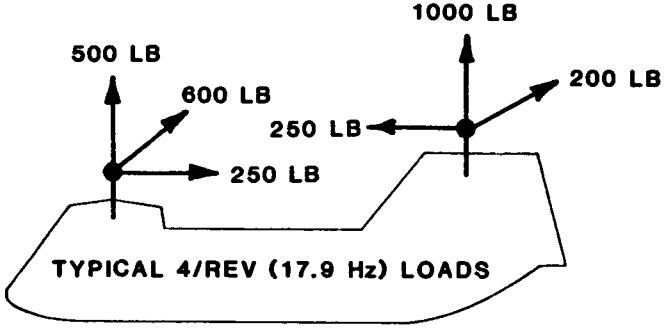

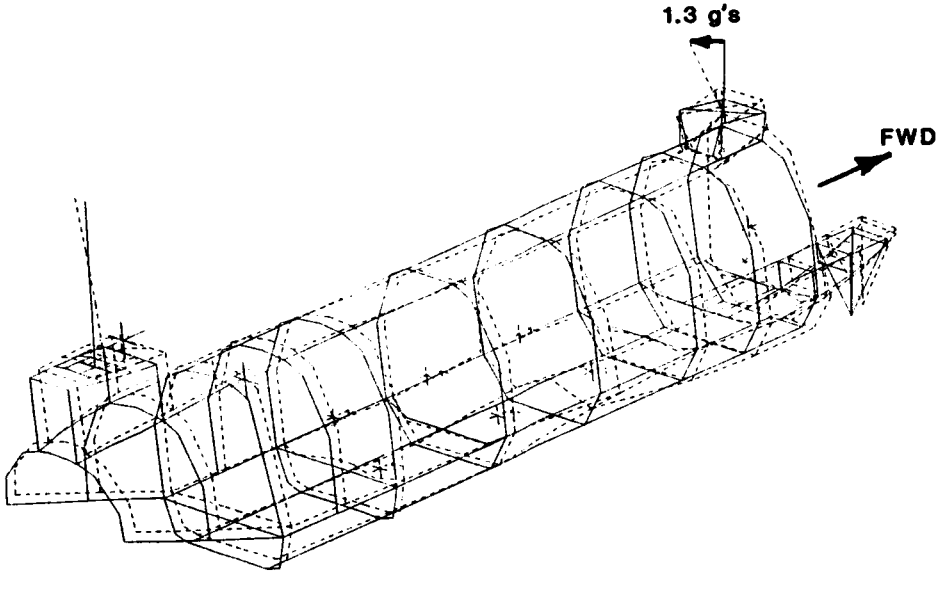

COMPLEX ACCELERATION VECTOR
(MAGNITUDE/PHASE)

POINT ID.	TYPE	T1	T2	T3
51	G	4.550118E-01 341.5156	2.444409E-01 348.6511	3.162162E-01 11.8353
52	G	5.113727E-01 342.6069	1.438370E-01 9.7140	4.047808E-01 6.6928
347	G	4.831087E-01 341.5889	1.526982E-01 357.3269	4.442678E-01 351.3696
383	G	4.880970E-01 343.7505	8.911401E-02 13.2094	3.263945E-01 354.0868
384	G	5.227545E-01 343.3140	2.158444E-01 350.0430	4.403118E-01 354.3242
387	G	4.716969E-01 341.3560	1.445416E-01 359.0054	3.976015E-01 351.1812
388	G	4.992213E-01 341.9746	1.641724E-01 355.8296	4.806691E-01 351.8464
415	G	1.517773E+00 148.8287	1.784953E-01 177.8416	1.531331E-01 37.9244
441	G	2.597423E-01 127.9989	1.864645E-01 349.4238	2.314020E-01 114.5406
457	G	2.185888E-01 121.1939	6.639117E-02 351.4050	2.117628E-01 2.5870
458	G	1.767315E-01 114.2428	5.744375E-02 354.4470	3.947464E-01 359.1655
469	G	4.472799E-01 138.5083	7.883410E-02 4.5548	7.242765E-01 343.1086
637	G	4.229437E-01 339.9268	1.515412E-01 357.1458	3.998097E-01 347.2439

BLANK
PAGE

5.0 Correlation Guides

CORRELATION GUIDES

TEST CONDITIONS AND PARAMETERS

The measured vibration characteristics are available as plots of the magnitude and phase of the transfer function as a function of frequency. The transfer function is defined here as the acceleration divided by the force input of the master shaker (only the master shaker force is used regardless of whether there are one or two shakers). Analytical results will, therefore, be presented in the same normalized fashion.

In the interest of time and economy (and a need to limit the volume of the results presented) only selected results will be presented. Expected test results include data for ten shaker configurations - vertical, lateral, longitudinal pitch and roll at both the forward and aft rotor heads. Correlation plots will be presented for each of the ten shaker configurations at six agreed upon aircraft locations. These locations will be scattered throughout the aircraft and include:

1.) rotor hubs

2.) cockpit

3.) cabin

4.) aft fuselage

5.) engines

CORRELATION GUIDES
TEST CONDITIONS AND PARAMETERS

- **FORMAT OF TEST DATA DICTATES THAT RESULTS BE PRESENTED AS PLOTS OF TRANSFER FUNCTION MAGNITUDE AND PHASE VERSUS FREQUENCY WHERE THE TRANSFER FUNCTION IS DEFINED AS:**
  - **ACCELERATION/MASTER SHAKER FORCE**
- **DATA FOR SIX AGREED UPON AIRCRAFT LOCATIONS WILL BE SHOWN IN THREE AXES (X, Y, Z DIRECTIONS) FOR EACH OF THE TEN TEST SHAKER CONFIGURATIONS. SUGGESTED LOCATIONS INCLUDE:**
  - **ROTOR HUBS**
  - **COCKPIT**
  - **CABIN**
  - **AFT FUSELAGE**
  - **ENGINES**

CORRELATION GUIDES

BASIS FOR CORRELATION

The general ground rules for the correlation effort are summarized on this chart. Adjustments, as required, will be made to the FEM so that it conforms to the test article. Test apparatus other than the hub fixtures (suspension system, shakers, etc.) will not be considered. Forced responses will be calculated for the test conditions with the model in a free-free condition. Test and analytical results displaying forced response as a function of frequency will be compared in graphical form.

CORRELATION GUIDES
BASIS FOR CORRELATION

- THE MODEL 360 NASTRAN FEM WILL BE ADJUSTED TO CONFORM TO THE TEST CONFIGURATION. TEST APPARATUS OTHER THAN THE HUB FIXTURES WILL NOT BE MODELED.

- ROTOR HEAD EXCITING FORCES REPRESENTATIVE OF TEST CONDITIONS WILL BE APPLIED TO THE NASTRAN MODEL TO PREDICT FORCED RESPONSE AS A FUNCTION OF FREQUENCY. THIS ANALYSIS WILL BE PERFORMED WITH THE MODEL IN THE FREE-FREE CONDITION.

- COMPARISONS OF TEST AND ANALYTICAL FORCED RESPONSE WILL CONSTITUTE THE SOLE METHOD OF CORRELATION. RESULTS DISPLAYING STEADY STATE RESPONSE MAGNITUDE AND PHASE AS A FUNCTION OF FREQUENCY WILL BE PRESENTED IN GRAPHICAL FORM.

CORRELATION GUIDES

SAMPLE CORRELATION PLOT

The typical planned format for the forced response correlation plots is illustrated in the accompanying figure. Transfer function magnitude and phase in three axes (x, y, z directions) are shown for one aircraft location. A total of sixty (60) sheets will be required to present the planned data.

CORRELATION GUIDES - SAMPLE CORRELATION PLOT

SIXTY (60) SHEETS REQUIRED

EXCITATION: FWD HUB LONGITUDINAL RESPONSE: FWD HUB (LOC. 2)

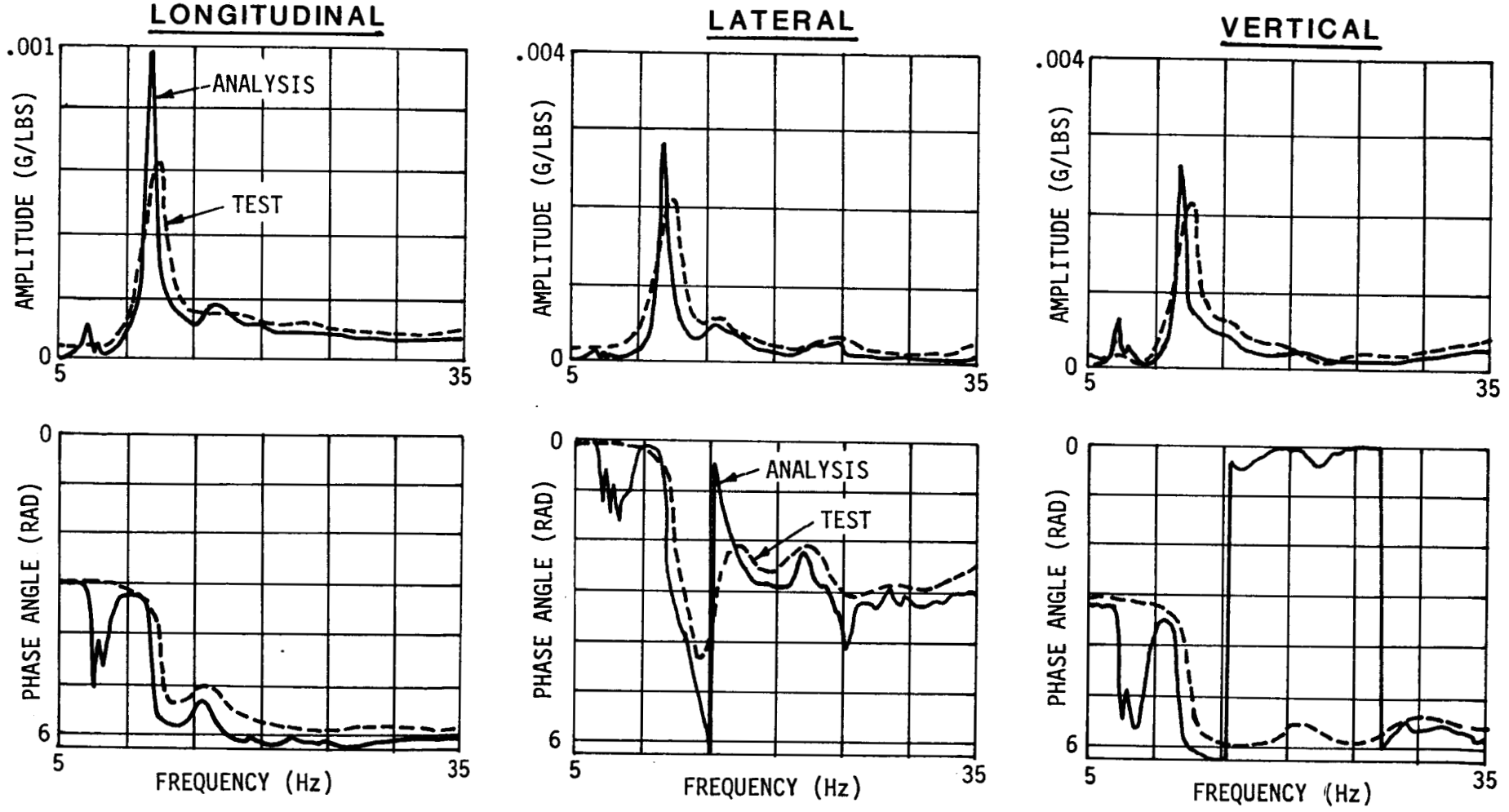

6.0 Modeling Documentation

PRECEDING PAGE BLANK NOT FILMED

PAGE 142 INTENTIONALLY BLANK

6.1 Actual versus Planned Guides

ACTUAL VS PLANNED GUIDES - BACKGROUND

Correlation data, Reference 1, was obtained from a test vehicle which differed significantly from the flight configuration. Modeling activity was directed solely toward the test configuration to reduce effort and cost. This approach eliminated the need for static modeling of items not installed for the test, such as the landing gear. Mass modeling was generally simplified and only one mass model was required. Finally, the vibration model for the computational demonstration and the correlation analysis are the same.

ACTUAL VS PLANNED GUIDES - BACKGROUND

SHAKE TEST DATA FOR MODEL CORRELATION WAS OBTAINED EARLY IN THE PROGRAM USING A TEST VEHICLE (STRIPPED AIRFRAME) WHICH DIFFERED SIGNIFICANTLY FROM THE FLIGHT CONFIGURATION. TO REDUCE EFFORT AND COST, MODELING ACTIVITY WAS DIRECTED SOLELY TOWARD THE TEST CONFIGURATION. THIS ACCOMPLISHED THE FOLLOWING:

- **STATIC MODELING** - ITEMS NOT INSTALLED FOR TEST (SUCH AS LANDING GEAR) WERE NOT MODELED
- **MASS MODELING** - ONLY ONE MASS MODEL REQUIRED. ABSENCE OF NON-STRUCTURAL DISTRIBUTED WEIGHT IN THE TEST CONFIGURATION SIMPLIFIED MASS MODELING.
- **VIBRATION MODELING** - THE MODEL USED FOR THE COMPUTATIONAL DEMONSTRATION IS THE SAME AS THAT USED FOR THE CORRELATION ANALYSIS.

ACTUAL VS PLANNED GUIDES - BACKGROUND

TEST VEHICLE CONFIGURATION

Weight of the test hub fixture included the hub weight plus 70% of the flapping mass. The airframe of the test vehicle was in a stripped condition; i.e., only the basic structure was utilized. Landing gear, the nose enclosure, ramp, doors, some windows, hatches, fairings, avionics, controls, and other non-structural items were not installed. Isolation systems for the cockpit and cabin floor/fuel modules were locked out. Ballast was installed on the cockpit and cabin floor/fuel modules to induce significant inertial loading into the structure.

ACTUAL VS PLANNED GUIDES - BACKGROUND
TEST VEHICLE CONFIGURATION

- TEST HUB FIXTURE EQUAL TO HUB WEIGHT + 70% FLAPPING MASS.
- STRIPPED AIRFRAME: LANDING GEAR, NOSE ENCLOSURE, RAMP, DOORS, WINDOWS, HATCHES, FAIRINGS, AVIONICS, CONTROLS AND OTHER NON-STRUCTURAL ITEMS WERE NOT INSTALLED.
- COCKPIT AND CABIN FLOOR/FUEL MODULE ISOLATION SYSTEMS INACTIVE. (LOCKED OUT)
- COCKPIT AND CABIN FLOOR/FUEL MODULES (NO FUEL) BALLASTED TO OBTAIN MEANINGFUL INERTIA LOADS ON PRIMARY STRUCTURE.

ACTUAL VERSUS PLANNED STATIC MODELING GUIDES

STRUCTURE NOT MODELED

The figure illustrates the additional items not installed in the test vehicle and, consequently, not modeled. However, the support structure for these items was on the aircraft and was, therefore, modeled.

ACTUAL VS PLANNED STATIC MODELING GUIDES
STRUCTURE NOT MODELED

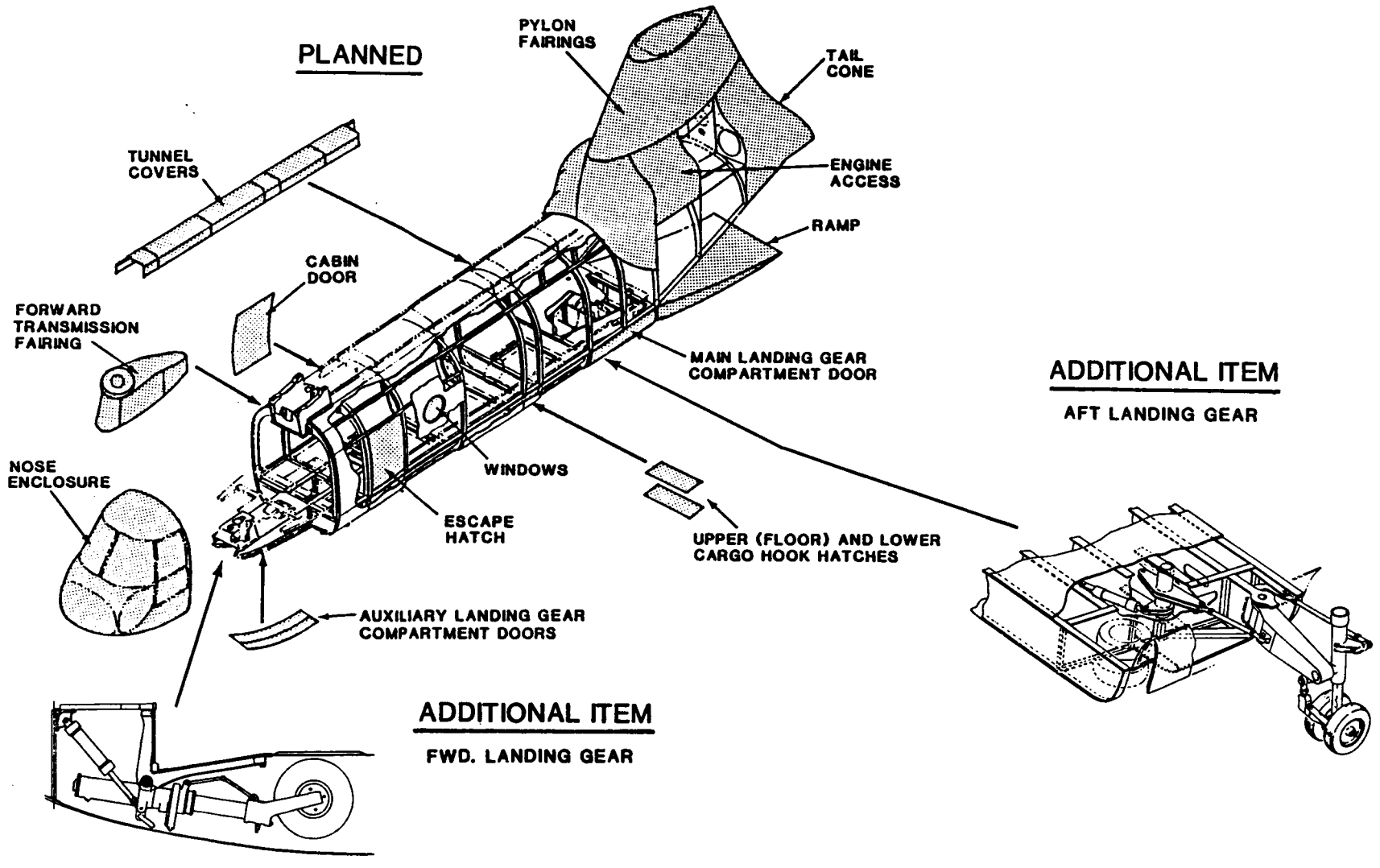

ACTUAL VS PLANNED STATIC MODELING GUIDES

ISOLATOR MODELING - CABIN FLOOR

Changes in the isolator modeling were superficial. The CELAS element intended to represent the isolator static stiffness was replaced by a CONROD to model the floor in the locked condition.

ACTUAL VS PLANNED STATIC MODELING GUIDES
ISOLATOR MODELING – CABIN FLOOR

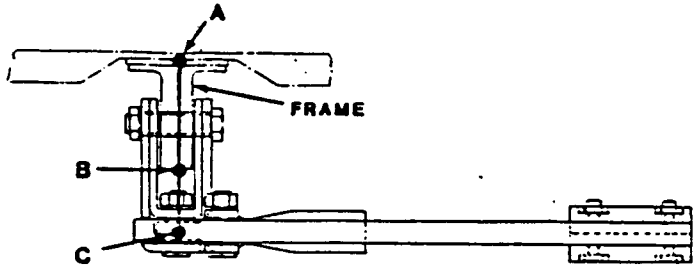

TOP VIEW

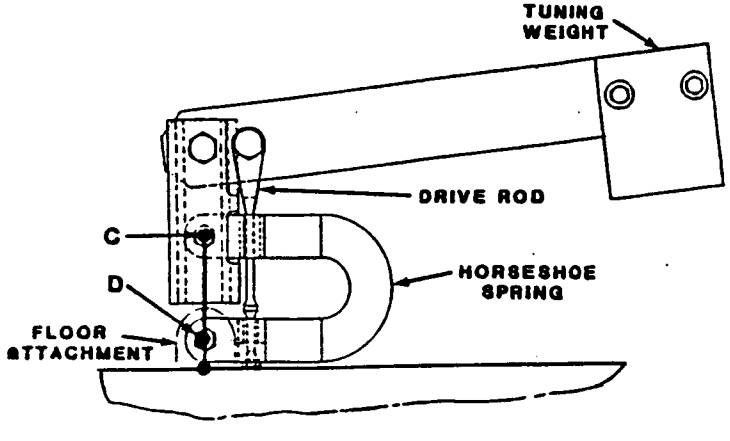

SIDE VIEW

PLANNED MODELING

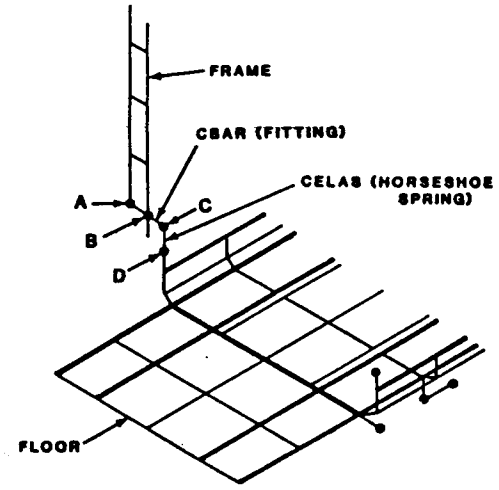

- DUPLICATES ISOLATOR STATIC STIFFNESS

ACTUAL MODELING

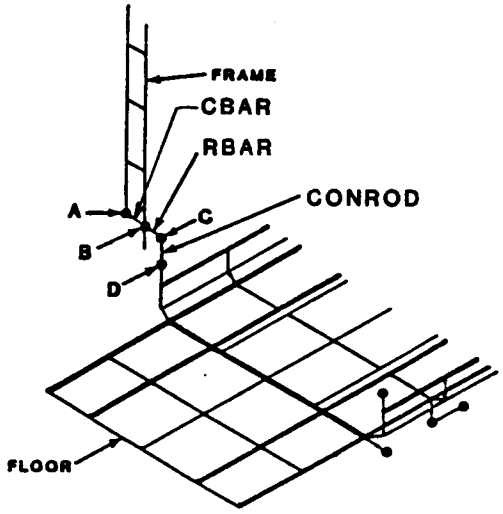

- LOCKED CONFIGURATION

ACTUAL VERSUS PLANNED STATIC MODELING GUIDES

FORWARD TRANSMISSION COVER AND ROTOR SHAFT

Static test load deflection data was used as the basis for modeling the transmission cover. Consequently, the simplest model capable of matching the measured hub deflection data was used. The rotor shaft stiffness was calculated as previously outlined in the modeling guides, and the cover properties were selected to match the measured hub load deflection data.

ACTUAL VS PLANNED STATIC MODELING GUIDES
FORWARD TRANSMISSION COVER AND ROTOR SHAFT

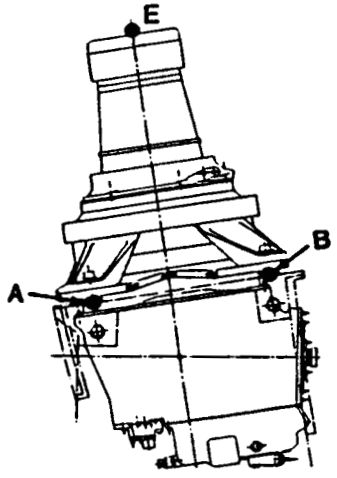

PLANNED MODELING

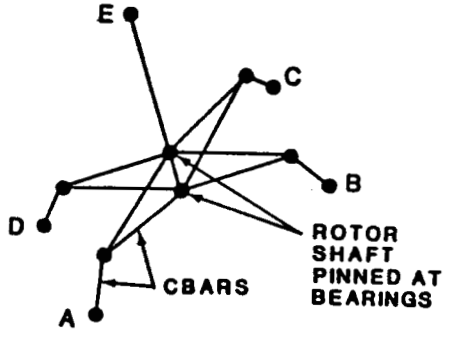

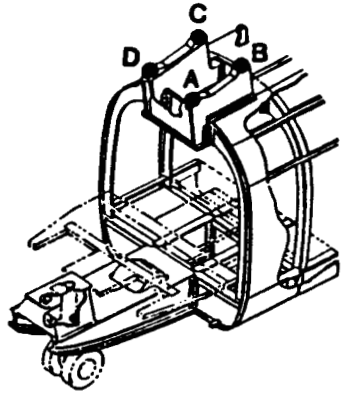

ACTUAL MODELING

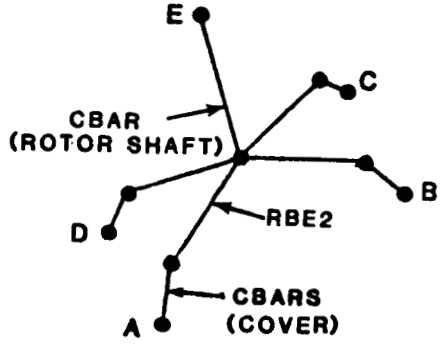

- CALCULATED ROTOR SHAFT PROPERTIES
- CBAR PROPERTIES FOR COVER SELECTED TO MATCH STATIC TEST DATA AT HUB

ACTUAL VS PLANNED STATIC MODELING GUIDES

AFT TRANSMISSION COVER AND ROTOR SHAFT

The final configuration of the aft transmission cover more nearly resembles the actual cover geometry. Element properties were based on a detailed analysis of the aft cover.

ACTUAL VS PLANNED STATIC MODELING GUIDES
AFT TRANSMISSION COVER AND ROTOR SHAFT

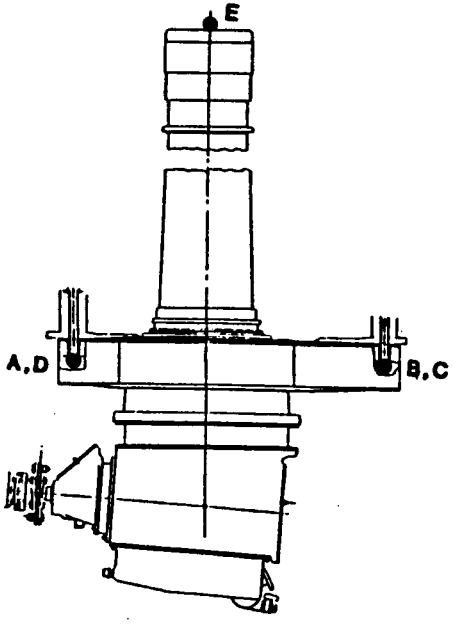

PLANNED MODELING

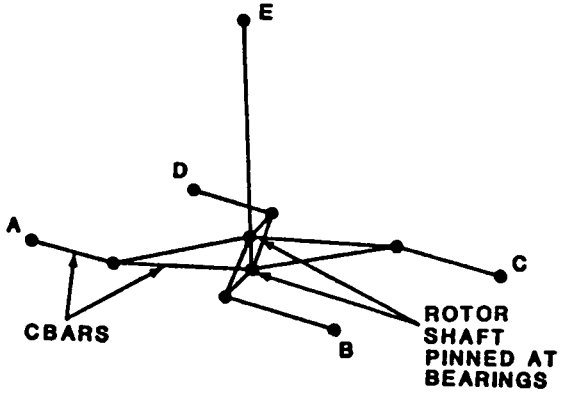

ACTUAL MODELING

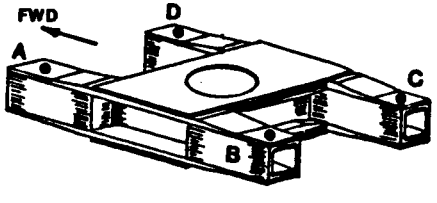

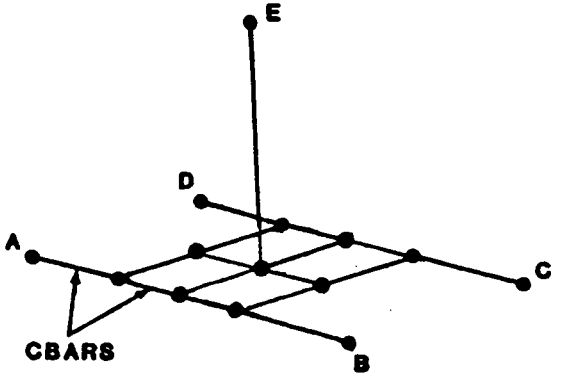

ACTUAL VERSUS PLANNED MASS MODELING GUIDES

TREATMENT OF DISTRIBUTED MASS ITEMS

No computer-based weight records were maintained for the Model 360 and a panel point loading diagram was not available. In lieu of the planned modeling, the procedure outlined on the following page was employed. The distributed mass was identified as being composed of the primary structure (3029 lb.) plus secondary structure and equipment (1515 lb.). Weight of the primary structure was handled as follows:

a) Actual frame weights (11 frames) were distributed by the weights engineer to an average of 12 grid points on the outer frame cap.

b) Drive shaft tunnel beam weight was manually distributed to the connecting points on the outer frame caps assuming uniform beam weight.

c) Skin weight and other QUAD4 items were obtained from the grid point weight generator using the true density values.

d) The remaining structural weight was assumed to be concentrated in the CBAR elements. Density was adjusted until the grid point weight generator indicated the correct total primary structure weight.

The cabin floor assembly (643 lb.) is the single largest piece of secondary structure. The weight was manually distributed to grid points in the assembly assuming a uniform structural weight. Remaining miscellaneous structure and equipment was distributed manually to appropriate grid points.

ACTUAL VS PLANNED MASS MODELING GUIDES
TREATMENT OF DISTRIBUTED MASS ITEMS

PLANNED MODELING

MASS MODELING GUIDES

TREATMENT OF DISTRIBUTED MASS ITEMS

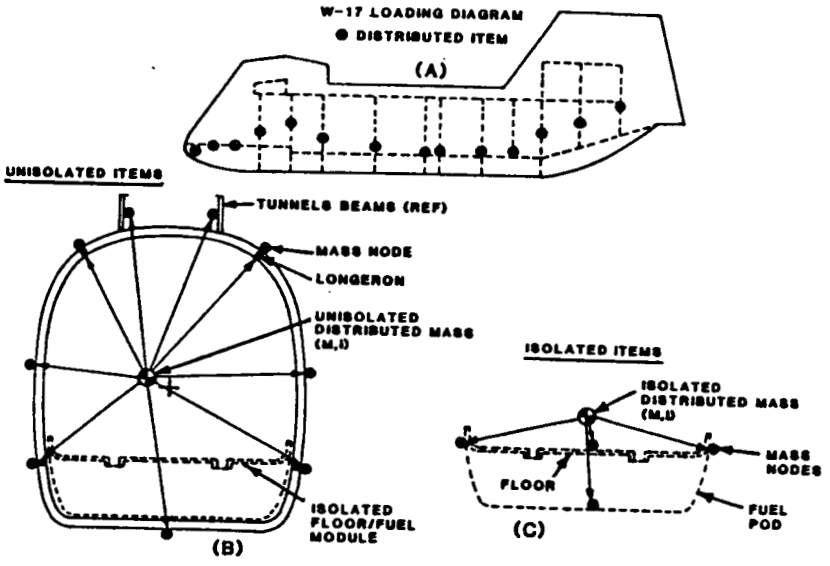

- DISTRIBUTED MASS ITEMS LUMPED AT NODES AS SHOWN
- MAINTAIN VERTICAL AND HORIZONTAL CG, AND THE ROLL INERTIA WITHIN THE LIMITS OF THE NASTRAN MODEL

ACTUAL MODELING

PRIMARY STRUCTURE

- ACTUAL FRAME WEIGHTS MANUALLY DISTRIBUTED TO GRID POINTS ON OUTER CAP.
- TUNNEL BEAM WEIGHT MANUALLY DISTRIBUTED TO CONNECTING POINTS ON OUTER FRAME CAPS ASSUMING UNIFORM BEAM WEIGHT
- SKIN WEIGHTS AND OTHER QUAD 4 ITEMS OBTAINED FROM GRID POINT WEIGHT GENERATOR USING TRUE DENSITY.
- REMAINING STRUCTURE (LONGERONS, BEAM ETC.) MODELED WITH CBARS USING EFFECTIVE AREA. DENSITY ADJUSTED TO OBTAIN CORRECT TOTAL WEIGHT FROM GRID POINT WEIGHT GENERATOR.

SECONDARY STRUCTURE & EQUIPMENT

- CABIN FLOOR/FUEL ASSEMBLY WEIGHT MANUALLY DISTRIBUTED TO ASSEMBLY GRID POINTS ASSUMING UNIFORM STRUCTURAL WEIGHT.
- MISCELLANEOUS STRUCTURE AND EQUIPMENT DISTRIBUTED MANUALLY TO APPROPRIATE GRID POINTS.

ACTUAL VS PLANNED MASS MODELING GUIDES

WEIGHT DISTRIBUTION PROCEDURE FOR UNIFORM STRUCTURE

Illustrated in this figure is the method used to distribute the weight of the cabin floor/fuel assembly. Since this structure is composed principally of large honeycomb panels, the assumption of a uniform structural weight seems justified. Using the procedure shown, weight is distributed to all of the grid points in the assembly.

ACTUAL VS PLANNED MASS MODELING GUIDES
WEIGHT DISTRIBUTION PROCEDURE FOR UNIFORM STRUCTURE

0 ASSUMPTION : STRUCTURE COMPRISED OF PANELS HAVING CONSTANT WEIGHT PER UNIT AREA

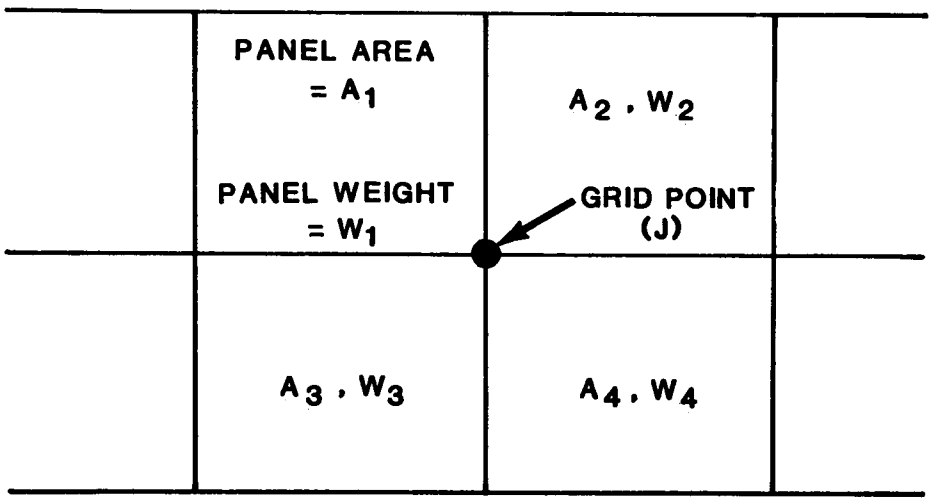

$$\text{TOTAL AREA} = \Sigma A_i$$

$$\text{PANEL WEIGHT} = W_i = \frac{A_i \times \text{TOTAL WT.}}{\Sigma A_i}$$

$$\text{GRID POINT (J) WT.} = W_J = \frac{W_1 + W_2 + W_3 + W_4}{4}$$

ACTUAL VS PLANNED MASS MODELING GUIDES

TREATMENT OF CONCENTRATED MASS ITEMS

Concentrated masses were treated as originally planned except for two items. The rotor mass was reduced to include only 70% of the flapping mass in order to match the shake test configuration. Similarly, the landing gear was not included in the model since it was not installed.

ACTUAL VS PLANNED MASS MODELING GUIDES
TREATMENT OF CONCENTRATED MASS ITEMS

CONCENTRATED MASS ITEMS TREATED AS PLANNED WITH THE FOLLOWING EXCEPTIONS:

- ROTOR MASS INCLUDED ONLY 70% OF FLAPPING MASS
- LANDING GEAR NOT INCLUDED IN MODEL

ACTUAL VS PLANNED VIBRATION MODELING GUIDES

CHANGES FROM STATIC TO VIBRATION FEM

Since the static model reflected the test configuration, planned changes from the static to vibration model were not necessary. Based on results of an early check run, the forward engine attachment to the support beams was modified.

ACTUAL VS PLANNED VIBRATION MODELING GUIDES
CHANGES FROM STATIC TO VIBRATION FEM

PLANNED CHANGES

- REDUCE ROTOR FLAPPING MASS FROM 100% TO 70%
- CONVERT FLOOR ISOLATION SYSTEMS TO LOCKED CONFIGURATION

ACTUAL CHANGES

- ABOVE ITEMS INCLUDED IN THE STATIC MODEL , NO CHANGE REQUIRED
- MODIFIED ENGINE ATTACHMENT TO SUPPORT BEAM

ACTUAL VERSUS PLANNED COMPUTATIONAL DEMONSTRATION

DEMONSTRATION CASES

Original planning specified a number of demonstration cases that were to be performed for a 30,500 lb. gross weight flight configuration. Changes to the planned demonstration were as follows:

1. Analysis was performed for the shake test configuration and gross weight.

2. In lieu of the 3 g pull-up, static internal loads were calculated for a laboratory static test condition with the aircraft supported at the rotors and a load applied at the center cargo hook.

3. No forced vibration was performed for the demonstration case. Since the configuration was the same as the test configuration, forced response was confined to the analysis for correlation.

ACTUAL VS PLANNED COMPUTATIONAL DEMONSTRATION
DEMONSTRATION CASES

FOR 30,500 LB DESIGN GROSS WEIGHT PERFORM FOLLOWING:

- **RIGID BODY CHECK**
- **STATIC ANALYSIS FOR INTERNAL MEMBER LOADS**
  - **3.0g PULL-UP FROM SYMMETRIC DIVE**
- **NORMAL MODES ANALYSIS**
  - **NATURAL FREQUENCIES AND MODES**
- **FORCED VIBRATION ANALYSIS**
  - **REPRESENTATIVE b/REV LOADS**

PLANNED DEMONSTRATION

CHANGES TO PLANNED DEMONSTRATION

- ANALYSIS PERFORMED FOR SHAKE TEST AIRCRAFT CONFIGURATION AND GROSS WEIGHT
- STATIC INTERNAL LOADS ANALYSIS FOR LABORATORY TEST CONFIGURATION WITH APPLIED LOAD AT THE CARGO HOOK REACTED AT THE HUBS
- NO FORCED VIBRATION AS PART OF DEMONSTRATION. FORCED RESPONSE CONFINED TO ANALYSIS FOR CORRELATION WITH SHAKE TEST

ACTUAL VERSUS PLANNED COMPUTATIONAL DEMONSTRATION

ACTUAL STATIC LOAD CASE

The accompanying figure shows the loading used for static analysis to determine internal member loads. This configuration duplicates a static test condition and was used in lieu of the 3.0 g pull-up condition originally planned.

ACTUAL VS PLANNED COMPUTATIONAL DEMONSTRATION
ACTUAL STATIC LOAD CASE

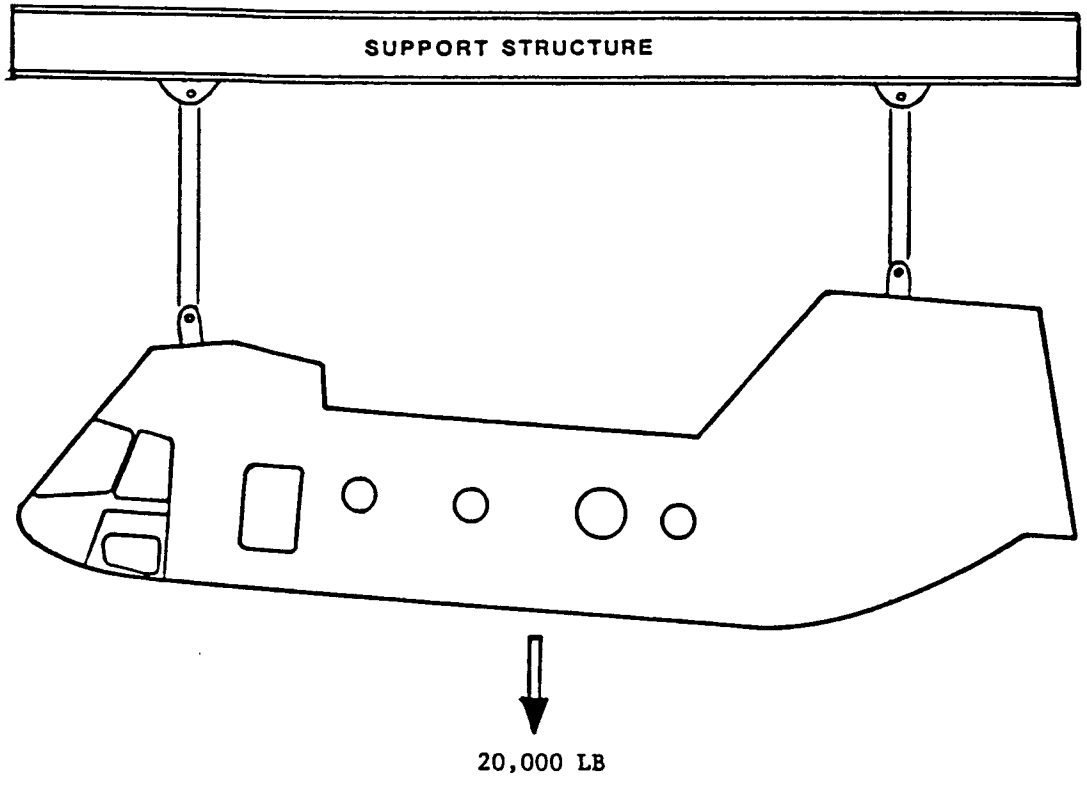

ACTUAL VS PLANNED CORRELATION GUIDES

TEST CONDITIONS AND PARAMETERS

For one airframe location, an analysis versus test comparison consists of 6 plots; i.e., amplitude and phase in the X, Y and Z directions. As a cost saving measure, the total number of comparisons was reduced from 60 (360 plots) to 28 (168 plots). Comparison plots were prepared for the following locations/conditions:

1) Rotor hub drive point response for three rotor forces and two moments. Forward hub response shown for forward rotor excitation and aft hub response for aft rotor excitation.

2) Response at three airframe locations for three forward and three aft rotor exciting forces.

ACTUAL VS PLANNED CORRELATION GUIDES
TEST CONDITIONS AND PARAMETERS

DATA FOR SIX AGREED UPON AIRCRAFT LOCATIONS WILL BE SHOWN IN THREE AXES (X, Y, Z DIRECTIONS) FOR EACH OF THE TEN TEST SHAKER CONFIGURATIONS. SUGGESTED LOCATIONS INCLUDE:

- ROTOR HUBS
- COCKPIT
- CABIN
- AFT FUSELAGE
- ENGINES

PLANNED GUIDE

CHANGES TO PLANNED GUIDE

FOR COST REASONS, THE TOTAL NUMBER OF ANALYSIS VERSUS TEST COMPARISONS (AMPLITUDE AND PHASE - X,Y,Z DIRECTIONS) WAS REDUCED TO THE FOLLOWING:

- DRIVE POINT (ROTOR HUB) RESPONSE FOR THREE ROTOR FORCES AND TWO MOMENTS
  - FORWARD HUB RESPONSE FOR FORWARD ROTOR EXCITATION
  - AFT HUB RESPONSE FOR AFT ROTOR EXCITATION
- RESPONSE AT THREE AIRFRAME LOCATIONS FOR THREE FORWARD AND THREE AFT ROTOR EXCITING FORCES

6.2 Static Modeling

PRECEDING PAGE BLANK NOT FILMED

STATIC MODELING

CURRENT MODEL 360 NASTRAN STRUCTURAL MODEL

The accompanying figure shows the NASTRAN structural model developed under this program. Statistics for the model indicate a total of 2869 structural nodes (grid points) and 5686 structural elements. Subsequent figures in this section present a more detailed view of each superelement comprising the complete model. It should be noted that the new model has roughly twice the number of elements and grid points as the earlier model.

STATIC MODELING

CURRENT MODEL 360 NASTRAN STRUCTURAL MODEL

2869 STRUCTURAL NODES
5686 STRUCTURAL ELEMENTS

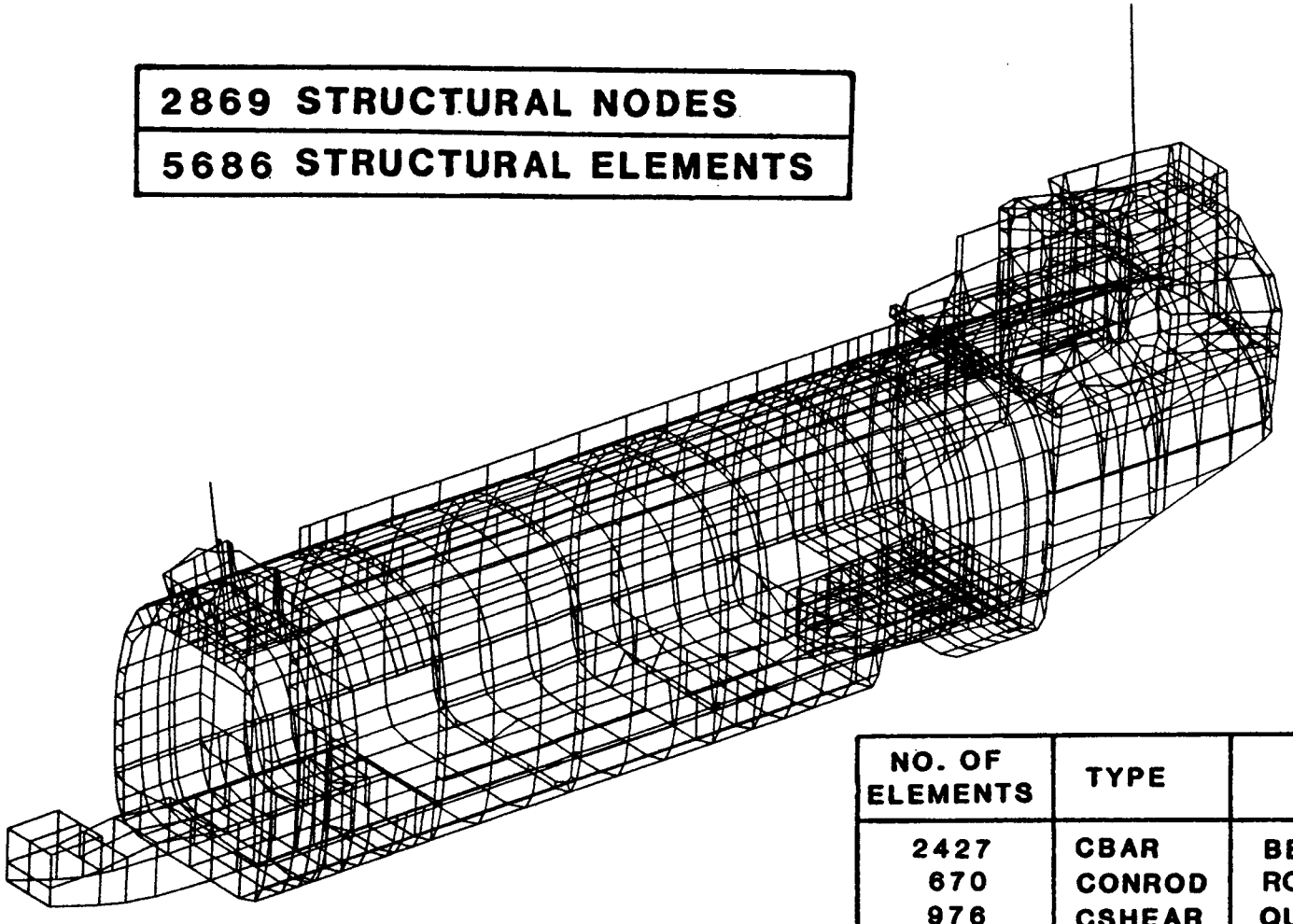

NO. OF ELEMENTS	TYPE	DESCRIPTION
2427	CBAR	BEAM
670	CONROD	ROD
976	CSHEAR	QUADRILATERAL SHEAR
1512	CQUAD4	QUADRILATERAL PLATE
101	CTRIA3	TRIANGULAR PLATE

STATIC MODELING

FORWARD FUSELAGE/COCKPIT - SUPERELEMENT NO. 1

This figure illustrates the NASTRAN model for the forward fuselage/cockpit superelement. For clarity, the cockpit floor panel is shown separately. In a normal installation, the cockpit floor panel is supported from the airframe on isolators. For the test configuration modeled here, the isolators were locked. Included in this superelement are the forward transmission and rotor shaft.

STATIC MODELING
FORWARD FUSELAGE/COCKPIT – SUPERELEMENT NO. 1

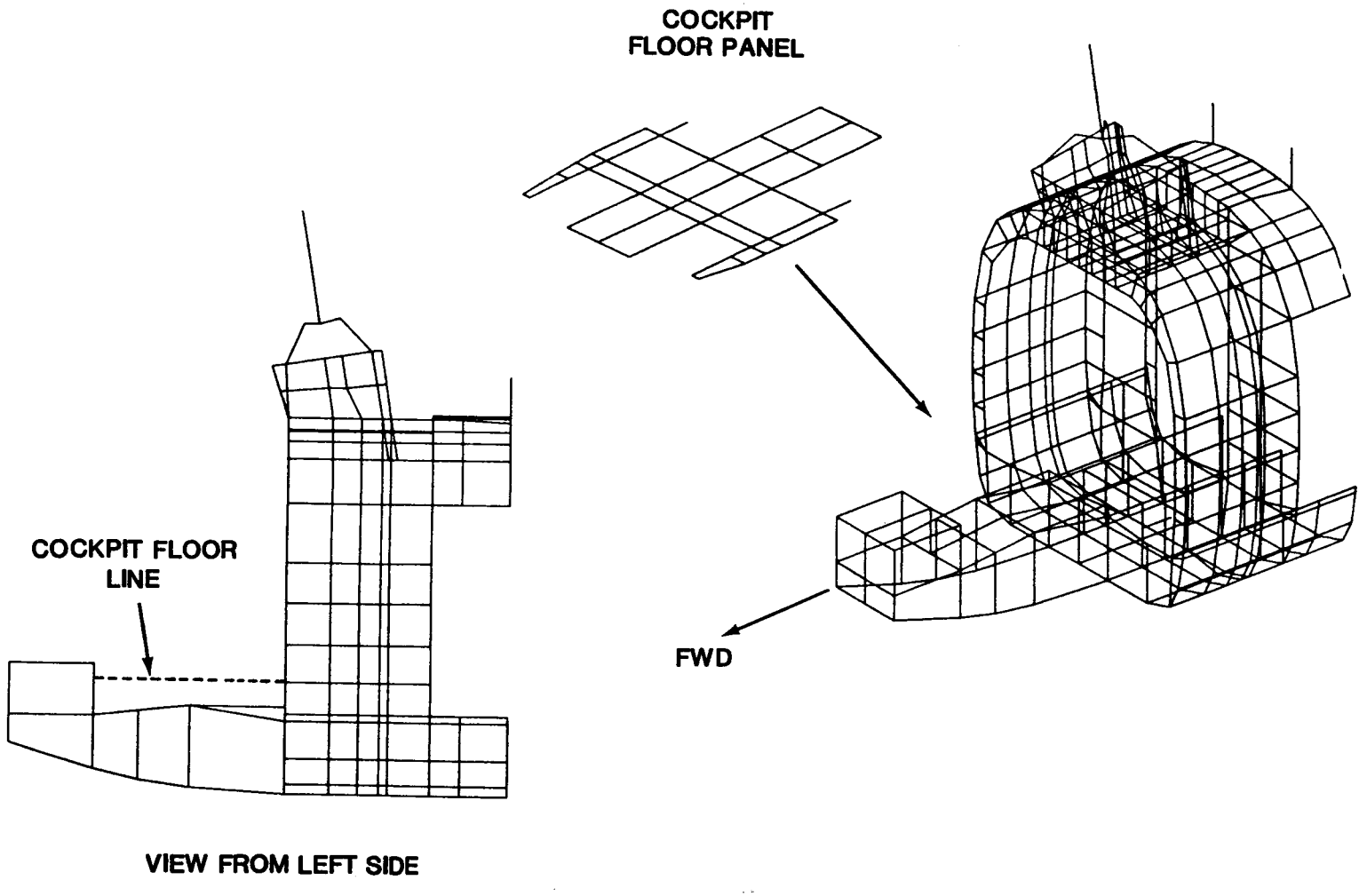

STATIC MODELING

CENTER FUSELAGE - SUPERELEMENT NO. 2

The NASTRAN model of the center fuselage, superelement No. 2, is shown in this figure. Note that the floor, which is an independent structural element, is not part of the superelement.

STATIC MODELING
CENTER FUSELAGE - SUPERELEMENT NO. 2

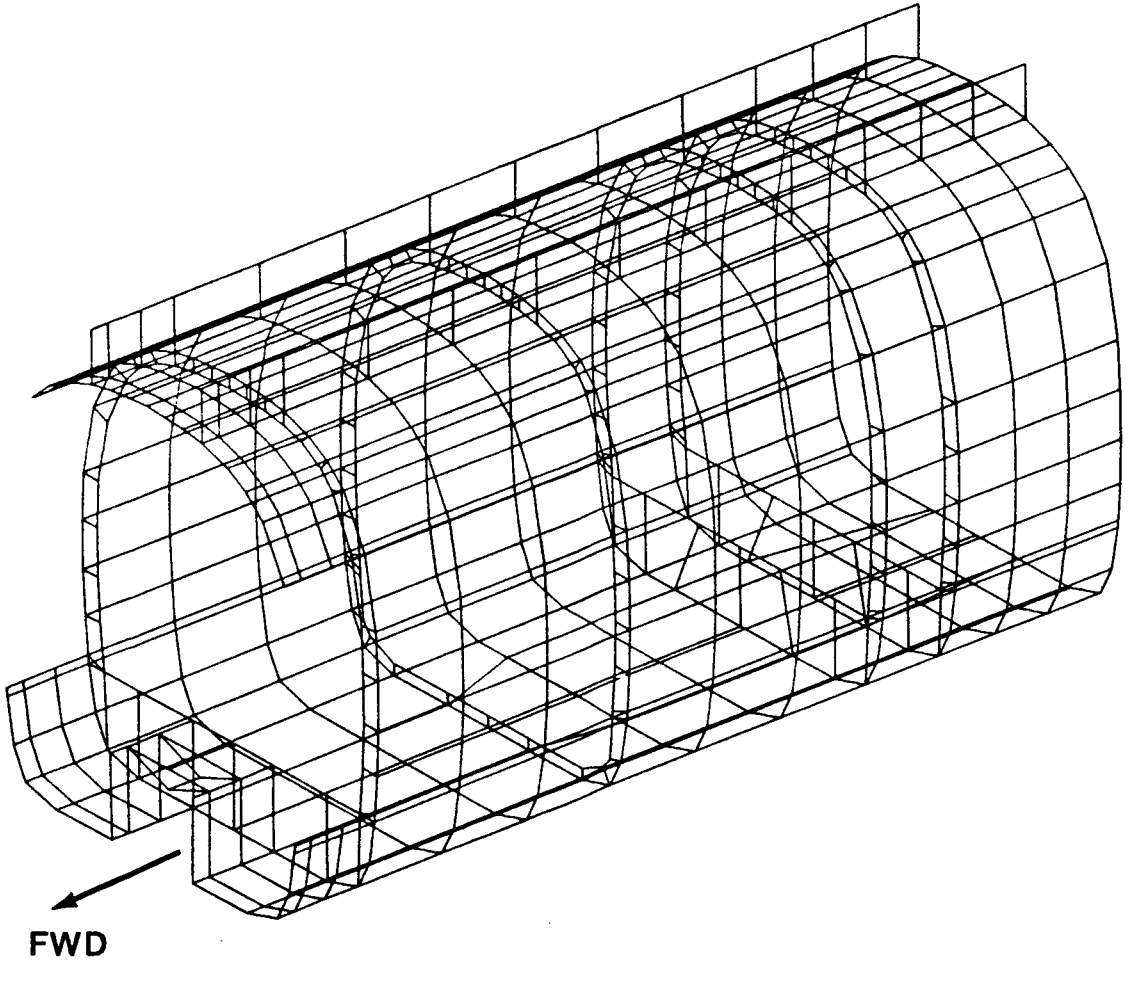

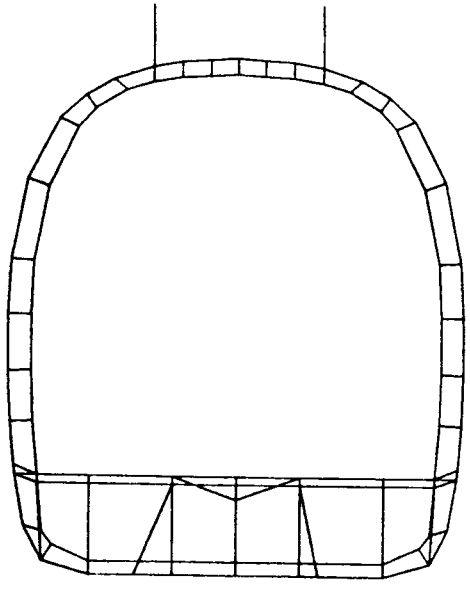

VIEW LOOKING AFT

STATIC MODELING

CABIN FLOOR/FUEL ASSEMBLY - SUPERELEMENT NO. 3

As illustrated here, the upper surface of the cabin floor/fuel assembly is a flat panel with a rolled up edge on each side. Below the top surface are three box-like compartments which house the fuel cells. The floor assembly is supported from the cabin structure at four locations on each side.

STATIC MODELING

CABIN FLOOR/FUEL ASSEMBLY - SUPERELEMENT NO. 3

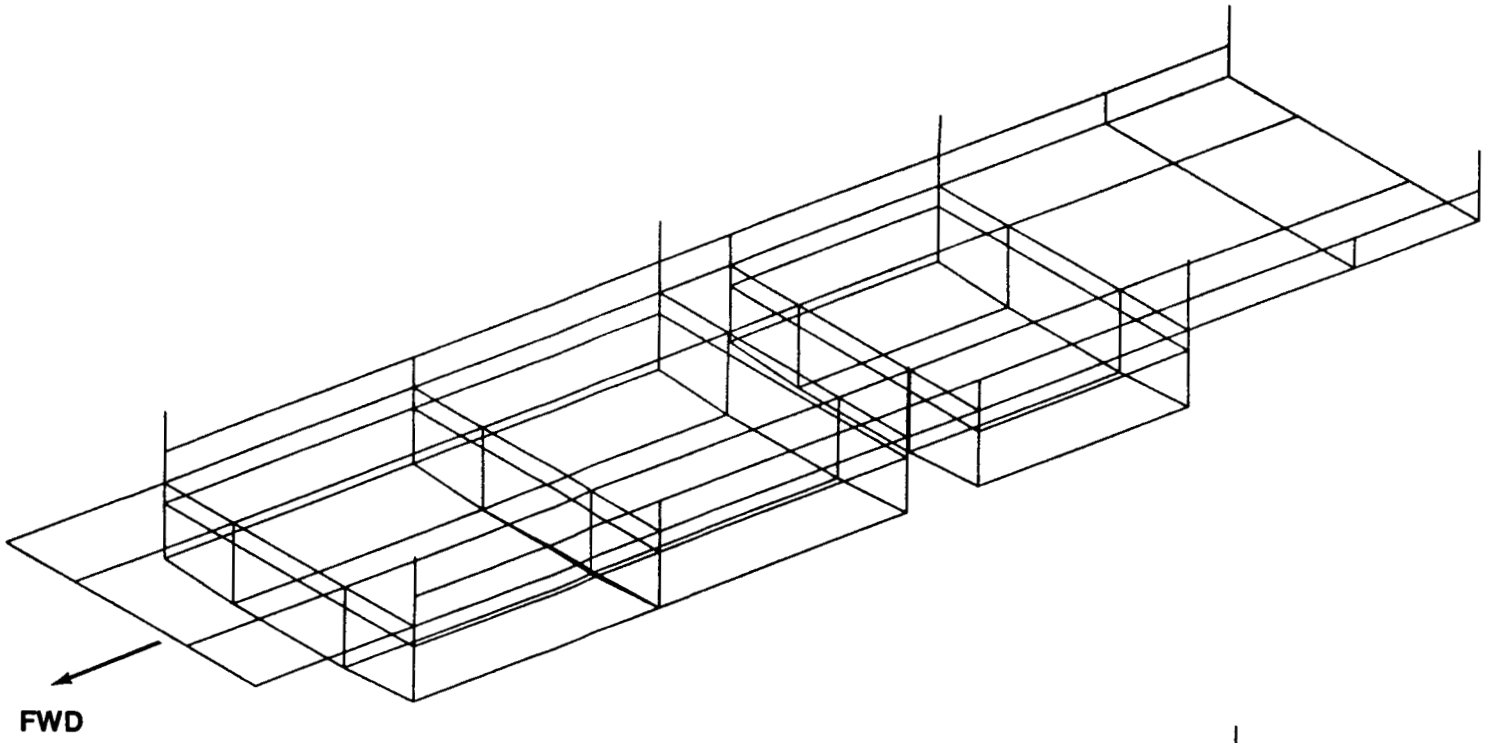

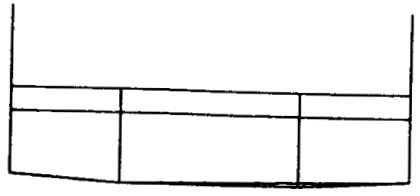

VIEW LOOKING AFT

STATIC MODELING

MAIN LANDING GEAR COMPARTMENT - SUPERELEMENT NO. 4

Shown here is the NASTRAN model of the main landing gear compartment, superelement No. 4, which contains all of the support provisions for the retractable main gear. Not included in the model are the landing gear, linkages, actuators and doors.

STATIC MODELING
MAIN LANDING GEAR COMPARTMENT - SUPERELEMENT NO. 4

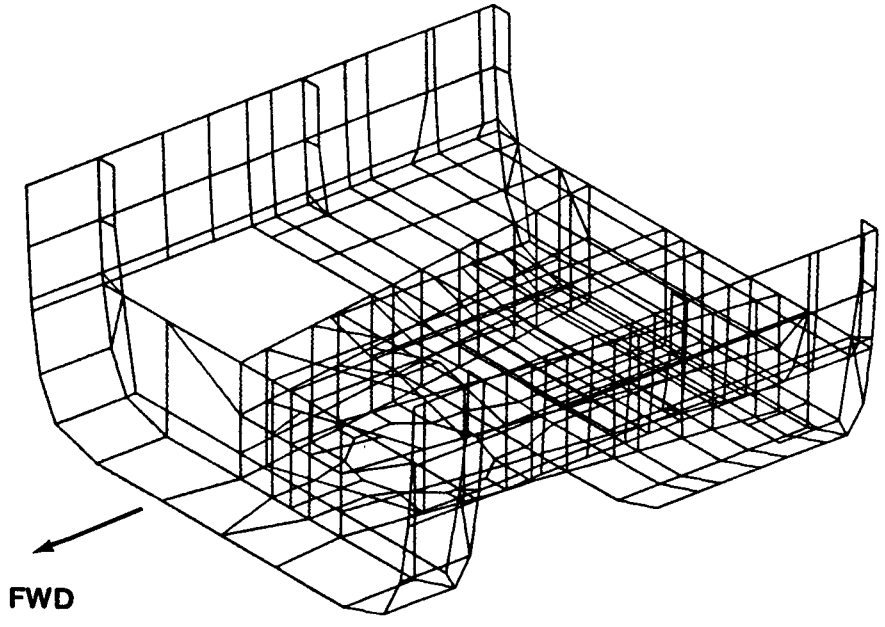

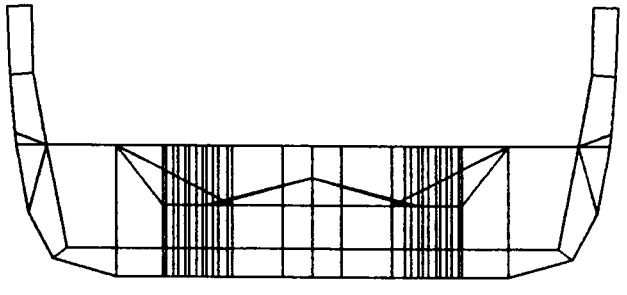

VIEW LOOKING AFT

STATIC MODELING

AFT FUSELAGE - SUPERELEMENT NO. 5

Superelement No. 5 presented in this figure includes the portion of the center cabin above the landing gear compartment in addition to the aft fuselage. The aft rotor shaft, transmission cover and engines are also a part of this model.

STATIC MODELING
AFT FUSELAGE - SUPERELEMENT NO. 5

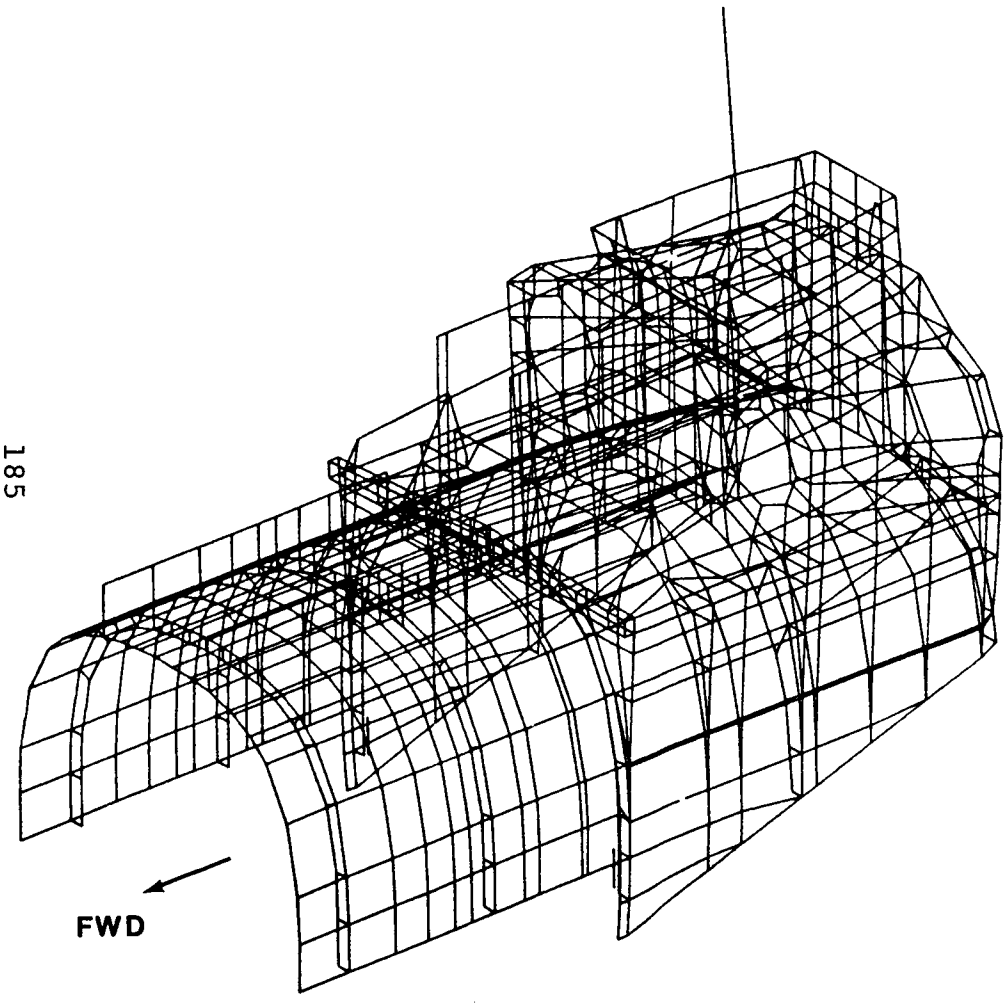

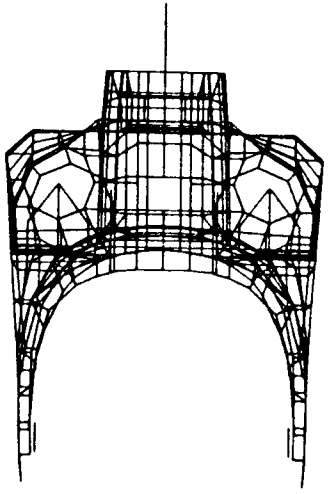

VIEW LOOKING AFT

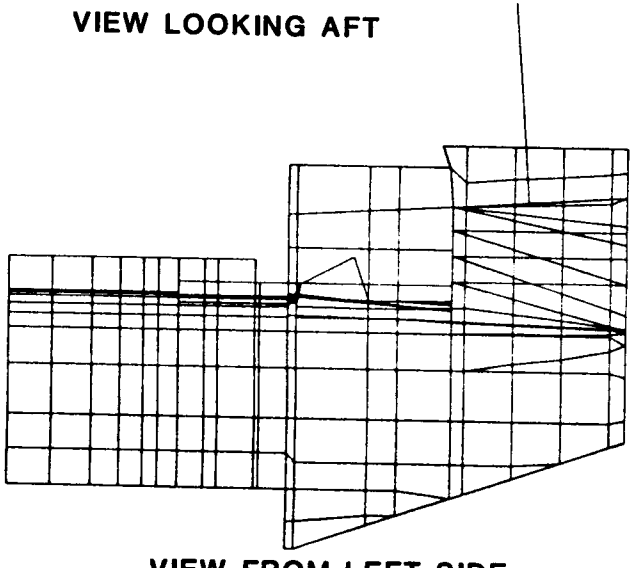

VIEW FROM LEFT SIDE

6.3 Mass Modeling

MASS MODELING

COMPARISON OF FEM AND TEST VEHICLE

The accompanying comparison between the NASTRAN model weight and the test vehicle shows a small difference of 128 lb. in the weight and 4.9 inches in the center of gravity location. Efforts to improve the agreement were not successful.

MASS MODELING
COMPARISON OF FEM AND TEST VEHICLE

	FEM	TEST VEHICLE
PRIMARY STRUCTURE	3029	3029
SECONDARY STRUCTURE & EQUIPMENT	1515.2	———
CONCENTRATED ITEMS	13613.5	———
TOTAL WEIGHT	18157.7 LB	18285.5 LB
CENTER OF GRAVITY	STA. 280.6	STA. 285.5

MASS MODELING

DISTRIBUTION OF MODEL WEIGHT

The accompanying chart shows the distribution of weight within the model. Out of a total of 3029 lb. of primary structure, 75% or 2282 lb. was distributed by the grid point weight generator. The remaining model weight, which totals 15,876 lbs., was manually distributed to 330 locations using CONM2 mass elements.

MASS MODELING
DISTRIBUTION OF MODEL WEIGHT

- 75% (2282 LB) OF PRIMARY STRUCTURE WEIGHT DISTRIBUTED BY GRID POINT WEIGHT GENERATOR

GRID POINT WEIGHT GENERATOR		
— QUAD 4's	708	2282
— CBARS	1574	
FRAME WEIGHT		555
TUNNEL BEAM WEIGHT		81
WEIGHT ADJUSTMENT (SEE NOTE)		111
TOTAL PRIMARY STRUCTURE		3029 LB

NOTE: ACTUAL ERROR IN PREDICTED WEIGHT DUE TO UNDEFINED FILLING AND SHIMMING IN AFT FUSELAGE

- REMAINING MODEL WEIGHT (15876 LB) MANUALLY DISTRIBUTED TO 330 LOCATIONS USING CONM2 MASS ELEMENTS

MASS MODELING

SECONDARY STRUCTURE, EQUIPMENT AND CONCENTRATED WEIGHTS

Items grouped into the categories of secondary structure and equipment and concentrated weights are summarized in the accompanying figure. The sum of the concentrated weights (13613.5 lb) constitutes 75% of the total aircraft weight.

MASS MODELING

SECONDARY STRUCTURE, EQUIPMENT AND CONCENTRATED WEIGHTS

SECONDARY STRUCTURE & EQUIPMENT

FLOOR ASSEMBLY	643.
FUEL CELLS	350.
FUEL SYSTEM (PARTIAL)	123.1
FLOOR INSTALLATION RIGGING	26.3
COCKPIT & CABIN ISOLATION UNITS	191.
WINDOWS (4)	19.5
RAMP HINGE & ACTUATOR FITTINGS	32.2
COCKPIT FLOOR PANEL	68.
FWD LANDING GEAR SKIN PANELS	24.
JACK PADS	10.9
MISC. SUPPORT PROVISIONS	22.2
STRAIN GAGE WIRING	5.
	1515.2 LB

CONCENTRATED WEIGHT ITEMS

FORWARD HUB ASSEMBLY	1471.5
FORWARD ROTOR TRANSMISSION	861.5
COCKPIT BALLAST (INCLUDING SEATS)	1521
CABIN BALLAST	5100
COMBINING TRANSMISSION	248
ENGINE & TRANSMISSIONS	1838
AFT ROTOR TRANSMISSION	1108
AFT HUB ASSEMBLY	1465.5
	13613.5 LB

6.4 Vibration Modeling

PRECEDING PAGE BLANK NOT FILMED

VIBRATION MODELING

MODEL CONFIGURATION

The model configuration for vibration modeling is summarized in this figure. Over the frequency range of interest, the free-free condition is assumed to adequately represent the shake test suspension. The structural model and weight distribution were based on the configuration of the shake test vehicle which included ballast in both the cockpit and cabin. Cockpit and cabin isolation in the test vehicle (and the model) were locked to reduce the dynamic complexity. Based on preliminary rotor-fuselage coupling studies, the test hub weight included only 70% of the rotor flapping mass.

VIBRATION MODELING
MODEL CONFIGURATION

- FREE – FREE CONDITION
- SHAKE TEST CONFIGURATION WITH COCKPIT AND CABIN BALLAST
- COCKPIT AND CABIN ISOLATORS LOCKED
- 70% ROTOR FLAPPING MASS

VIBRATION MODELING

CHANGE IN ENGINE MODEL

Based on an early check run, attachment of the engine mass to the support beam at the forward end of the engine was modified. The original model was connected to the support beam at only two points and showed large local deflections. Investigation indicated that the support beam was correctly modeled as a built-up box beam. However, the engine fitting which actually spans the upper surface of the beam was not correctly modeled. The model was, therefore, modified to provide attachment at grid points on both the forward and aft edge of the support beam. The pictorial representation of the engine is purely a cosmetic change that shows how a single NASTRAN rigid-body element (RBE) was specified to connect the engine c.g. and the three support points.

VIBRATION MODELING
CHANGE IN ENGINE MODEL

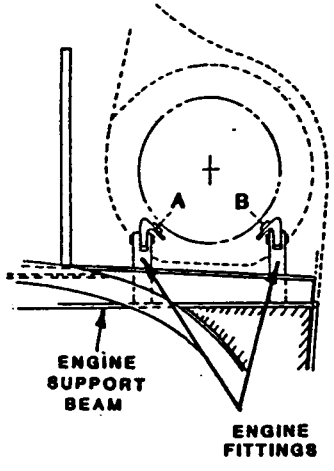

STA 480
FORWARD SUPPORT

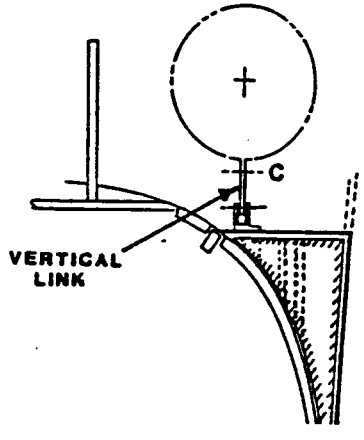

STA 451
AFT SUPPORT

STATIC MODELING

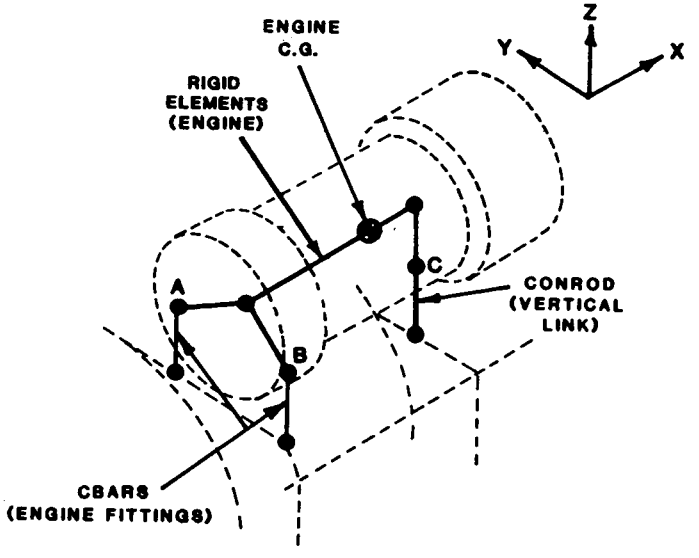

VIBRATION MODELING

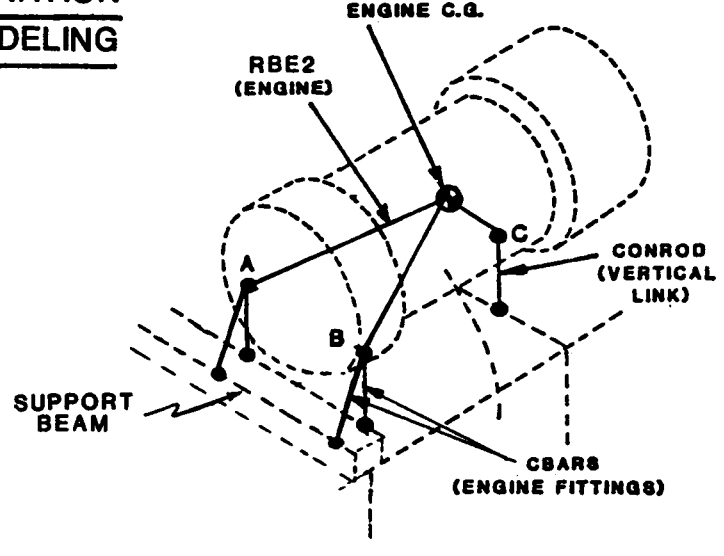

6.5 Computational Demonstration

DEMONSTRATION CASES

Several demonstration cases were performed to show that the FEM generates reasonable (error-free) results. Rigid body checks were performed using the method of enforced displacement to ensure that all grid points were connected and SPC forces were near zero. Static internal loads were examined for a static test configuration with a 20,000 lb. load applied at the cargo hook and reacted at the rotor hubs. The vibrations model was used to obtain natural frequencies and modes corresponding to the shake test configuration. All calculations were performed using the MSC NASTRAN code.

Version 65 was used for static calculations and Version 64 for the dynamic analysis. There are no differences between Version 64 and Version 65 that affect the analysis results. The static analysis was performed on the VAX 8800 computer where only Version 65 is available. The dynamic analysis was executed on the IBM 3090 mainframe with Version 64a - the only version of NASTRAN residing on this machine.

DEMONSTRATION CASES

- RIGID-BODY CHECK
  - ENFORCED DISPLACEMENT AT FORWARD HUB
- STATIC INTERNAL LOADS
  - 20,000 LB LOAD AT THE CENTER CARGO HOOK REACTED AT THE ROTOR HUBS
  - DUPLICATES STATIC TEST CONFIGURATION
- NATURAL FREQUENCIES AND MODES
  - SHAKE TEST AIRCRAFT CONFIGURATION

DEMONSTRATION CASES

RIGID-BODY CHECK

Results for an enforced longitudinal displacement of 1 inch at the forward rotor hub are shown in the accompanying figure. A typical portion of the displacement vector shows a unit displacement in the x-direction and near zero for the remaining coordinates. Non-zero SPC forces are extremely small, indicating the SPC's will have no impact on either the static or dynamic analysis.

DEMONSTRATION CASES
RIGID-BODY CHECK

ENFORCED DISPLACEMENT SET: 1 INCH AT FWD HUB

D I S P L A C E M E N T V E C T O R

POINT ID.	TYPE	T1	T2	T3	R1	R2	R3
82226	G	1.000000E+00	1.446933E-14	5.621783E-14	-1.475775E-15	1.311279E-14	1.007874E-15
82227	G	1.000000E+00	6.629246E-15	6.890604E-14	-3.218508E-15	1.306755E-14	2.334938E-15
82228	G	1.000000E+00	1.222500E-15	8.571645E-14	-5.209277E-15	1.303281E-14	2.291258E-15
82229	G	1.000000E+00	-7.762361E-15	1.307496E-13	-8.915022E-15	4.071743E-13	-6.265474E-14
82230	G	1.000000E+00	-2.429107E-14	1.639142E-13	-1.057044E-14	4.752240E-13	-7.286879E-14
82231	G	1.000000E+00	-5.915095E-14	2.141406E-13	-1.164415E-14	4.810596E-13	-1.207307E-13
82232	G	1.000000E+00	-1.510799E-13	2.989602E-13	-1.098620E-14	3.856819E-13	-3.220263E-13
82233	G	1.000000E+00	-2.348200E-13	3.482211E-13	-3.676704E-15	3.042332E-13	-6.289465E-13
82234	G	1.000000E+00	-2.076691E-13	3.762121E-13	5.703500E-15	2.389172E-13	-7.500615E-13
82235	G	1.000000E+00	-1.236346E-13	3.923303E-13	1.244376E-14	1.374910E-13	-8.641024E-13
82236	G	1.000000E+00	-3.116498E-14	3.963923E-13	-1.714794E-15	1.531597E-14	-9.562802E-13
82237	G	1.000000E+00	5.044822E-14	3.900462E-13	-2.073546E-16	-4.199419E-13	-8.471479E-13
82238	G	1.000000E+00	5.312807E-14	3.876335E-13	-1.736214E-16	-5.120304E-13	-7.255793E-13
82239	G	1.000000E+00	5.658561E-14	3.876060E-13	-3.834942E-18	2.338558E-14	-2.676678E-15
82241	G	1.000000E+00	5.848559E-14	3.859084E-13	-3.051817E-16	2.314295E-14	-1.303570E-15
82252	G	1.000000E+00	-4.914024E-12	3.334131E-13	-1.023555E-15	2.188553E-14	-1.014690E-13
82254	G	1.000000E+00	-4.914024E-12	3.536611E-13	-1.023555E-15	2.188553E-14	-1.014690E-13
82255	G	1.000000E+00	-4.913980E-12	3.601661E-13	-1.263556E-15	2.142192E-14	-1.014606E-13
85101	G	1.000000E+00	0.0	0.0	0.0	0.0	0.0
85102	G	1.000000E+00	6.136768E-16	9.850919E-15	1.275853E-17	6.513019E-15	-1.317933E-16
85202	G	1.000000E+00	6.136768E-16	9.680134E-15	1.275853E-17	6.513019E-15	-1.317933E-16
89101	G	1.000000E+00	9.887924E-17	-1.567496E-14	1.275853E-17	6.513019E-15	-1.317933E-16
91101	G	1.000000E+00	4.238363E-14	-2.869233E-14	-5.741935E-15	1.039880E-14	-2.728720E-15

F O R C E S O F S I N G L E - P O I N T C O N S T R A I N T

POINT ID.	TYPE	T1	T2	T3	R1	R2	R3
44101	G	0.0	0.0	-1.602984E-11	0.0	0.0	0.0
85101	G	2.655050E-08	-7.648711E-10	-1.480006E-10	-1.631275E-08	-2.007421E-06	4.417706E-08
106104	G	0.0	0.0	0.0	0.0	0.0	4.547474E-13
160139	G	0.0	0.0	0.0	0.0	-3.116821E-12	0.0
160141	G	0.0	0.0	0.0	0.0	-3.183139E-12	0.0
160239	G	0.0	0.0	0.0	0.0	-3.109747E-12	0.0
370202	G	0.0	-3.183231E-12	0.0	0.0	0.0	0.0
406101	G	0.0	0.0	0.0	0.0	0.0	5.080171E-13
406117	G	0.0	0.0	0.0	0.0	-1.394140E-15	0.0
406201	G	0.0	0.0	0.0	0.0	0.0	-1.362164E-13
406217	G	0.0	0.0	0.0	0.0	1.467044E-14	0.0
417201	G	0.0	0.0	0.0	0.0	0.0	1.152896E-12
451130	G	0.0	3.418437E-20	0.0	0.0	0.0	0.0
451230	G	0.0	3.925834E-20	0.0	0.0	0.0	0.0

DEMONSTRATION CASES

TYPICAL STATIC INTERNAL LOADS - STA. 82 R/H FRAME

Typical internal loads are presented for the static load condition with a 20,000 lb. vertical load at the cargo hook. In the following figures, loads are displayed for the upper right hand frame structure at Station 82 (below forward transmission). The information shown includes:

1) Grid point displacements
2) Forces in bar and rod elements
3) Forces acting on shear elements
4) Grid point force balance at selected points

DEMONSTRATION CASES

TYPICAL STATIC INTERNAL LOADS - STA. 82 R/H FRAME

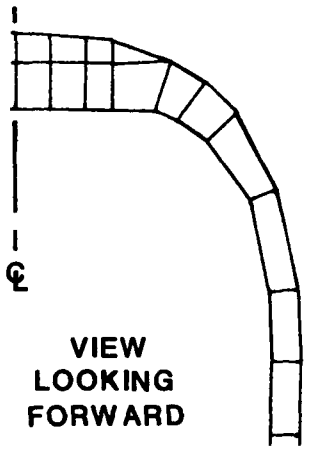

C-3

207

DISPLACEMENT VECTOR

POINT ID.	TYPE	T1	T2	T3	R1	R2	R3
82101	G	-3.384671E-02	-7.097971E-04	-3.088432E-03	-7.140311E-06	-6.016243E-03	-1.265701E-04
82102	G	-2.728638E-02	-3.016429E-03	-2.568668E-03	2.228883E-04	-4.467682E-03	-1.493237E-03
82103	G	-1.223528E-02	-5.330883E-03	-8.818208E-05	6.115850E-04	-2.927273E-03	-4.393756E-03
82104	G	3.256298E-03	-6.831753E-03	3.028251E-03	8.375054E-04	-4.432335E-04	-8.675791E-05
82105	G	-1.597310E-03	-5.609576E-03	1.550536E-02	1.633808E-03	-6.610354E-04	8.679638E-04
82106	G	-2.619076E-03	-2.239840E-03	2.591435E-02	1.941537E-03	-2.042347E-04	3.157772E-04
82107	G	1.608144E-03	5.478666E-03	3.760052E-02	2.076081E-03	-1.078097E-03	4.812745E-04
82108	G	2.049032E-03	2.649045E-02	5.073838E-02	1.408408E-03	-1.368044E-03	-9.056741E-04
82109	G	6.948860E-04	3.311425E-02	5.086535E-02	-4.013993E-04	6.484361E-04	-8.240645E-04
82110	G	-4.344753E-06	2.084921E-02	4.838563E-02	-1.500744E-03	2.210061E-04	-1.908370E-04
82111	G	5.478968E-04	-4.661605E-04	4.629843E-02	-1.827565E-03	1.253555E-04	8.939654E-04
* 82121	G	0.0	-7.255326E-04	-3.213326E-03	0.0	0.0	0.0
* 82122	G	0.0	-1.787827E-03	-2.577853E-03	0.0	0.0	0.0
* 82123	G	0.0	-2.747819E-03	-1.233802E-04	0.0	0.0	0.0
82124	G	4.866563E-03	-3.831771E-03	2.951117E-03	9.196440E-04	-5.001569E-04	-9.104519E-05
82125	G	1.089894E-02	-7.479408E-04	-3.288655E-03	-7.010667E-06	-5.788049E-04	-7.746473E-06
82126	G	1.060645E-02	4.395614E-04	-2.586286E-03	2.879000E-04	-5.673928E-04	8.404921E-05
82127	G	9.703988E-03	1.830040E-03	-1.712372E-04	6.011084E-04	-5.553094E-04	3.456571E-04
82128	G	8.611457E-03	2.940426E-03	2.966240E-03	9.808065E-04	-5.461349E-04	-9.993498E-05
82129	G	7.915702E-03	4.672497E-03	1.191116E-02	1.770173E-03	1.564239E-03	2.892590E-04
82130	G	4.372590E-03	7.804375E-03	1.847234E-02	2.066387E-03	1.903586E-03	3.481222E-04
82131	G	-3.554265E-03	1.413556E-02	2.840621E-02	2.183025E-03	1.920597E-03	5.586918E-04
82132	G	-2.415609E-02	2.912464E-02	4.449347E-02	1.775083E-03	1.452915E-03	1.232340E-03
82133	G	-4.461195E-02	3.494984E-02	5.306794E-02	-2.074938E-04	8.388708E-04	1.358034E-03
82134	G	-4.983867E-02	2.124527E-02	5.619703E-02	-1.818522E-03	3.362980E-05	9.981238E-04
82135	G	-4.409248E-02	-2.549811E-04	5.523486E-02	-2.661200E-03	-1.185525E-03	4.669777E-04

* SPC IN X-DIRECTION

DEMONSTRATION CASES

TYPICAL STATIC INTERNAL LOADS - STA. 82 R/H FRAME (CONT'D)

FORCES IN BAR ELEMENTS (CBAR)

ELEMENT ID.	BEND-MOMENT END-A PLANE 1	BEND-MOMENT END-A PLANE 2	BEND-MOMENT END-B PLANE 1	BEND-MOMENT END-B PLANE 2	- SHEAR - PLANE 1	- SHEAR - PLANE 2	AXIAL FORCE	TORQUE
131705	1.436647E+03	-3.073384E+03	9.547534E+02	-1.745491E+03	1.417334E+02	-3.905566E+02	9.002927E+02	3.033877E-02
131706	9.547534E+02	-1.745491E+03	-2.321327E+01	1.497849E+01	1.387187E+02	-2.497120E+02	-8.513092E+01	3.033877E-02
131707	2.570938E+00	-2.993160E+00	5.449301E-01	-7.867212E+01	3.964274E-01	1.480804E+01	-2.187934E+03	1.662132E-01
131708	5.452181E-01	-7.867212E+01	5.970526E+00	-5.167185E+01	-1.002701E+00	-4.990169E+00	-2.268107E+03	1.652664E-01
131709	5.966737E+00	-5.167185E+01	-1.972816E+01	-4.798389E+01	6.246846E+00	-8.966037E-01	-2.353401E+03	2.693371E-01
131710	-2.556941E-01	-5.952996E+01	2.890479E-02	-6.651830E+01	-5.580371E-02	1.370263E+00	1.173532E+03	1.163591E-03
131711	2.890478E-02	-6.651830E+01	-6.393231E-01	-5.991350E+01	1.237459E-01	-1.223112E+00	1.330224E+03	1.163591E-03
131712	-6.393231E-01	-5.991349E+01	2.008703E+00	-1.419563E+02	-6.458601E-01	2.001043E+01	1.586770E+03	1.163591E-03
131713	-1.860181E+00	-1.144688E+02	7.397916E-01	-3.936520E+01	-2.768279E-01	-7.996535E+00	-1.649951E+03	-2.831145E-02
131714	-4.451009E-01	-1.272201E+02	-3.064462E-01	-1.364825E+02	-2.124977E-02	1.419531E+00	1.538557E+03	1.681831E-01
131715	1.085587E+00	-2.716076E+01	-5.580456E-01	-6.491335E+01	2.710446E-01	6.225621E+00	-1.845954E+03	5.746698E-02
131716	-3.471761E-01	-1.364825E+02	-2.679597E-01	-3.672304E+01	-2.124977E-02	-2.676045E+01	6.226061E+02	4.078698E-02
131717	3.279268E+00	-8.962927E+01	-2.413565E+00	4.419249E+01	8.524068E-01	-2.003758E+01	-1.322076E+03	-9.354560E-02
131718	-2.705972E-01	-3.672305E+01	-1.547267E-01	1.044464E+01	-2.124977E-02	-8.650193E+00	-2.315657E+02	-1.559156E-02
131719	-2.903403E+00	-2.850042E+01	3.796181E+00	1.276480E+02	-5.194598E-01	-1.210714E+01	-4.485195E+02	6.884816E-02
131720	-1.424782E-01	1.044464E+01	8.643629E-02	3.607704E+01	-2.124977E-02	-2.379415E+00	-1.094670E+03	-6.231716E-02
131721	-2.299135E+00	5.440306E+01	6.797819E-01	3.089375E+01	-1.921146E-01	1.516149E+00	1.781167E+02	2.054634E-02
131722	1.051043E-01	3.607704E+01	4.063161E-01	4.456143E+00	-2.124977E-02	2.230779E+00	-1.152227E+03	-1.754246E-02
131723	1.473013E+00	3.699969E+01	-9.968134E-01	-5.003694E+00	2.377095E-01	4.042634E+00	2.861439E+02	-9.461089E-02
131724	4.038487E-01	4.456141E+00	6.186843E-01	-4.405305E-01	-2.124977E-02	4.843385E-01	-4.888913E+02	4.802837E-02
131725	8.577424E-01	3.385183E+01	-7.443120E-01	-2.455010E+01	1.507816E-01	5.496653E+00	3.217733E+02	-1.531486E-01
131726	6.159334E-01	-4.405307E-01	8.401185E-01	2.453373E+00	-2.124977E-02	-2.743036E-01	1.206584E+02	7.551841E-02

FORCES IN ROD ELEMENTS (CONROD)

ELEMENT ID.	AXIAL FORCE	TORQUE	ELEMENT ID.	AXIAL FORCE	TORQUE
141707	-4.374154E+01	0.0	141708	-3.733303E+01	0.0
141709	-5.551948E+01	0.0	141710	-2.857701E+01	0.0
141711	7.468824E+01	0.0	141712	8.361098E+00	0.0
141713	4.744974E+01	0.0	141714	2.694406E+02	0.0
141715	1.958068E+02	0.0	141716	1.113911E+02	0.0
141717	-3.693991E+02	0.0	141718	-9.581181E+01	0.0
141719	-1.678402E+01	0.0	141720	-3.853830E-01	0.0
141721	1.701793E+01	0.0	141722	8.815919E+01	0.0

DEMONSTRATION CASES

TYPICAL STATIC INTERNAL LOADS - STA. 82 R/H FRAME (CONT'D)

FORCES ACTING ON SHEAR PANEL ELEMENTS (CSHEAR)

ELEMENT ID	POINT 1 F-FROM-4 / KICK-1	POINT 1 F-FROM-2 / SHEAR-12	POINT 2 F-FROM-1 / KICK-2	POINT 2 F-FROM-3 / SHEAR-23	POINT 3 F-FROM-2 / KICK-3	POINT 3 F-FROM-4 / SHEAR-34	POINT 4 F-FROM-3 / KICK-4	POINT 4 F-FROM-1 / SHEAR-41
161707	2.93970E+01	3.69136E+01	-3.69136E+01	-3.17806E+01	3.17806E+01	3.68365E+01	-3.68365E+01	-2.93970E+01
	0.0	1.44457E+01	0.0	1.56170E+01	0.0	1.44457E+01	0.0	1.33623E+01
161708	2.82394E+01	4.09637E+01	-4.09637E+01	-3.08135E+01	3.08135E+01	4.08828E+01	-4.08828E+01	-2.82394E+01
	0.0	1.51418E+01	0.0	1.65220E+01	0.0	1.51418E+01	0.0	1.38769E+01
161709	2.31085E+01	2.79563E+01	-2.79563E+01	-2.53514E+01	2.53510E+01	2.78662E+01	-2.78662E+01	-2.31085E+01
	0.0	1.35933E+01	0.0	1.49126E+01	0.0	1.35933E+01	0.0	1.23906E+01
161710	4.22464E+01	3.05612E+01	-3.05612E+01	-0.22464E+01	4.22464E+01	3.05612E+01	-3.05612E+01	-0.22460E+01
	0.0	1.19848E+01	0.0	1.19848E+01	0.0	1.19848E+01	0.0	1.19848E+01
161711	5.32008E+01	4.07496E+01	-4.07496E+01	-5.32008E+01	5.32008E+01	0.07496E+01	-4.07496E+01	-5.32008E+01
	0.0	1.50924E+01	0.0	1.50924E+01	0.0	1.50924E+01	0.0	1.50924E+01
161712	7.94170E+01	4.61858E+01	-4.61858E+01	-7.94170E+01	7.94170E+01	4.61858E+01	-4.61858E+01	-7.94170E+01
	0.0	2.25297E+01	0.0	2.25297E+01	0.0	2.25297E+01	0.0	2.25297E+01
161713	-3.75901E+02	-3.34351E+02	3.34351E+02	3.78783E+02	-3.78783E+02	-4.49062E+02	4.49062E+02	3.75901E+02
	0.0	-7.50593E+01	0.0	-9.68829E+01	0.0	-1.37644E+02	0.0	-1.06638E+02
161714	-4.91539E+02	-2.55288E+02	2.55288E+02	5.38844E+02	-5.38844E+02	-4.16838E+02	4.16838E+02	0.91539E+02
	0.0	-8.41969E+01	0.0	-1.49768E+02	0.0	-2.23633E+02	0.0	-1.25723E+02
161715	-4.03205E+02	-3.42508E+02	3.42508E+02	4.59836E+02	-4.59836E+02	-0.25650E+02	4.25650E+02	4.03205E+02
	0.0	-1.02570E+02	0.0	-1.42890E+02	0.0	-1.56122E+02	0.0	-1.12068E+02
161716	-1.51686E+02	-3.71436E+02	3.71436E+02	2.24008E+02	-2.24008E+02	-4.47233E+02	4.47233E+02	1.51686E+02
	0.0	-5.75993E+01	0.0	-1.01465E+02	0.0	-8.30320E+01	0.0	-4.71351E+01
161717	9.43944E+01	3.10525E+02	-3.10525E+02	-9.64547E+01	9.64547E+01	3.39641E+02	-3.39641E+02	-9.43944E+01
	0.0	4.00524E+01	0.0	4.48911E+01	0.0	4.79218E+01	0.0	4.27564E+01
161718	1.33050E+02	3.06224E+02	-3.06224E+02	-1.30324E+02	1.30324E+02	3.14572E+02	-3.14572E+02	-1.33050E+02
	0.0	5.89053E+01	0.0	5.92372E+01	0.0	6.22297E+01	0.0	6.19231E+01
161719	1.22057E+02	2.92655E+02	-2.92655E+02	-1.22087E+02	1.22087E+02	2.94735E+02	-2.94735E+02	-1.22057E+02
	0.0	5.50880E+01	0.0	5.54796E+01	0.0	5.58740E+01	0.0	5.54796E+01

DEMONSTRATION CASES

TYPICAL STATIC INTERNAL LOADS - STA. 82 R/H FRAME (CONCLUDED)

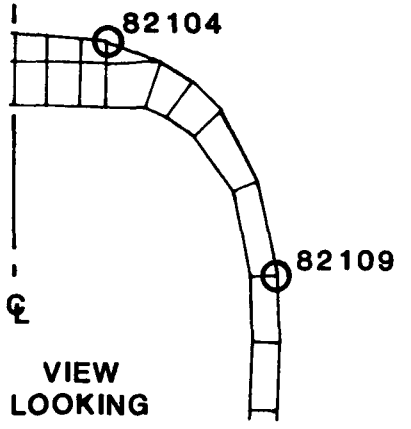

GRID POINT FORCE BALANCE

POINT-ID	ELEMENT-ID	SOURCE	T1	T2	T3	R1	R2	R3
82104	131704	BAR	8.309871E+00	1.600339E+01	-2.411943E+01	-8.132816E+01	2.851407E+00	-2.505818E+01
82104	131705	BAR	1.417334E+02	3.905566E+02	-9.002927E+02	3.073384E+03	-1.436647E+03	-3.033876E-02
82104	131709	BAR	-6.246846E+00	2.345743E+03	-1.897042E+02	-4.798389E+01	-1.851236E+00	-1.964296E+01
82104	131713	BAR	-2.768279E-01	-1.560961E+03	5.346053E+02	1.144688E+02	5.673512E-01	1.771776E+00
82104	131907	BAR	1.842421E+02	2.285135E+02	-5.675302E+02	-3.107348E+03	9.592687E+02	-1.714823E+02
82104	131910	BAR	-8.783007E+02	-4.535924E+01	-5.628059E+01	1.542106E+00	4.958310E+02	2.076938E+02
82104	151908	QUAD4	-1.971530E+02	-2.098030E+02	7.041743E+01	4.726554E+01	-2.001989E+01	6.748277E+00
82104	161706	SHEAR	7.352186E+00	1.370182E+01	-2.227048E+01	0.0	0.0	0.0
82104	161709	SHEAR	0.0	2.786617E+01	2.310854E+01	0.0	0.0	0.0
82104	161905	SHEAR	6.114102E+02	0.0	-1.802945E+02	0.0	0.0	0.0
82104	161906	SHEAR	1.264507E+02	0.0	9.375343E+01	0.0	0.0	0.0
82104	171701	TRIA3	0.0	-1.206261E+03	1.310171E+03	0.0	0.0	0.0
82104	171751	TRIA3	2.478951E+00	0.0	-9.156386E+01	0.0	0.0	0.0
82104		*TOTALS*	-2.870593E-12	-2.671641E-12	-7.105427E-13	7.080558E-12	5.243361E-12	8.482104E-14
82109	131721	BAR	1.921146E-01	-3.372139E+01	1.749020E+02	3.089375E+01	6.623081E-01	1.545108E-01
82109	131723	BAR	2.377095E-01	1.138571E+01	-2.859459E+02	-3.699969E+01	-1.475971E+00	1.508154E-02
82109	141718	CONROD	0.0	9.564954E+01	5.573987E+00	0.0	0.0	0.0
82109	151912	QUAD4	3.492992E+02	-9.798801E+01	4.886793E+02	3.209799E+01	1.098574E+00	-5.448071E+00
82109	151913	QUAD4	-3.497290E+02	-1.667724E+01	2.290966E+02	-2.599204E+01	-2.849113E-01	5.278479E+00
82109	161717	SHEAR	0.0	1.576716E+02	-2.987866E+02	0.0	0.0	0.0
82109	161718	SHEAR	0.0	-1.163202E+02	-3.135193E+02	0.0	0.0	0.0
82109		*TOTALS*	1.634248E-13	-4.014566E-13	-1.378453E-12	-2.131628E-14	8.167078E-15	-2.009504E-14

DEMONSTRATION CASES

MODAL ANALYSIS - NATURAL FREQUENCIES

Calculated natural frequencies for the first 20 flexible modes are presented in the following figure along with a line spectrum showing frequency placement relative to the rotor harmonic frequencies. Principal identifying motions at each frequency are noted in the tabulated results.

The flexible mode frequencies and shapes seem reasonable and the extremely low rigid-body frequencies (modes 1-6) confirm the absence of any spurious constraints. Placement of the lower modes also compares favorably with results from an earlier NASTRAN model. Of particular interest is the large number of modes between 1P and 4P.

DEMONSTRATION CASES
MODAL ANALYSIS - NATURAL FREQUENCIES

MODE	FREQUENCY (HZ)	DESCRIPTION
1-6	<0.0001	RIGID BODY
7	5.68	AFT PYLON LATERAL
8	6.17	AFT PYLON LONGITUDINAL
9	7.33	COCKPIT FLOOR
10	8.08	FWD. PYLON LONGITUDINAL
11	8.56	SYMMETRIC ENGINE LATERAL
12	9.14	ASYMMETRIC ENGINE LATERAL
13	9.21	COCKPIT FLOOR
14	10.12	FUSELAGE 1st VERTICAL
15	10.46	FUSELAGE TORSION
16	11.56	ENGINE/CABIN FLOOR YAW
17	11.83	COCKPIT FLOOR
18	13.41	FUSELAGE LATERAL
19	13.67	COCKPIT FLOOR
20	14.16	AFT FUSELAGE LATERAL
21	14.44	COCKPIT FLOOR
22	15.56	ENGINE LONGITUDINAL/CABIN FLOOR VERTICAL
23	16.79	CABIN FLOOR 2nd VERTICAL
24	17.51	CABIN FLOOR TORSION
25	18.76	ENGINE PITCH/FUSELAGE 2nd VERTICAL
26	19.45	NOSE LATERAL

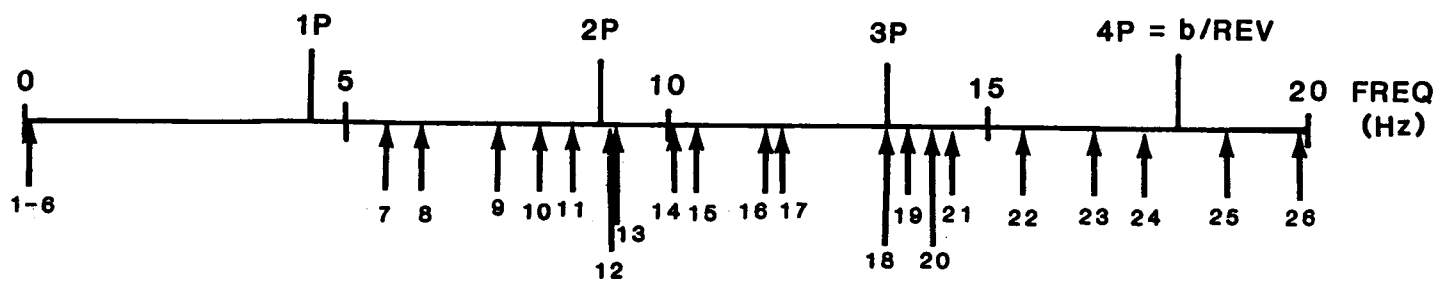

DEMONSTRATION CASES

MODAL ANALYSIS - NATURAL MODES

Mode shapes corresponding to modes 7, 8 and 10, which illustrate some of the more fundamental and readily identifiable modes, are shown in the following figures. Mode 7 shown here is the fundamental torsion mode with the hubs moving in opposition. Because the mode is dominated by relatively large aft rotor hub lateral motions, this mode is generally referred to as the "aft pylon lateral mode".

DEMONSTRATION CASES
MODAL ANALYSIS - NATURAL MODES

MODE 7, FREQUENCY = 5.68 Hz

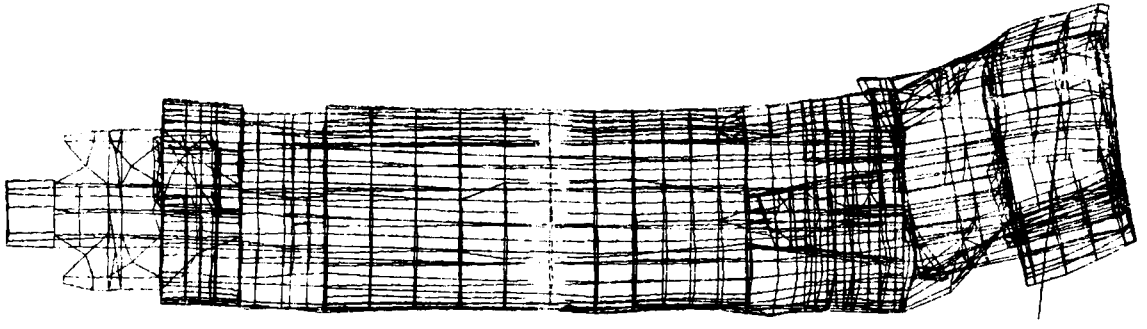

VIEW FROM ABOVE

AFT
HUB

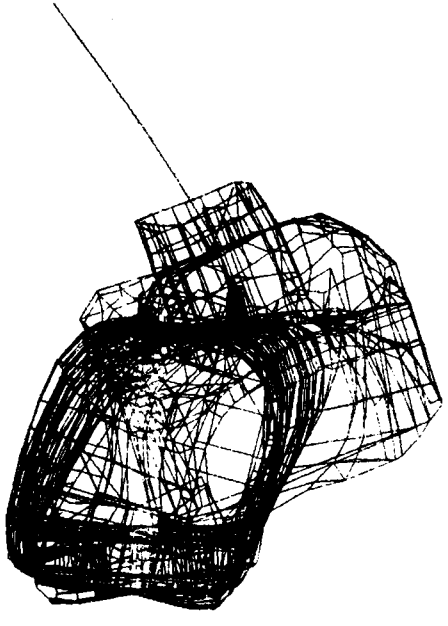

VIEW LOOKING FORWARD

DEMONSTRATION CASES

MODAL ANALYSIS - NATURAL MODES

Mode 8 is the first vertical bending mode with opposing longitudinal motions of the rotor heads. The mode is characterized by the large pitching motion of the aft pylon structure and rotor shafts. For obvious reasons, the mode is identified as the "aft pylon longitudinal mode".

DEMONSTRATION CASES
MODAL ANALYSIS - NATURAL MODES

MODE 8, FREQUENCY = 6.17 Hz

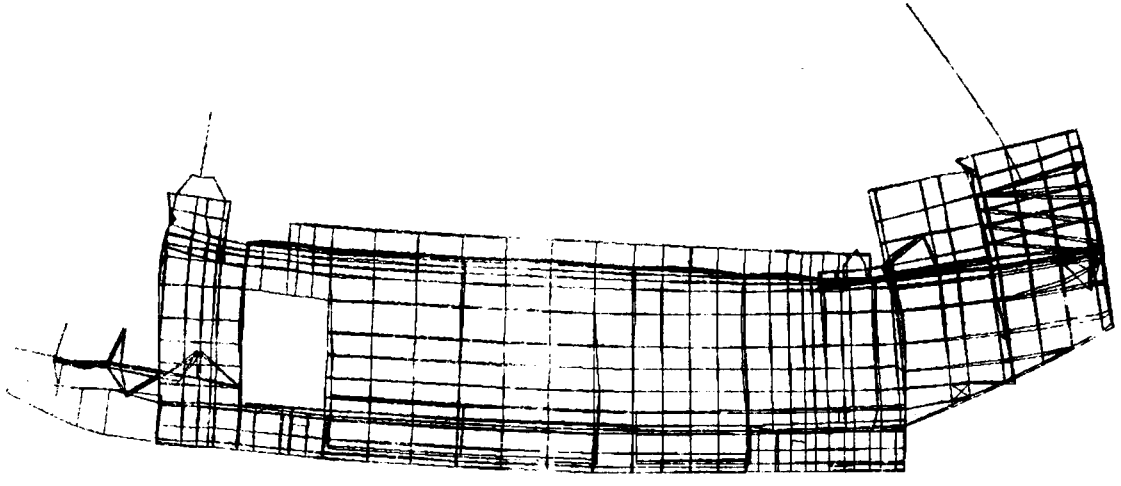

DEMONSTRATION CASES

MODAL ANALYSIS - NATURAL MODES

Mode 10 shown in the accompanying figure is somewhat unusual. The motion is confined almost exclusively to the forward end of the aircraft. A large longitudinal pitching motion of the forward transmission and rotor is opposed by a vertical pitching motion of the cockpit beam and floor.

DEMONSTRATION CASES
MODAL ANALYSIS - NATURAL MODES

MODE 10, FREQUENCY = 8.08 Hz

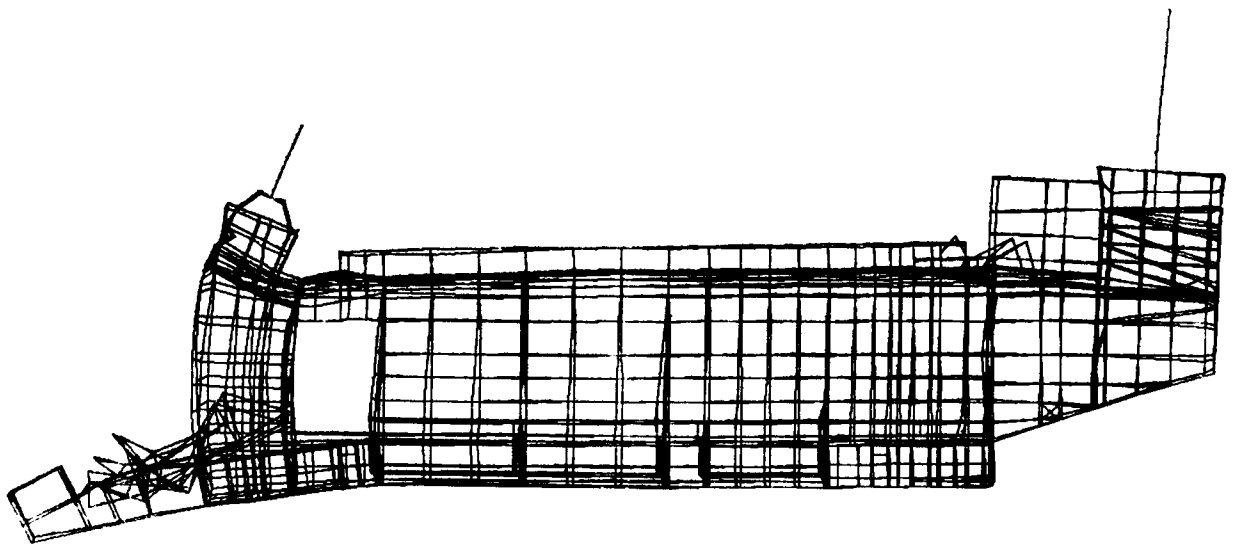

7.0 Comparison of Test and Analytical Frequency Response

COMPARISON OF TEST AND ANALYTICAL FREQUENCY RESPONSE

TEST MEASUREMENT LOCATIONS

Measurement locations from the Reference 1 shake test of the Model 360 airframe are displayed in the following figure. Frequency response data at selected locations are compared with analytical results in this section.

COMPARISON OF TEST AND ANALYTICAL FREQUENCY RESPONSE
TEST MEASUREMENT LOCATIONS

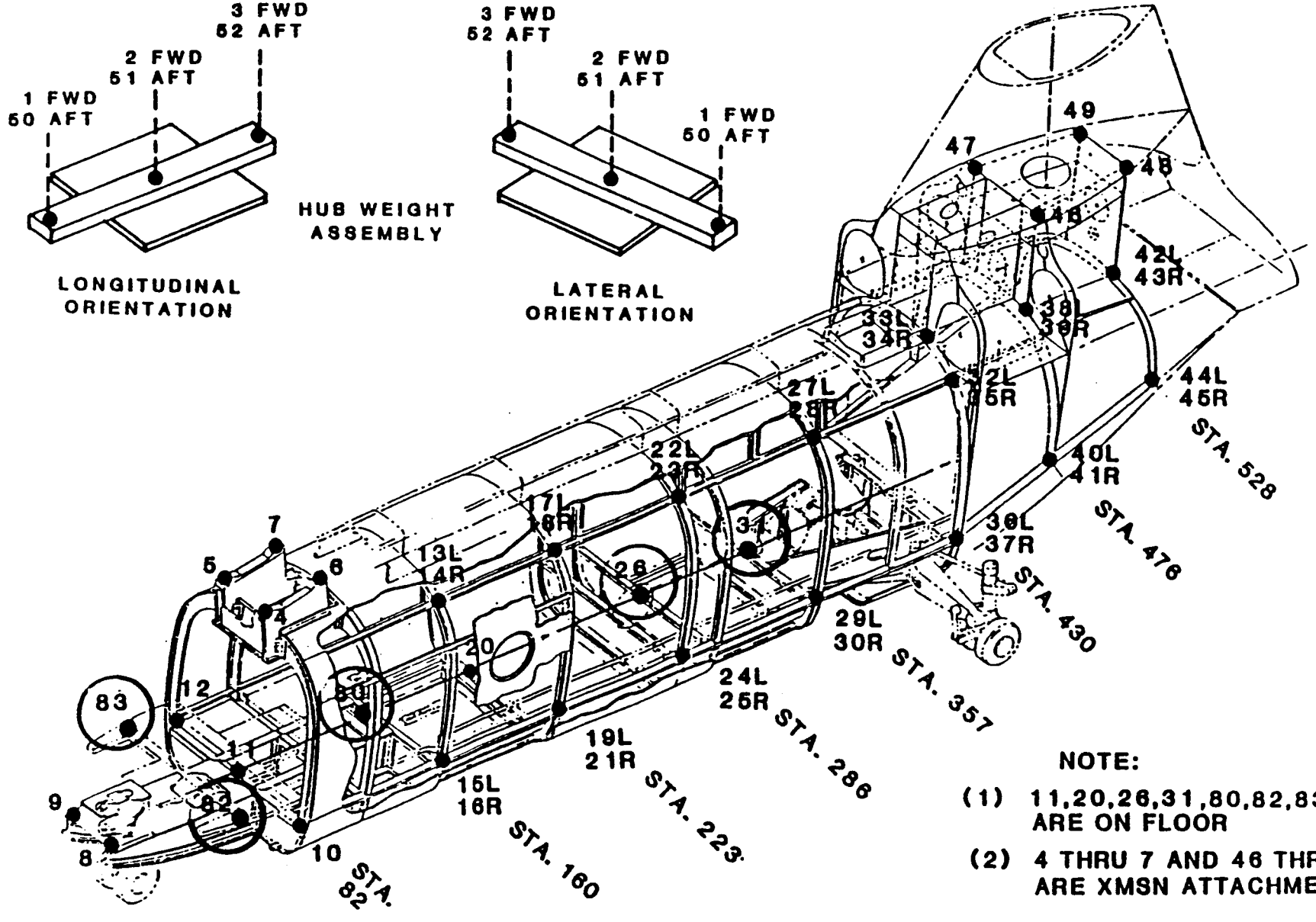

COMPARISON OF TEST & ANALYTICAL FREQUENCY RESPONSE

CORRESPONDING TEST AND NASTRAN LOCATIONS.

The accompanying figure presents a tabulation of the NASTRAN grid points which correspond to the test measurement locations. A descriptive location indicating identifiable points on the structure is also provided. At a few locations, notably the center line of the cabin floor, there is no NASTRAN grid point. Providing a NASTRAN grid point at these locations would require a minimum of 32 additional elements in the floor model.

COMPARISON OF TEST & ANALYTICAL FREQUENCY RESPONSE
CORRESPONDING TEST AND NASTRAN LOCATIONS

MEASUREMENT LOCATION	NASTRAN GRID POINT	DESCRIPTION
1	NONE	FWD HUB, FRONT OF BEAM
2	085103	℄ FWD. HUB
3	NONE	FWD. HUB, REAR OF BEAM
4	081201	L/H FWD } BOLT HEAD, FWD. XMSN MNTG.
5	081101	R/H FWD
6	103201	L/H AFT
7	103101	R/H AFT
8	010204	STA. 10 L/H COCKPIT BEAM
9	010104	STA. 10 R/H
10	082213	STA. 82 L/H LOWER LONGERON
11	082151	STA. 82 ℄ COCKPIT FLOOR
12	082113	STA. 82 R/H LOWER LONGERON
13	160206	STA. 160 L/H UPPER
14	160106	STA. 160 R/H
15	160213	STA. 160 L/H LOWER
16	160113	STA. 160 R/H
17	223206	STA. 223 L/H UPPER
18	223106	STA. 223 R/H
19	223213	STA. 223 L/H LOWER
20	NONE	STA. 223 ℄ CABIN FLOOR
21	223113	STA. 223 R/H LOWER LONGERON
22	286206	STA. 286 L/H UPPER
23	286106	STA. 286 R/H
24	286213	STA. 286 L/H LOWER
25	286113	STA. 286 R/H
26	NONE	STA. 304 ℄ CABIN FLOOR
27	357206	STA. 357 L/H UPPER LONGERON
28	357106	STA. 357 R/H
29	357213	STA. 357 L/H LOWER
30	357113	STA. 357 R/H
31	NONE	STA. 357 ℄ CABIN FLOOR
32	430211	STA. 430 L/H INBD. ENG. ATTACH

MEASUREMENT LOCATION	NASTRAN GRID POINT	DESCRIPTION
33	430207	STA. 430 L/H CROWN @ B.L. BEAM
34	430107	STA. 430 R/H
35	430111	STA. 430 R/H INBD. ENG. ATTACH
36	430226	STA. 430 L/H LOWER LONGERON
37	430126	STA. 430 R/H
38	476239	STA. 476 L/H CROWN @ B.L. BEAM
39	476139	STA. 476 R/H
40	476253	STA. 476 L/H LOWER LONGERON
41	476153	STA. 476 R/H
42	528235	STA. 528 L/H CROWN @ B.L. BEAM
43	528135	STA. 528 R/H
44	528244	STA. 528 L/H LOWER LONGERON
45	528144	STA. 528 R/H
46	480205	L/H FWD } BOLT HEAD, AFT XMSN MNTG
47	480105	R/H FWD
48	523205	L/H AFT
49	523105	R/H AFT
50	NONE	AFT HUB, FRONT OF BEAM
51	493102	℄ AFT ROTOR HUB
52	NONE	AFT HUB, REAR OF BEAM
53	421200	VERT., LONG. } L/H ENGINE G/B
	421201	LAT.
54	421100	VERT., LONG. } R/H ENGINE G/B
	421101	LAT.
55	458200	VERT., LONG. } L/H COMBUSTOR
	458201	LAT.
56	458100	VERT., LONG. } R/H COMBUSTOR
	458101	LAT.
80	NONE	STA. 160 ℄ CABIN FLOOR
82	063254	STA. 63 L/H COCKPIT FLOOR
83	063154	STA. 63 R/H

COMPARISON OF TEST & ANALYTICAL FREQUENCY RESPONSE

NASTRAN FORCED RESPONSE

The NASTRAN forced response was performed using RIGID FORMAT SOL 30 with the first 51 free-free natural modes as the degrees of freedom. A uniform value of 3.0% critical damping was assumed based on test data average.

COMPARISON OF TEST & ANALYTICAL FREQUENCY RESPONSE
NASTRAN FORCED RESPONSE

- **MODAL FORCED RESPONSE (SOL 30) USING THE FIRST 51 NATURAL MODES AS D.O.F.**

- **UNIFORM VALUE OF 3.0% CRITICAL DAMPING ASSUMED BASED ON TEST DATA AVERAGE**

COMPARISON OF TEST & ANALYTICAL FREQUENCY RESPONSE

FORWARD HUB RESPONSE

Forward hub response in 3 axes is presented for three hub forces and two hub moments. Overall correlation of the amplitude response is generally poor. Consequently, comparison of the phase responses has been omitted. Specific comments are as follows:

Vertical Excitation - The vertical response misses the two major test peaks by approximately 5 Hz.

Lateral Excitation - The lateral response shows good agreement at the lowest frequency peak (aft pylon mode). A second major peak near 25 Hz shows a 5 Hz error.

Longitudinal Excitation - The calculated longitudinal response is similar to the test except the major peaks are in error by 2-3 Hz.

Pitch Excitation - Again, the calculated longitudinal response is similar to the test. The same 2-3 Hz error in the two major peaks noted with longitudinal response is evident.

Roll Excitation - The lateral response in the 20 to 30 Hz range shows some similarity, but the calculated levels are low.

FREQUENCY RESPONSE - FORWARD VERTICAL EXCITATION
RESPONSE: FORWARD HUB (LOC. 2)

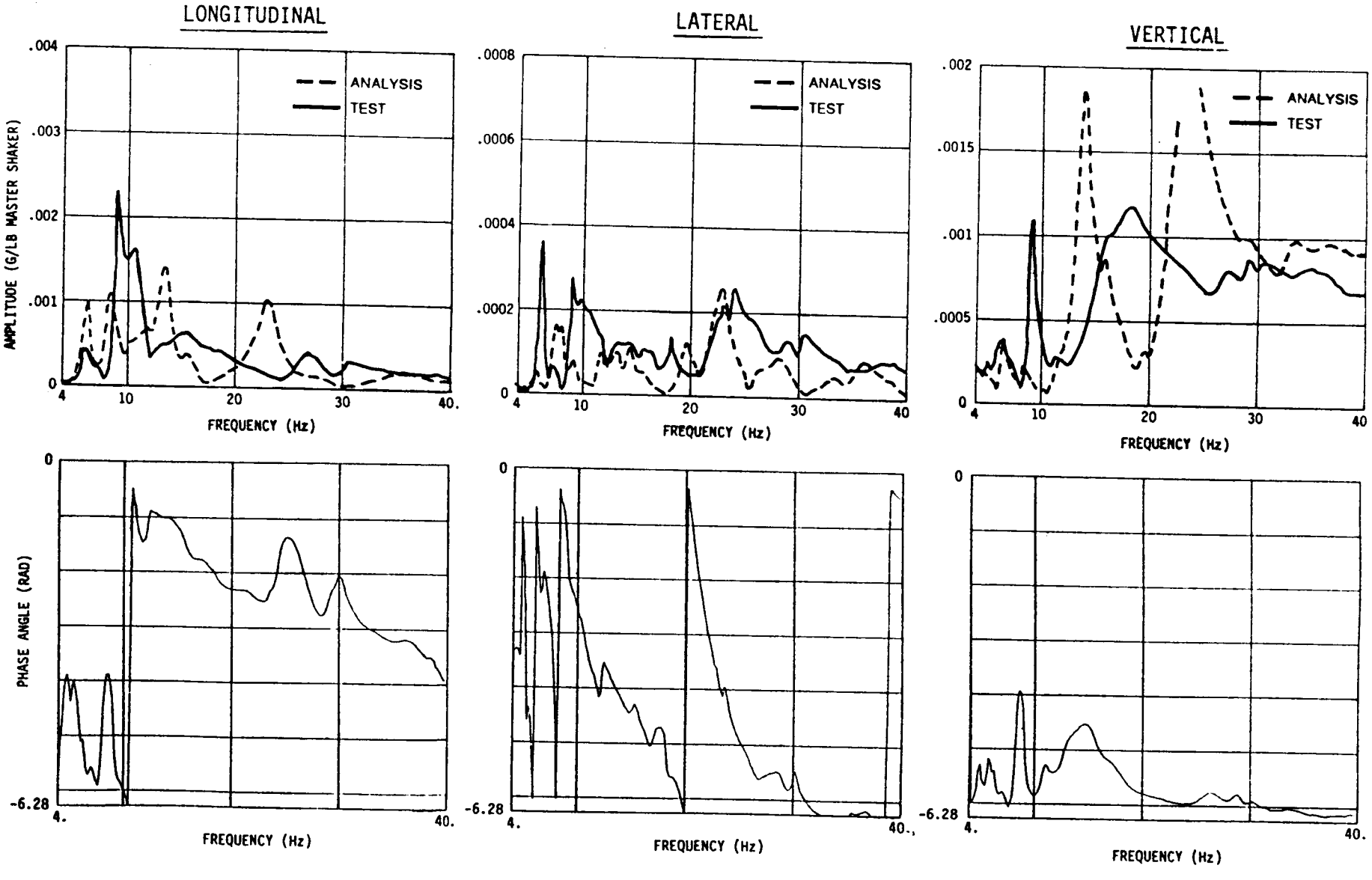

FREQUENCY RESPONSE - FORWARD LATERAL EXCITATION

RESPONSE: FORWARD HUB (LOC. 2)

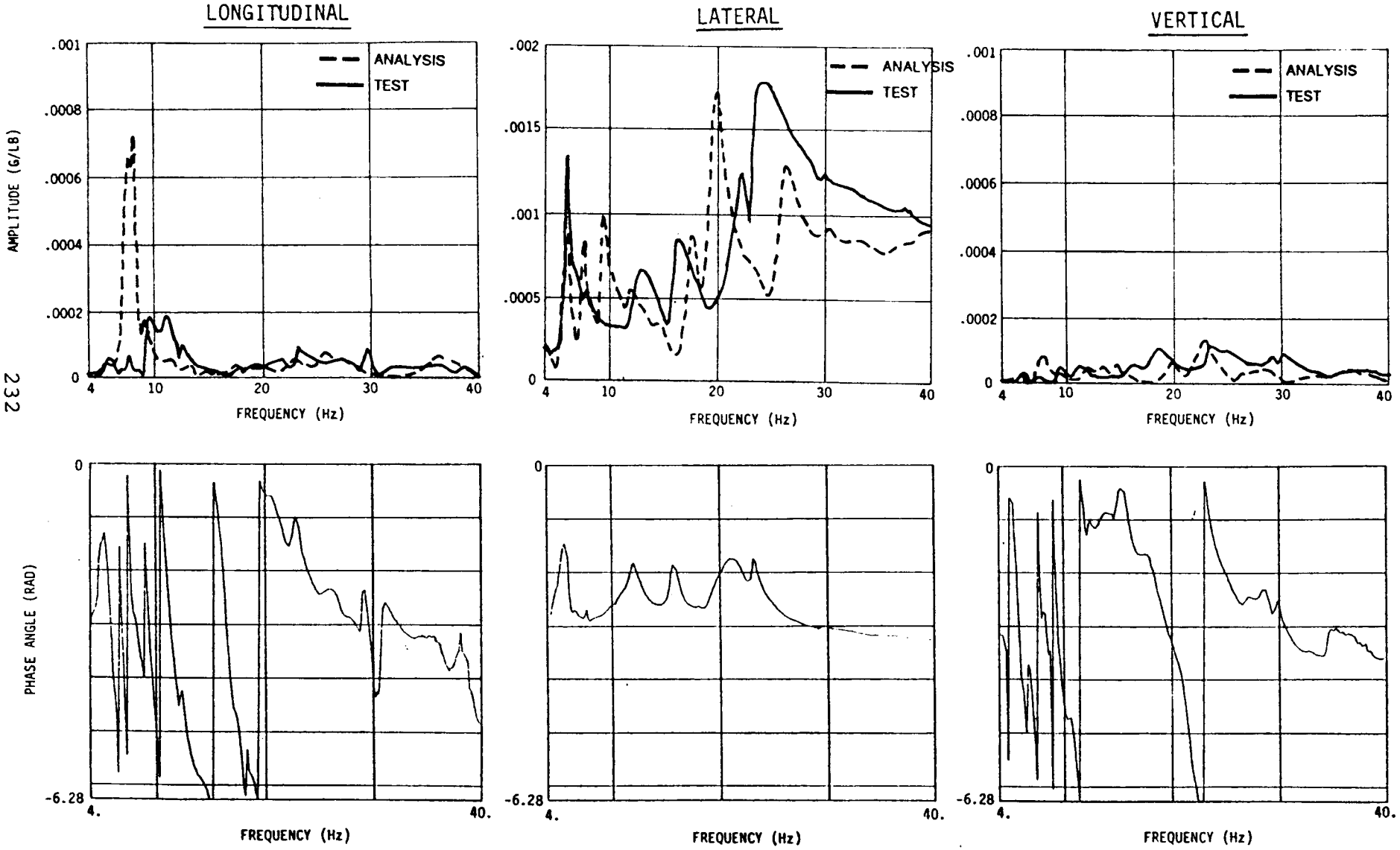

FREQUENCY RESPONSE - FORWARD LONGITUDINAL EXCITATION

RESPONSE: FORWARD HUB (LOC. 2)

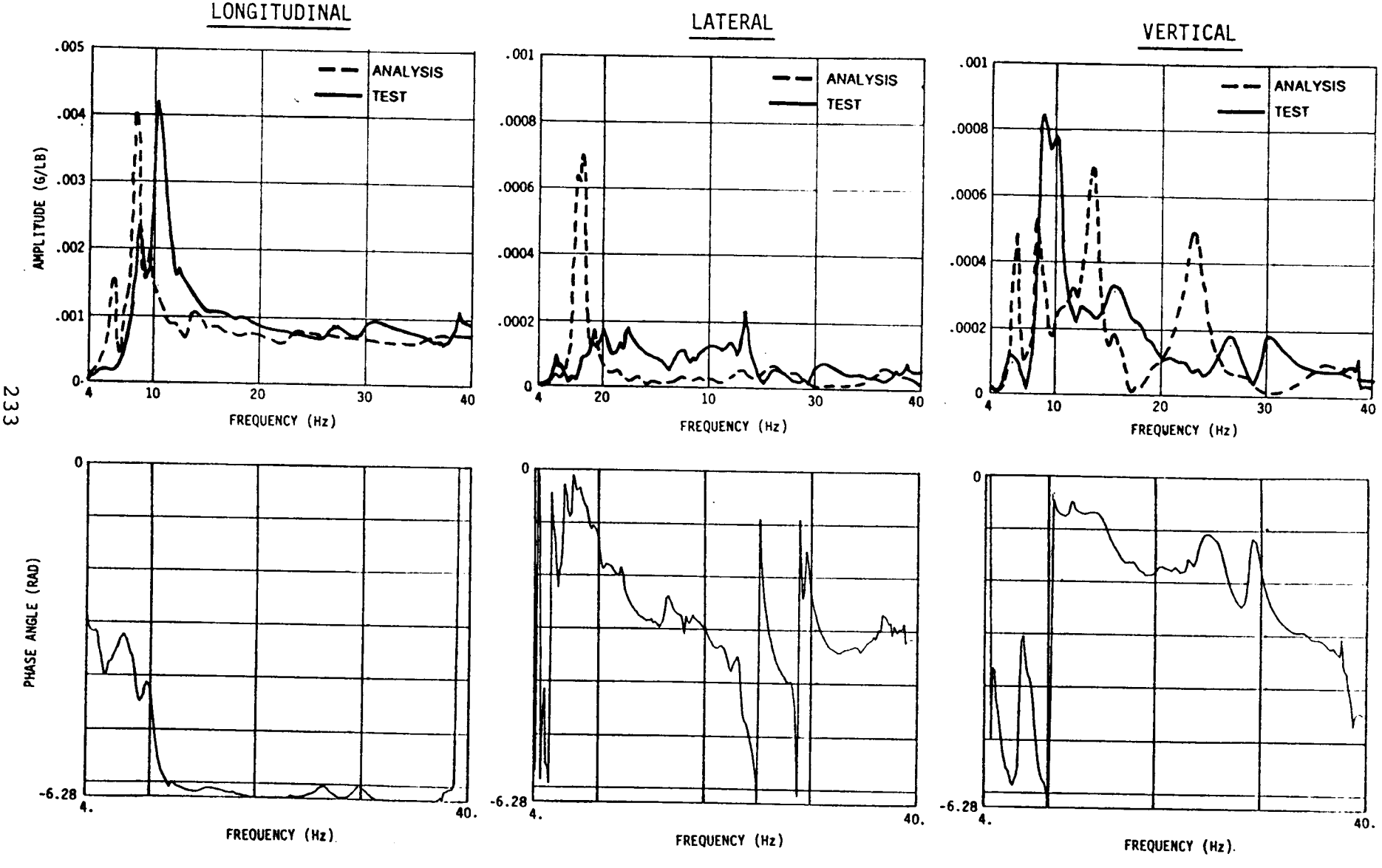

FREQUENCY RESPONSE - FORWARD PITCH EXCITATION

RESPONSE: FORWARD HUB (LOC. 2)

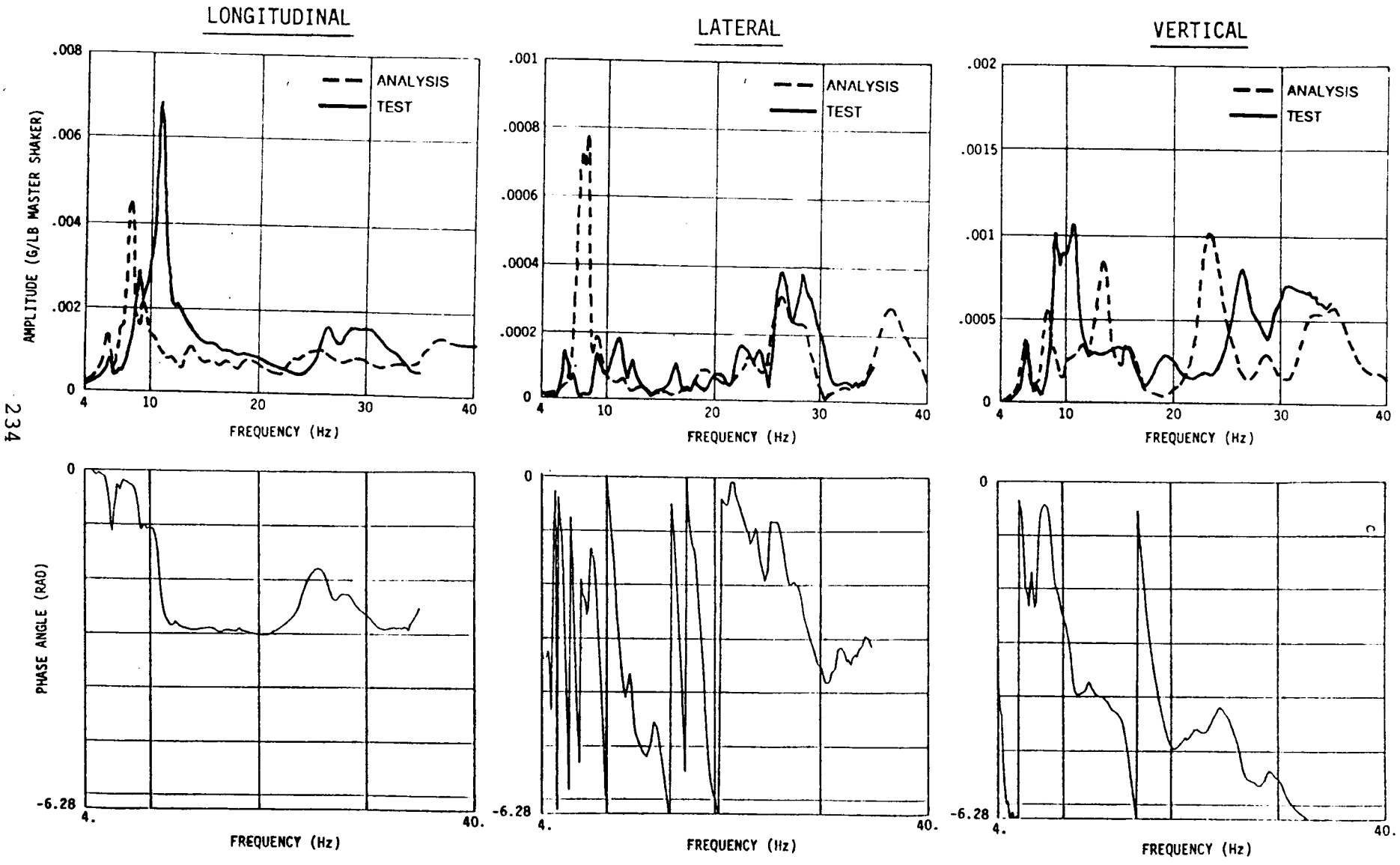

FREQUENCY RESPONSE – FORWARD ROLL EXCITATION
RESPONSE: FORWARD HUB (LOC. 2)

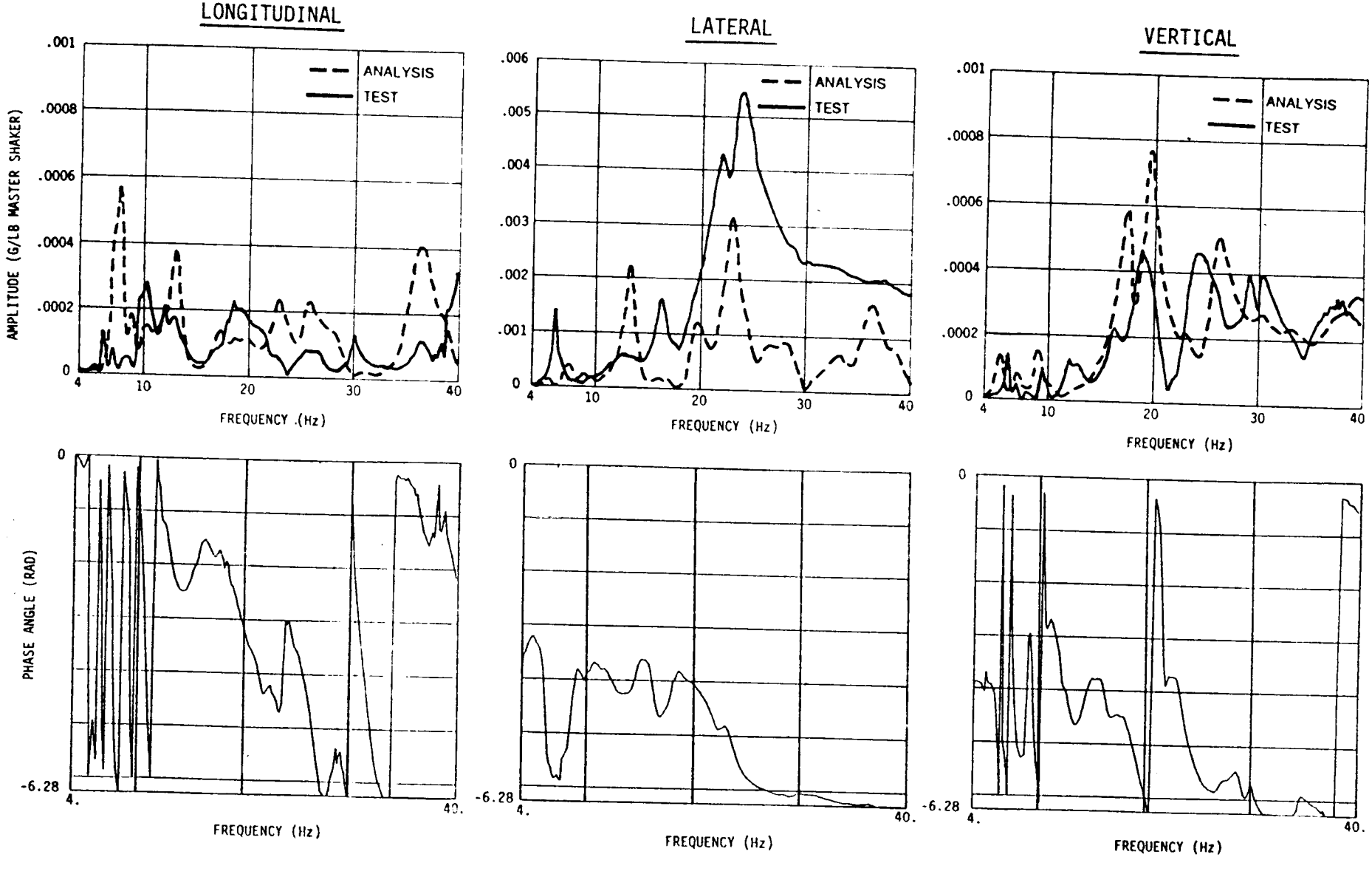

COMPARISON OF TEST & ANALYTICAL FREQUENCY RESPONSE

AFT HUB RESPONSE

Aft hub response to aft hub forces and moments is presented in the following figures. Responses in the direction of the exciting force appear to show better correlation than those for the forward rotor. However, this may be deceiving due to the fact that most of the primary test responses have only one or two peaks below 10 Hz and a relatively flat response over the remainder of the frequency range. Specific comments are as follows:

Vertical Excitation - There is little correlation between the test and analysis. Calculated peaks near the two major test peaks are 2-4 Hz in error and have significantly lower amplitude. In addition, the calculated response shows several large amplitude peaks between the major test peaks near 9 and 29 Hz.

Lateral Excitation - The lateral response shows reasonable agreement in the frequency of the lowest test peak; however, the amplitude of the calculated response is too high. A second low frequency test peak (below 10 Hz) is not detected by the analysis.

Longitudinal Excitation - The calculated longitudinal response is similar to the test except that the amplitude of the single peak below 10 Hz is higher than the test value.

Pitch Excitation - Again, the calculated longitudinal response is similar to the test. However, the calculated amplitude of the peak near 6 Hz is high and several smaller test peaks below 10 Hz are not indicated by the analysis.

Roll Excitation - The calculated amplitude of the peak near 6 Hz is again high. A second test peak near 8 Hz is missed by the analysis.

FREQUENCY RESPONSE - AFT VERTICAL EXCITATION
RESPONSE: AFT HUB (LOC. 51)

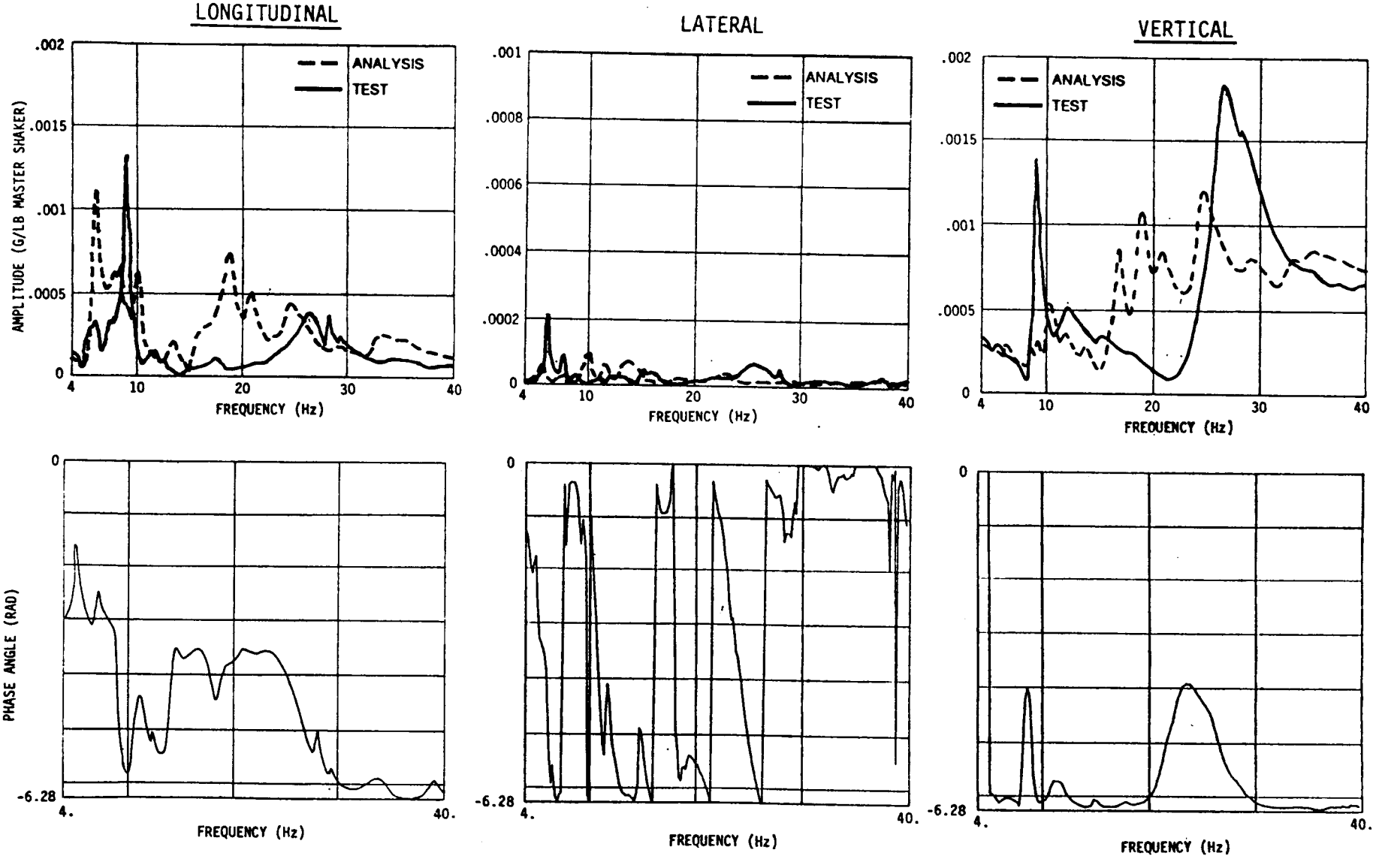

FREQUENCY RESPONSE - AFT LATERAL EXCITATION
RESPONSE: AFT HUB (LOC. 51)

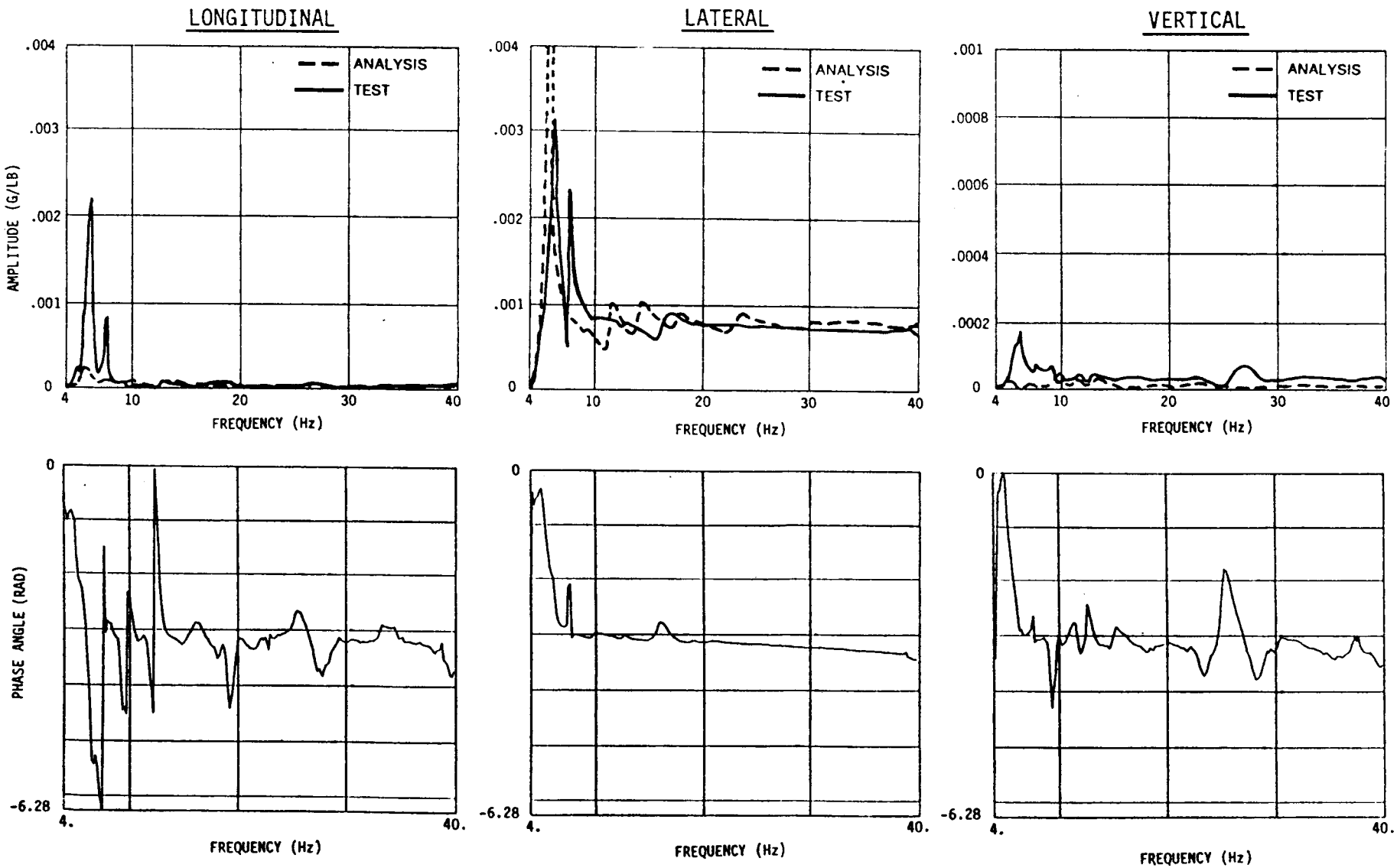

FREQUENCY RESPONSE – AFT LONGITUDINAL EXCITATION
RESPONSE: AFT HUB (LOC. 51)

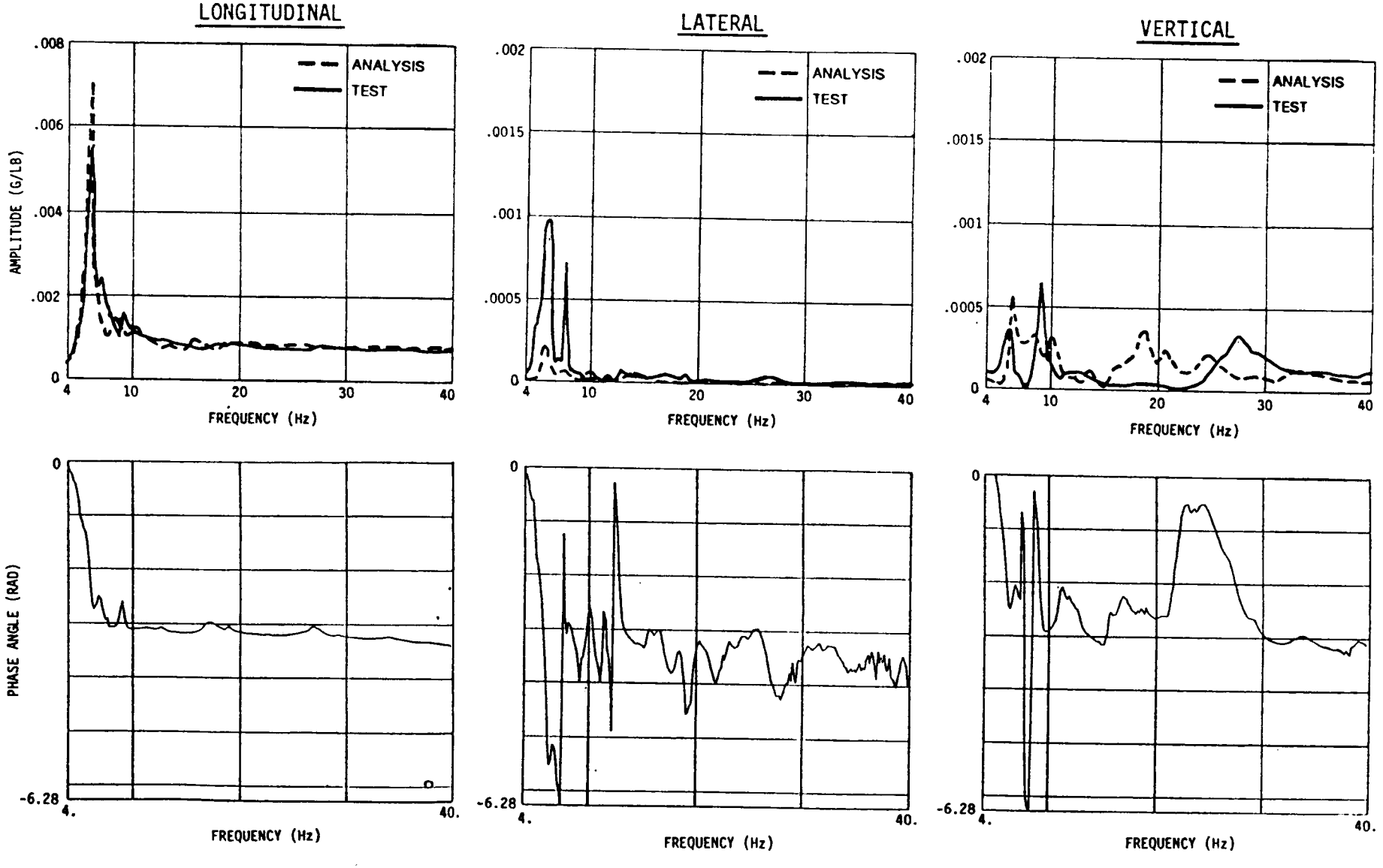

FREQUENCY RESPONSE - AFT PITCH EXCITATION
RESPONSE: AFT HUB (LOC. 51)

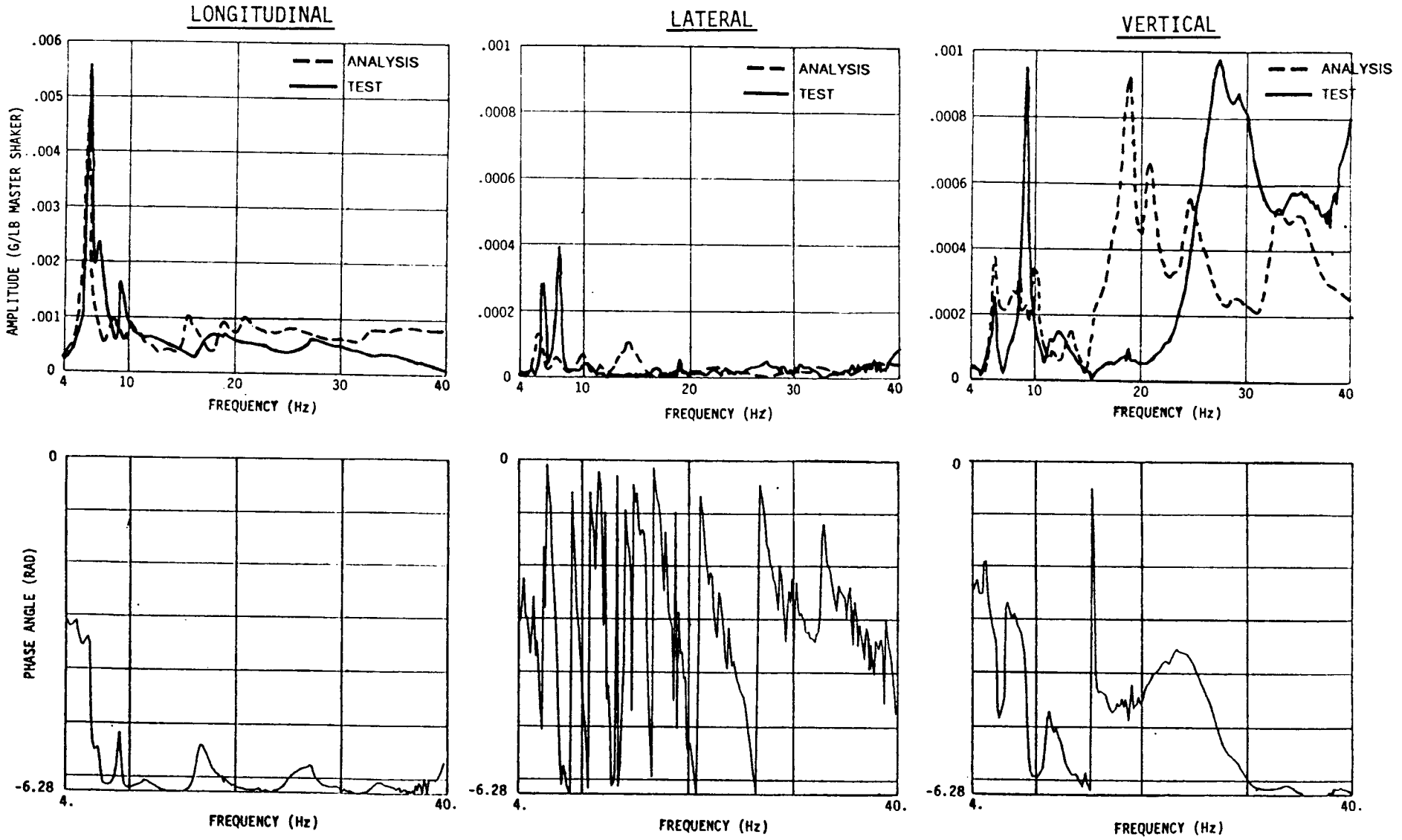

FREQUENCY RESPONSE - AFT ROLL EXCITATION

RESPONSE: AFT HUB (LOC. 51)

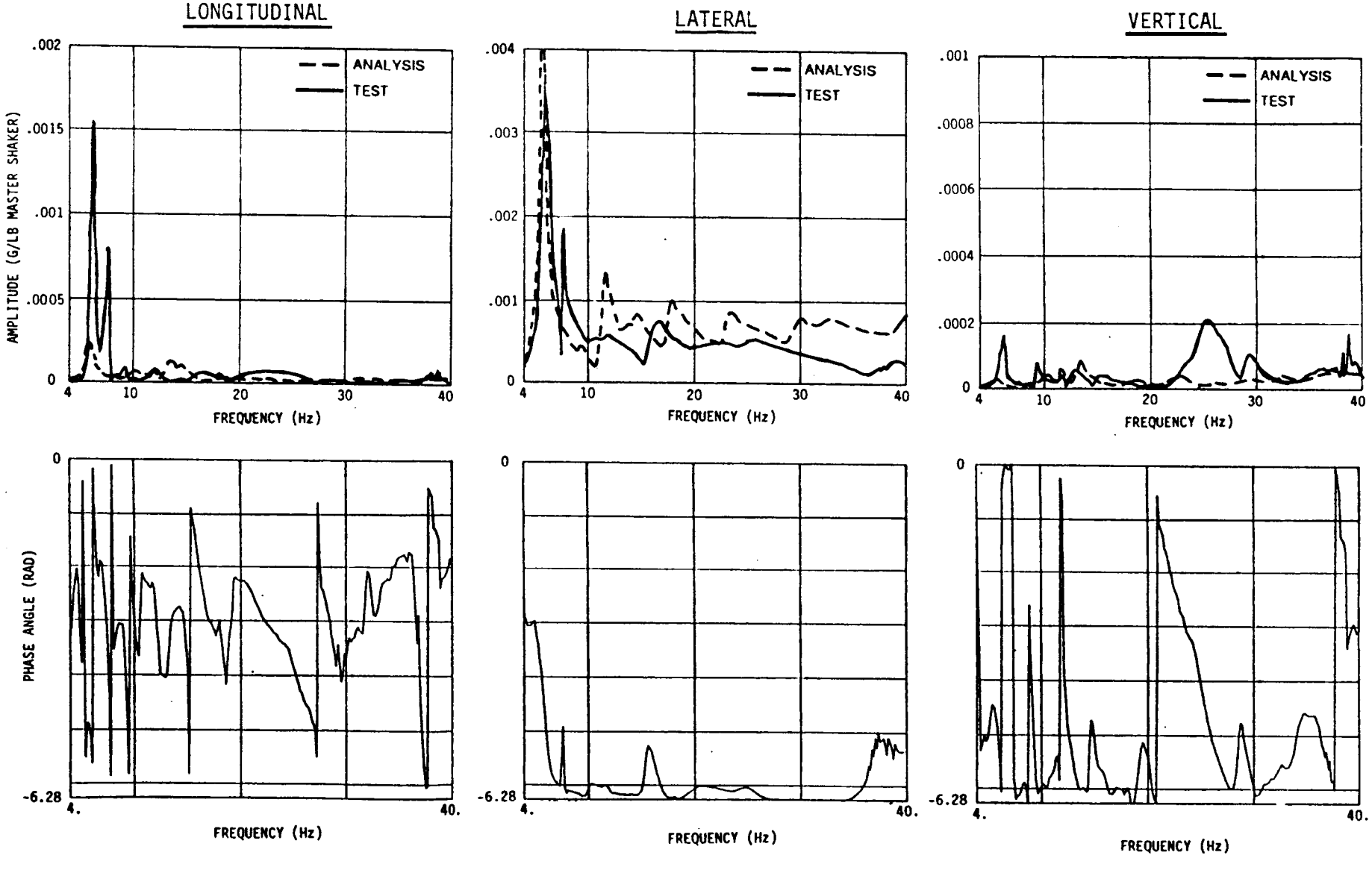

COMPARISON OF TEST & ANALYTICAL FREQUENCY RESPONSE

FORWARD COCKPIT RESPONSE

Forward cockpit response in 3 axes is presented in the following figures for both forward and aft hub forces. Correlation is relatively poor in terms of both frequency and amplitude. As a general observation, the amplitude response at this location gives indications of being significantly underdamped. Comments relative to the response in the directions corresponding to the applied hub forces are as follows:

Forward Vertical Excitation - Major analytical peaks in the 20 to 30 Hz range are near the centers of high test response but significantly underdamped.

Forward Lateral Excitation - Analytical peaks conceivably related to test frequencies are 2 to 6 Hz in error. Predicted response is underdamped below 27 Hz and overdamped above 27 Hz.

Forward Longitudinal Excitation - The major test peak at 10 Hz is underpredicted by 2 Hz and the analytical response is far too high. Above 10 Hz, numerous analytical peaks not present in the test data are evident.

Aft Vertical Excitation - The major test peak near 9 Hz is overpredicted by 1 Hz. Analytical response above 15 Hz is seriously underdamped and several peaks have no test counterpart.

Aft Lateral Excitation - The predominant low frequency test peak near 7 Hz is reasonably well predicted. The analysis shows several relatively high amplitude peaks not evident in the test response.

Aft Longitudinal Excitation - The analytical response is seriously underdamped. Only the peak near 7 Hz shows any correlation with a test peak.

FREQUENCY RESPONSE – FORWARD VERTICAL EXCITATION
RESPONSE: STA. 10 R/H FORWARD COCKPIT (LOC. 9)

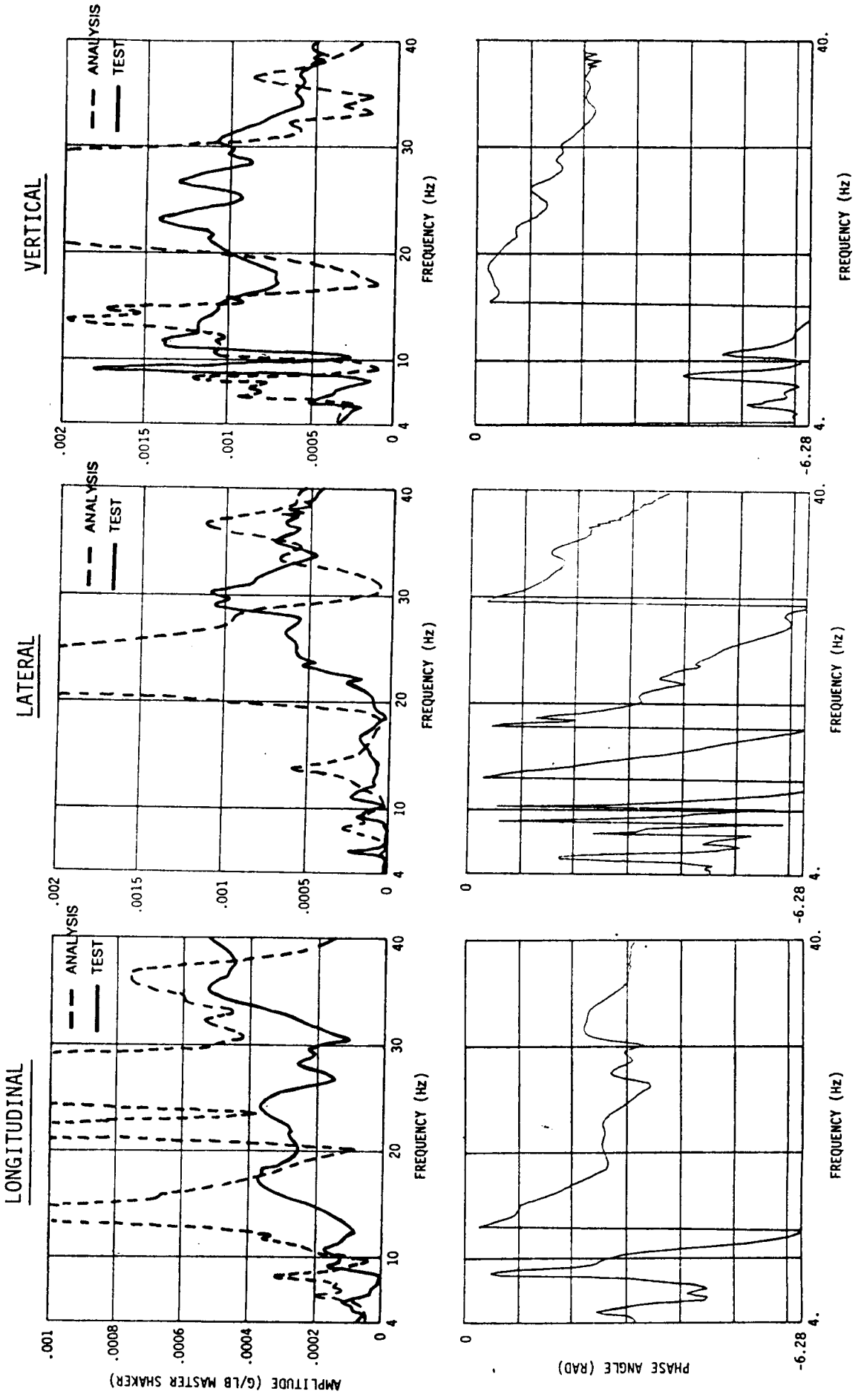

FREQUENCY RESPONSE - FORWARD LATERAL EXCITATION
RESPONSE: STA. 10 R/H FORWARD COCKPIT (LOC. 9)

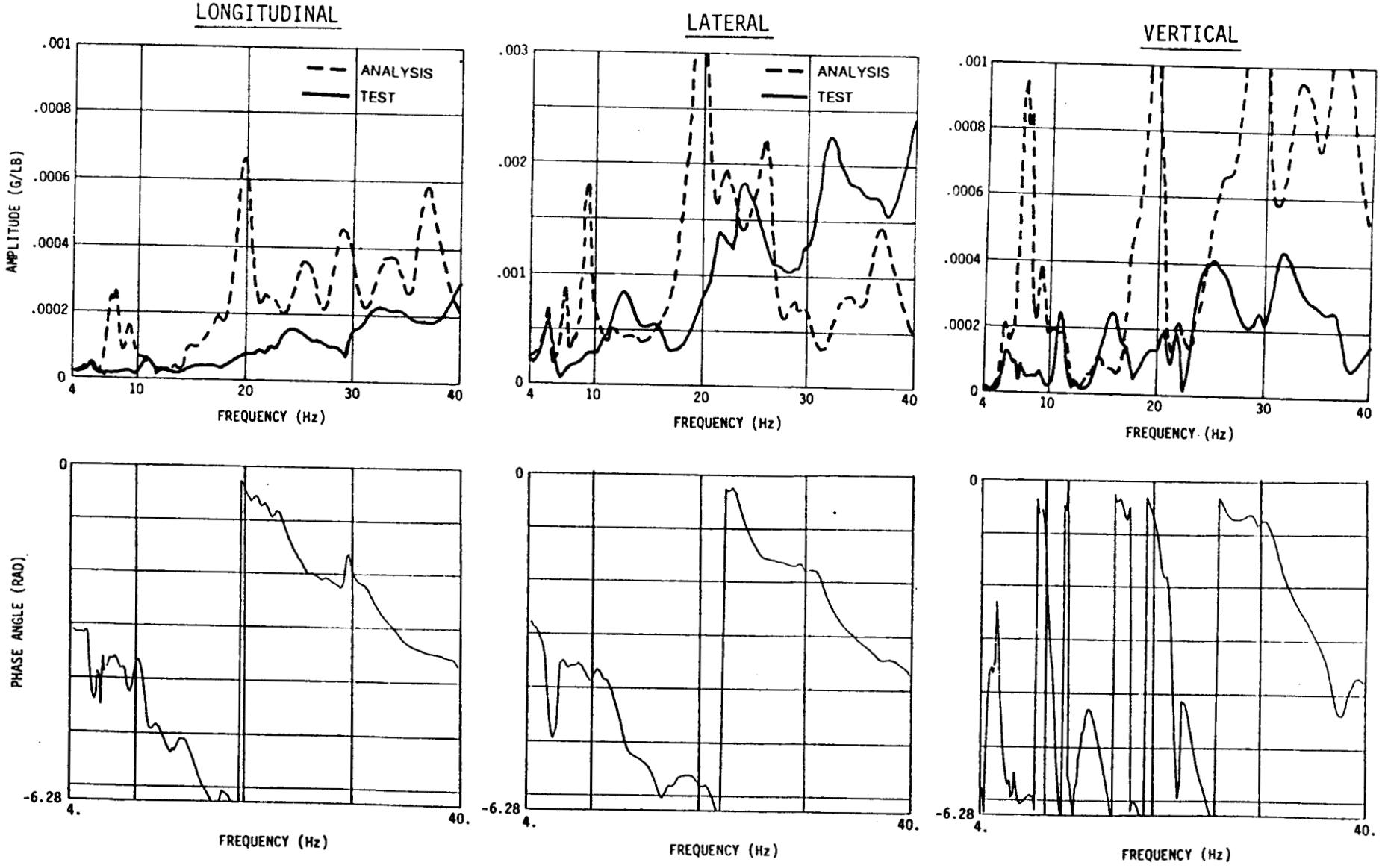

FREQUENCY RESPONSE - FORWARD LONGITUDINAL EXCITATION

RESPONSE: STA. 10 R/H FORWARD COCKPIT (LOC. 9)

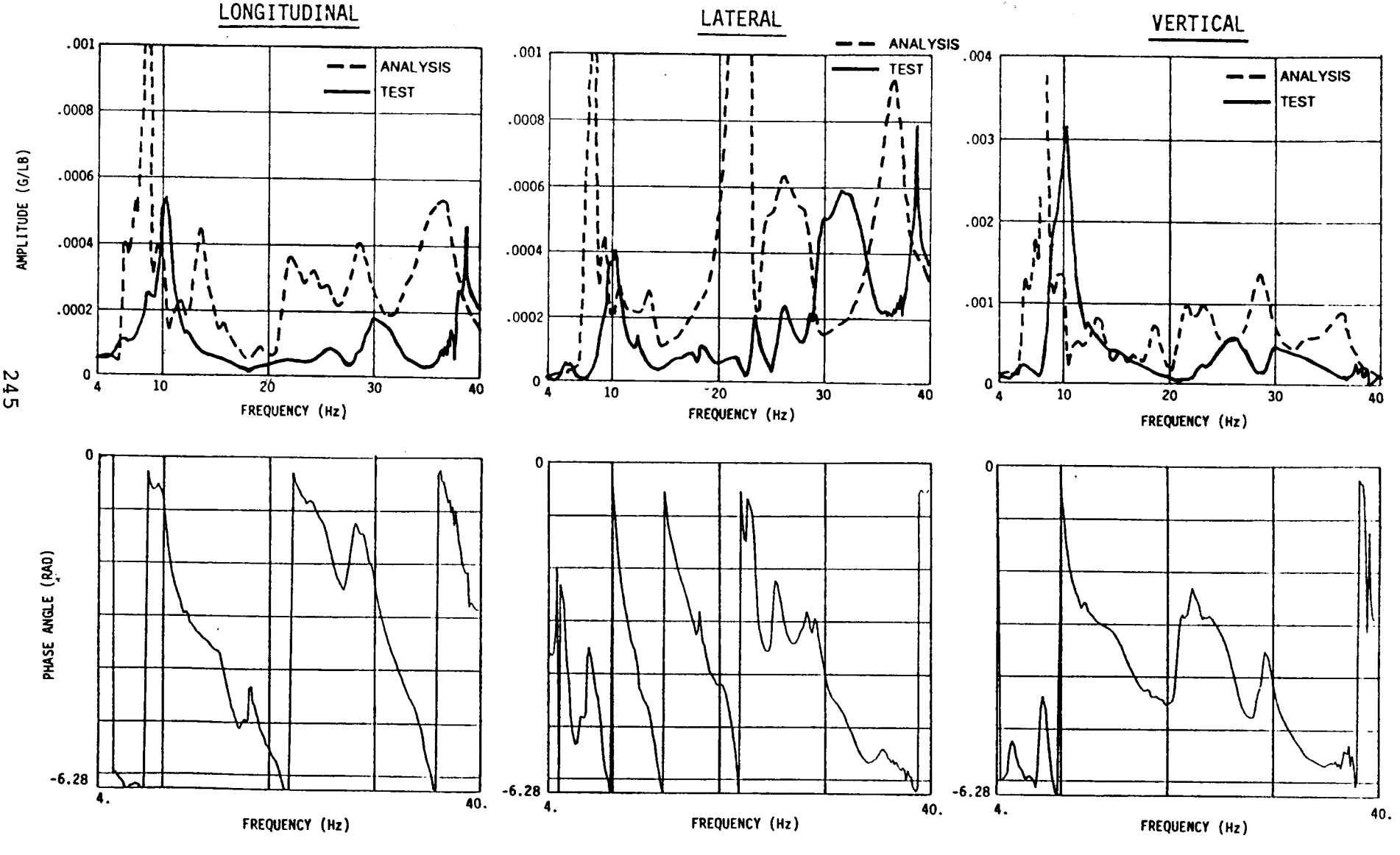

FREQUENCY RESPONSE - AFT VERTICAL EXCITATION
RESPONSE: STA. 10 R/H FORWARD COCKPIT (LOC. 9)

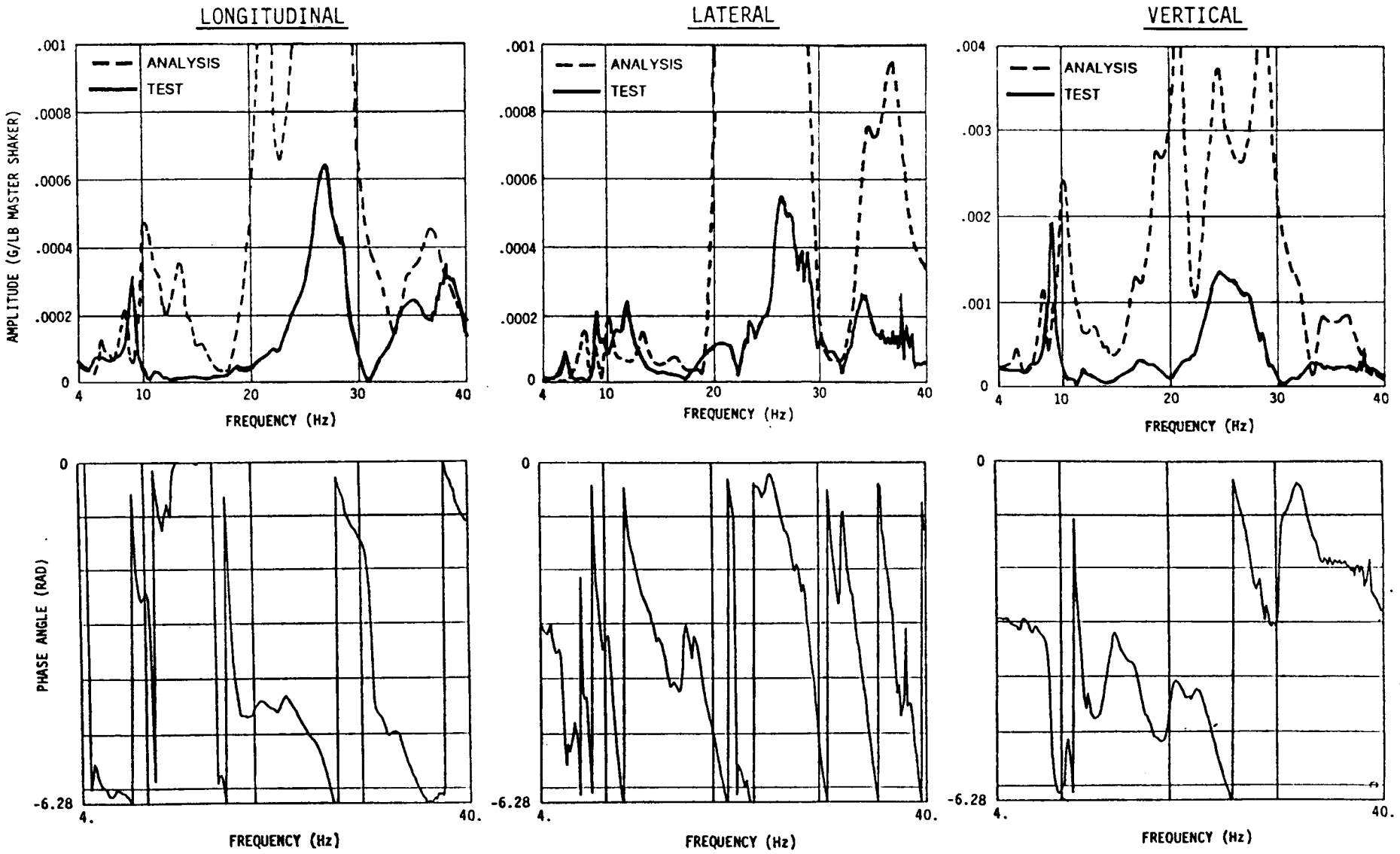

FREQUENCY RESPONSE - AFT LATERAL EXCITATION
RESPONSE: STA. 10 R/H FORWARD COCKPIT (LOC. 9)

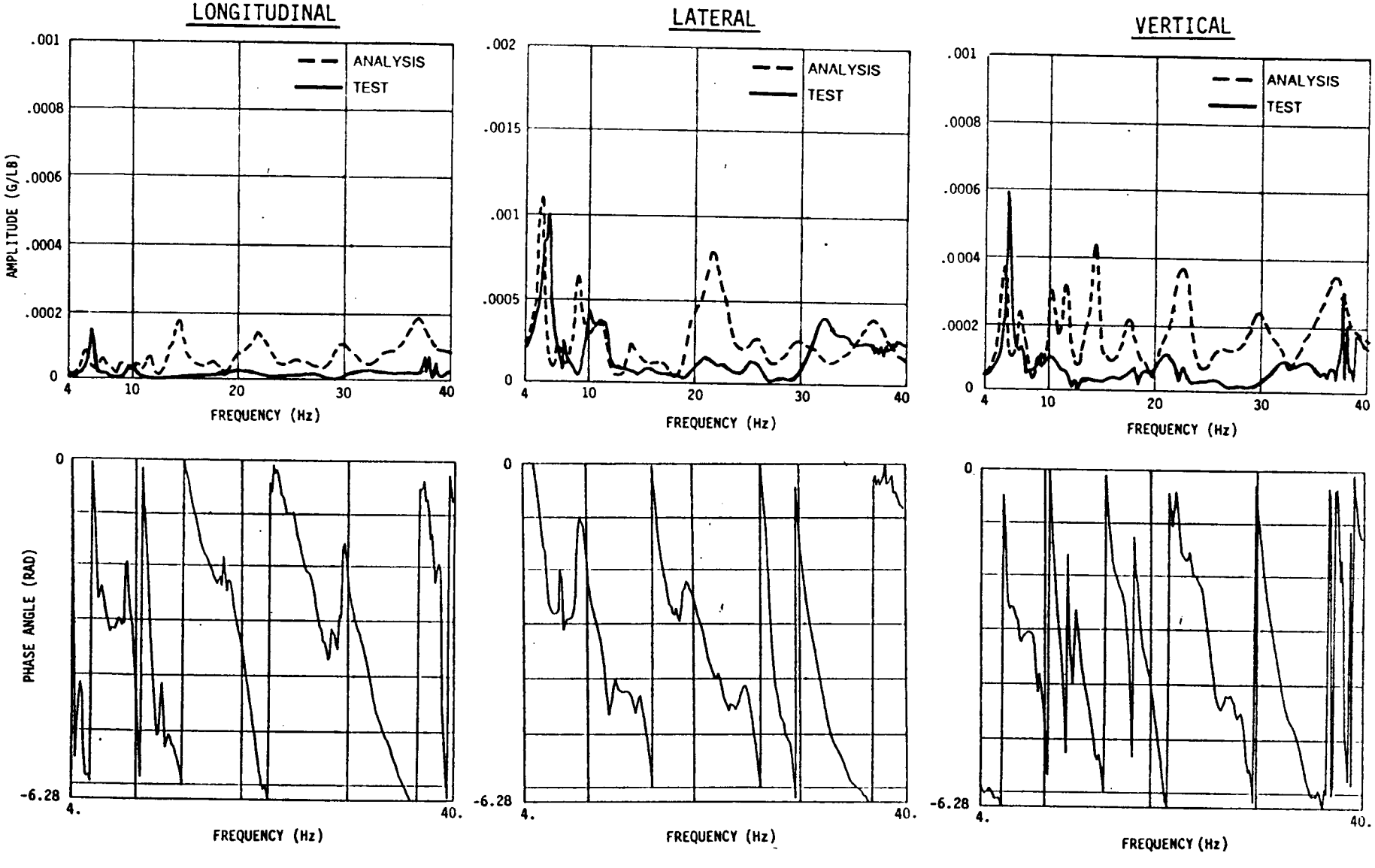

FREQUENCY RESPONSE - AFT LONGITUDINAL EXCITATION
RESPONSE: STA. 10 R/H FORWARD COCKPIT (LOC. 9)

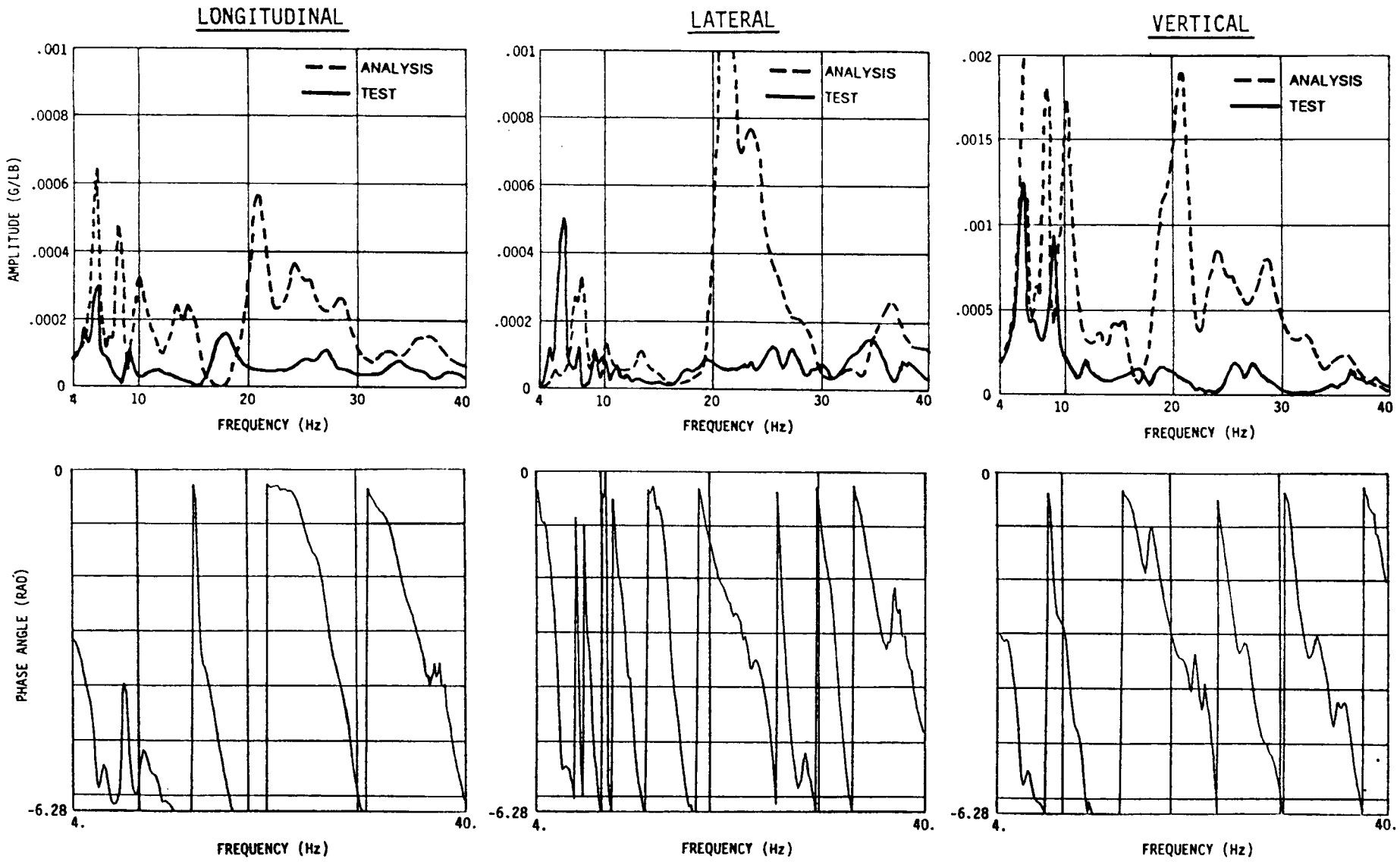

8.0 Comparison of Analysis and Estimated Test Natural Frequencies

COMPARISON OF ANALYSIS AND ESTIMATED TEST NATURAL FREQUENCIES

ANALYTICAL MODE AT 6.17 HZ

In this section, an effort is made to identify test natural frequencies and match them to the calculated natural frequencies based on an examination of the forced response mode shapes. The objective is to identify errors in the analytical model which contribute to the rather poor correlation evident in the comparison of test and analytical frequency response.

The accompanying chart shows a comparison of analytical and test frequencies. Based on mode shape, the comparison is divided into vertical/longitudinal responses and lateral/torsion responses. Of interest here is the analytical aft pylon longitudinal mode at 6.17 HZ and the corresponding test mode at 6.2 HZ (shaded area of chart).

The following pages show: (1) typical test and analytical forced response versus frequency; (2) the natural mode shape from the analysis; and (3) the forced response mode shape from the test. Examination of the test and analytical shapes confirms that both display the characteristic large aft pylon longitudinal/pitch motion.

COMPARISON OF ANALYSIS AND ESTIMATED TEST NATURAL FREQUENCIES

ANALYTICAL MODE AT 6.17 Hz

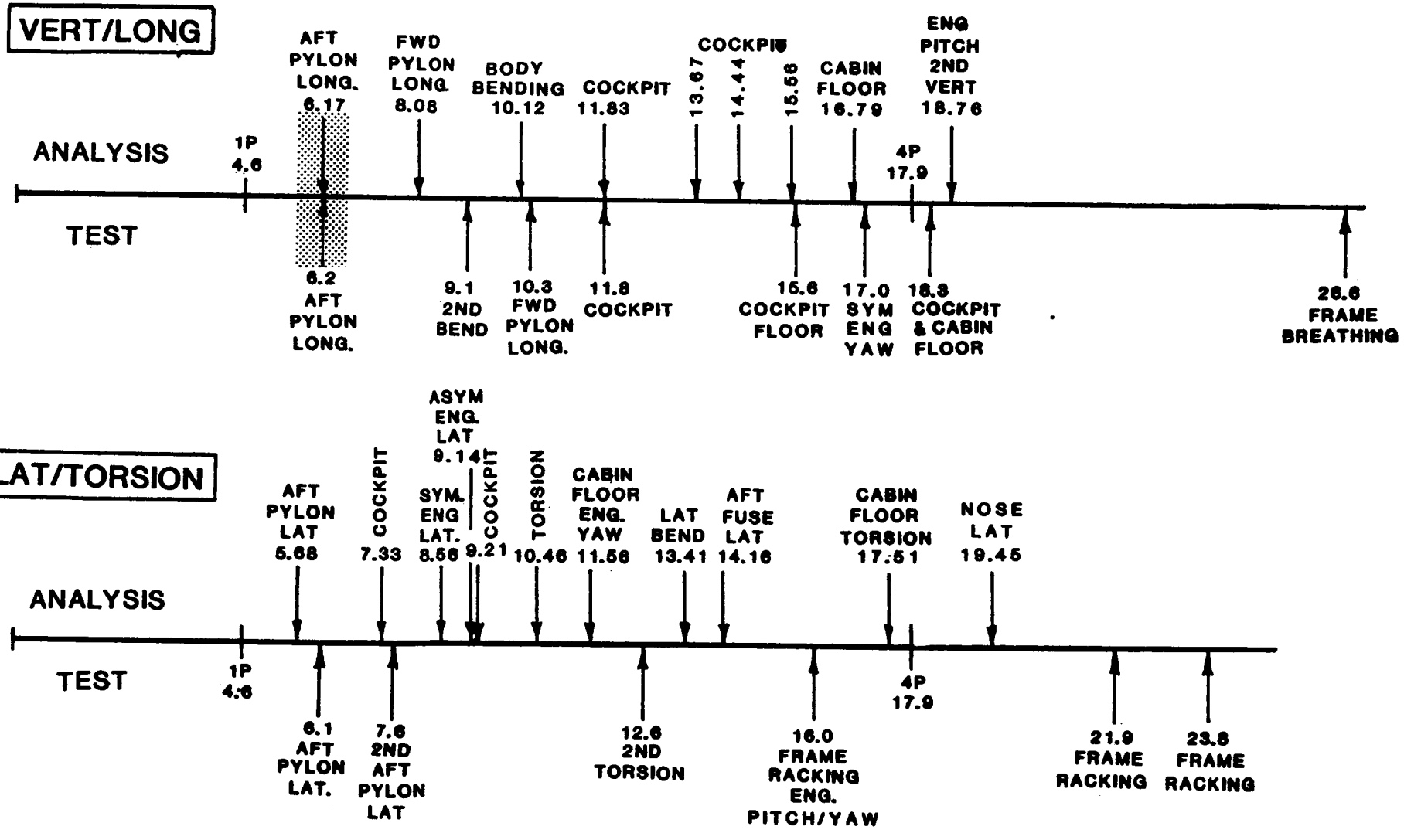

COMPARISON OF ANALYSIS AND ESTIMATED TEST NATURAL FREQUENCIES
ANALYTICAL MODE AT 6.17 Hz

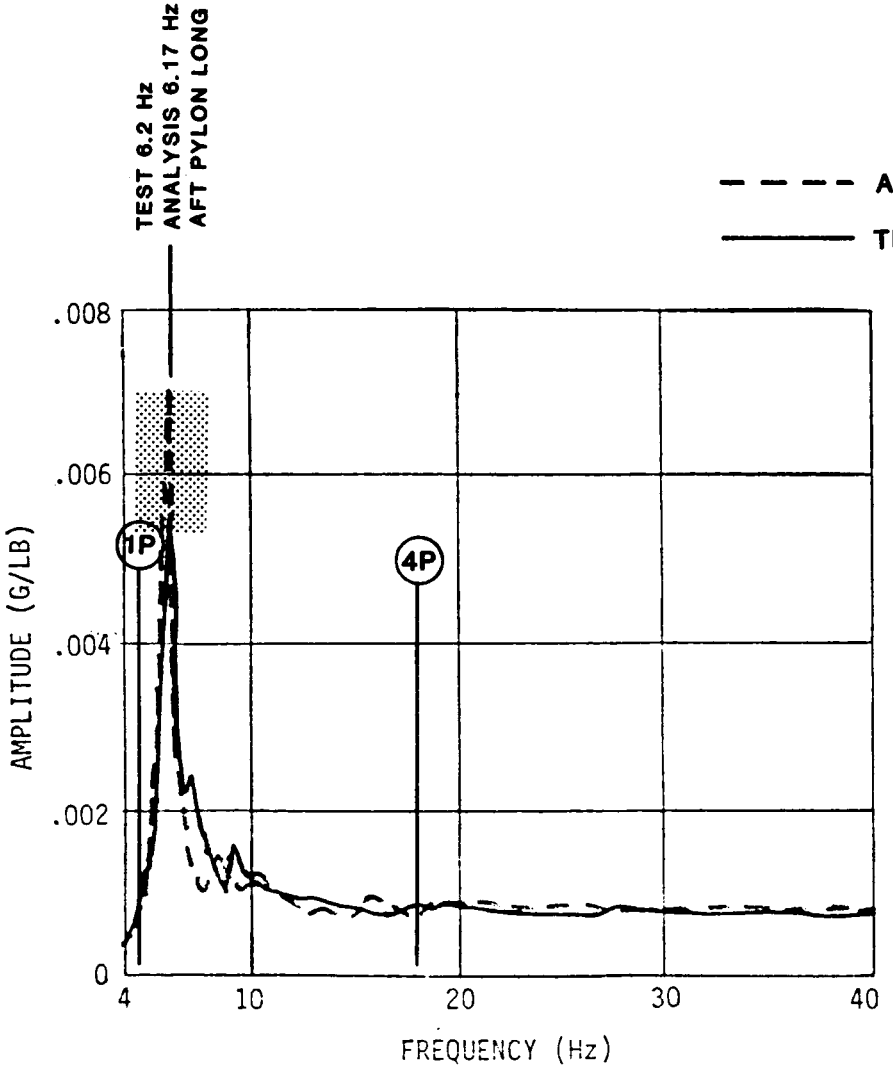

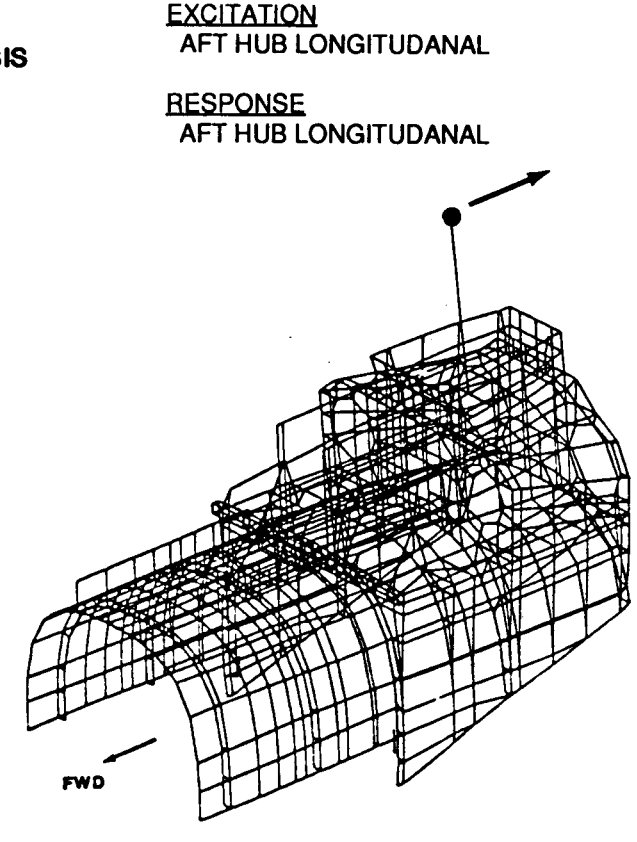

ANALYTICAL RESULTS - NATURAL MODES

MODE 8, FREQUENCY = 6.17 Hz

AFT PYLON LONGITUDINAL

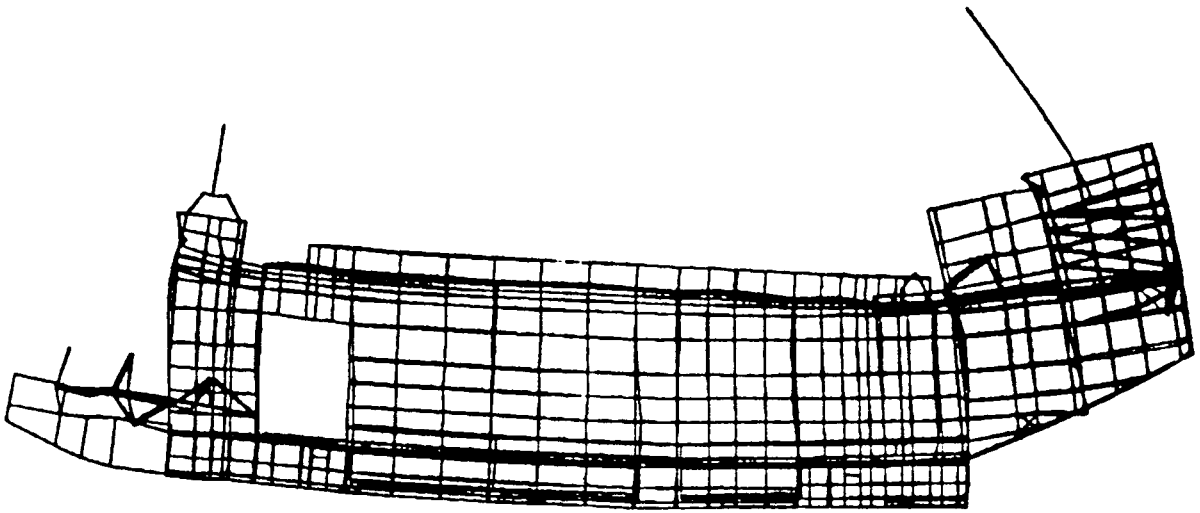

TEST RESULTS - FORCED RESPONSE MODE SHAPES
AFT HUB LONGITUDINAL EXCITATION AT 6.2 Hz

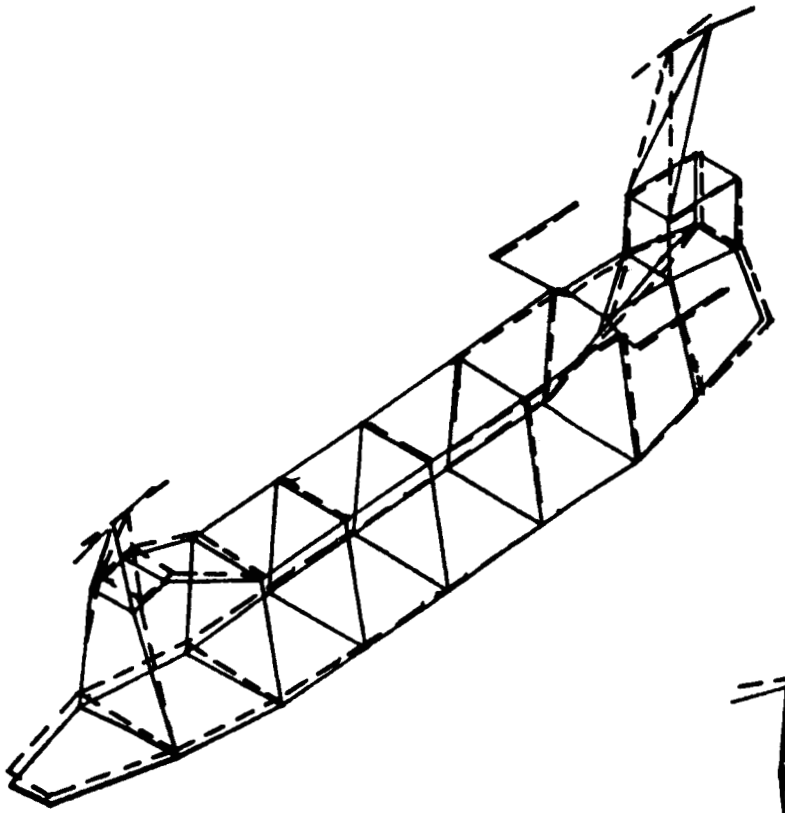

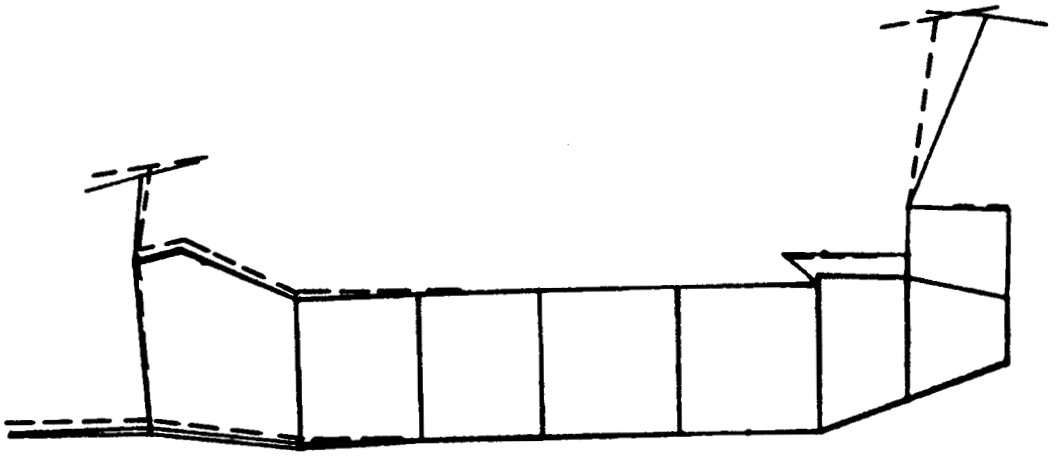

DYNAMIC

UNDEFLECTED

SIDE VIEW

COMPARISON OF ANALYSIS AND ESTIMATED TEST NATURAL FREQUENCIES

ANALYTICAL MODE AT 8.08 HZ

Based on the response shapes, the 8.08 HZ mode is best matched by the test mode at 10.3 HZ. Both display large longitudinal pitch motions of the forward pylon which is opposed by a vertical motion of the cockpit.

COMPARISON OF ANALYSIS AND ESTIMATED TEST NATURAL FREQUENCIES

ANALYTICAL MODE AT 8.08 Hz

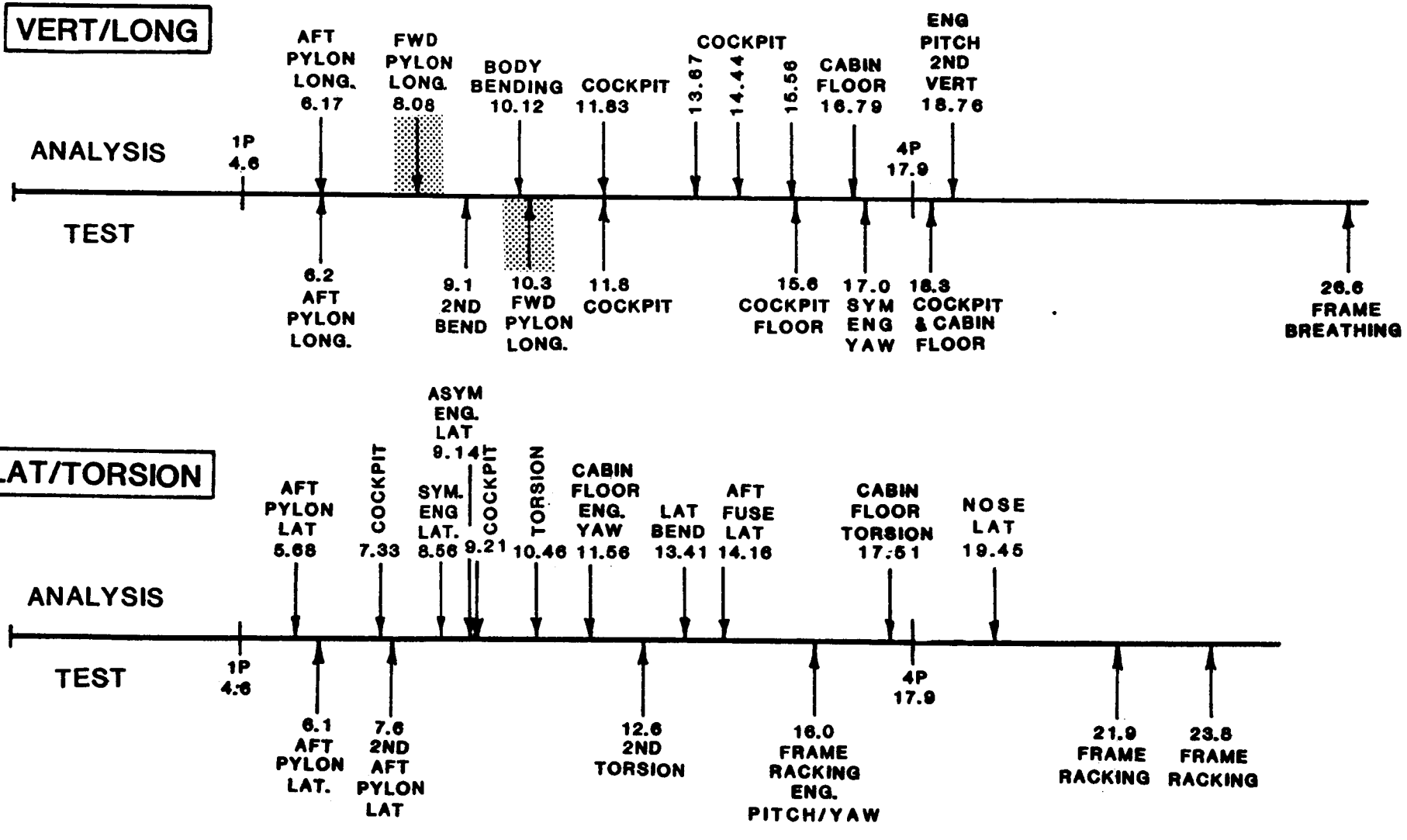

COMPARISON OF ANALYSIS AND ESTIMATED TEST NATURAL FREQUENCIES ANALYTICAL MODE AT 8.08 Hz

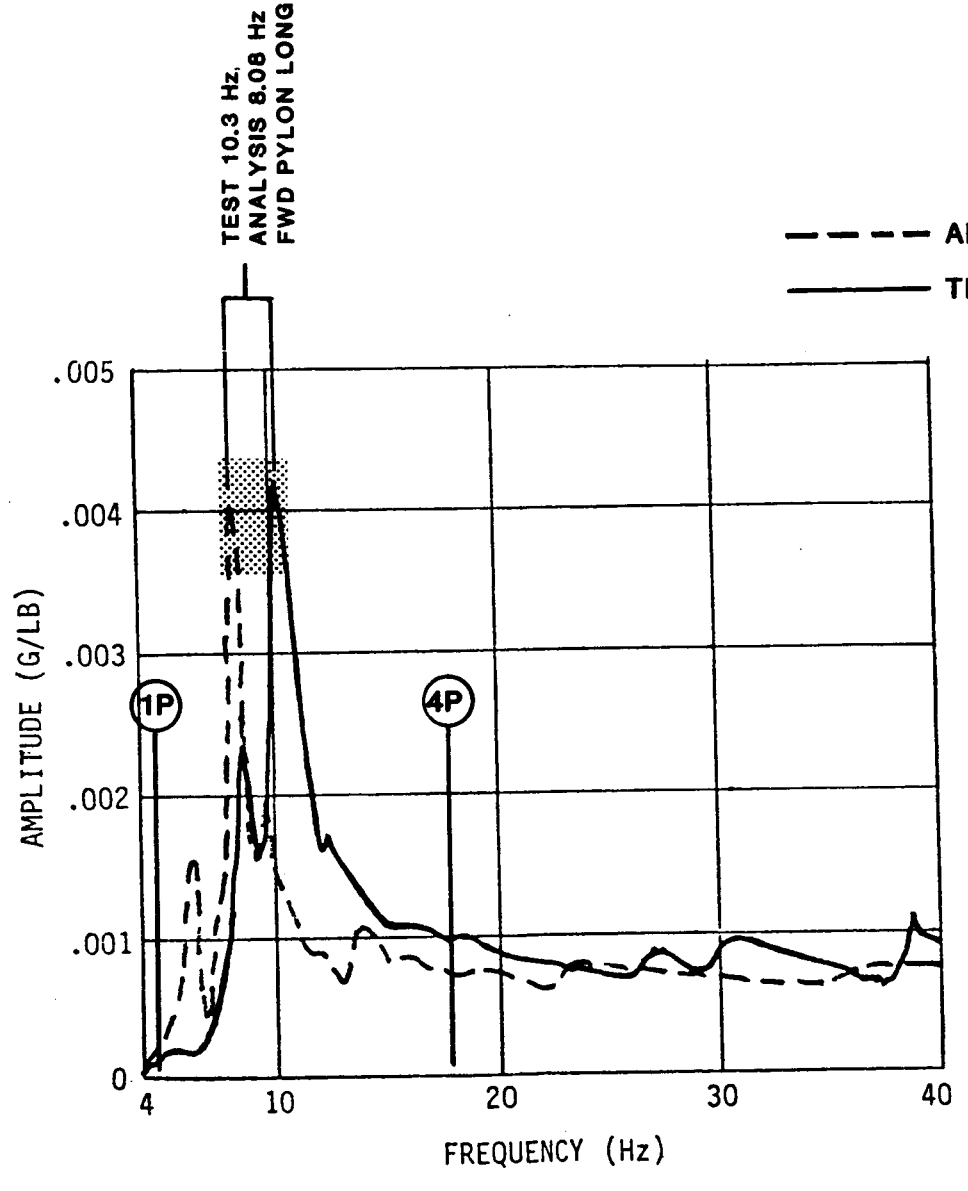

EXCITATION
FWD HUB LONGITUDANAL

RESPONSE
FWD HUB LONGITUDANAL

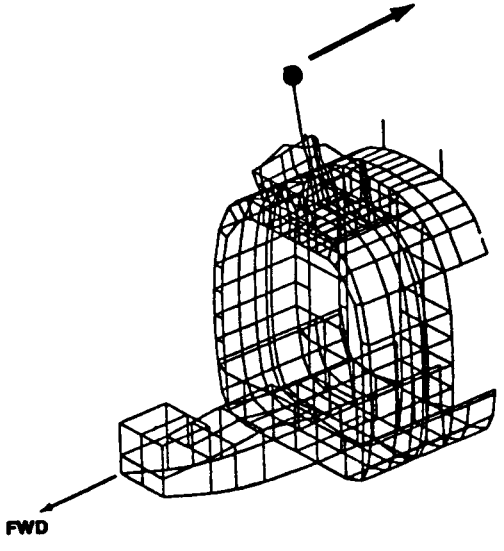

ANALYTICAL RESULTS - NATURAL MODES

MODE 10, FREQUENCY = 8.08 Hz

FWD PYLON LONGITUDINAL

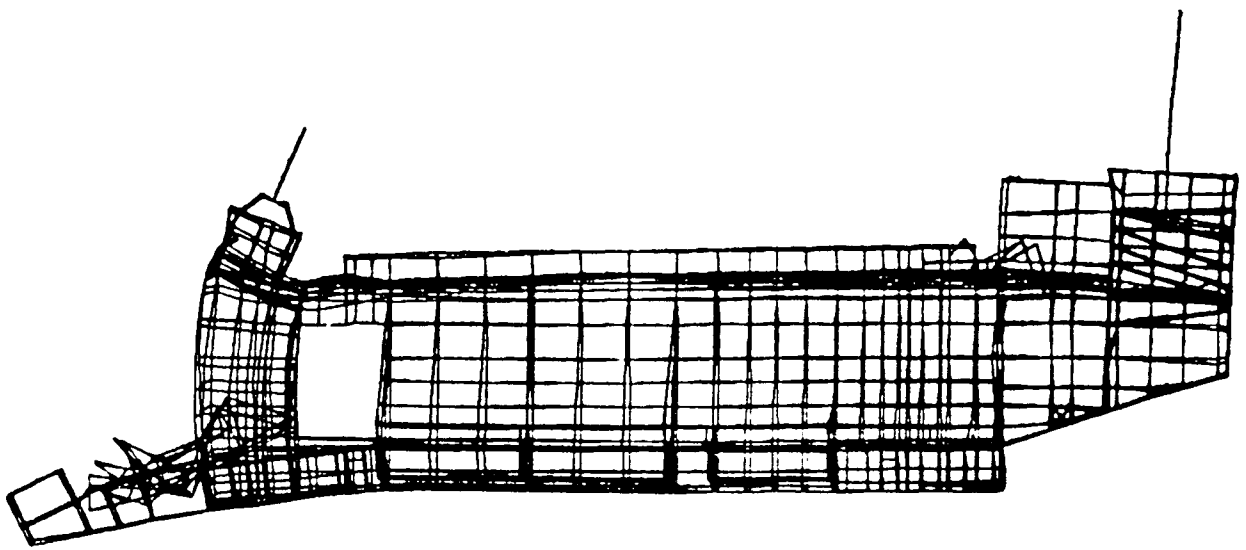

TEST RESULTS - FORCED RESPONSE MODE SHAPES
FORWARD HUB LONGITUDINAL EXCITATION AT 10.3 Hz

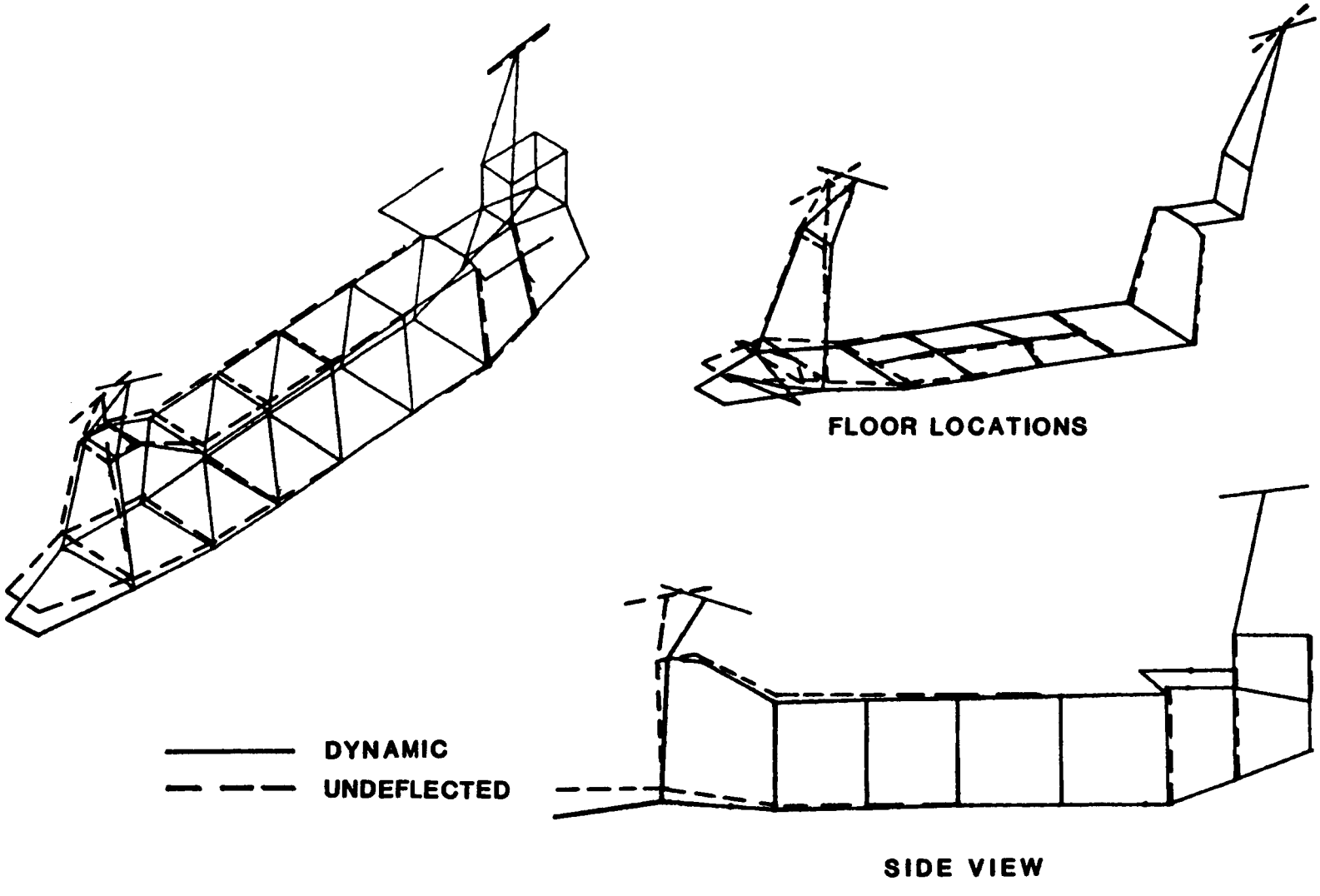

COMPARISON OF ANALYSIS AND ESTIMATED TEST NATURAL FREQUENCIES

ANALYTICAL MODE AT 10.12 HZ

The test mode at 9.1 HZ is best paired with the analytical mode at 10.12 HZ. Forced response test data shows a strong peak in the aft hub vertical response. The corresponding analytical response is not as strong. Both mode shapes display significant bending motion, particularly at the floor line. The test mode shows large vertical motions in the aft fuselage, which is not evident in the analytical mode.

COMPARISON OF ANALYSIS AND ESTIMATED TEST NATURAL FREQUENCIES

ANALYTICAL MODE AT 10.12 Hz

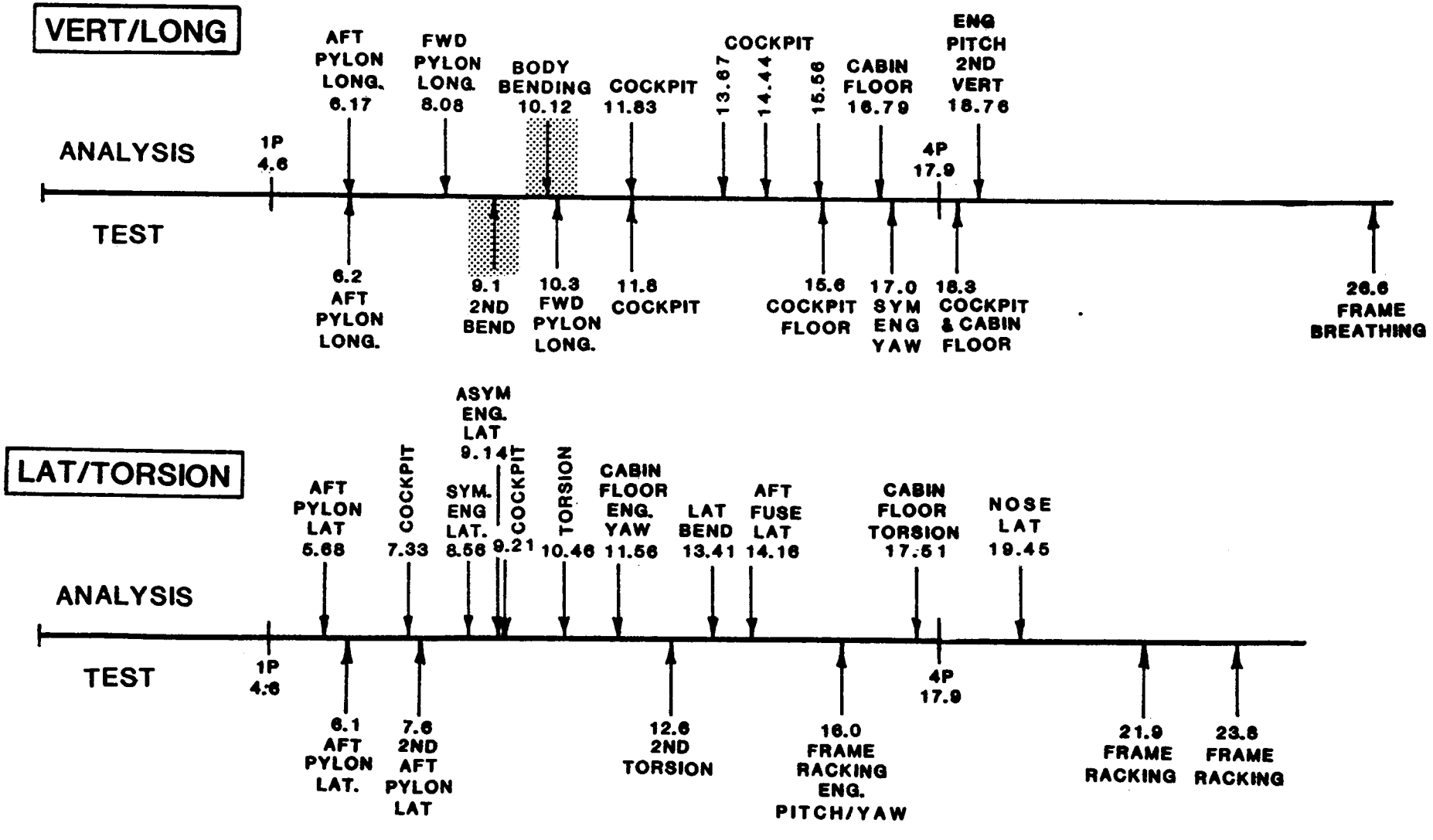

COMPARISON OF ANALYSIS AND ESTIMATED TEST NATURAL FREQUENCIES
ANALYTICAL MODE AT 10.12 Hz

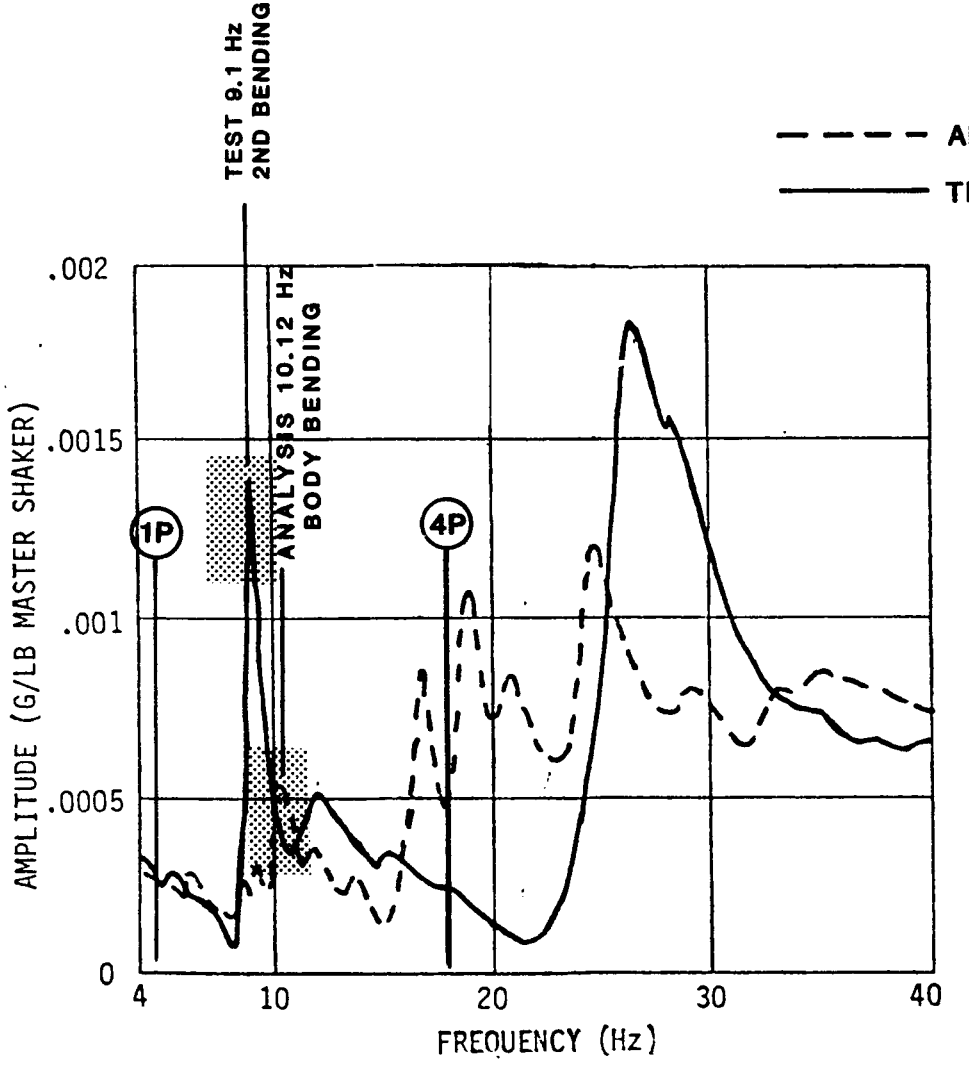

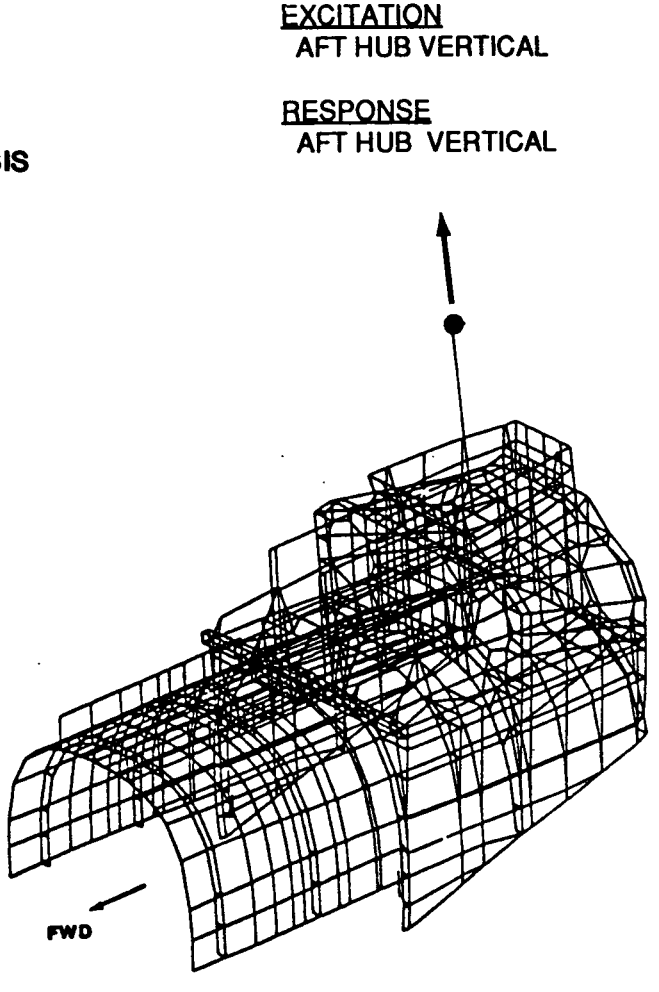

ANALYTICAL RESULTS - NATURAL MODES

MODE 14, FREQUENCY = 10.12 Hz

BODY BENDING

TEST RESULTS - FORCED RESPONSE MODE SHAPES
FORWARD HUB VERTICAL EXCITATION AT 9.1 Hz

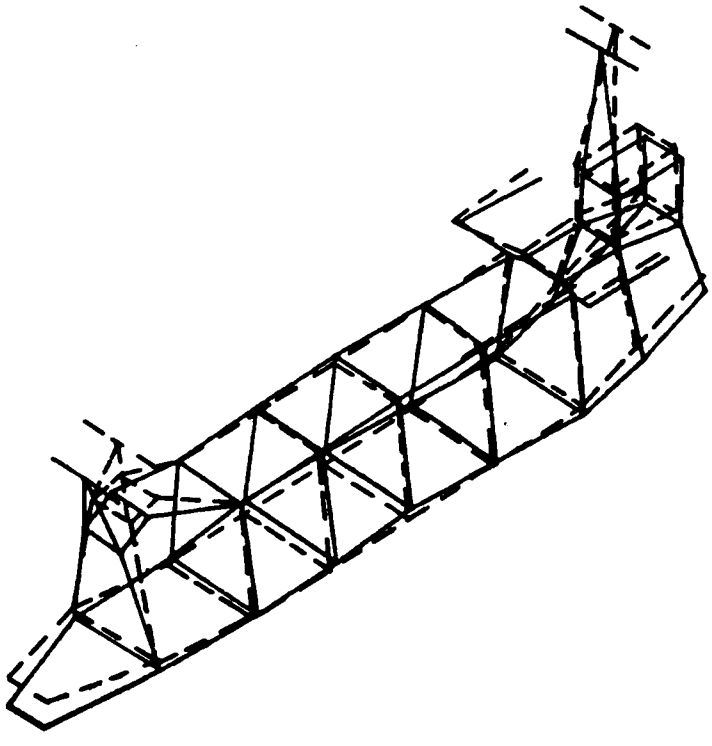

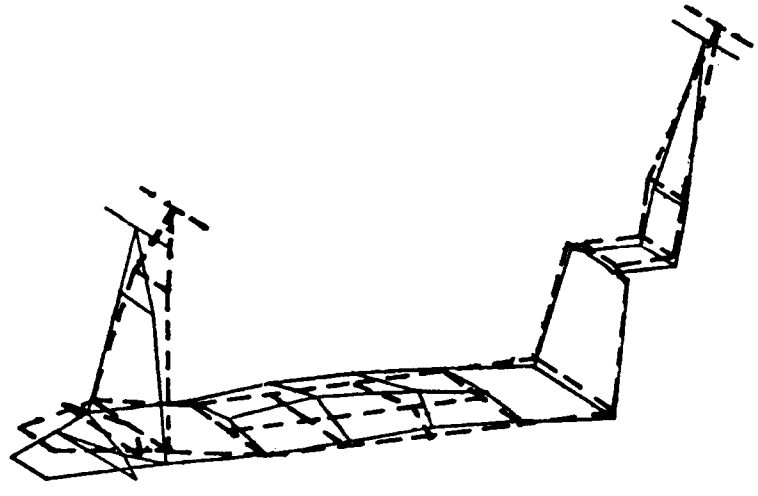

FLOOR LOCATIONS

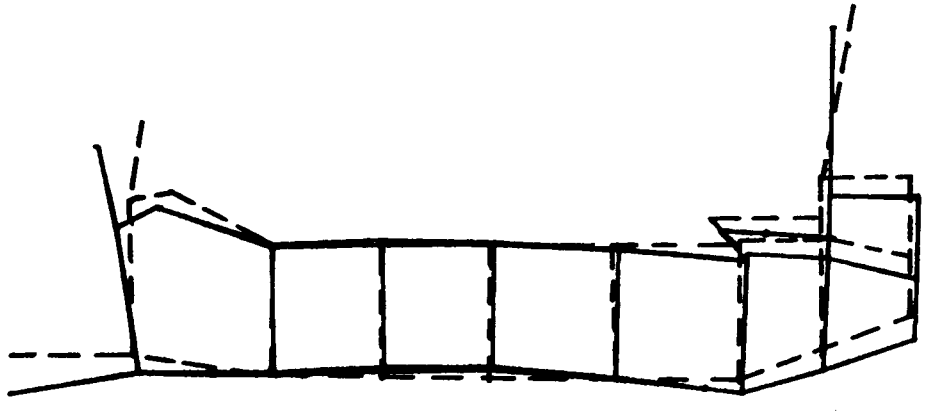

SIDE VIEW

DYNAMIC

UNDEFLECTED

COMPARISON OF ANALYSIS AND ESTIMATED TEST NATURAL FREQUENCIES

ANALYTICAL MODES AT 11.83, 13.67 AND 14.4 HZ

The only test response in this area, 11.8 HZ, seems best matched with the analytical mode at 11.83 HZ. The motion in both cases is largely confined to the cockpit. At 13.67 HZ the analytical mode shows activity over most of the airframe with some torsional motion involved. The largest motions, however, involve concentrated masses on the cockpit floor. At 14.44 HZ, the motion is again confined largely to the cockpit. Comparison with the mode at 11.83 HZ shows a phase change in the vertical motion of the cockpit beam and more local responses. In general, all of the modes appear to be local modes of the seats, console and equipment cabinets which are all mounted on the cockpit floor pallet.

COMPARISON OF ANALYSIS AND ESTIMATED TEST NATURAL FREQUENCIES

ANALYTICAL MODES AT 11.83, 13.67 AND 14.4 Hz

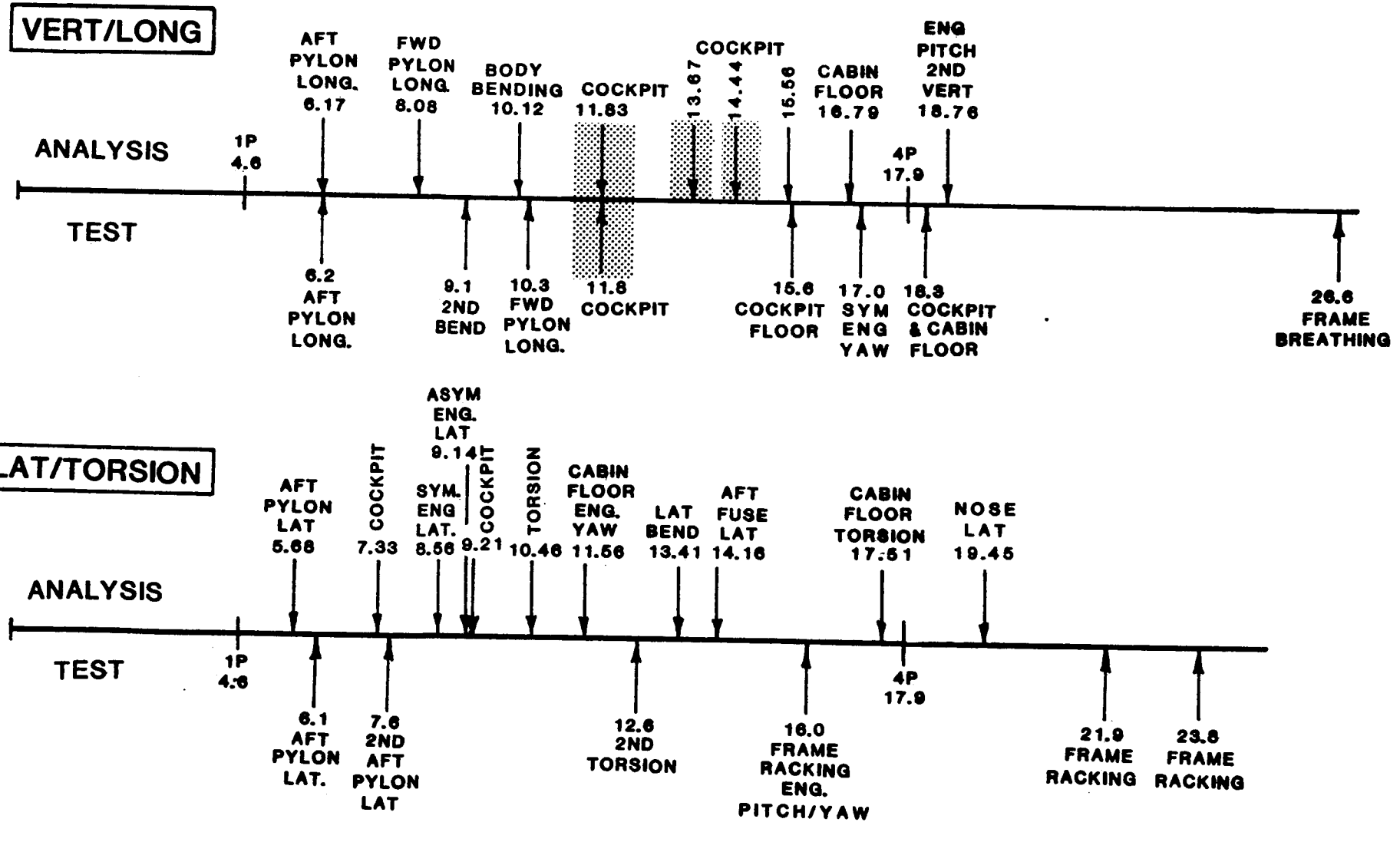

COMPARISON OF ANALYSIS AND ESTIMATED TEST NATURAL FREQUENCIES ANALYTICAL MODES AT 11.83, 13.67 AND 14.4 Hz

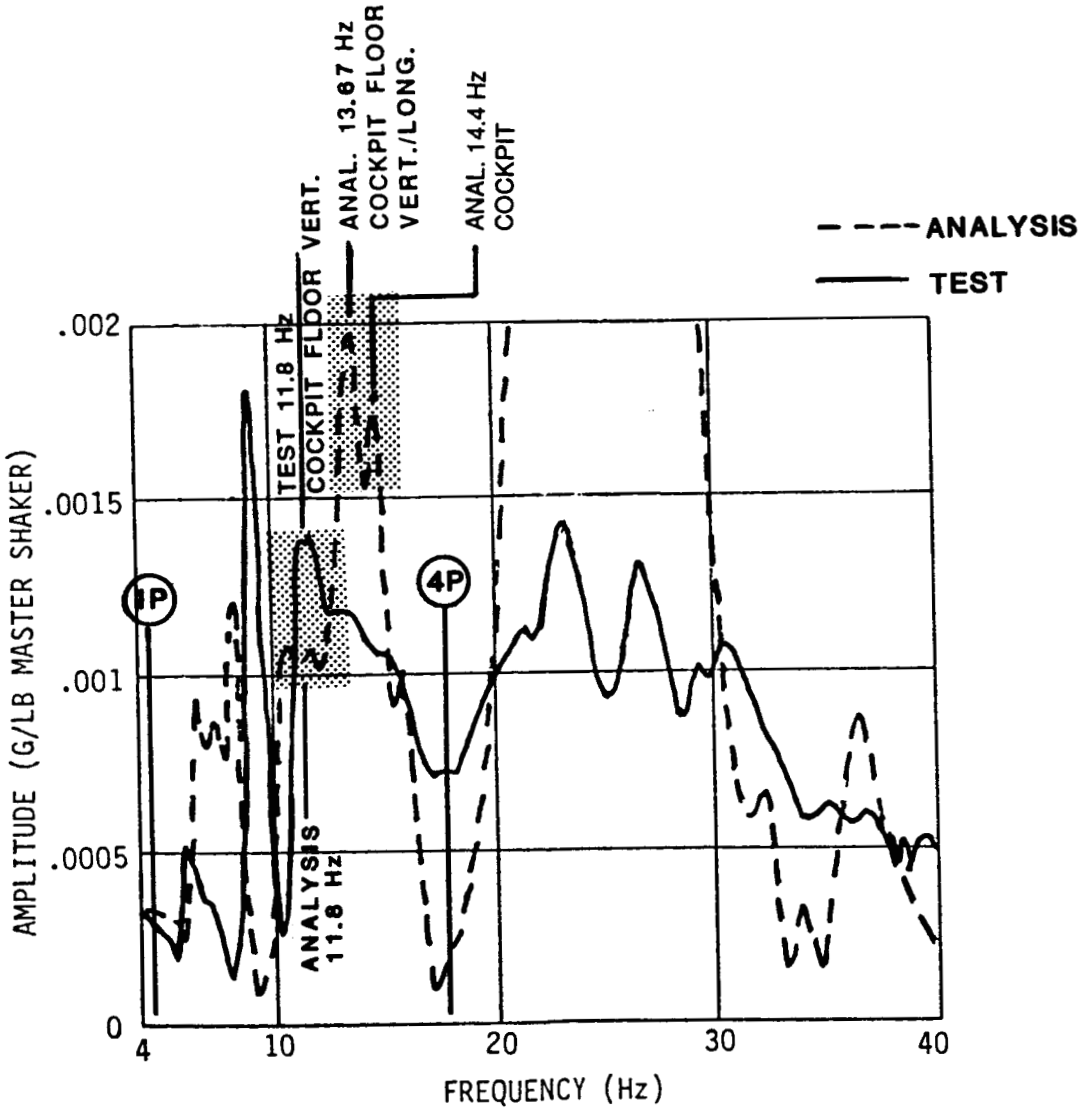

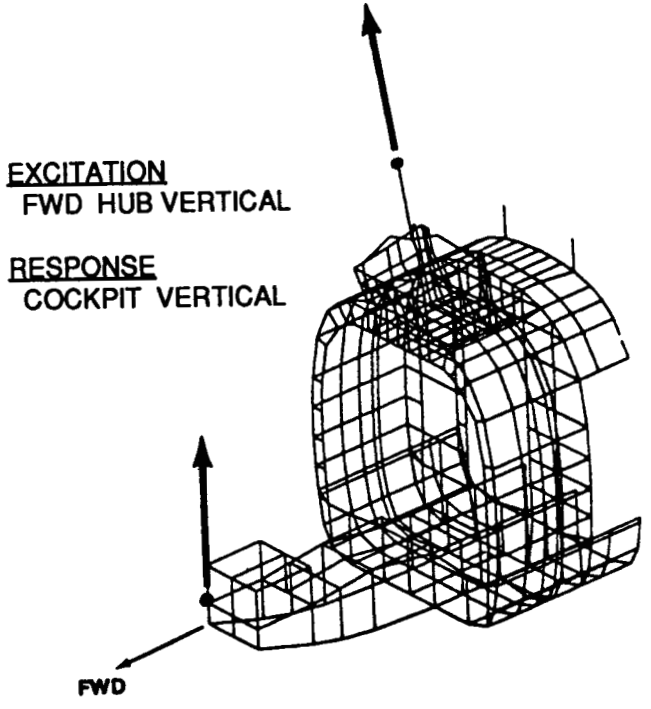

ANALYTICAL RESULTS - NATURAL MODES

MODE 17, FREQUENCY = 11.83 Hz
COCKPIT FLOOR VERTICAL

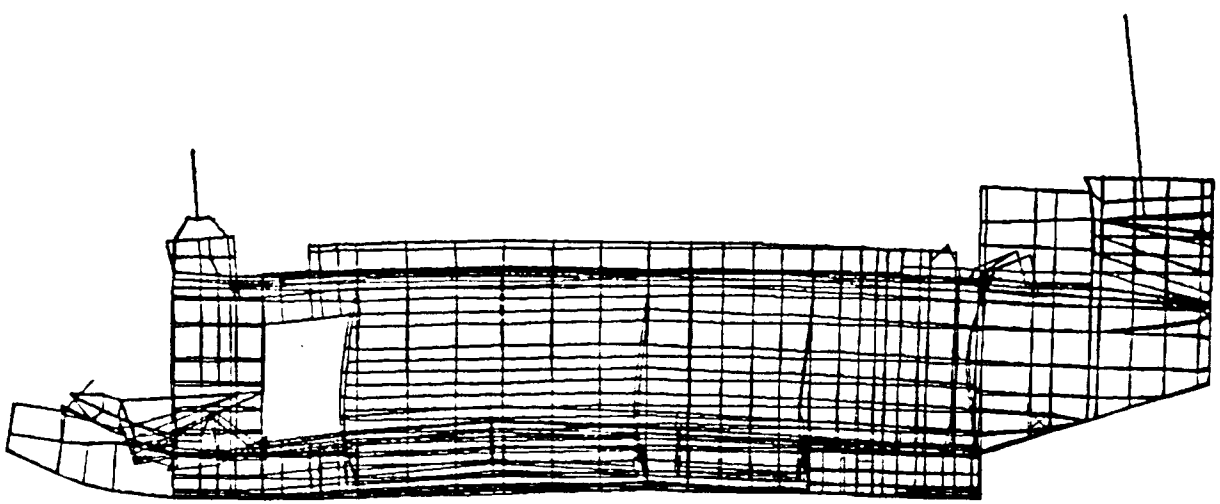

TEST RESULTS - FORCED RESPONSE MODE SHAPES
FORWARD HUB VERTICAL EXCITATION AT 11.8 Hz

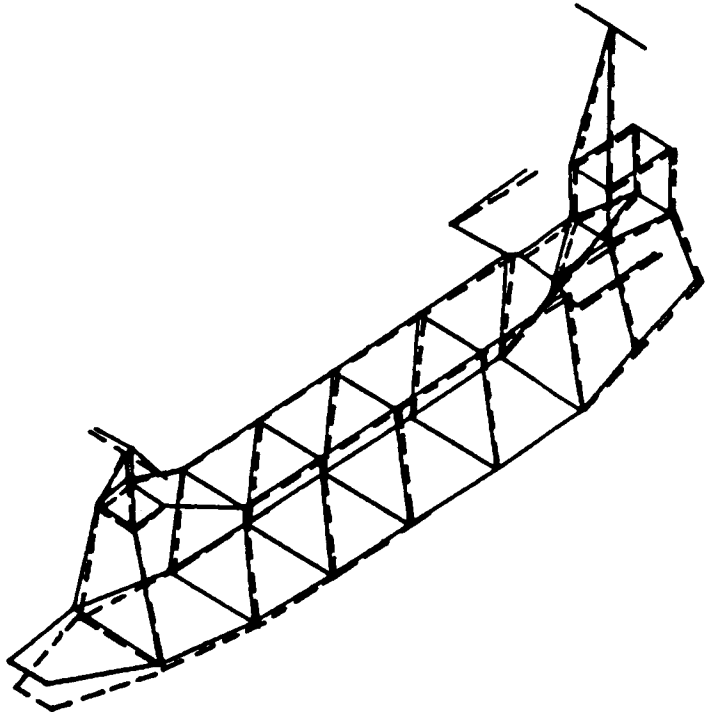

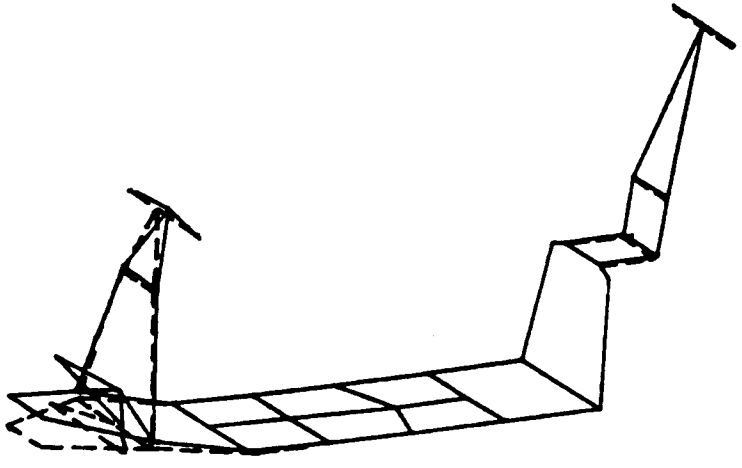

FLOOR LOCATIONS

DYNAMIC

UNDEFLECTED

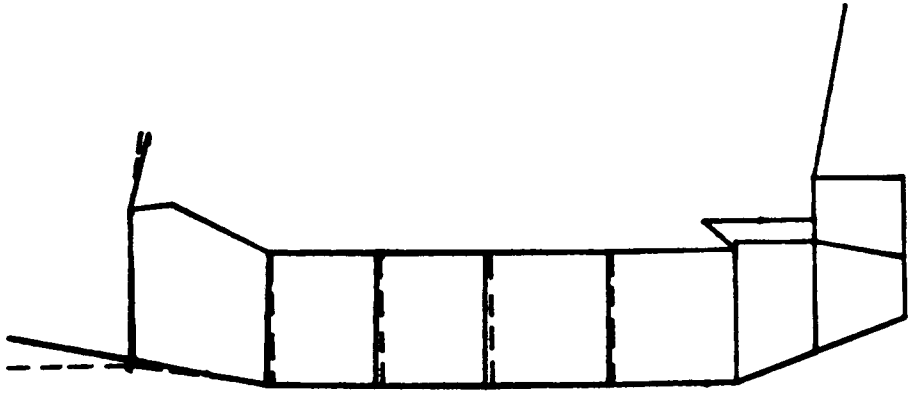

SIDE VIEW

ANALYTICAL RESULTS - NATURAL MODES

MODE 19 13.67 Hz

COCKPIT FLOOR VERT/LONG

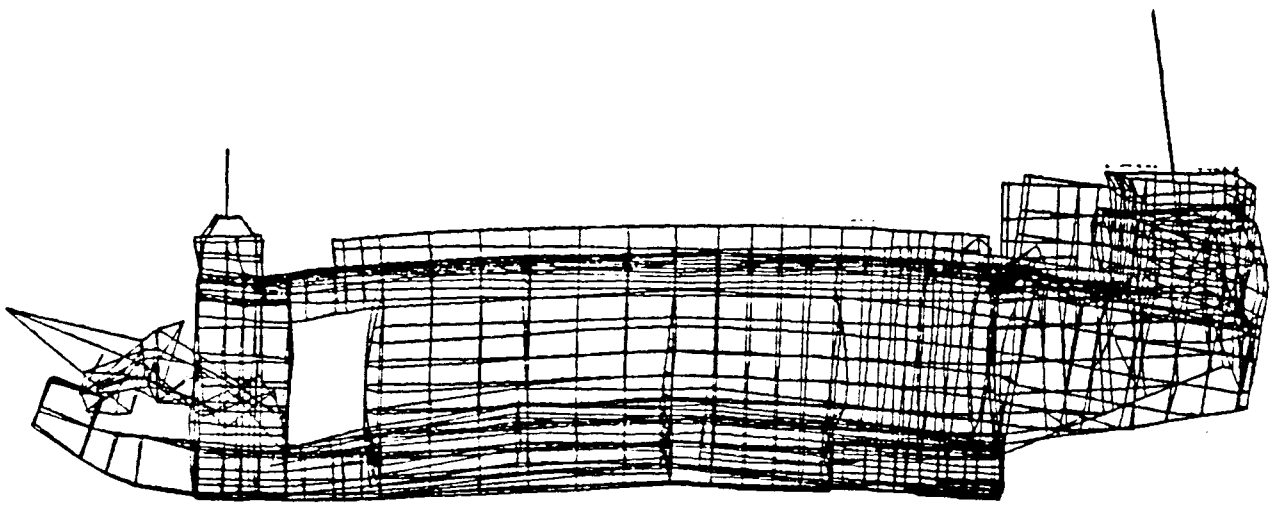

ANALYTICAL RESULTS - NATURAL MODES

MODE 21 14.44 Hz

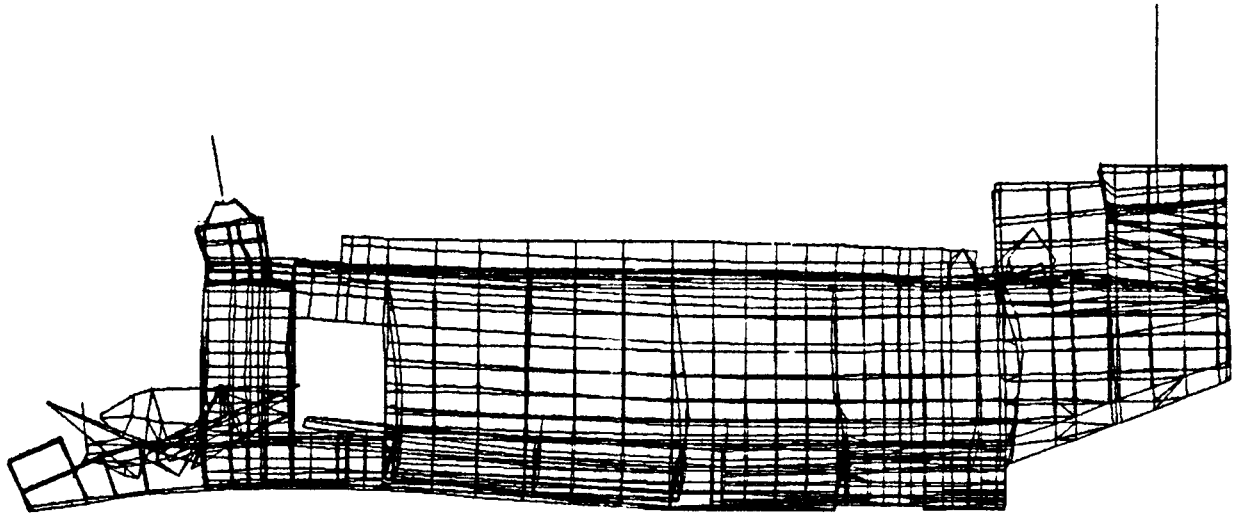

COMPARISON OF ANALYSIS AND ESTIMATED TEST NATURAL FREQUENCIES

ANALYTICAL MODE AT 15.56 HZ

The 15.56 Hz analysis mode and the 15.6 Hz test mode are similar in that both show large vertical motions near Sta. 223. However, the phase of the test mode in the region of the forward hub and cockpit is opposite to that of the analysis. Additionally, the analysis shows large motions in the aft pylon which are absent in the test response.

COMPARISON OF ANALYSIS AND ESTIMATED TEST NATURAL FREQUENCIES

ANALYTICAL MODE AT 15.56 Hz

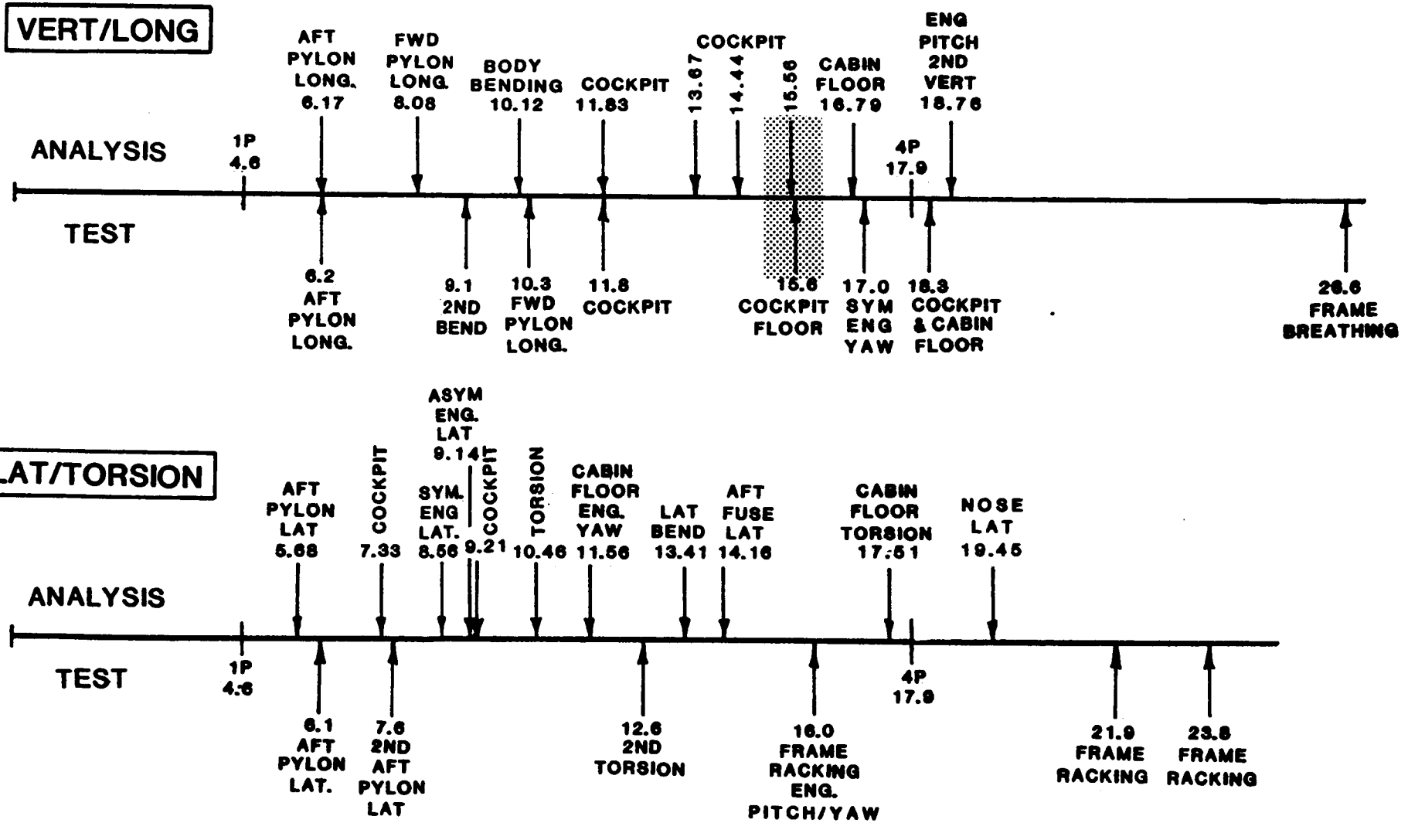

COMPARISON OF ANALYSIS AND ESTIMATED TEST NATURAL FREQUENCIES ANALYTICAL MODE AT 15.56 Hz

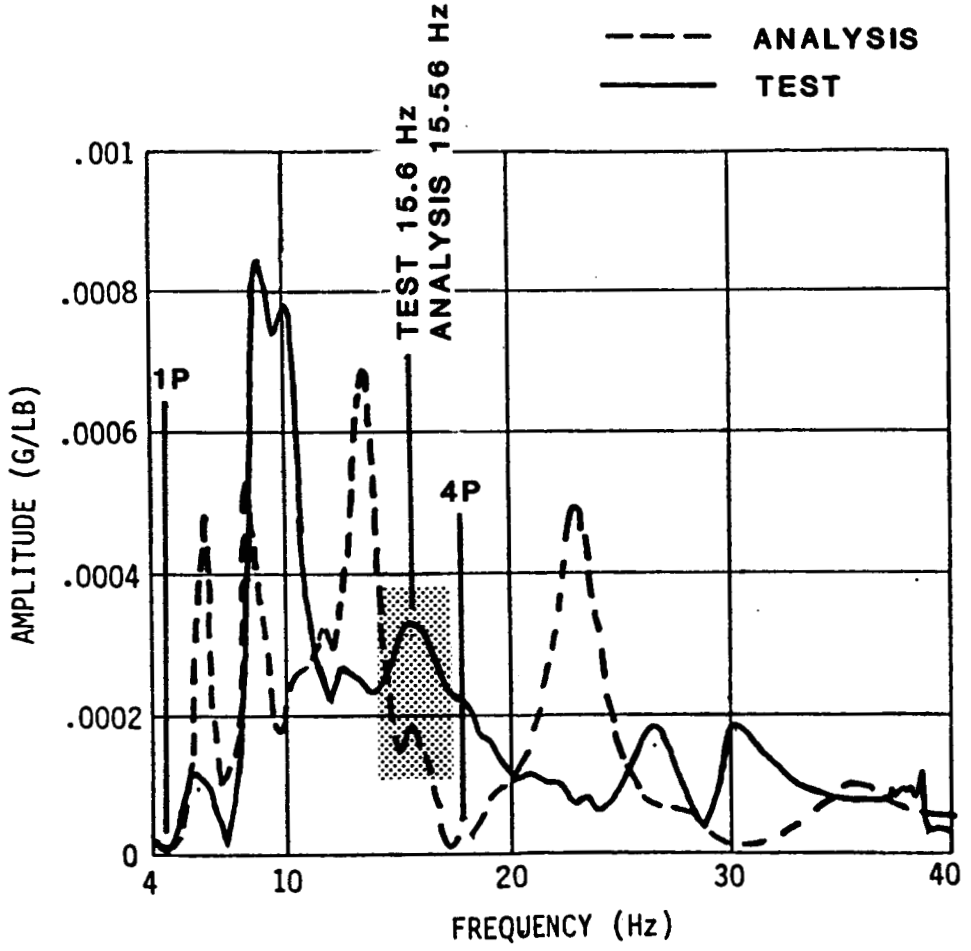

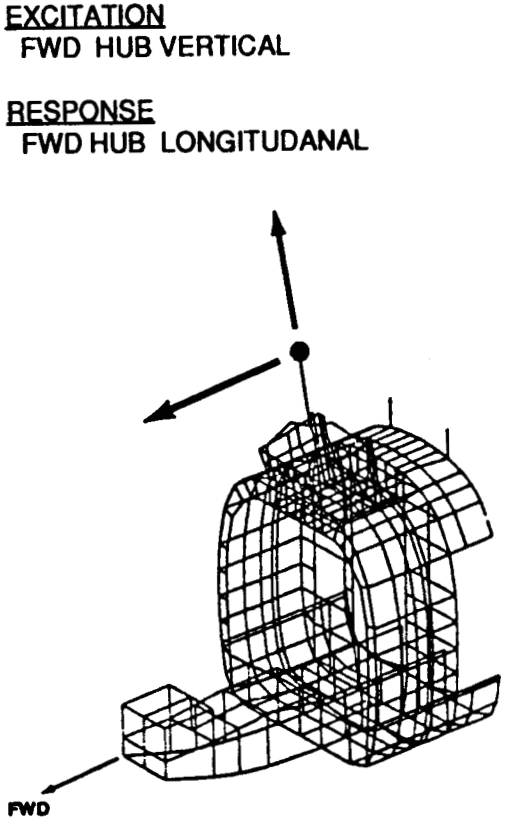

ANALYTICAL RESULTS - NATURAL MODES

MODE 22 15.56 Hz

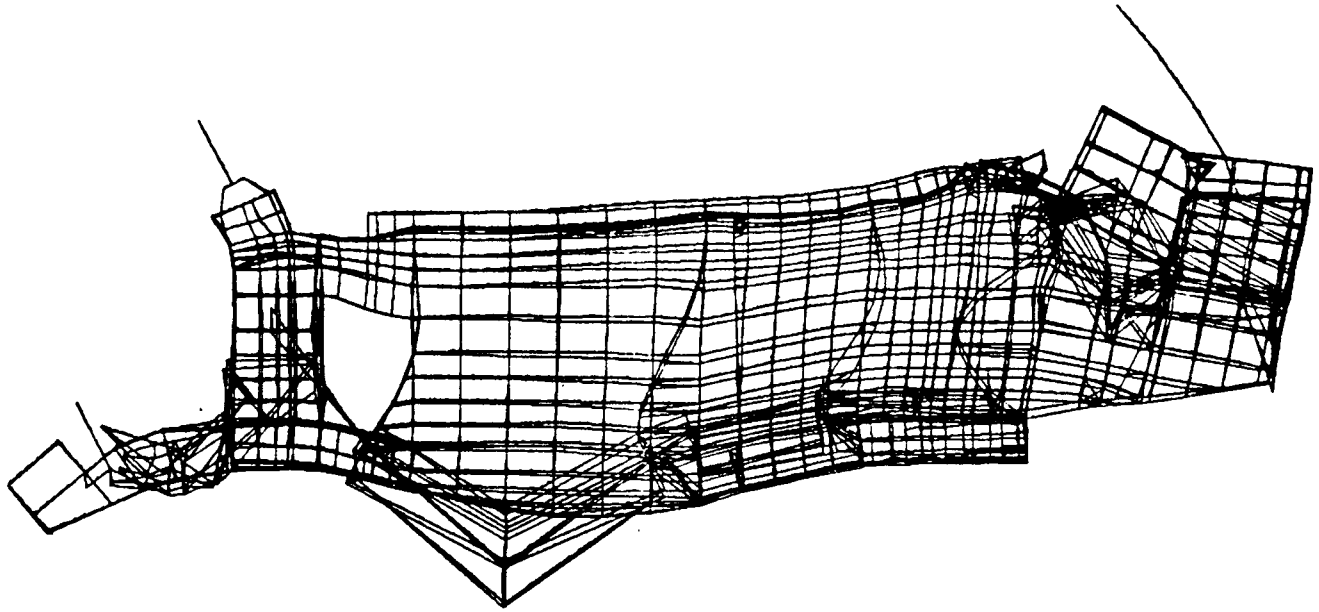

TEST RESULTS - FORCED RESPONSE MODE SHAPES
FORWARD HUB VERTICAL EXCITATION AT 15.6 Hz

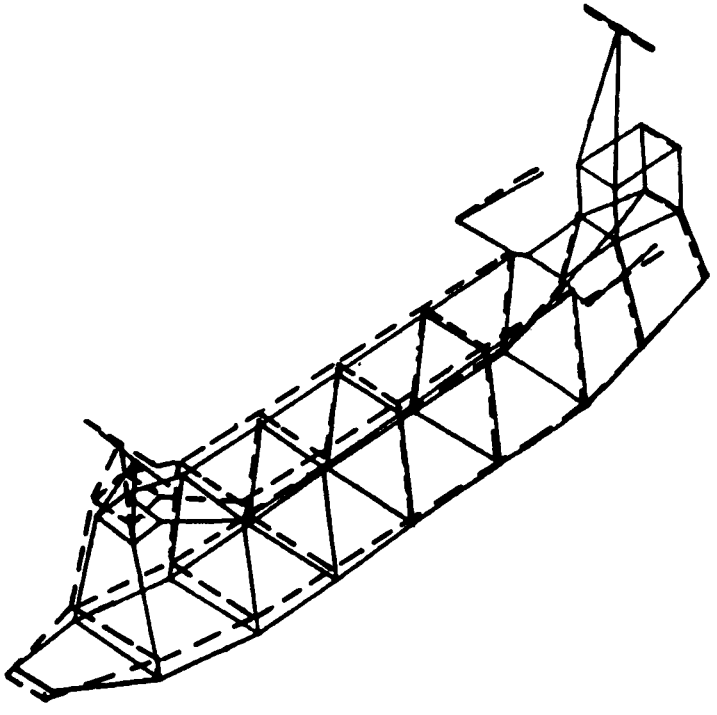

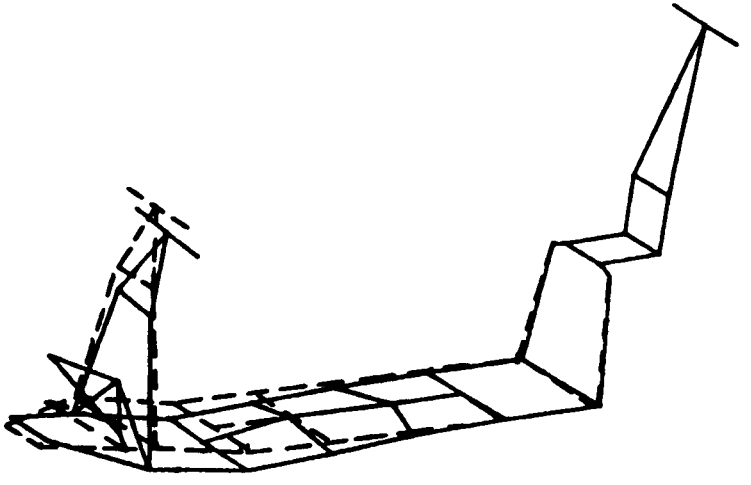

FLOOR LOCATIONS

DYNAMIC

UNDEFLECTED

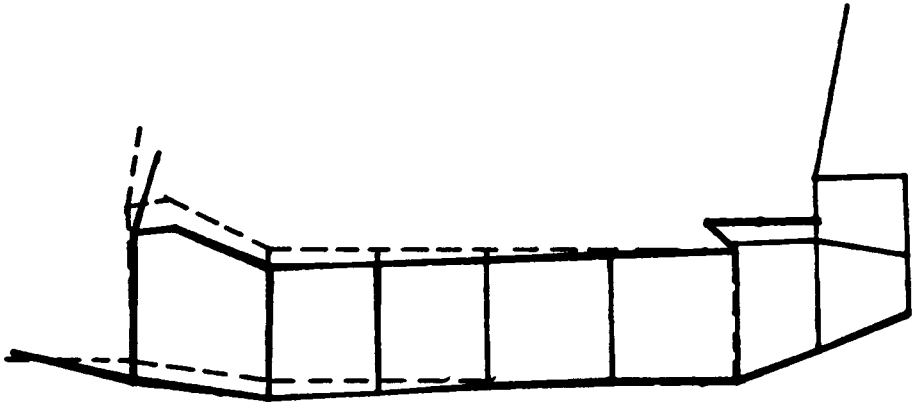

SIDE VIEW

COMPARISON OF ANALYSIS AND ESTIMATED TEST NATURAL FREQUENCIES

ANALYTICAL MODE AT 16.79 HZ

The test response at 17 HZ and the analytical mode at 16.79 HZ seem well matched; however, the mode shapes are distinctly different. The analytical mode displays an overall response dominated by the cabin floor. In contrast, the most distinctive feature of the test shape is the large symmetric engine yaw motion.

COMPARISON OF ANALYSIS AND ESTIMATED TEST NATURAL FREQUENCIES

ANALYTICAL MODE AT 16.79 Hz

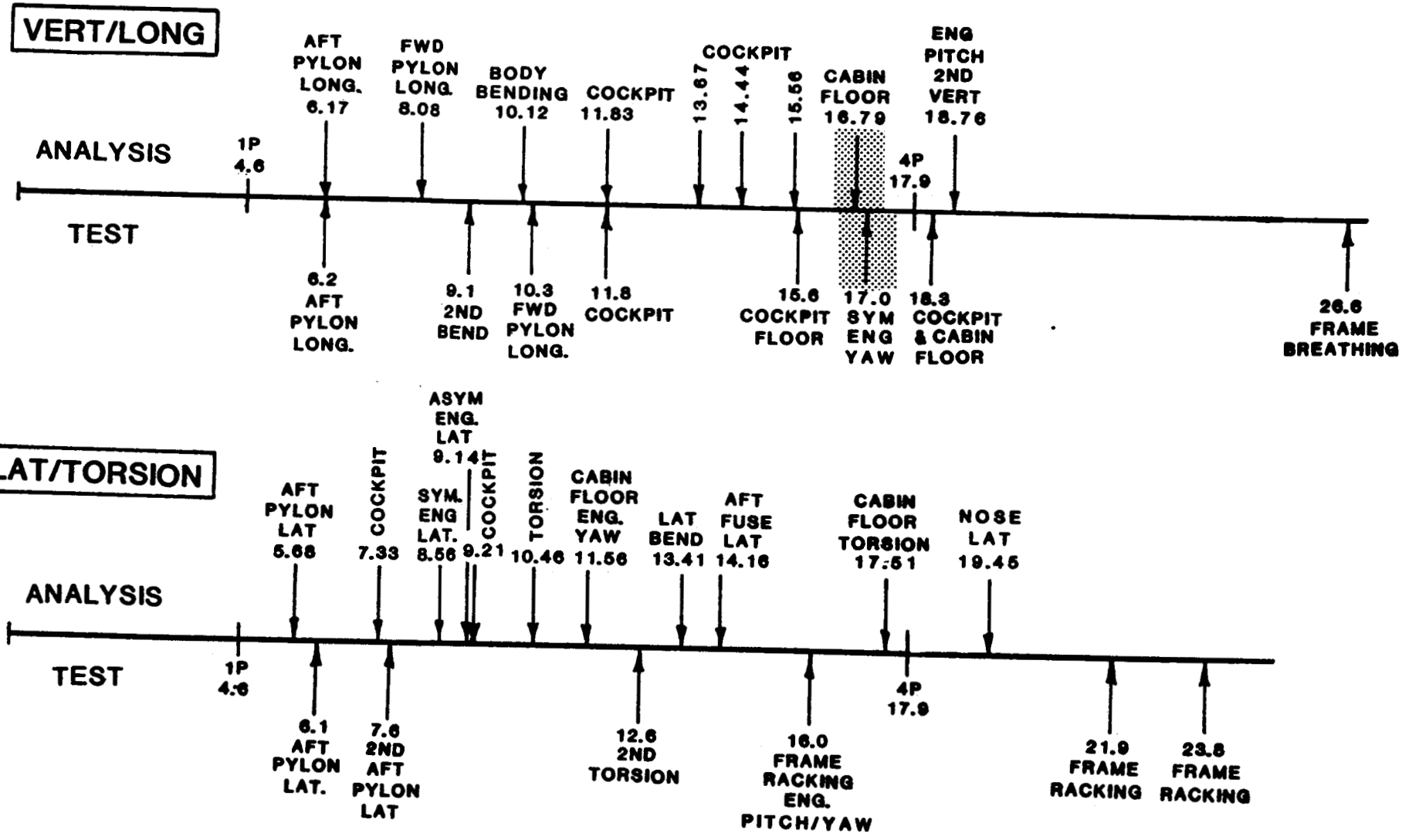

COMPARISON OF ANALYSIS AND ESTIMATED TEST NATURAL FREQUENCIES
ANALYTICAL MODE AT 16.79 Hz

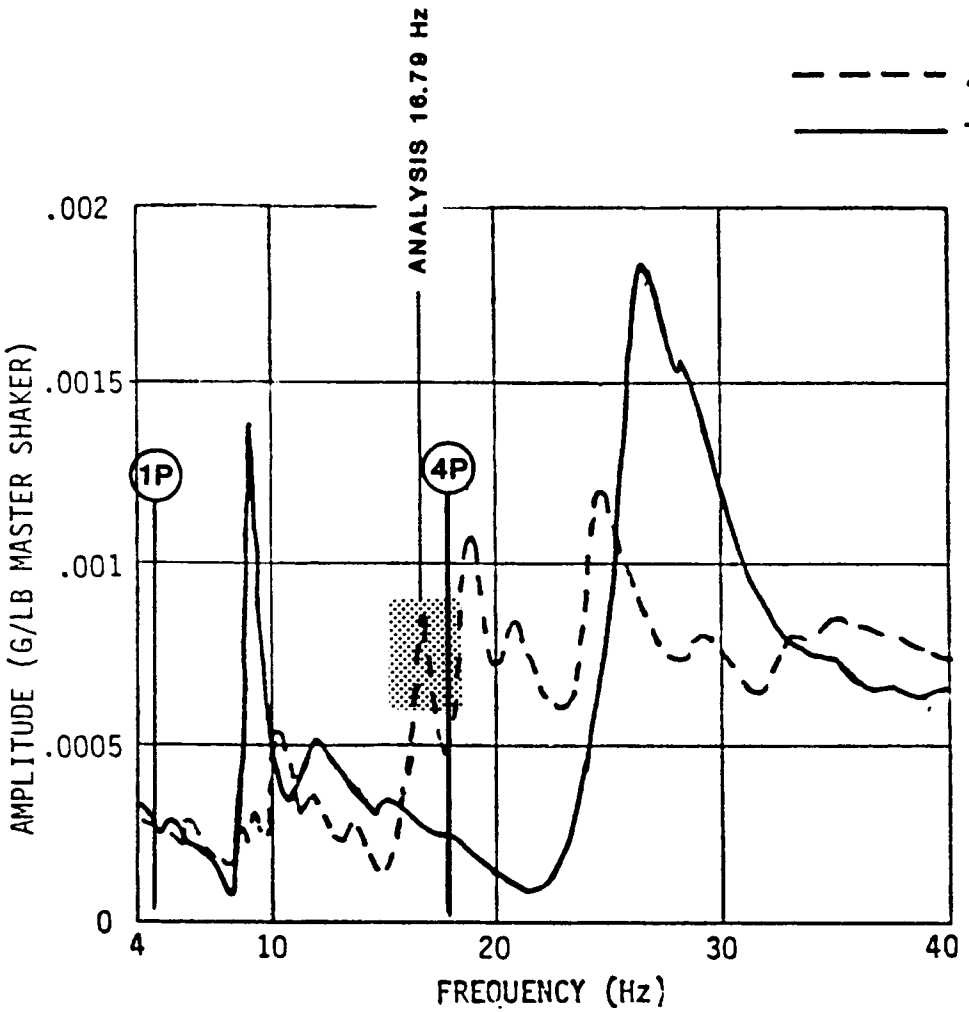

EXCITATION
AFT HUB VERTICAL

RESPONSE
AFT HUB VERTICAL

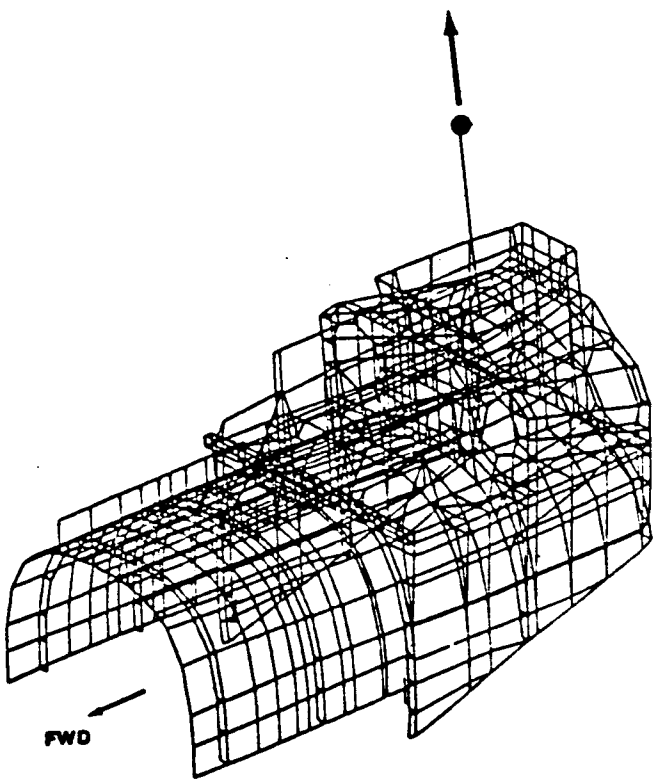

COMPARISON OF ANALYSIS AND ESTIMATED TEST NATURAL FREQUENCIES
ANALYTICAL MODE AT 16.79 Hz

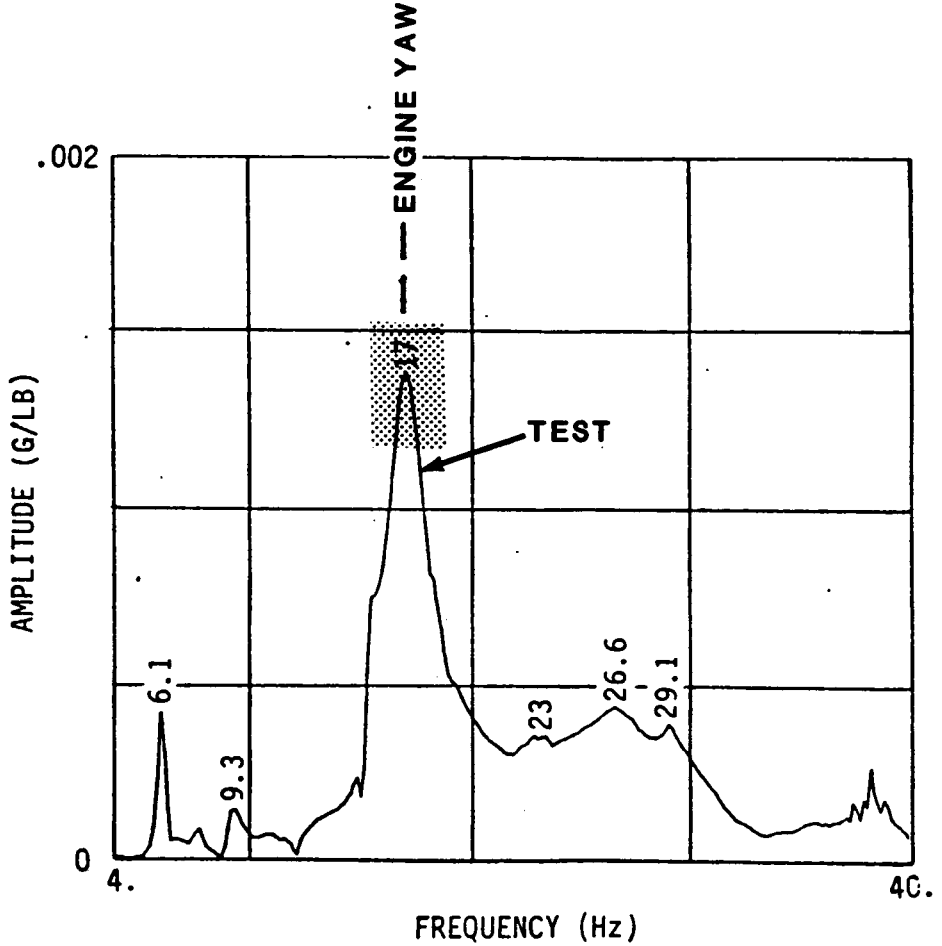

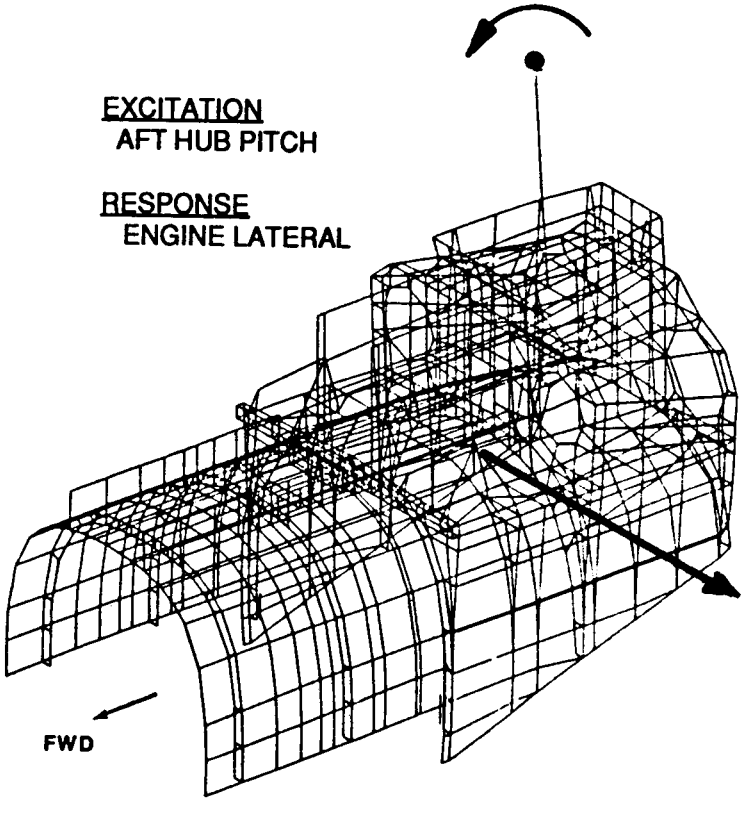

ANALYTICAL RESULTS - NATURAL MODES

MODE 23 16.79 Hz

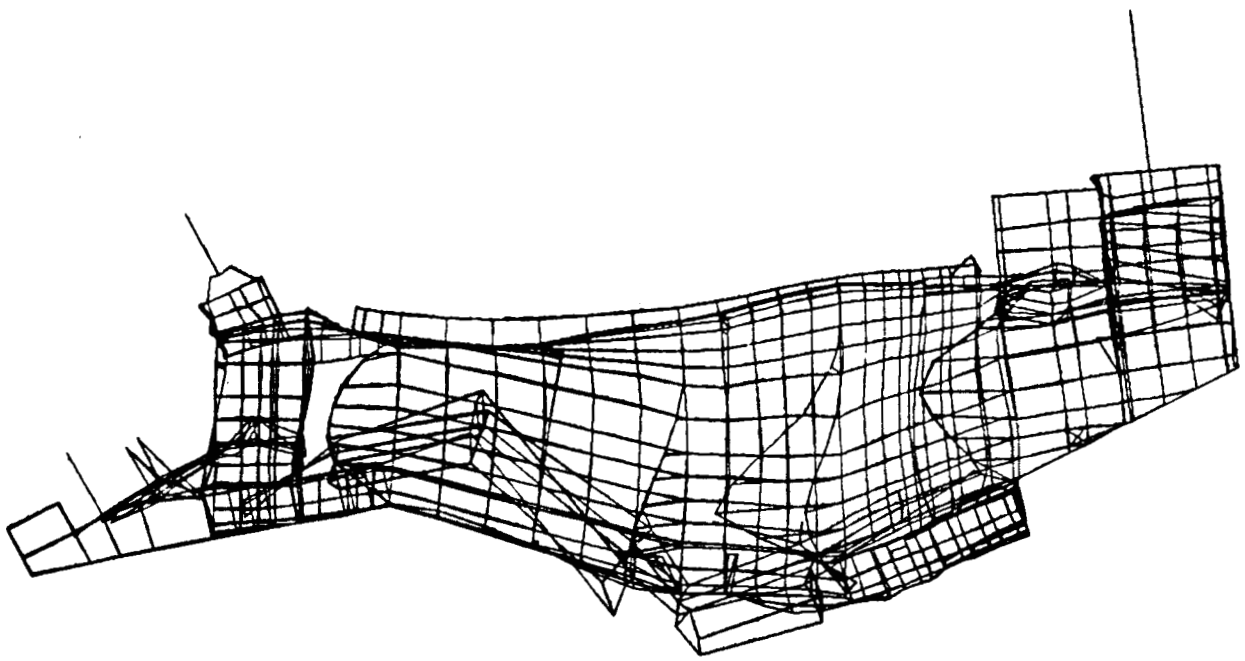

TEST RESULTS - FORCED RESPONSE MODE SHAPES
AFT HUB PITCH EXCITATION AT 17.0 Hz

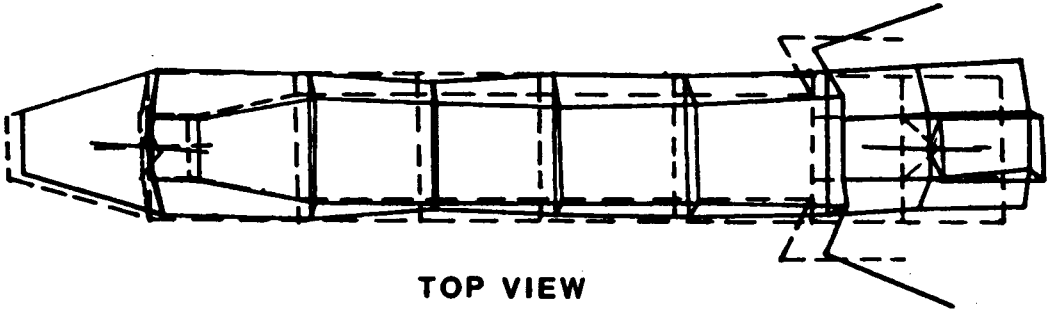

TOP VIEW

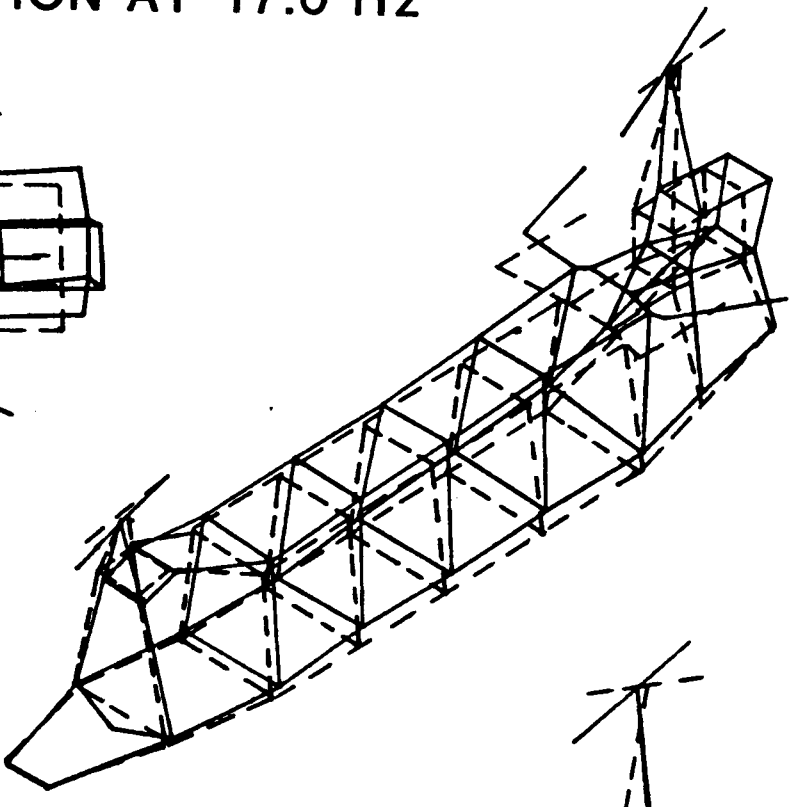

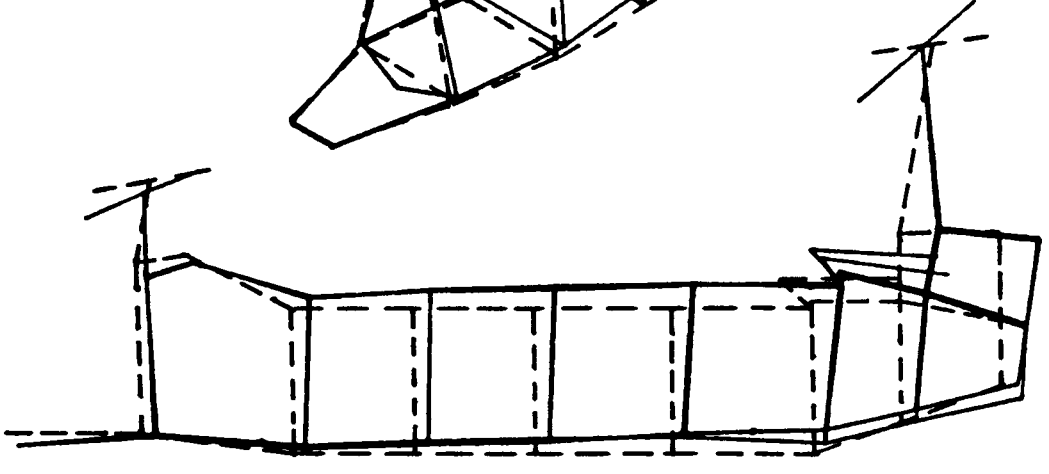

SIDE VIEW

——— DYNAMIC

– – – UNDEFLECTED

COMPARISON OF ANALYSIS AND ESTIMATED TEST NATURAL FREQUENCIES

ANALYTICAL MODE AT 18.76 HZ

The analytical mode at 18.76 HZ displays large cockpit and cabin floor response together with a symmetric engine pitch motion. The test shape (forward rotor vertical forcing) at 18.3 Hz shows somewhat similar cockpit and cabin floor motions; however, the engine pitching motion is absent.

COMPARISON OF ANALYSIS AND ESTIMATED TEST NATURAL FREQUENCIES

ANALYTICAL MODE AT 18.76 Hz

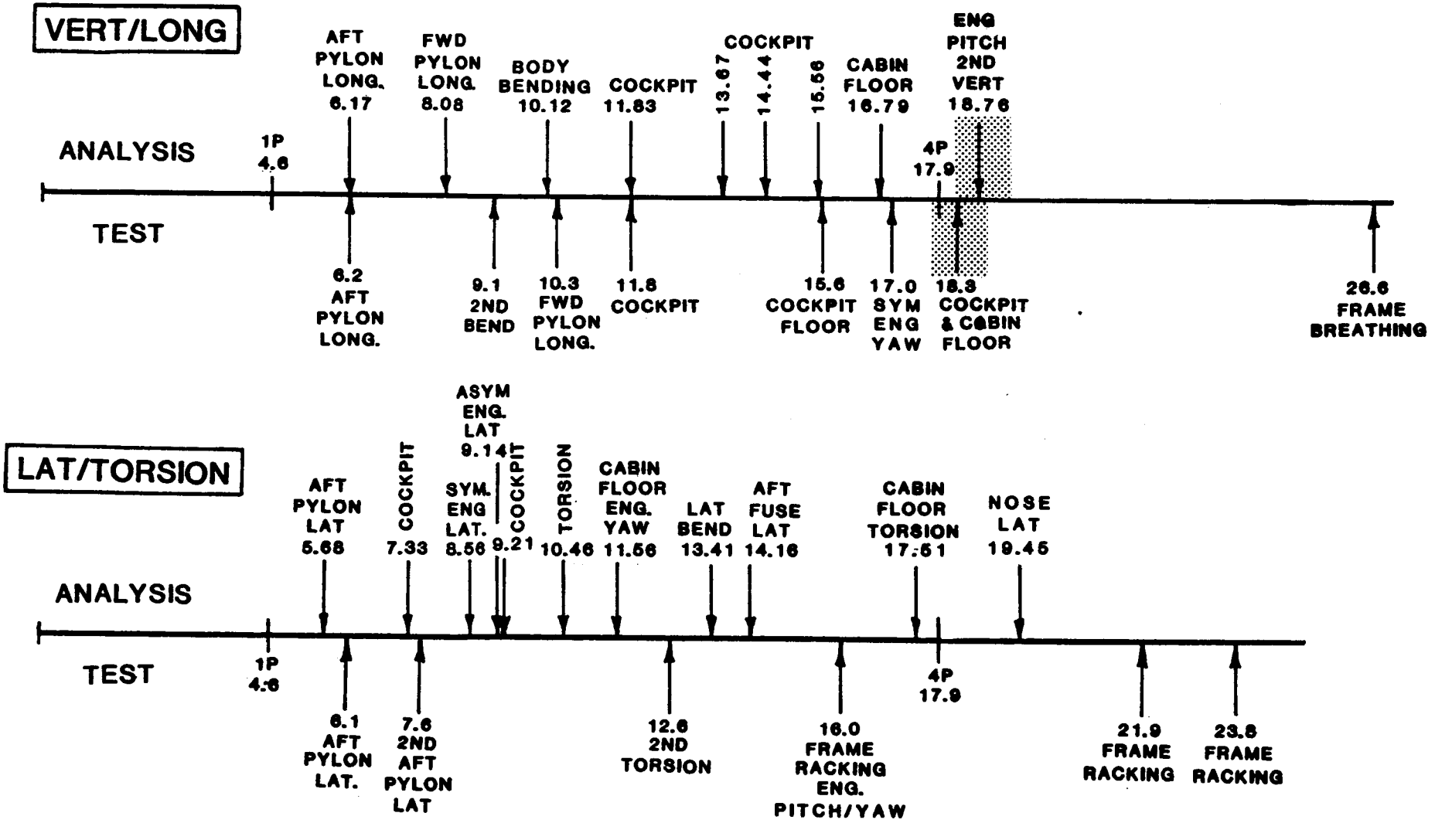

COMPARISON OF ANALYSIS AND ESTIMATED TEST NATURAL FREQUENCIES
ANALYTICAL MODE AT 18.76 Hz

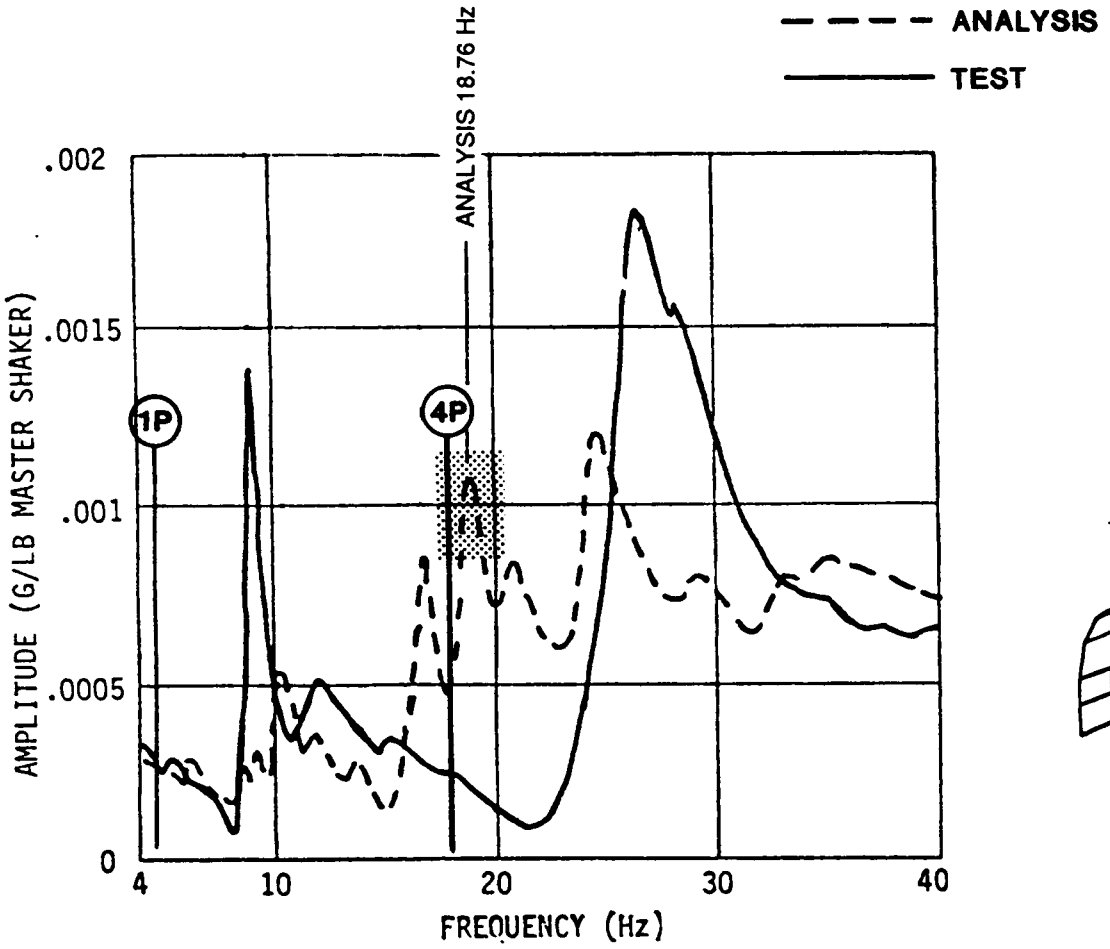

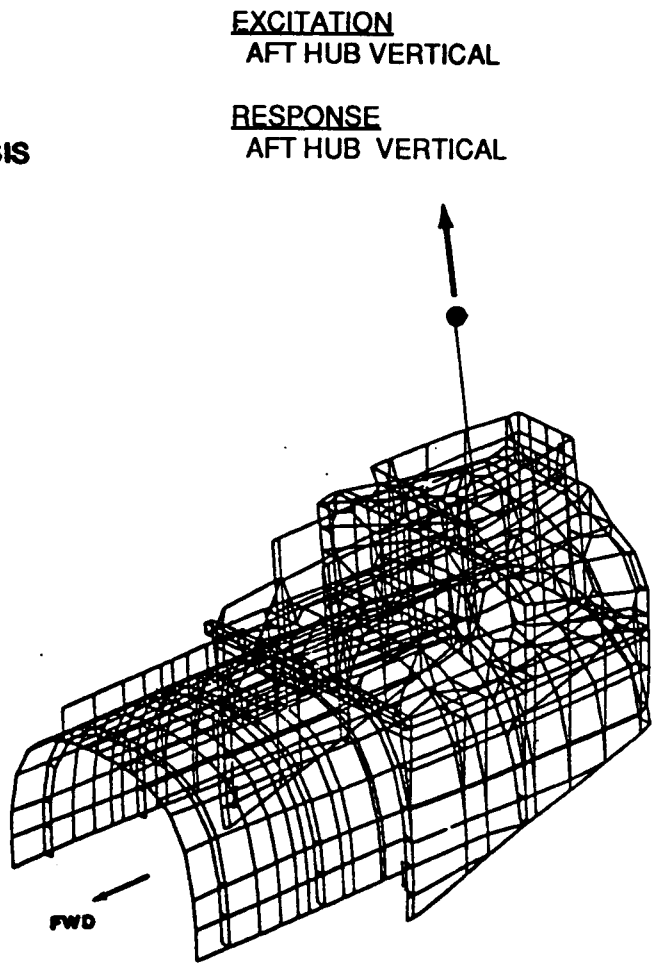

COMPARISON OF ANALYSIS AND ESTIMATED TEST NATURAL FREQUENCIES
ANALYTICAL MODE AT 18.76 Hz

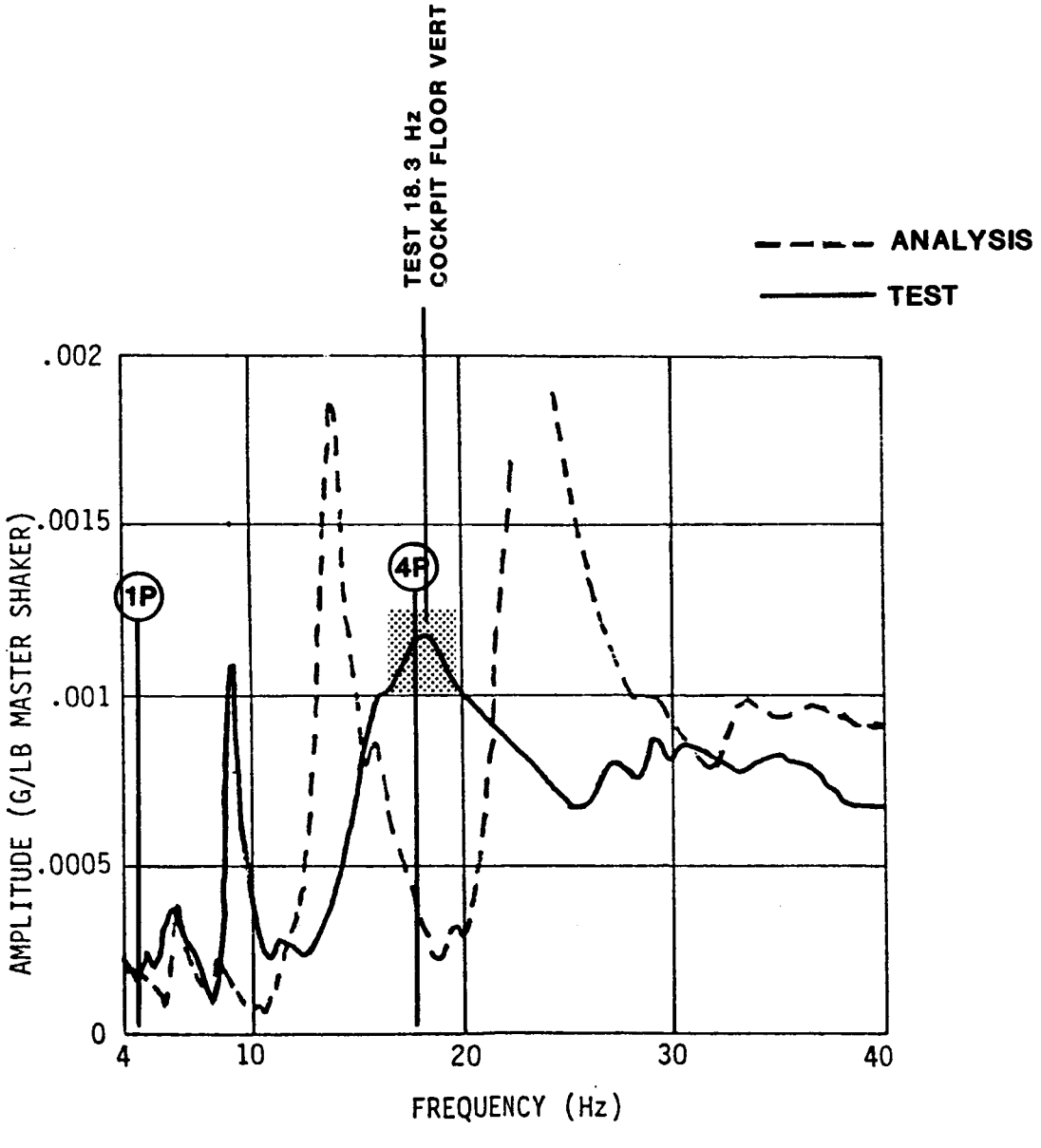

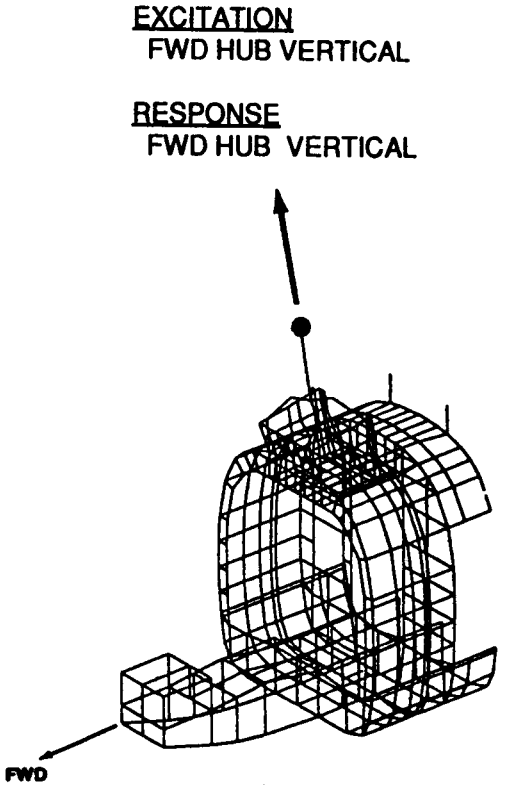

ANALYTICAL RESULTS - NATURAL MODES

MODE 25 18.76 Hz

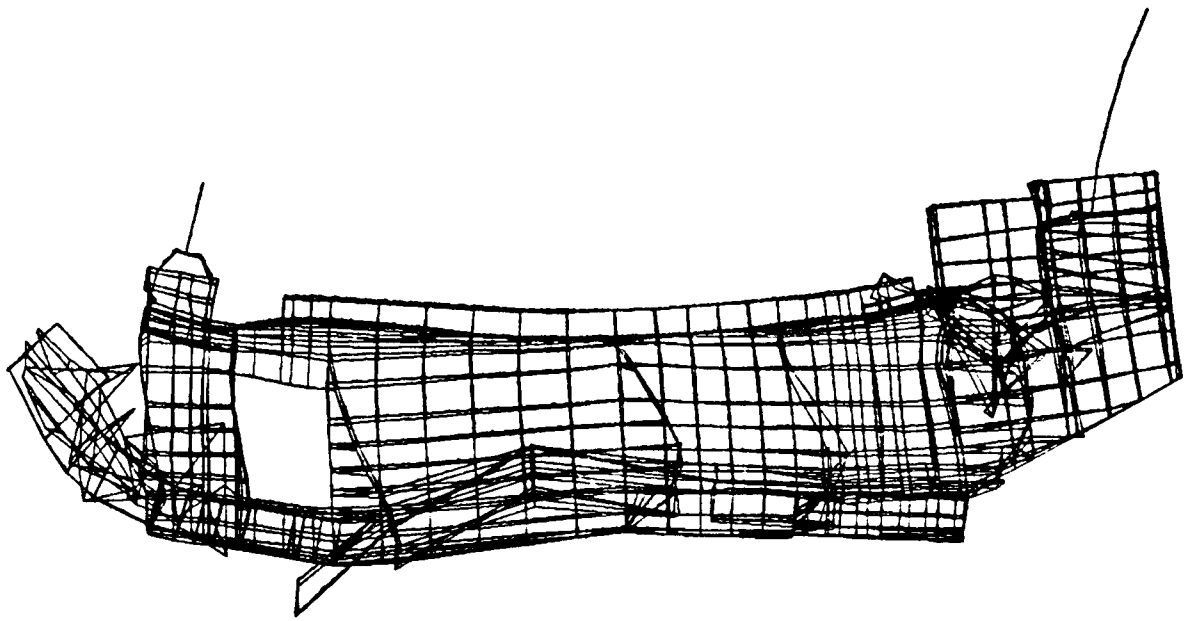

TEST RESULTS - FORCED RESPONSE MODE SHAPES
FORWARD HUB VERTICAL EXCITATION AT 18.3 Hz

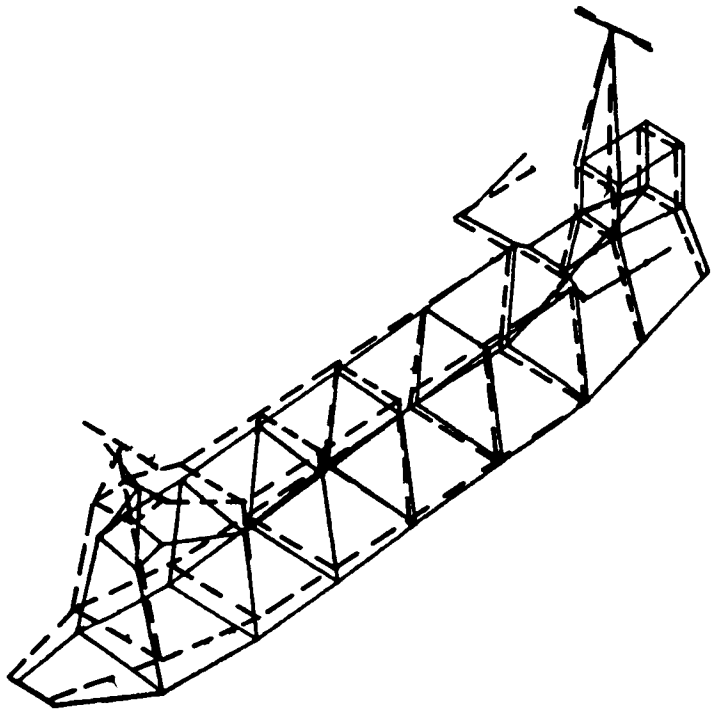

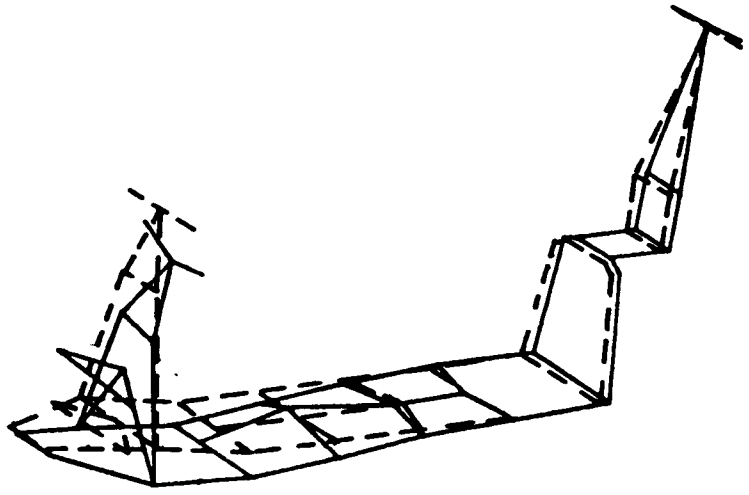

FLOOR LOCATIONS

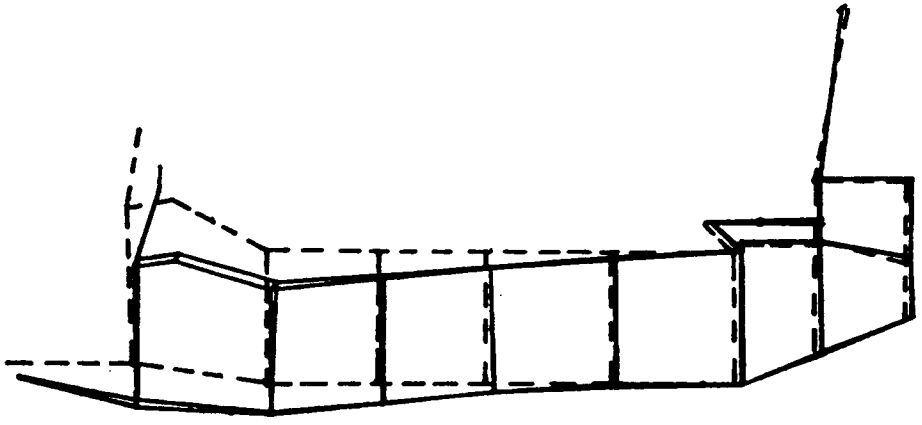

SIDE VIEW

——— DYNAMIC

– – – UNDEFLECTED

COMPARISON OF ANALYSIS AND ESTIMATED TEST NATURAL FREQUENCIES

ANALYTICAL MODES AT 5.68 and 7.33 HZ

The analytical mode at 5.68 HZ and the test mode at 6.1 HZ both show the same characteristic aft pylon lateral/roll motion and are obviously the same mode.

On the other hand, the analytical and test response at 7.33 and 7.6 HZ appear unrelated. The analytical mode appears to be a local mode of one or more of the cockpit masses, while the test mode at 7.6 HZ is hardly distinguishable from the test mode at 6.1 HZ. It should be noted, however, that the test instrumentation was not adequate to identify a local mode if one were actually present.

COMPARISON OF ANALYSIS AND ESTIMATED TEST NATURAL FREQUENCIES

ANALYTICAL MODES AT 5.68 AND 7.33 Hz

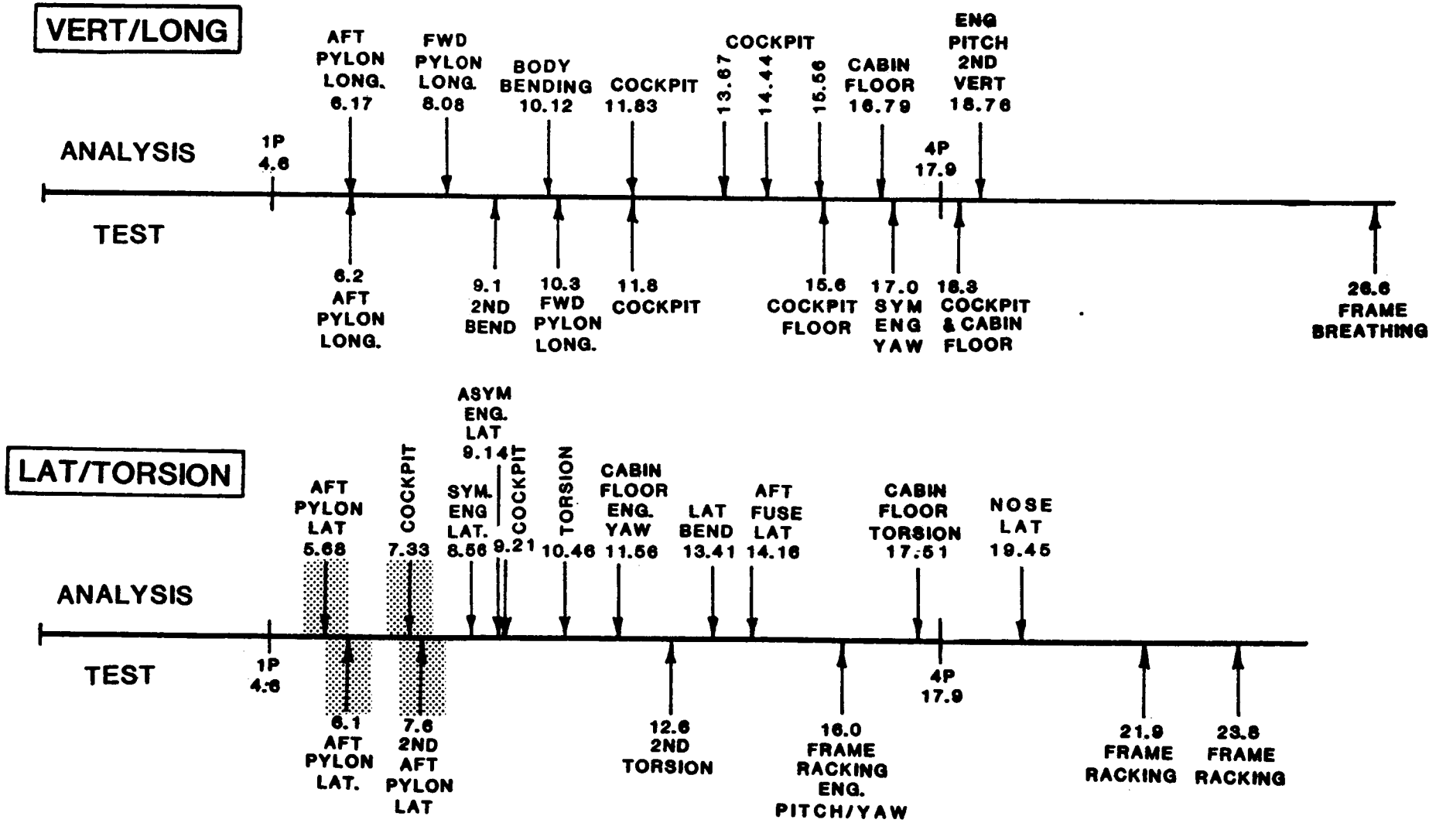

COMPARISON OF ANALYSIS AND ESTIMATED TEST NATURAL FREQUENCIES ANALYTICAL MODES AT 5.68 AND 7.33 Hz

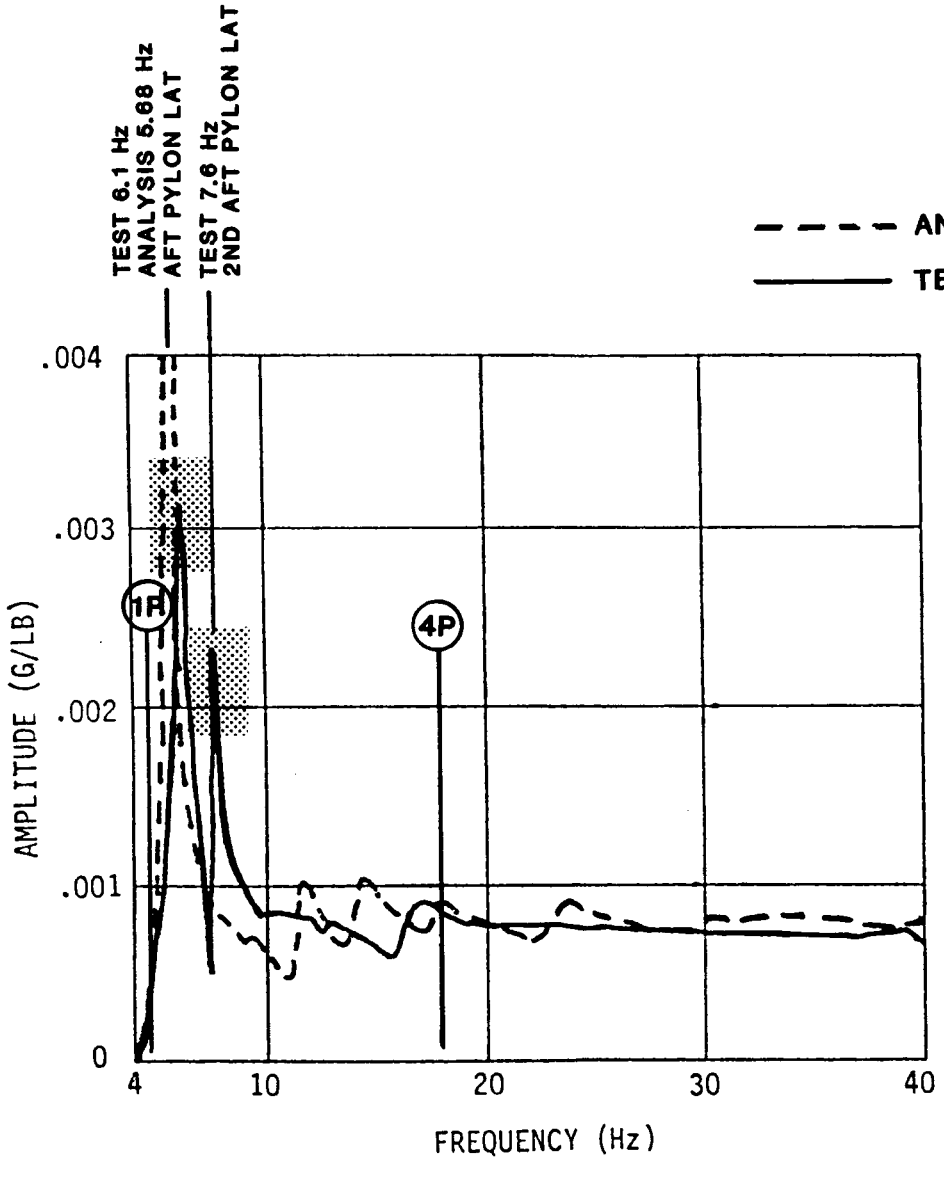

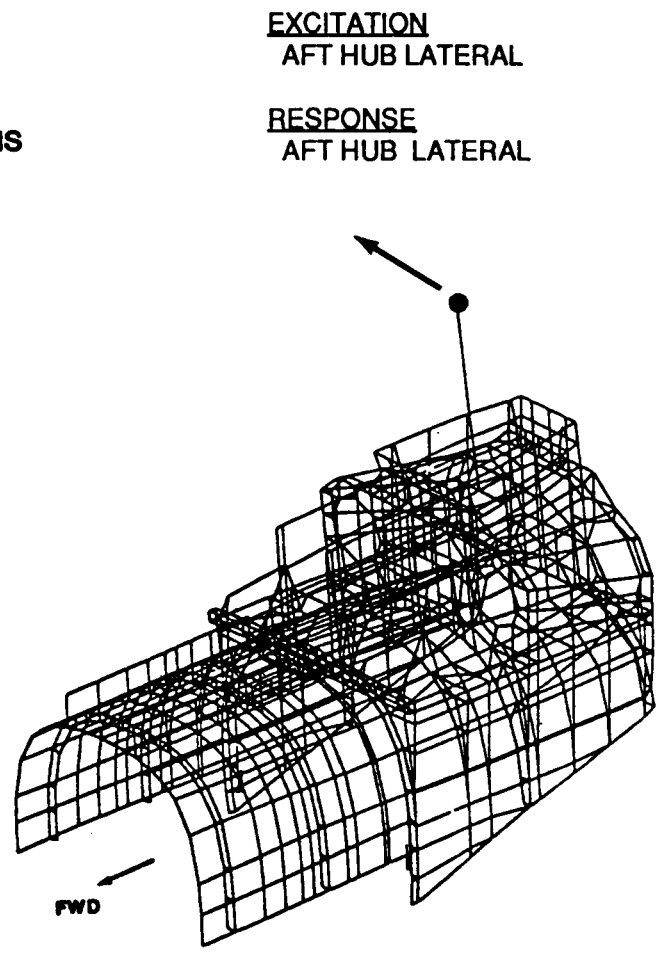

ANALYTICAL RESULTS - NATURAL MODES

MODE 7, FREQUENCY = 5.68 Hz

AFT PYLON LATERAL

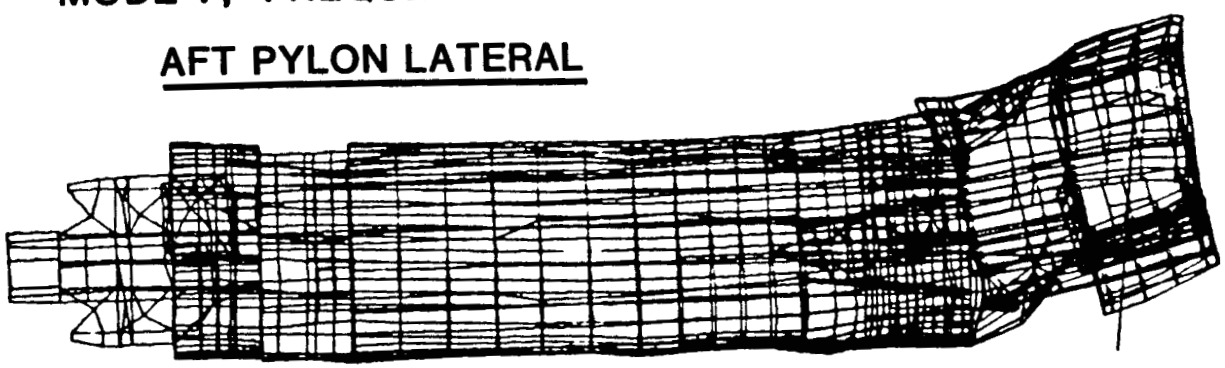

VIEW FROM ABOVE

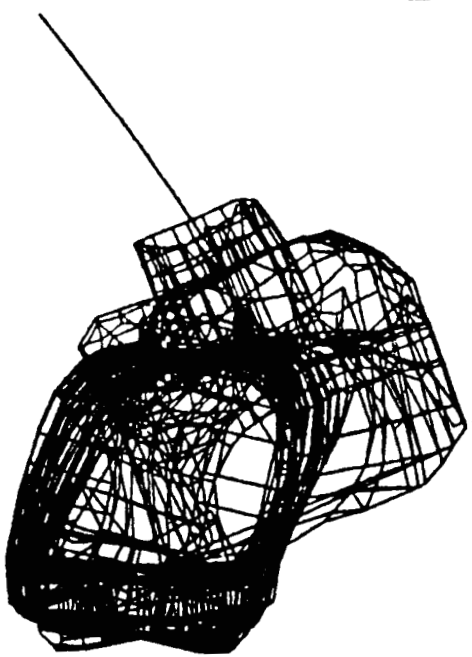

VIEW LOOKING FORWARD

TEST RESULTS - FORCED RESPONSE MODE SHAPES
AFT HUB LATERAL EXCITATION AT 6.1 Hz

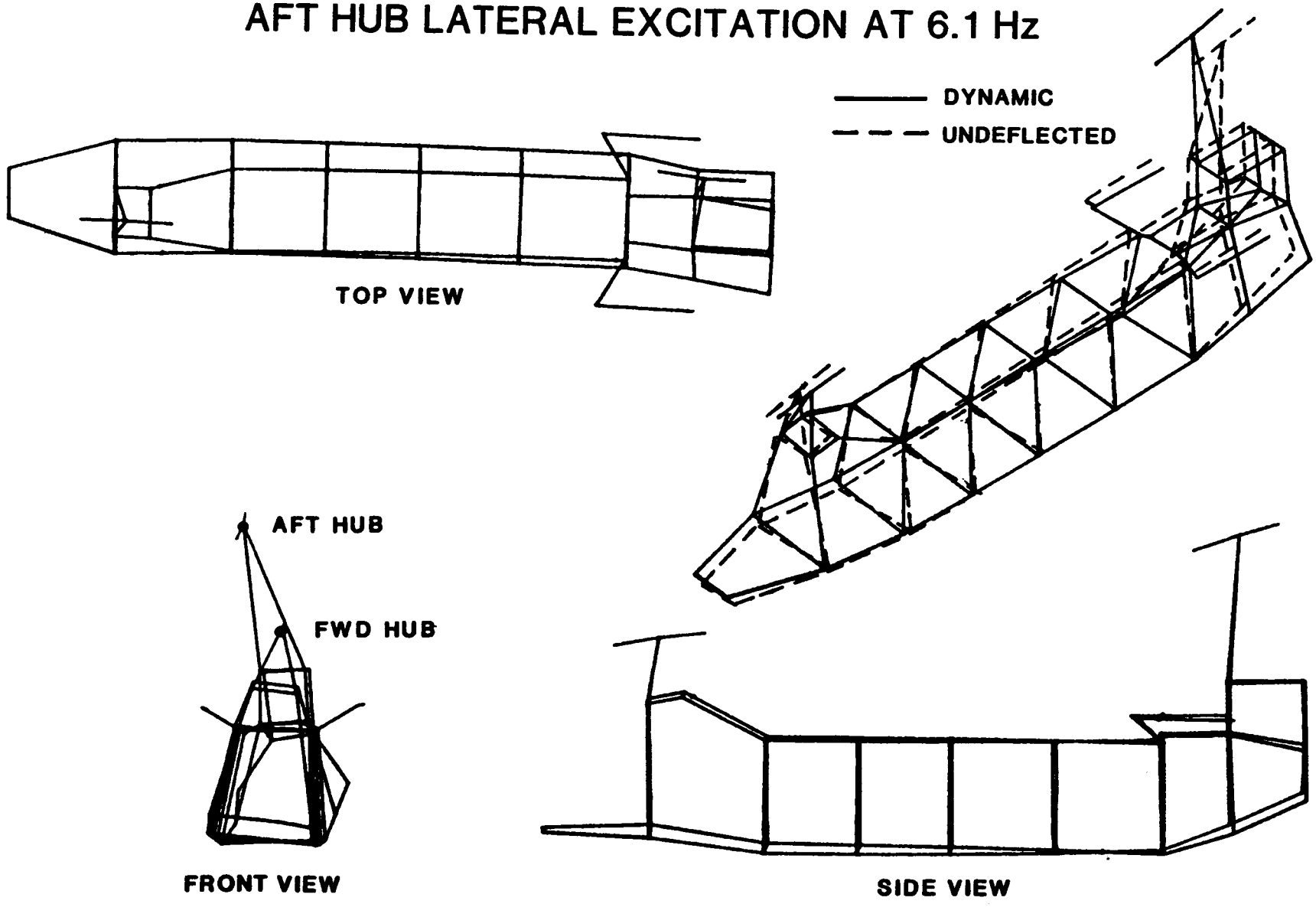

ANALYTICAL RESULTS - NATURAL MODES

MODE 9 FREQUENCY = 7.33 Hz

COCKPIT FLOOR LATERAL

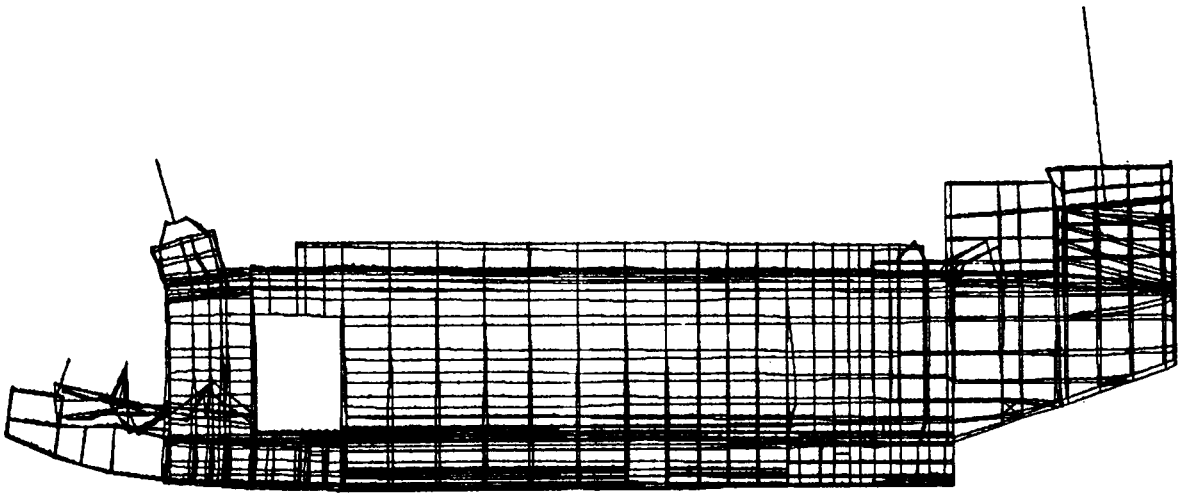

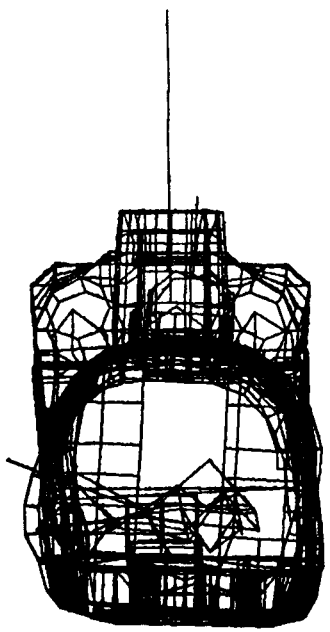

TEST RESULTS - FORCED RESPONSE MODE SHAPES
AFT HUB LATERAL EXCITATION AT 7.6 Hz

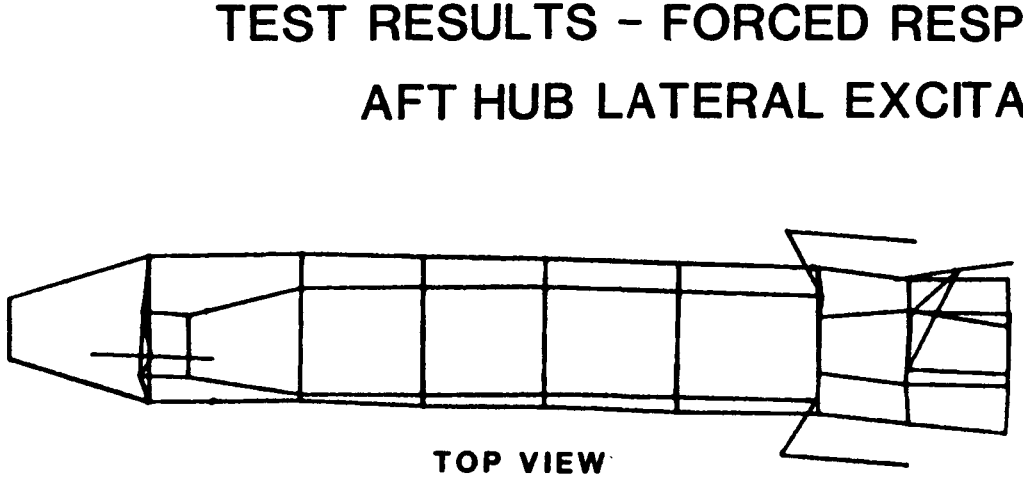

TOP VIEW

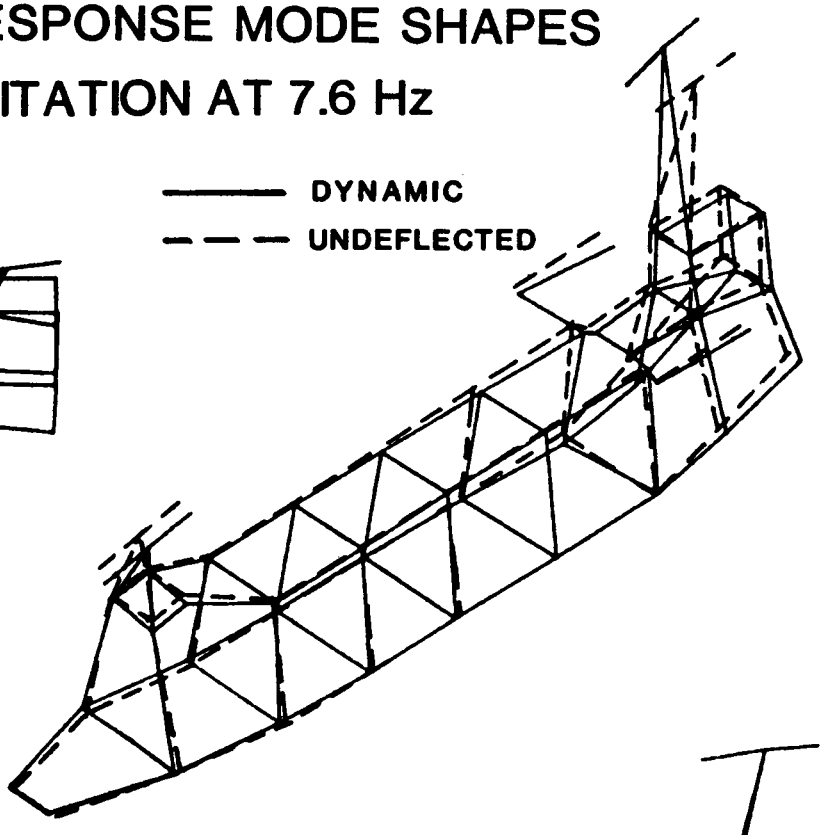

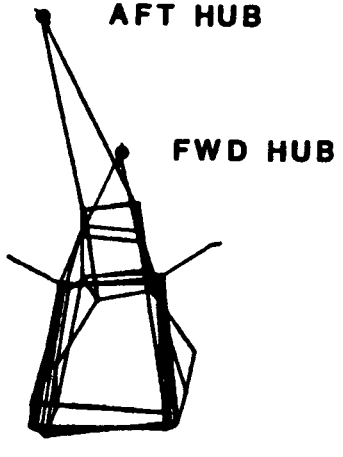

FRONT VIEW

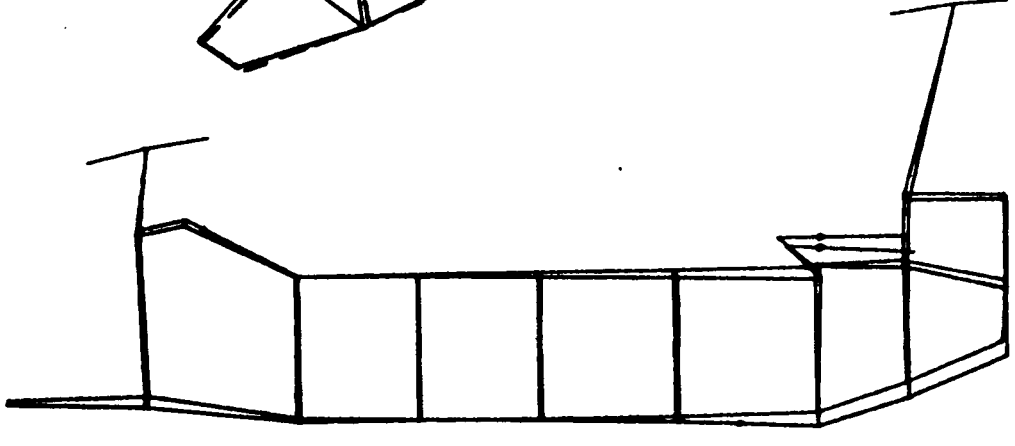

SIDE VIEW

COMPARISON OF ANALYSIS AND ESTIMATED TEST NATURAL FREQUENCIES

ANALYTICAL MODES AT 8.56, 9.14, 9.21, AND 10.46 HZ

There appears to be no test counterpart for these analytical modes. The first mode at 8.56 HZ is a virtually uncoupled symmetric engine lateral (yaw) mode. An asymmetric engine lateral motion coupled with a mild fuselage lateral/torsion motion characterizes the mode at 9.14 HZ. At 9.21 HZ, the mode involves a local motion of the cockpit console. Finally, the mode at 10.46 HZ is a torsion mode with a lateral/rolling motion of the cockpit and racking motion of the forward fuselage.

COMPARISON OF ANALYSIS AND ESTIMATED TEST NATURAL FREQUENCIES

ANALYTICAL MODES AT 8.56, 9.14, 9.21 AND 10.46 Hz

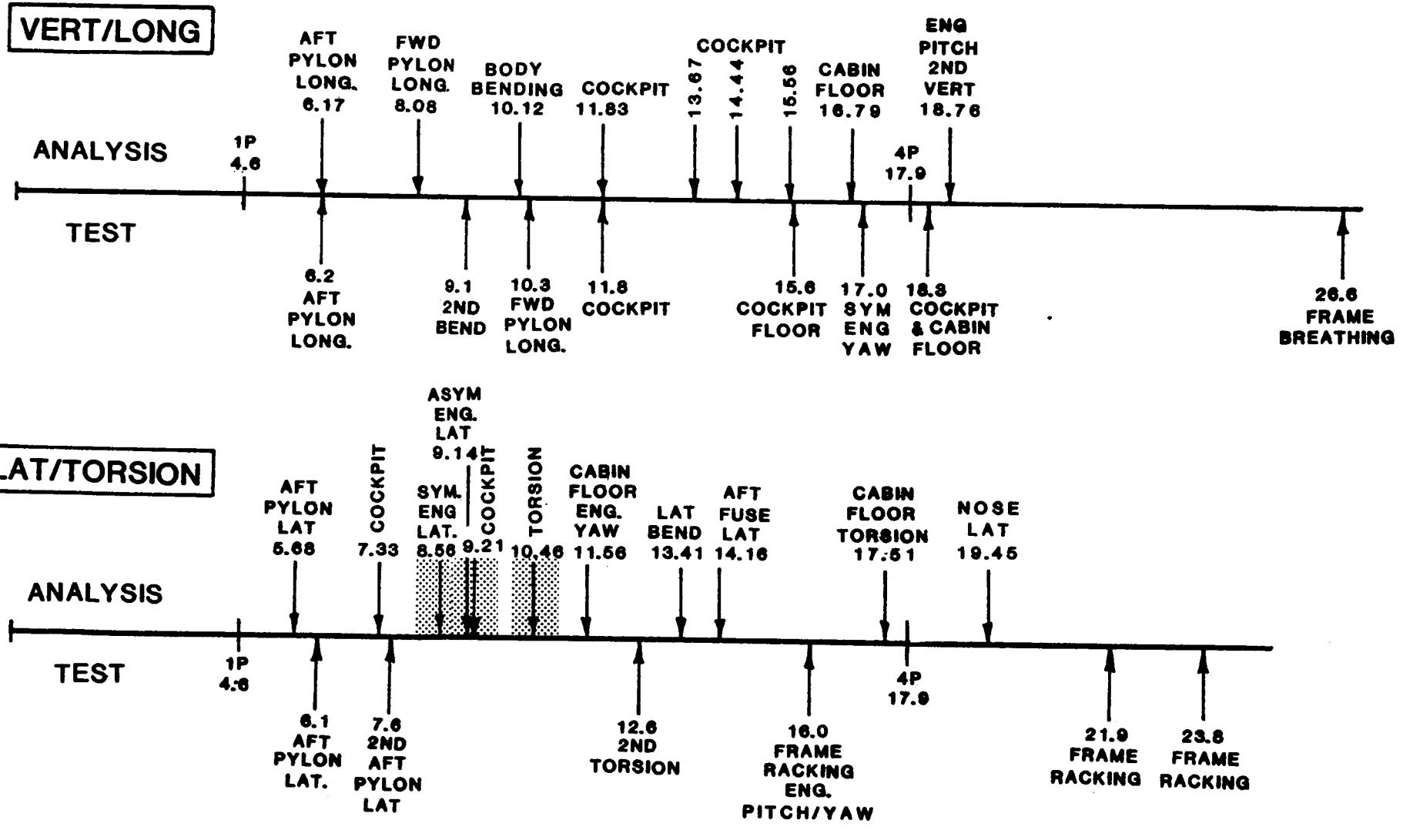

COMPARISON OF ANALYSIS AND ESTIMATED TEST NATURAL FREQUENCIES ANALYTICAL MODES AT 8.56, 9.14, 9.21 AND 10.46 Hz

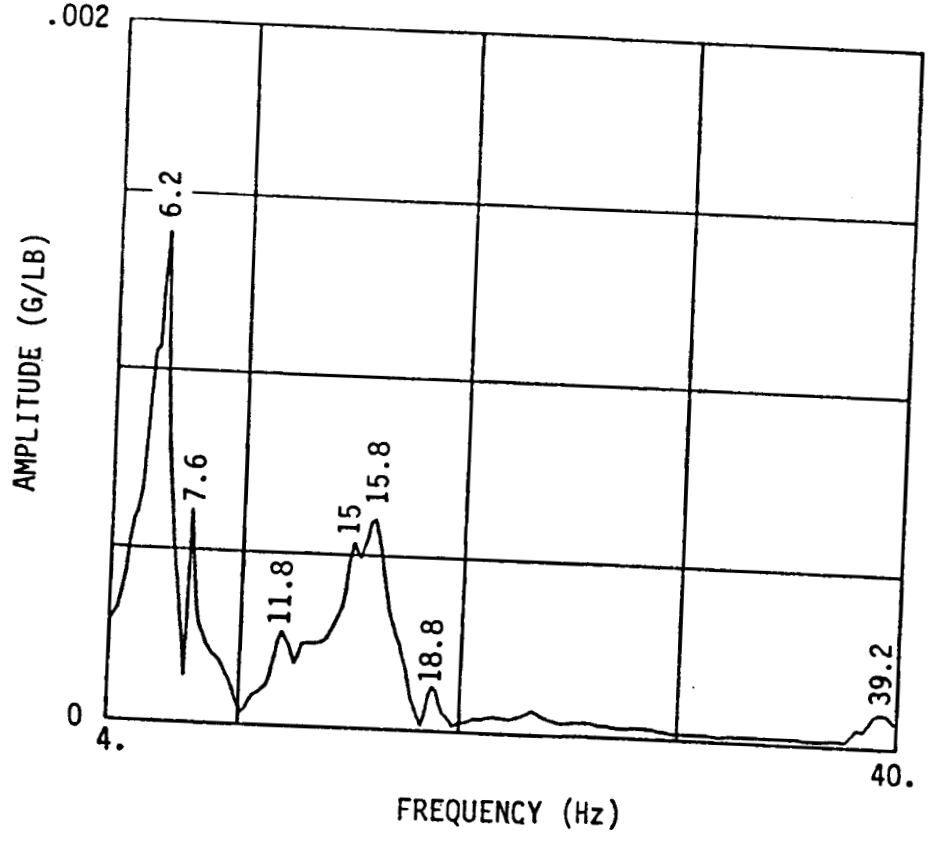

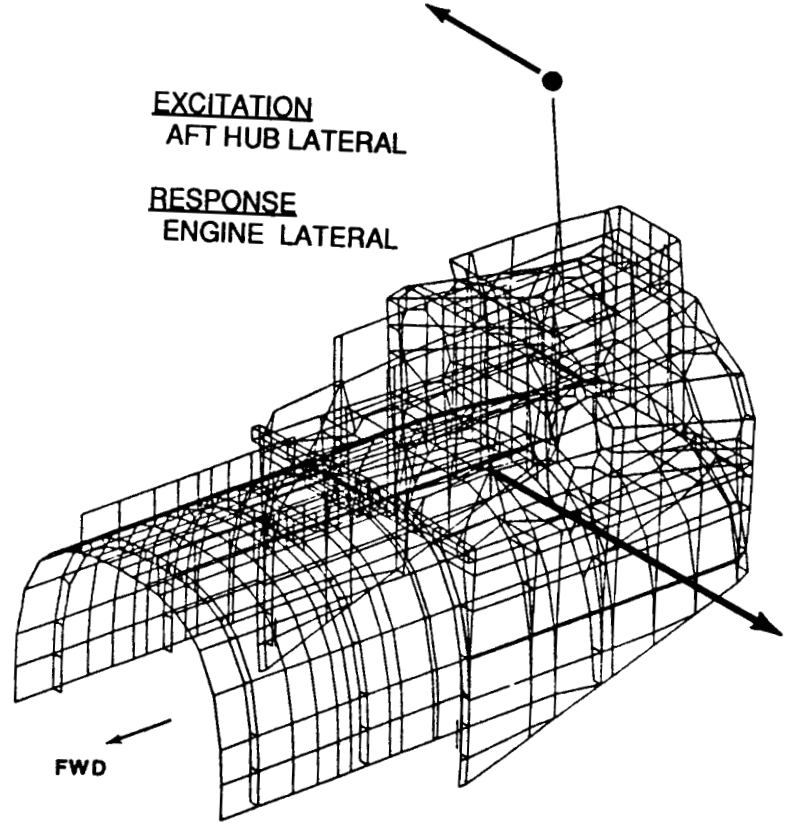

ANALYTICAL RESULTS - NATURAL MODES

MODE 11 8.56 Hz

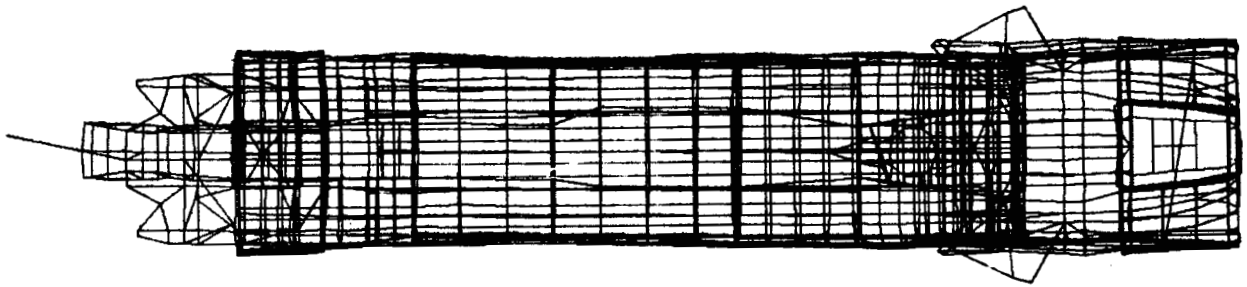

VIEW FROM ABOVE

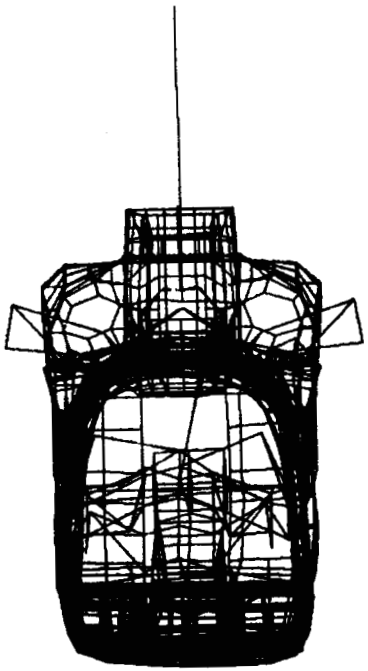

VIEW LOOKING FORWARD

ANALYTICAL RESULTS - NATURAL MODES

MODE 12 9.14 Hz

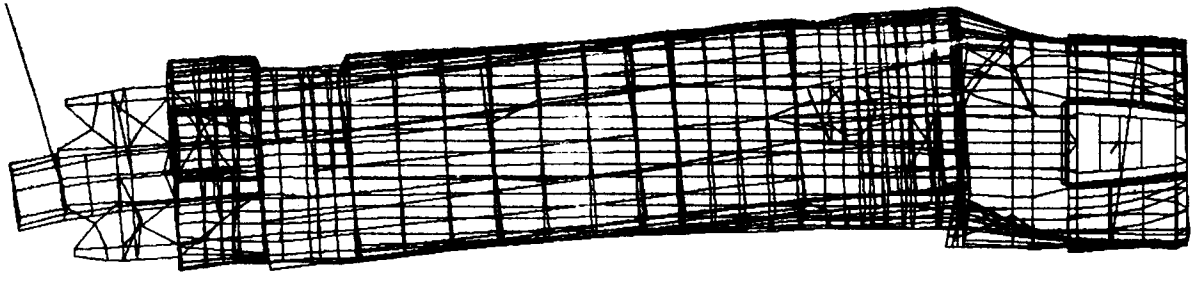

VIEW FROM ABOVE

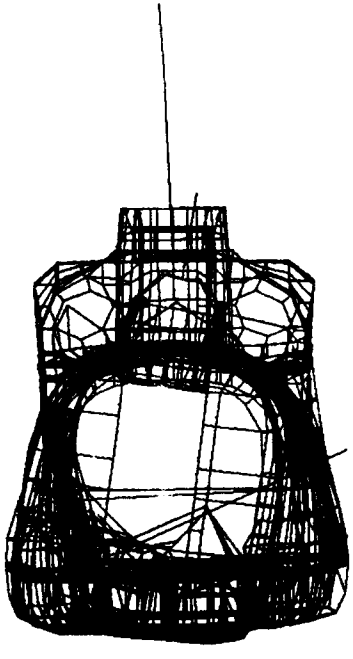

VIEW LOOKING FORWARD

ANALYTICAL RESULTS - NATURAL MODES

MODE 13 9.21 Hz

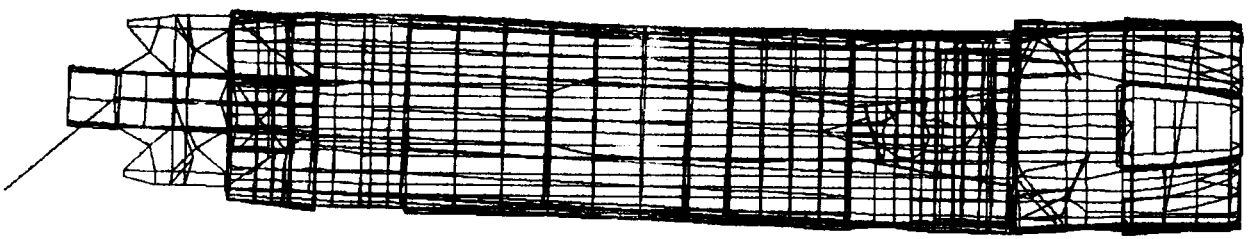

VIEW FROM ABOVE

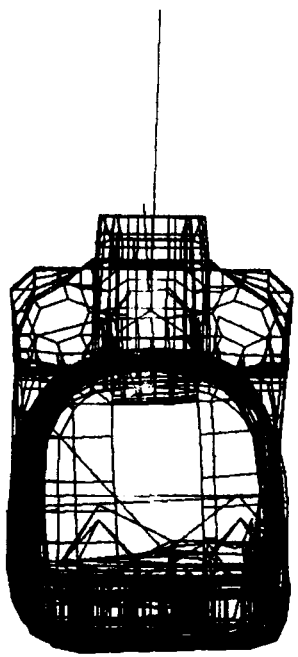

VIEW LOOKING FORWARD

ANALYTICAL RESULTS - NATURAL MODES

MODE 15 10.46 Hz

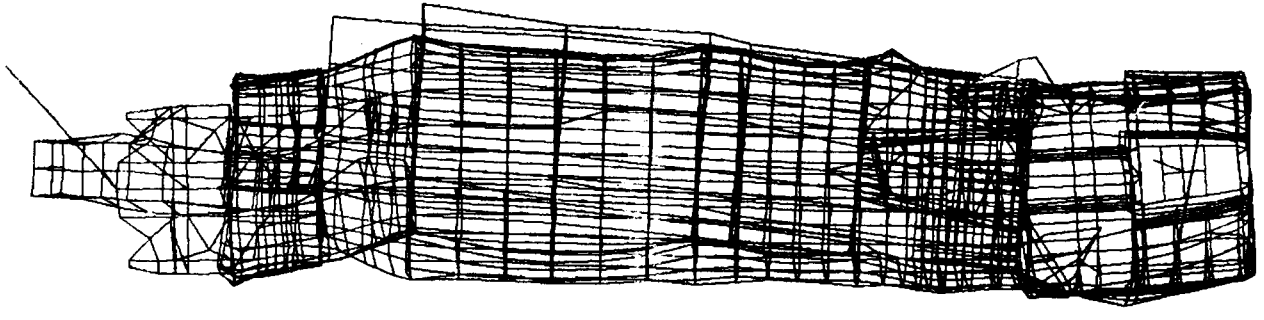

VIEW FROM ABOVE

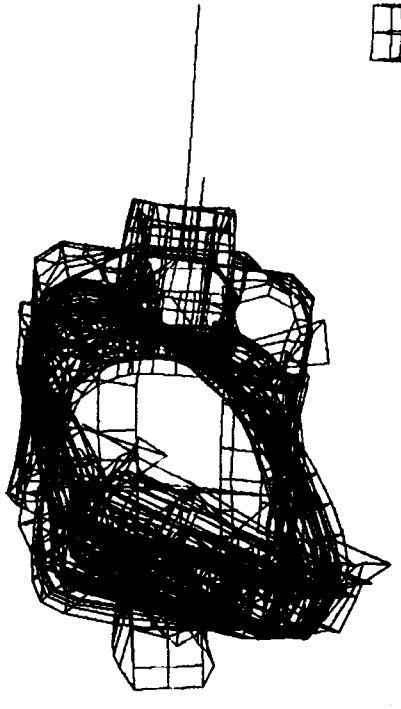

VIEW LOOKING FORWARD

COMPARISON OF ANALYSIS AND ESTIMATED TEST NATURAL FREQUENCIES

ANALYTICAL MODE AT 11.56 HZ

The analytical mode at 11.56 HZ and the test shape at 12.6 HZ appear to be essentially the same type of mode. The motion can be best described as a racking motion due to differential yawing of the fuselage floor and crown.

COMPARISON OF ANALYSIS AND ESTIMATED TEST NATURAL FREQUENCIES

ANALYTICAL MODE AT 11.56 Hz

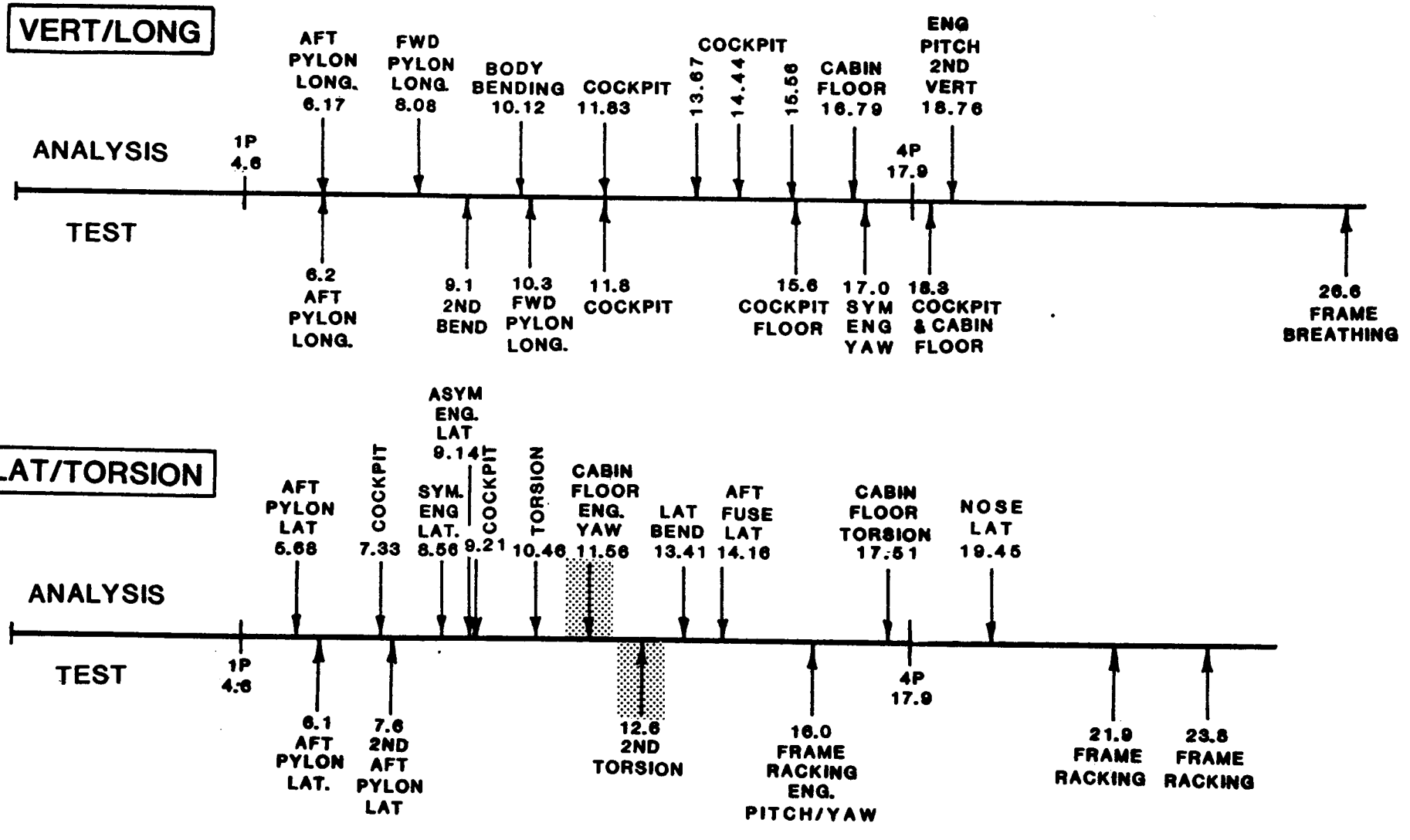

COMPARISON OF ANALYSIS AND ESTIMATED TEST NATURAL FREQUENCIES ANALYTICAL MODE AT 11.56 Hz

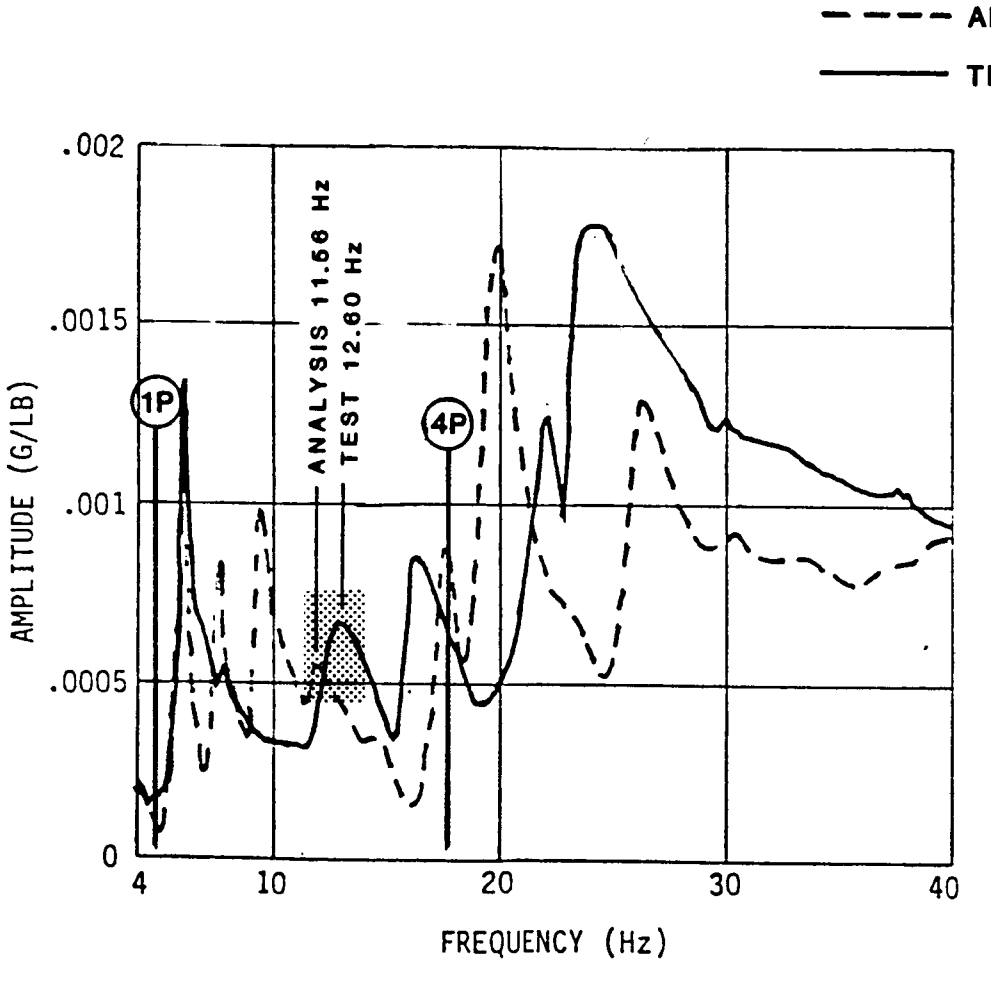

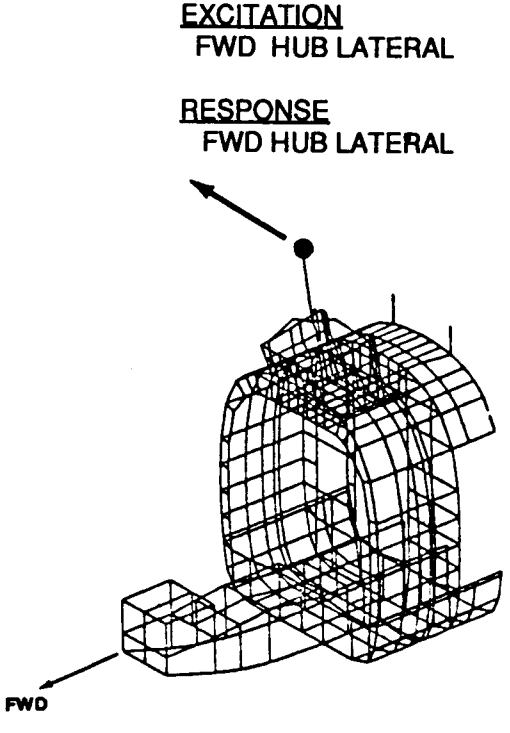

ANALYTICAL RESULTS - NATURAL MODES

MODE 16 11.56 Hz

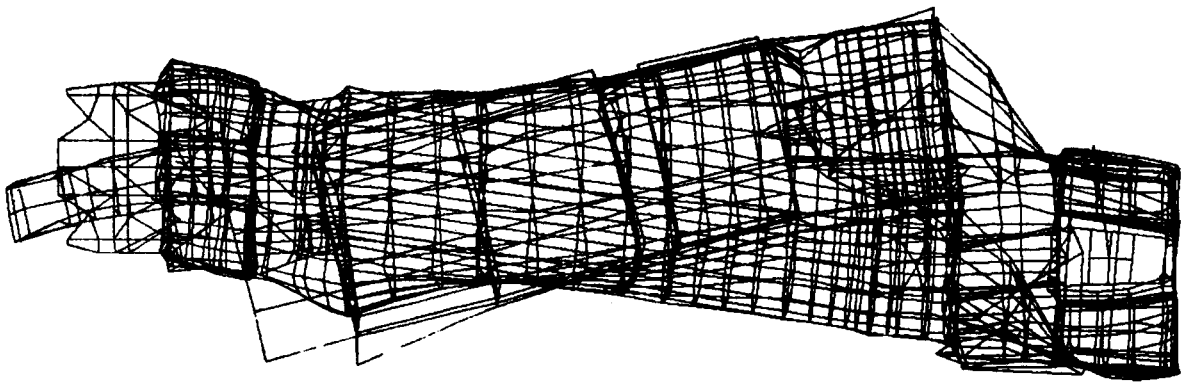

VIEW FROM ABOVE

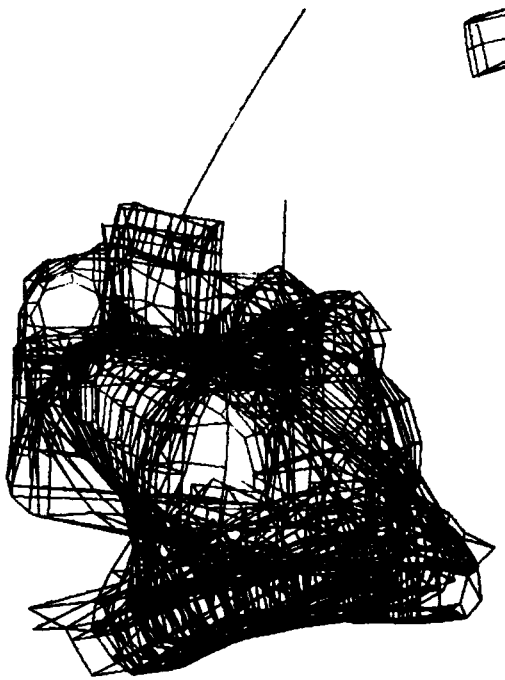

VIEW LOOKING FORWARD

TEST RESULTS - FORCED RESPONSE MODE SHAPES
FORWARD HUB LATERAL EXCITATION AT 12.6 Hz

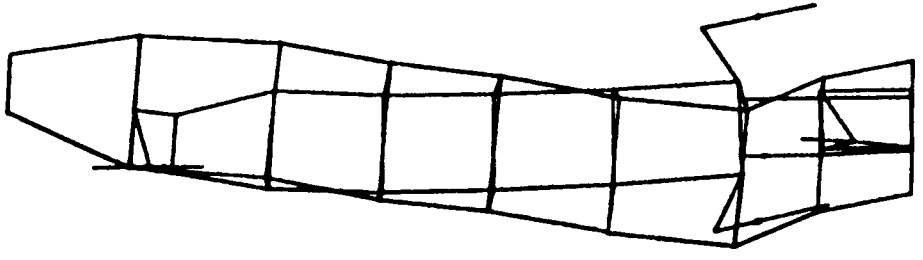

TOP VIEW

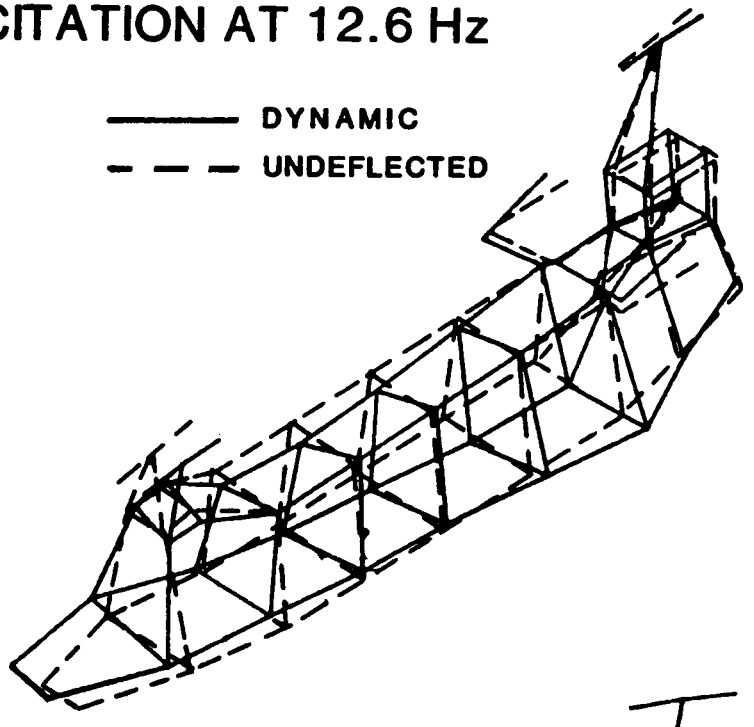

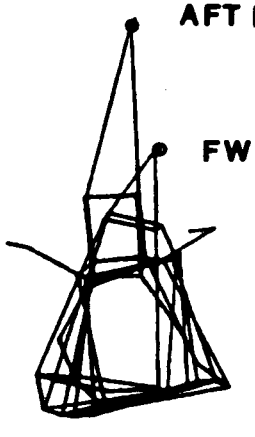

FRONT VIEW

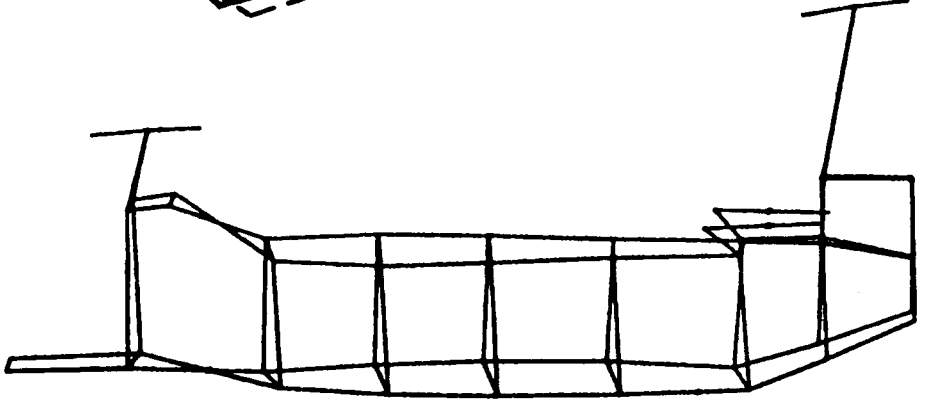

COMPARISON OF ANALYSIS AND ESTIMATED TEST NATURAL FREQUENCIES

ANALYTICAL MODES AT 13.41, 14.16, 17.51 AND 19.45 HZ

Here there are four analytical modes to consider and only one test mode. With the exception of the 19.45 HZ mode, which is confined mainly to the cockpit area, all of the analytical modes involve complex lateral/torsional motions. The test shape at 16 HZ, with significant lateral bending, most resembles the analytical mode at 13.41 HZ which also has a strong lateral bending component.

COMPARISON OF ANALYSIS AND ESTIMATED TEST NATURAL FREQUENCIES

ANALYTICAL MODES AT 13.41, 14.16, 17.51 AND 19.45 Hz

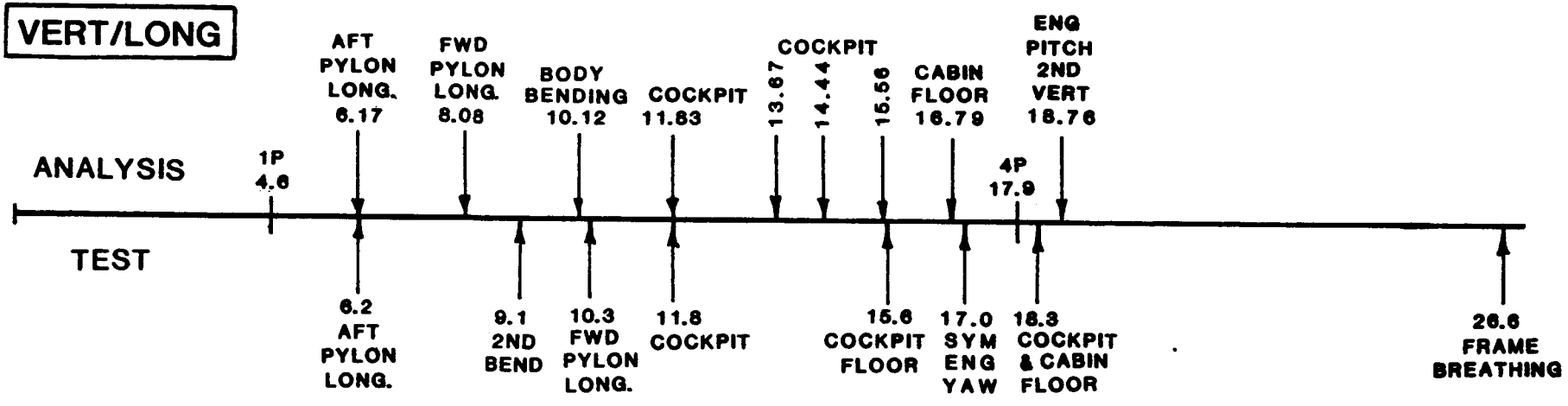

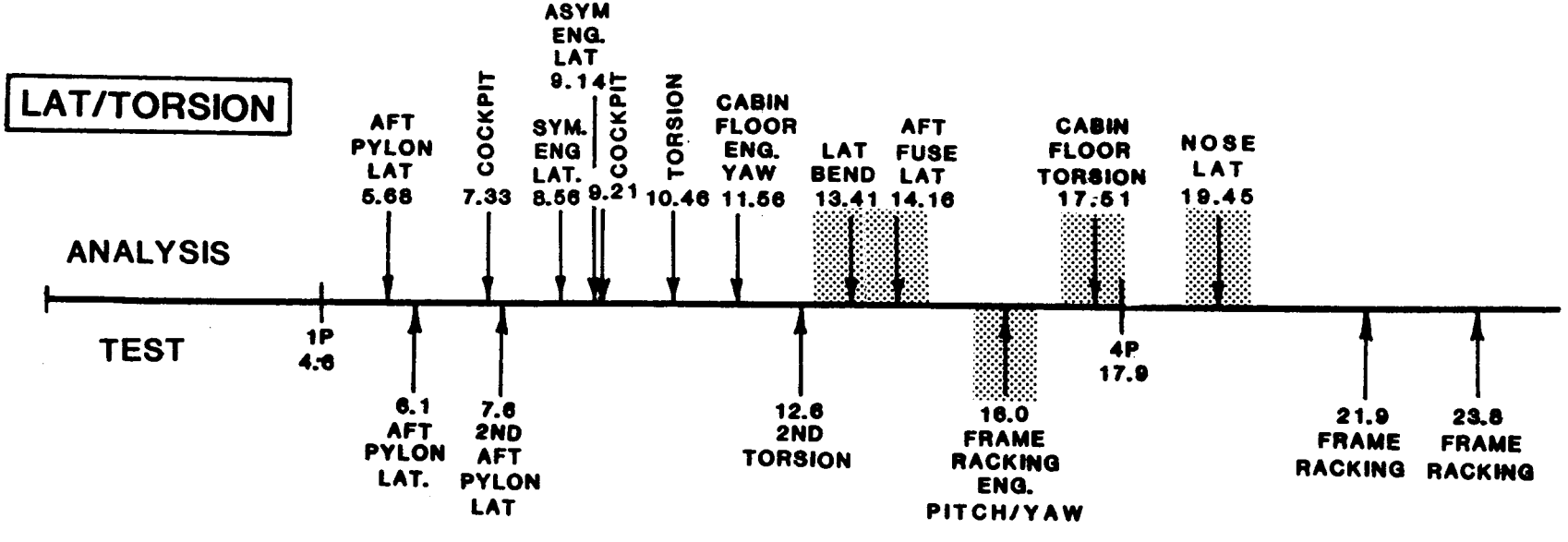

COMPARISON OF ANALYSIS AND ESTIMATED TEST NATURAL FREQUENCIES ANALYTICAL MODES AT 13.41, 14.16, 17.51 AND 19.45 Hz

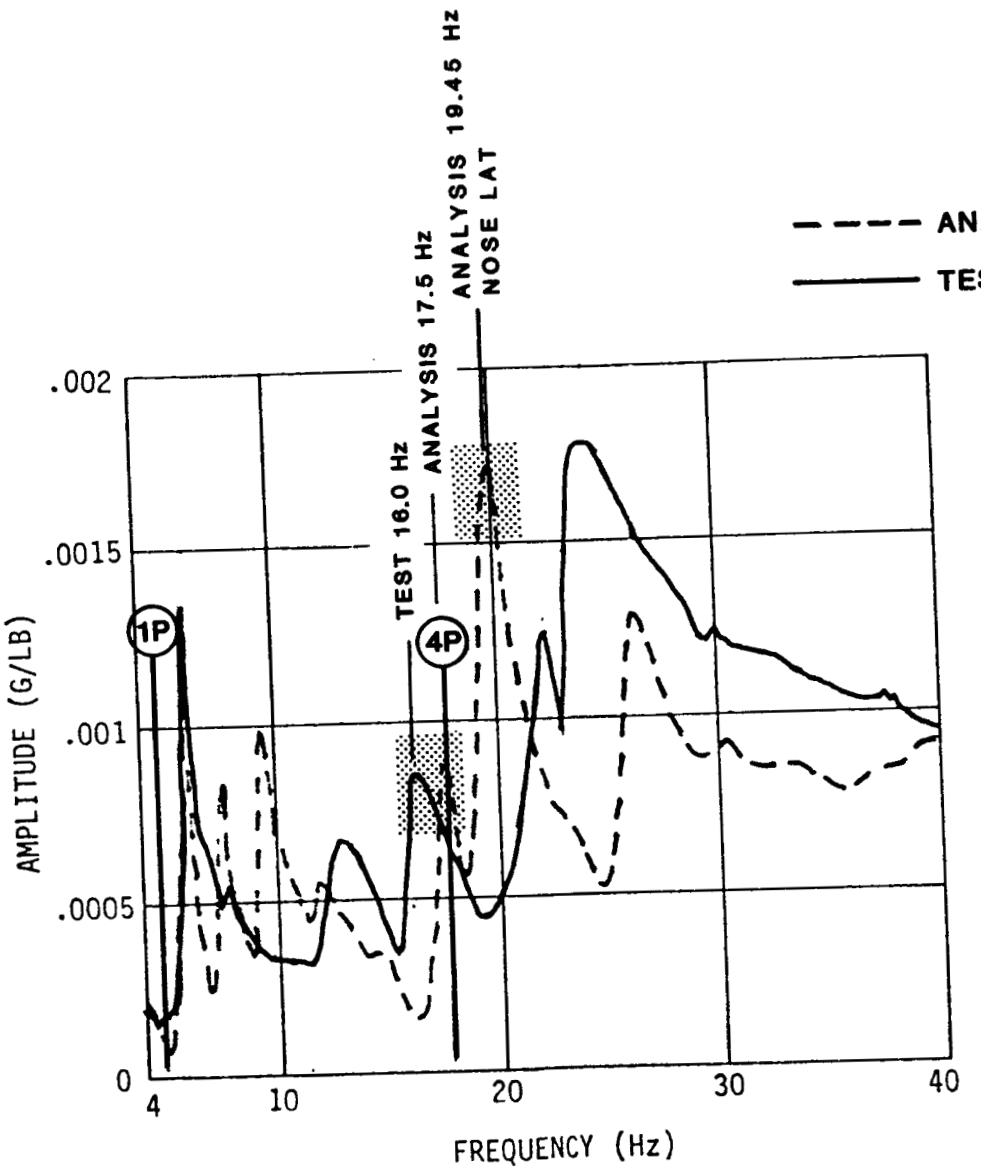

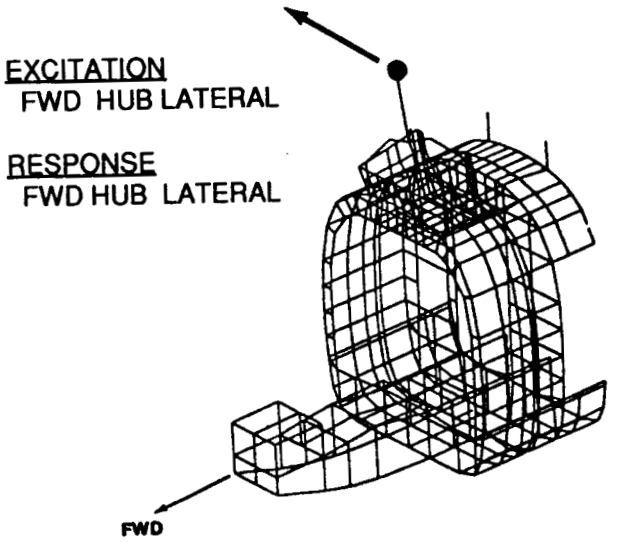

ANALYTICAL RESULTS - NATURAL MODES

MODE 18 13.41 Hz

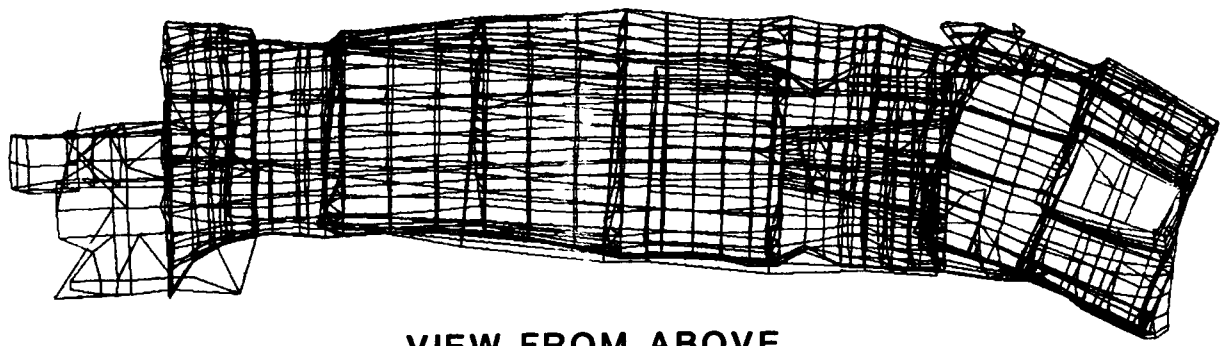

VIEW FROM ABOVE

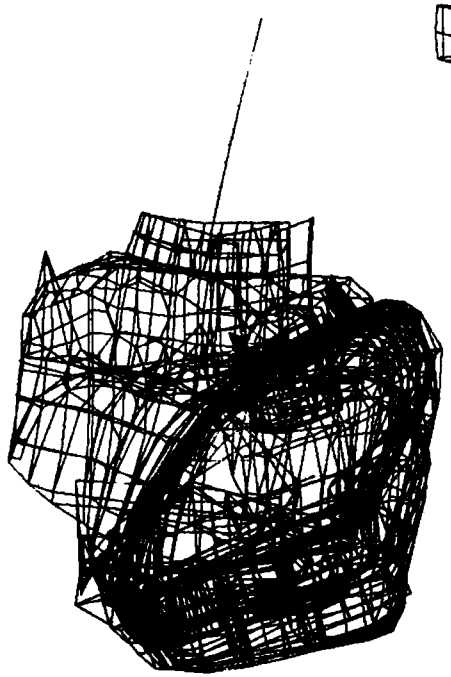

VIEW LOOKING FORWARD

TEST RESULTS - FORCED RESPONSE MODE SHAPES
FORWARD HUB LATERAL EXCITATION AT 16.0 Hz

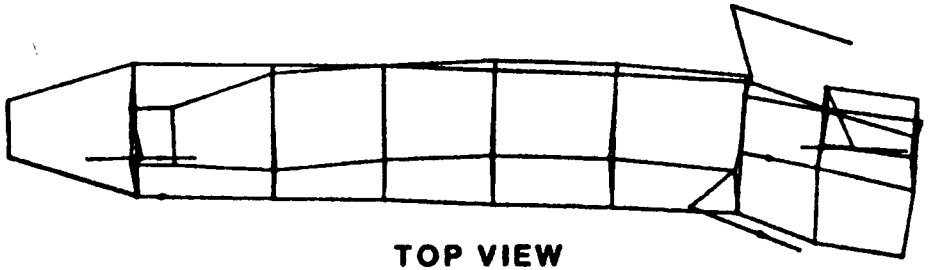

TOP VIEW

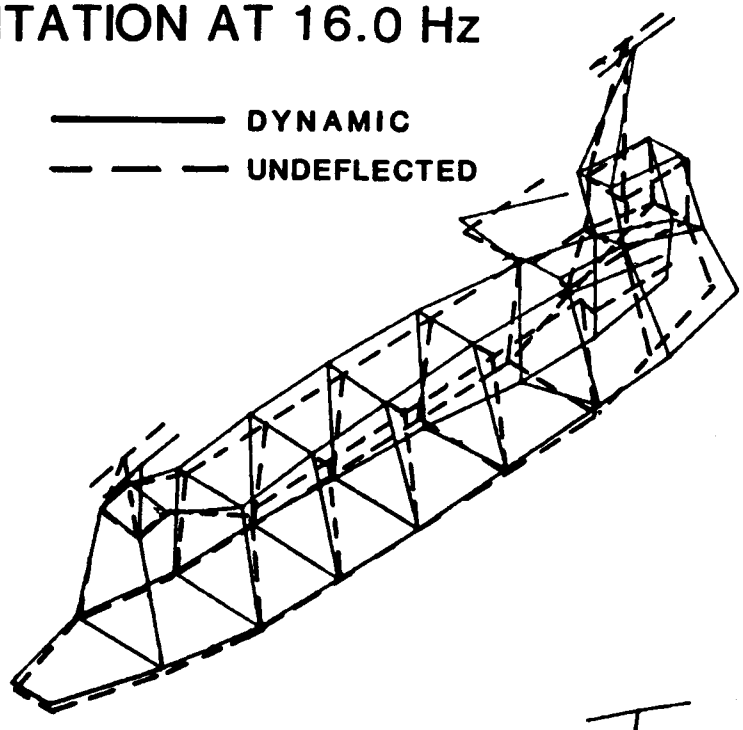

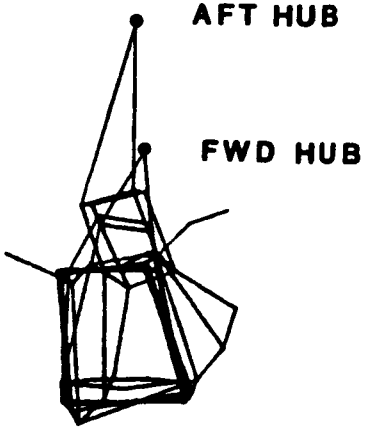

FRONT VIEW

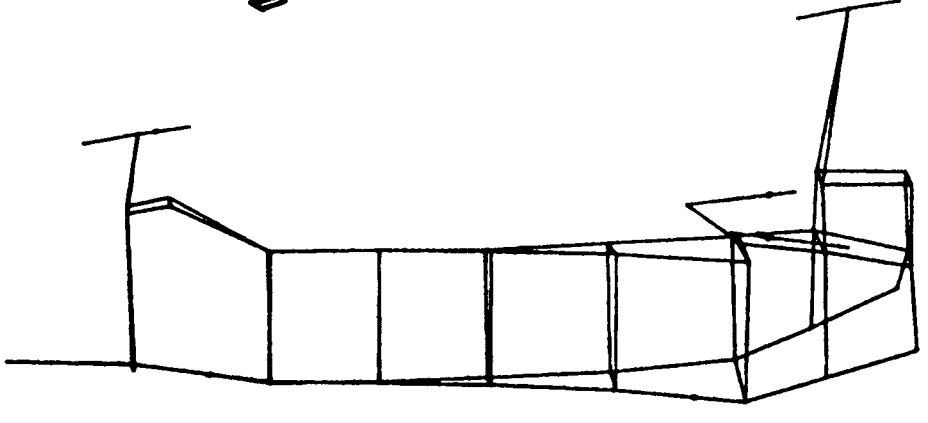

SIDE VIEW

ANALYTICAL RESULTS - NATURAL MODES

MODE 20 14.16 Hz

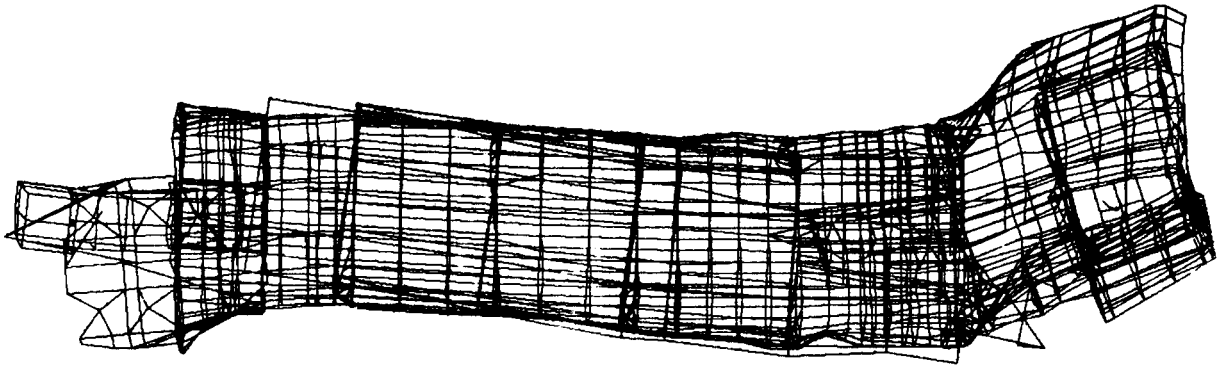

VIEW FROM ABOVE

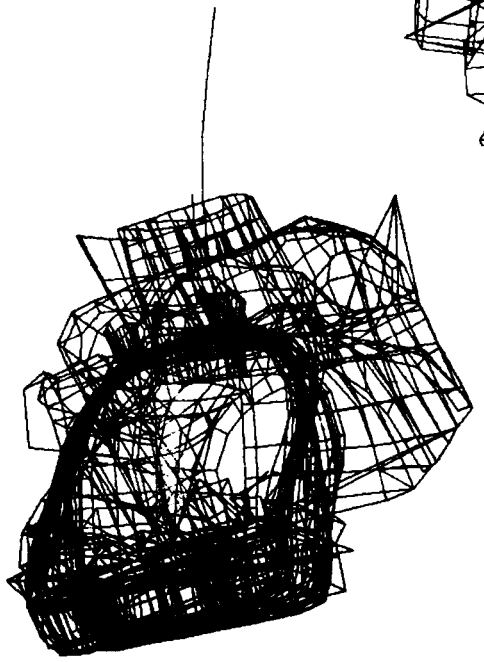

VIEW LOOKING FORWARD

ANALYTICAL RESULTS - NATURAL MODES

MODE 24 17.51 Hz

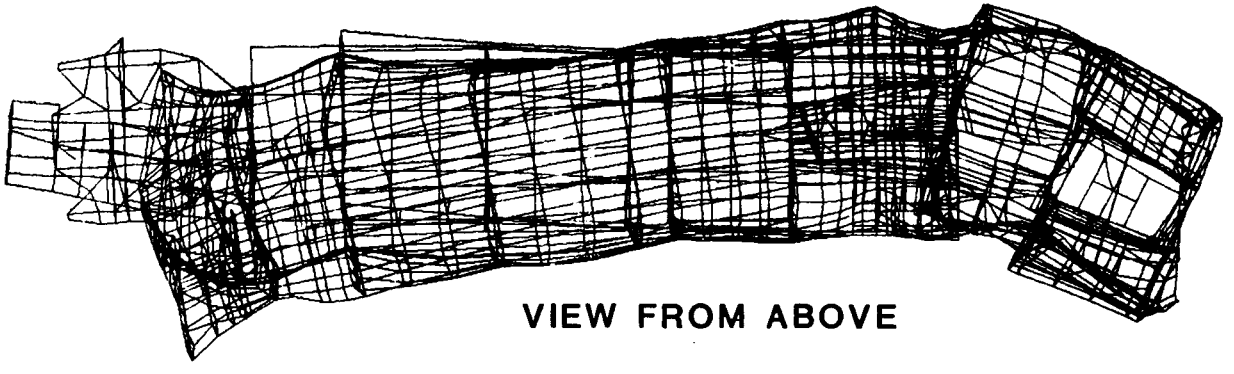

VIEW FROM ABOVE

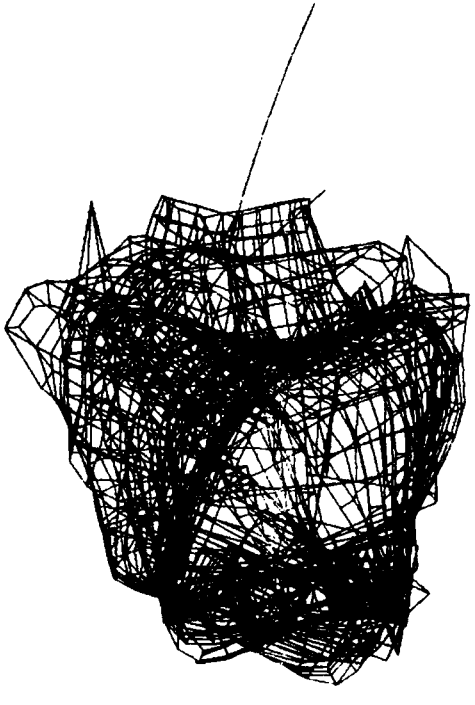

VIEW LOOKING FORWARD

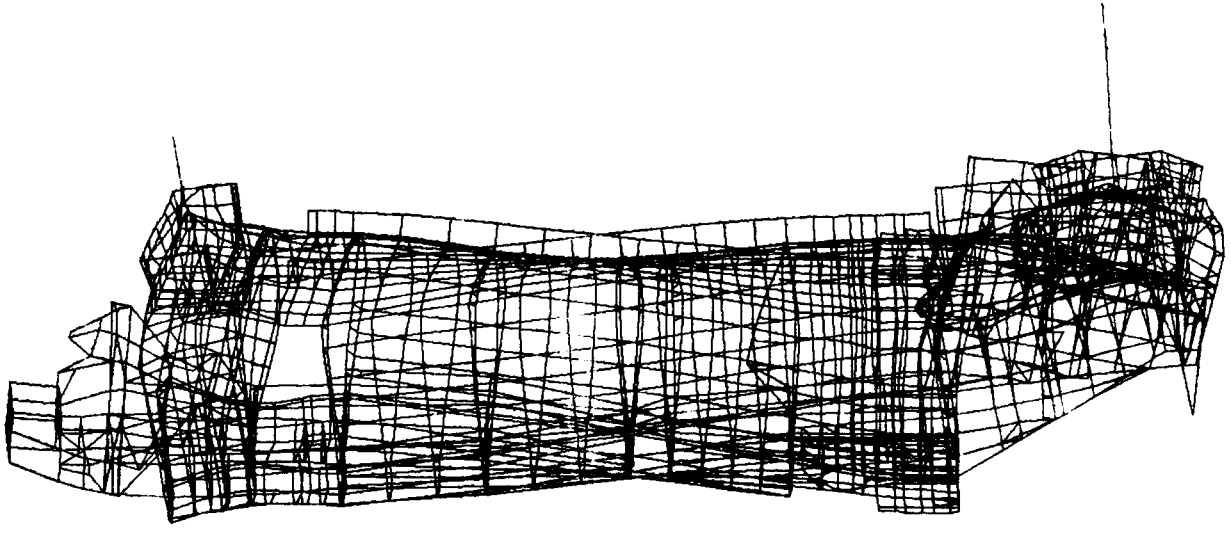

SIDE VIEW

ANALYTICAL RESULTS - NATURAL MODES

MODE 26 19.45 Hz

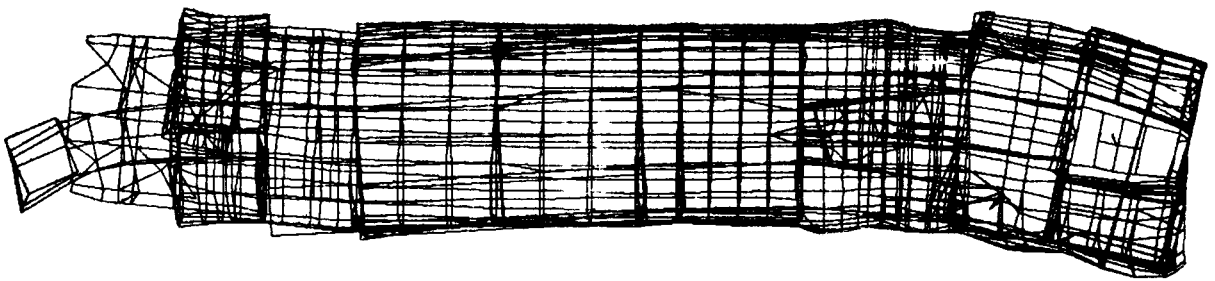

VIEW FROM ABOVE

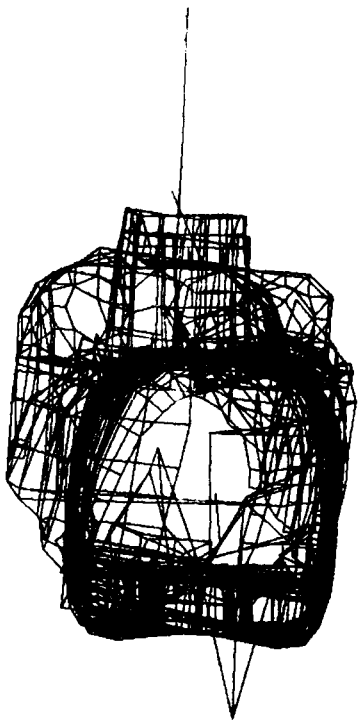

VIEW LOOKING FORWARD

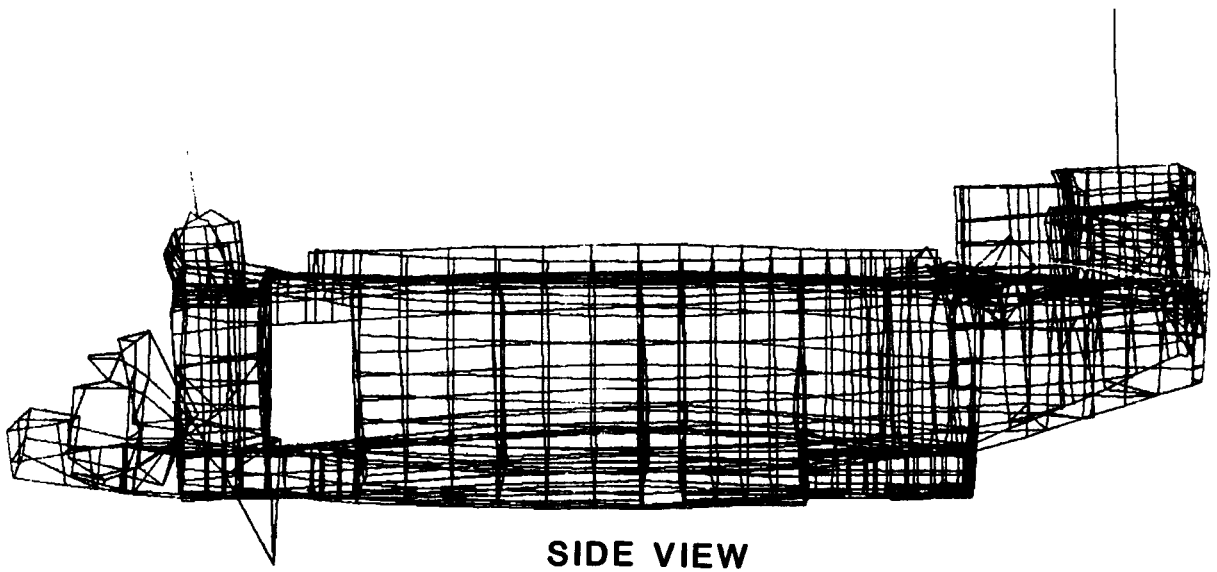

SIDE VIEW

9.0 Conclusions

CONCLUSIONS - MODELING

The modeling effort involved both the preparation of comprehensive modeling guides and formulation of a vibration model for the Model 360 helicopter composite airframe. Following is a summary of conclusions relative to these modeling activities:

1. Modeling of a composite airframe is more time consuming than a comparable metal aircraft because physical properties of equivalent elements must be developed for multi-ply structures.

2. Experience with the grid and element numbering system used in this program demonstrated that the system was extremely flexible and well suited to partitioning of the modeling tasks.

3. In general, the treatment of mass modeling tends to be somewhat superficial compared to stiffness modeling. Considering the modal complexity near b/rev, more detailed modeling seems necessary.

CONCLUSION - MODELING

- MODELING OF A COMPOSITE AIRCRAFT IS MORE TIME CONSUMING THAN A COMPARABLE METAL AIRCRAFT BECAUSE PHYSICAL PROPERTIES OF EQUIVALENT ELEMENTS MUST BE DEVELOPED FOR MULTI-PLY STRUCTURES.

- THE GRID AND ELEMENT NUMBERING SYSTEM USED IN THIS PROGRAM PROVED EXTREMELY FLEXIBLE AND IS WELL SUITED TO PARTITIONING OF THE MODELING TASKS.

- MASS MODELING IN GENERAL TENDS TO BE RATHER SUPERFICAL COMPARED TO STIFFNESS MODELING. CONSIDERING THE MODAL COMPLEXITY NEAR B/REV, MORE DETAILED MODELING IS NEEDED.

CONCLUSIONS - CORRELATION

The correlation effort included a comparison of analytical and test frequency response at selected locations, and a comparison of calculated natural mode shapes with test forced response mode shapes. Conclusions pertinent to this effort are as follows:

1. The correlation between test and analytical frequency response was poor in terms of both frequency placement and amplitude.

2. A number of potential problem areas in the model were identified from a comparison of natural mode shapes and test forced response mode shapes. These areas include:

    - Cockpit Module
    - Cabin Floor/Fuel Module
    - Forward Pylon and Transmission

3. In most cases, the combination of analytical and test results suggest that more detailed modeling is necessary to improve correlation.

4. Frequent large disparities between test and analytical amplitudes indicates a need for improved modeling of damping.

CONCLUSIONS - CORRELATION

- THE CORRELATION BETWEEN TEST AND ANALYTICAL FREQUENCY RESPONSE WAS POOR IN TERMS OF BOTH FREQUENCY PLACEMENT AND AMPLITUDE.
- A NUMBER OF POTENTIAL PROBLEM AREAS IN THE MODEL WERE IDENTIFIED FROM A COMPARISON OF NATURAL MODE SHAPES AND TEST FORCED RESPONSE MODE SHAPES. THESE AREAS INCLUDE:
  - COCKPIT MODULE
  - CABIN FLOOR/FUEL MODULE
  - FORWARD PYLON AND TRANSMISSION
- IN MOST CASES,THE COMBINATION OF ANALYTICAL AND TEST RESULTS SUGGEST THAT MORE DETAILED MODELING IS NECESSARY TO IMPROVE CORRELATION.
- FREQUENT LARGE DISPARITIES BETWEEN TEST AND ANALYTICAL AMPLITUDES INDICATES A NEED FOR IMPROVED MODELING OF DAMPING.

10.0 References

REFERENCES

GABEL, R. AND REED, D.: GROUND SHAKE TEST OF THE BOEING MODEL 360 HELICOPTER AIRFRAME, NASA CONTRACTOR REPORT 181766, MARCH 1989.

APPENDIX A

SCHEDULE AND RESOURCES

SCHEDULE AND RESOURCES

COMPARISON OF PLANNED AND ACTUAL SCHEDULE

The projected and actual schedules, in terms of elapsed time for the principal program elements, are presented in the accompanying summary. A major delay in the program was encountered in the formation of the static model. Changes to the existing model were more extensive than anticipated. In addition, modeling of the composite structure was more time consuming than expected.

SCHEDULE AND RESOURCES
COMPARISON OF PLANNED AND ACTUAL SCHEDULE

	ELAPSED TIME-WEEKS	
	PLANNED	ACTUAL
• PLANNING		
PLAN MODELING AND CORRELATION PROGRAM AND PREPARE NASA/INDUSTRY PRESENTATION	5.5	9
• EXECUTION		
FORM STATIC MODEL	6	15
FORM VIBRATION MODEL	8.25	9
CORRELATION STUDY		
PREPARATION OF RESULTS		
PREPARE NASA/INDUSTRY PRESENTATION		
FINAL REPORT		

SCHEDULE AND RESOURCES

COMPARISON OF ESTIMATED AND ACTUAL MAN-HOURS

This figure summarizes the man-hour costs for the major program activities. A significant increase over the estimated hours was required in the formation of the static model. As indicated previously, this was due to under estimation of the extent and difficulty of changes to the existing model. An offsetting reduction in hours is exhibited in the formation of the vibration model, the correlation study and items associated with the preparation of analysis results and reports. Because of poor correlation observed at the outset, the extent of the correlation effort and the volume of data generated was sharply reduced. The total hours expended exceeds the estimated hours by approximately 9%.

SCHEDULE AND RESOURCES
COMPARISON OF ESTIMATED AND ACTUAL MAN-HOURS

		MAN-HOURS ESTIMATED	MAN-HOURS ACTUAL
• PLANNING			
PLAN MODELING AND CORRELATION PROGRAM AND PREPARE NASA/INDUSTRY PRESENTATION		740	1008
• EXECUTION			
FORM STATIC MODEL		2300	3361
FORM VIBRATION MODEL	560		
CORRELATION STUDY	600		
PREPARATION OF RESULTS	280	1820	905
PREPARE NASA/INDUSTRY PRESENTATION	240		
FINAL REPORT	140		
		4860	5274

NASA
National Aeronautics and Space Administration

Report Documentation Page

1. Report No.	2. Government Accession No.	3. Recipient's Catalog No.
NASA CR-181787		

4. Title and Subtitle	5. Report Date
Plan, Formulate, Discuss and Correlate a NASTRAN Finite Element Vibrations Model of the Boeing Model 360 Helicopter Airframe	April 1989
	6. Performing Organization Code

7. Author(s)	8. Performing Organization Report No.
R. Gabel, P. F. Lang, L. A. Smith and D. A. Reed	D210-12328-4
	10. Work Unit No. 505-63-51-01

9. Performing Organization Name and Address	11. Contract or Grant No.
Boeing Helicopters P.O. Box 16858 Phila., PA 19142-0858	NAS1-17497
	13. Type of Report and Period Covered: Contractor Report

12. Sponsoring Agency Name and Address	14. Sponsoring Agency Code
National Aeronautics and Space Administration Langley Research Center Hampton, VA 23665-5225	

15. Supplementary Notes

Langley Technical Monitor: R. G. Kvaternik
Final Report

16. Abstract

Boeing Helicopter, together with other U.S. Helicopter manufacturers, participated in a finite element applications program to emplace in the United States a superior capability to utilize finite element analysis models in support of helicopter airframe design. The program was sponsored by the NASA Langley Research Center. This report summarizes the activities relating to planning and creating a finite element vibrations model of the Boeing Model 360 composite airfame, and the subsequent analytical correlation with ground shake test data.

17. Key Words (Suggested by Author(s))	18. Distribution Statement
NASTRAN Model 360 Helicopter DAMVIBS Composite Airframe	Unclassified - Unlimited Subject Category 39

19. Security Classif. (of this report)	20. Security Classif. (of this page)	21. No. of pages	22. Price
Unclassified	Unclassified	344	A15